The Role of the Schwann Cell in the Induction of Elongative Central Axonal Growth

Devesh J Dhasmana
The Norman and Sadie Lee Research Centre,
Laboratory of Neurobiology,
National Institute for Medical Research,
Mill Hill,
London NW7 1AA

December 1998

A thesis submitted in partial fulfilment of the requirements of University College London for the degree of Doctor of Philosophy

Supervisors:
Dr G. Raisman
Dr M. Gassmann

ProQuest LLC.
789 East Eisenhower Parkway
P.O. Box 1346
Ann Arbor, MI 48106 – 1346

Abstract

The factors underlying the failure of axon regeneration in the CNS are thought to comprise of both the lack of supportive factors as well as the presence of inhibitory ones. Transplantation work has shown that the PNS is able to provide some of the necessary criteria and with it an increased capacity to regenerate. Studies have further shown that the crucial ingredient to such peripheral grafts is the presence of Schwann cells (SCs), the major glial cell of the PNS.

I have used an extrusion transplantation system, recently developed in this laboratory, to study the effects of a SC column placed into the origin of the septo-hippocampal cholinergic projection. These SC columns integrate with host glia with minimal tissue damage, form a tight and ordered column with aligned cellular processes, and are able to recruit modest numbers of axons. Immunostaining with a cholinergic axon marker suggests that these axons arise from the septal nuclei.

Given the limited availability and yield of primary SCs that current preparation protocols offer, I have engineered neonatal SC lines by transfecting the SV40 large T antigen into a population of primary neonatal rat SCs. Characterisation of these cell lines, with the use of immunocytochemistry, Western blotting and RT-PCR, shows that they retain the immunophenotype of primary SCs *in vitro*, although *in vivo* studies have posed more difficult with the lack of a suitable marker.

In addition, I have set up a retroviral transfection system with the use of a bicistronic vector containing the Green Fluorescent Protein. This would provide a means of unique and efficient labelling prior to transplantation, and moreover offer the potential for further transfections of an additional gene of interest within the same vector.

to rita

Acknowledgements

I would like to thank Geoff Raisman, Nick Mazarakis and Martin Gassmann for their supervision of different aspects of this project, Arjen Bakker for his tuition of retroviruses via the world wide web, Daqing Li and Abdul Sesay for showing me the techniques for the surgical procedures and Western blotting, respectively.

I would like to thank much of the division of Neurobiology upon whom I called for advice at some point in the course of this work, in particular, Bernice and Luca for their tissue culture work (Luca, take a break!), and Melvyn and Randa for making things easier for me.

I am also grateful to the British Neurological Research Trust and the International Spinal Research Trust for providing me with the financial support and the opportunity to work in this lab.

I would like to thank my Mother and Father for their constant support in my work, and praise their strength in difficult times. I would like to thank Rita for her guidance and her love which has seen me through my own difficult times.

Finally, I would like to thank Akash for his strength and his love and his guidance.

Contents

CHAPTER II

Abbreviations

BrdU	Bromo-deoxyuridine
BSA	Bovine Serum Albumin
ChAT	Choline acetyltransferase
CMV	Cytomegalovirus
CNS	Central Nervous System
CP	Calcium phosphate-mediated transfection
Cy2	Cyanine 2 dye
Cy3	Cyanine 3 dye
DAB	3,3 Diaminobenzidine
DMEM	Dulbecco's Modified Eagle Medium
DMEMF	DMEM with 10% Foetal Calf Serum
DMEMF/G	DMEMF with G418 at 600μg/ml
EF	Effectene-mediated transfection
FACS	Fluorescence-Activated Cell Sorting
FCS	Foetal Calf Serum
FITC	Fluorescein
fNX	Phoenix Packaging Cell Line
GalC	Galactocerebroside
GFAP	Glial Fibrillary Acidic Protein
GFP	Green Fluorescent Protein
G418	Geneticin
IMDM	Iscoves Modified Dulbecco's Medium
IMDMF	IMDM with 10% FCS
IR	Immunoreactivity

MAG	Myelin Associated Glycoprotein
NF	Neurofilament
NGF	Nerve growth factor
NRG	Neuregulin
(N)SC	(Neonatal) Schwann Cell
OEC	Olfactory ensheathing cell
P0	Peripheral myelin protein, Protein Zero
p75	low-affinity nerve growth factor receptor
PBS	Phosphate Buffer Solution
pCMV-g	CMV vector containing the gene encoding β-galactosidase
pCMV-T-neo	CMV vector containing the gene encoding large T antigen
PDGF	Platelet-Derived Growth Factor
PKC	Puromycin killing curve
PLL	Poly-L-Lysine
PNS	Peripheral Nervous System
PVDF	Polyvinylidene difluoride membranes
S001	Isotype of the GFP bicistronic expression vector
SC	Schwann cell
STAG	**S**chwann cell-large **T** **A**nti**G**en cell line
Tag	Large T antigen
TEF	Transfection Efficiency
TH	Tyrosine Hydroxylase
TRITC	Tetramethylrhodamine dye
TSA	Tyramide Signal Amplification

List of Figures

CHAPTER IV – EXTRUSION TRANSPLANTS OF NEONATAL SCHWANN CELLS INTO THE BASAL FOREBRAIN SYSTEM

CHAPTER V – RETROVIRAL TRANSFECTION OF GREEN FLUORESCENT PROTEIN

APPENDIX

CHAPTER I

CHAPTER I – INTRODUCTION

1.1 Regeneration in the nervous system

The ability of neurons in the peripheral nervous system (PNS) to regenerate is not shared by those in the central nervous system (CNS) (Ramon y Cajal, 1928). The clinical implications of this are that while a patient who suffers a leg injury with peripheral nerve involvement may experience some return of function, the spinal cord injured patient may remain unable to walk again.

The location of the major neuronal projecting process, the axon, in the CNS or PNS reflects its ability to regenerate. The CNS is composed of brain and spinal cord while the PNS constitutes the neurons and glia which reside outside of the CNS. Axons of the CNS, for example, those comprising the descending fibres of the corticospinal tract, the major mammalian motor projection which originates in the primary motor cortex of the brain and synapses in the ventral and lateral spinal cord, fail to show elongative growth following axonal injury. In contrast, axons of the PNS can show some regenerative growth. Regeneration in this case may take the form of collateral formation and/or elongative growth of cut axons.

An injury to the axons of the sciatic nerve leads to a number of events, including macrophage infiltration, glial cell proliferation and cytokine release, which together serve to induce re-extension of the cut axons and re-connection with the distal site. While an injury to the axons of the corticospinal tract leads to some similar initial responses, there may follow retrograde degeneration and cell death of neurons whose axons have been cut, as well as of neighbouring axons through secondary degeneration (Midha *et al.*, 1987; Pallini *et al.*, 1988). Although some tips of

corticospinal axons have been found to persist at the injury site long after the initial insult, they display only a sprouting form of growth and a failure to show elongative axonal growth (Li and Raisman, 1994; Li and Raisman, 1995).

For there to be successful regeneration of cut central axons, neurons must firstly survive the initial injury, and secondly, show long axonal growth and functional re-connection with their target cells distal to the lesion site.

1.2 Nervous system anatomy

In the CNS, *oligodendrocytes* and *astrocytes* make up the major non-neuronal or glial cells. The former constitute the myelinating glia of the CNS and fast conduction of information through central axons is dependent on the myelin sheath that the glia produce. Oligodendrocytes form the major target for the study and repair of demyelinating disease (Franklin and Blakemore, 1997). Astrocytes have been credited with multiple roles in the CNS which include trophic support and immune-system mediation (Aschner, 1998). Other CNS glia include microglia, important in an immunoeffector role and satellite cells (Gehrmann *et al.*, 1995).

In the PNS, the *Schwann cells* (SCs) constitute the myelinating glia and ensheathe axons in a 1:1 relationship. Satellite cells and the extracellular matrix in the PNS may also play important roles after neuronal injury (Carbonetto, 1991; Scherer, 1997).

1.3 Factors which may be important in nerve regeneration

There is much evidence to suggest that elements which are permissive and/or inhibitory to axonal growth reside in the developing nervous system (Tessier Lavigne

and Goodman, 1996). This can be extended to the adult nervous system and such elements may become more significant in the context of neuronal injury.

The neurotrophin family of nerve growth factors comprises of a growing number of factors, headed by the original and best-known of them, Nerve Growth Factor (NGF) (Levi-Montalcini, 1987; Levi-Montalcini and Hamburger, 1952). The list currently includes brain-derived neurotrophic factor (BDNF), NT-3 and NT-4/5, and more recently NT-6 and NT-7 isolated in lower vertebrates (Berkemeier *et al.*, 1991; Götz *et al.*, 1994; Hohn *et al.*, 1990; Lai *et al.*, 1998; Liebrock *et al.*, 1989). Other growth factors include ciliary neuronotrophic factor (CNTF), fibroblast growth factor (FGF) and glial cell-line derived neurotrophic factor (GDNF) (Eckenstein, 1994; Lin *et al.*, 1993; Manthorpe *et al.*, 1980). It is not clear to what extent or how such factors might play a role in regenerative growth *per se*, rather than one in survival and protection, roles which they do appear to play in development as evidenced by transgenic studies (Crowley *et al.*, 1994).

In addition, various cell adhesion molecules, extracellular matrix molecules and growth cone-associated molecules have been proposed to be permissive for axonal regeneration (Burden-Gulley *et al.*, 1997; Zhang *et al.*, 1995a; Zhang *et al.*, 1995b).

Inhibitory factors may be important following central axonal injury. It has been suggested that the presence of myelin products, designated *NI-35* and *NI-250*, are directly related to the failure of central axons to regenerate (Caroni and Schwab, 1988; Schnell and Schwab, 1990). Studies employing the application of antibodies against these factors (Bregman *et al.*, 1995) or delaying the onset of myelination in the developing chick (Keirstead *et al.*, 1992) suggest that there may be an important inhibitory contribution made by myelin or myelin-associated elements.

Astrocytes provide another source of factors which include those with both permissive and inhibitory potential (Rudge *et al.*, 1994). Chondroitin sulphate proteoglycans produced by astrocytes and/or expressed on their cell surfaces, may suppress elongative axonal growth in the CNS following axonal injury (McKeon *et al.*, 1991). A microtransplant study in the white matter tract, the corpus callosum, showed a correlation between the extension of dorsal root ganglion processes and the absence of inhibitory chondroitin sulphate proteoglycan (Davies *et al.*, 1997).

However, elongative growth of cut central axons has recently been demonstrated in the adult rat spinal cord (Li *et al.*, 1997). In this study, a transplant of olfactory ensheathing cells, placed across a small lesion of the corticospinal tract, was able to mediate successful elongative axonal growth across the lesion site, beyond which axons were remyelinated by host oligodendrocytes. Thus, at least in this model, any inhibition of central host glia can be circumvented under the right conditions.

In addition, Cheng et al., (1996) report, also in adult rat spinal cord, that cut axons can successfully be re-directed through adjacent grey matter bridged across the lesion site. Thus, given the right environment, cut central axons can show significant long axonal growth, a phenomenon which has become more evident with the development of peripheral nerve grafting.

1.4 Transplantation strategies to promote axon regeneration

The strategies of peripheral nerve grafting and cell transplantation require certain conditions for accurate histological analysis. This form of analysis requires principally that the donor transplant material can be cleanly distinguished from that of host tissue. This would involve the use of immunohistochemistry to distinguish antigens

specific to the transplant cell type from those of the host tissue. However, where the cell type of the donor material is similar to or identical to that of the cells of the host tissue, then alternatives may need to be sought in order to provide a more accurate histological analysis.

One method has exploited species differences in antigen expression; the polymorphism of the neuronal glycoprotein Thy1 in mice (Thy1.1 and Thy1.2) has been used to identify Thy1.1-positive donor cells transplanted into Thy1.2-positive (Thy1.1-negative) host brains (Charlton *et al.*, 1983; Lund and Hankin, 1995). Alternatively, the use of mouse donor cells in rat hosts can exploit species-specific antibodies to accurately recognise transplanted cells (Lund *et al.*, 1985); the mouse monoclonal antibody, M6 was used to identify transplanted mouse cells in this study. Indeed, the M6 antibody was used more recently to demonstrate that the adult CNS can support long axonal growth of embryonic neurons (Davies *et al.*, 1994; Li and Raisman, 1993).

When transplanted into the brain, donor tissue must also be compatible with the site into which it has been transplanted. Integration into the host tissue is important if there is to be good functional value to the graft. As part of this integration, it is important that the host immune system does not reject or otherwise destroy the graft.

Although regarded as an immunologically privileged site, the brain is not absolutely free from mounting a directed immune response. In this respect, microglia form the principal immunoeffector cell of the brain and spinal cord, while astrocytes play additional important roles (Gehrmann *et al.*, 1995; Aschner, 1998). Consequently, a cell that is introduced into the brain is vulnerable to an immune response by the host which is dependent on the nature of that cell type (aided also by the break in the blood-brain-barrier). Those cells which are normally foreign to the

brain, for example SCs and fibroblasts, may be more vulnerable, while transformed cells or otherwise genetically engineered cells are likely to be more immunogenic. The problems associated with such a host response may be most profound when they induce pathology either at or nearby to the site of the transplant. For example, this may take the form of transplant destruction with causing directly or indirectly demyelination of neighbouring axons (Matyszak and Perry, 1995; Selmaj *et al.*, 1991).

1.5 Peripheral nerve grafting to induce the repair of cut CNS axons

Peripheral nerve grafting has enjoyed a renaissance since the work of Aguayo et al., in the early 1980s. In a major report of central axonal elongation, they describe the extension of thoracic spinal axonal processes in an autologous peripheral nerve graft (Richardson *et al.*, 1980). Later studies demonstrated that an important determinant of axonal growth within such transplants was the distance between the neuronal cell body and the site of injury (Benfey and Aguayo, 1982; Richardson *et al.*, 1984).

In this and in later studies it was demonstrated that peripheral nerve grafts, which provided a growth-permissive environment and seclusion from the non-permissive CNS fibre tracts, could enable elongative growth of central axons within them. Studies subsequently progressed towards isolating the crucial element of these grafts.

Berry et al., described a peripheral nerve graft study in which they could evaluate the contribution of the SCs within the grafts (Berry *et al.*, 1988). They compared transplants of normal peripheral nerve with those which had been freeze-thawed and thereby rendered acellular. Although some regenerating axons could be found within the acellular grafts, they concluded that the presence of SCs within the grafts was the

key factor for elongative axonal growth within the transplants. This was consistent with the findings of a similar study in adult hamsters (Smith and Stevenson, 1988).

1.6 The importance of Schwann cells in CNS regeneration

SCs arise from the neural crest cells in development and through a process involving both intrinsic and environmental cues they differentiate into either a myelinating or a non-myelinating type (Jessen and Mirsky, 1997; Zorick and Lemke, 1996). In the adult, they have been shown to produce a plethora of growth-promoting factors including cell adhesion molecules, nerve growth factors including NGF and BDNF, and extracellular matrix molecules (Fu and Gordon, 1997; Jessen and Mirsky, 1991).

SCs have been used increasingly in recent years to stimulate the regenerative response of central axons. Studies have been carried out which seed SCs onto synthetic polymer tubes which are then implanted in the CNS to promote central axonal growth (Montgomery *et al.*, 1996; Xu *et al.*, 1997; Xu *et al.*, 1995). These tubes enable SCs to be placed in a defined location at high concentrations and have been shown to support some axonal growth. However, the transplantation procedure causes much local tissue damage and, with the inevitable astrogliosis, makes it difficult to interpret precisely the effect of placing SCs into the CNS environment. Nevertheless, the studies do support the idea that SCs can support axonal growth of cut central axons.

Another study carried out in this laboratory describes the transplantation of pure suspensions of SCs extruded into the thalamus to obtain discrete columnar transplants, which are able to support significant elongative growth of cut central

axons (Brook *et al.*, 1994). This is an example of SCs, *by themselves*, supporting elongative growth of central axons.

The neuronal phenotype of the axons which were recruited in the above study was not elucidated. However, a similar study which involved the transplantation of peripheral nerve into the body of the thalamus, and which reproduced the finding of significant elongative axonal growth, identified some of these axons as those of the thalamic reticular nucleus (Zhang *et al.*, 1995a). Indeed, induction of axonal growth of these same axons was initially described by the earlier studies of Aguayo et al. (Benfey *et al.*, 1985).

Although several studies of SCs in the CNS exist, it is not clear whether they show a specificity to recruit only certain classes of neurons. There are a number of studies which describe the induction of central axonal growth by SCs, and some demonstrate induction of a certain axonal phenotype (Benfey *et al.*, 1985; Brecknell and Fawcett, 1996; Montero-Menei *et al.*, 1992). However, it is possible that SCs support axonal growth of only certain classes of central neurons and this remains to be tested.

1.7 Preparation of Schwann cells

The ability to obtain large populations of human SCs is now possible through recent advances in SC expansion (Levi *et al.*, 1995) and suggests that one could consider the potential of autologous transplantation in the clinical situation. However, despite the recent improvements on cell culturing and yields, SC preparation remains time-consuming and difficult to generate pure populations. Primary SCs are generally quiescent and have a doubling rate of approximately 2 days when stimulated to divide

(Chen *et al.*, 1991). Although several mitogens have now been isolated (Dong *et al.*, 1997), there remains the presence of heterologous populations of SCs within each batch, a feature which may produce variable results in studies involving these cells. Studies would, therefore, benefit from more readily available homogeneous SC populations.

1.8 Gene transfection

There are currently a number of methods available which allow the transfection of a foreign gene into a host cell and these vary according to the nature of the study. In mammalian cell transfection, the major techniques include *calcium phosphate* ($CaPO_3$) transfection, where the plasmid is brought into the cell via a $CaPO_3$ precipitate, *liposome-mediated transfection*, where this is achieved by complexing with a lipid reagent and subsequent endocytosis, *electroporation* where the plasmid enters the cell through holes punched in the cell wall, and direct *microinjection* where the construct is injected directly into the nucleus of a single cell. Each technique offers its own advantages and disadvantages and the choice of method depends on a number of factors. These include the host cell type, the necessity for transient or stable transfection, the nature of the gene construct to be transfected and the nature of the experiment (Ridet and Privat, 1995).

In addition, viral vectors have been exploited for their natural affinity to mediate gene transfection with high efficiency (Breakefield, 1993). However, their natural ability to mediate gene transfection has also made them less attractive for reasons of safety. Recent studies have sought to improve their safety record and several defective viruses have since been generated which carry added stringent safety

measures incorporated within the viral construct (Kramm *et al.*, 1997; Pear *et al.*, 1993).

1.9 Retroviral transfection and the Green Fluorescent Protein

Retroviruses currently offer one of the highest transfection efficiencies of the viral transfection systems, although they show a preference for dividing cells. Replication-defective viral constructs are transfected into a *packaging cell line*, infectious viral particles can be packaged correctly and the supernatant from these cultures can be used to transfect dividing target cells with high efficiencies (Pawliuk *et al.*, 1998).

A third-generation retroviral cell line, termed the *Phoenix Cell Line* (fNX), has recently been generated and is claimed to produce high titre infectious virus with a further reduced risk of recombination, a rare but not impossible event in which the genetic elements of the virus are restored to their full potency (Pear *et al.*, 1993).

Green Fluorescent Protein (GFP) is a naturally fluorescent protein isolated from the jellyfish, *Aequorea victoria* (Prendergast and Mann, 1978). Its unique ability to fluoresce has made it an exceptionally useful tool in many fields, in particular, in those of Development and Gene Transfer (Okabe *et al.*, 1997; Ramiro *et al.*, 1998). With the isolation of brighter and more stable mutants, GFP is an ideal candidate for a reporter gene and cell tracking (Cormack *et al.*, 1996; Zhang *et al.*, 1996).

In addition, GFP has recently been coupled to the fNX line retroviral system and as such provides an attractive means of labelling and tracking a chosen cell population. An important implication of this is that a cell population, transfected with GFP and then transplanted into the brain or spinal cord, can easily and accurately be followed at later time points. Such a system would benefit transplant studies, where

selective identification of the transplanted cell is essential, and in particular, those which examine the migratory ability of the transplanted cell.

1.10 Aims of the project

Given the technical problems associated with working with primary SCs, conditionally immortalised SC lines were generated by liposome-mediated transfection of primary SCs with an expression vector encoding a thermosensitive mutant allele of the large T antigen. The SC lines were characterised extensively *in vitro* and transplanted *in vivo* to compare their properties with those of the original primary cell type.

In addition, suspensions of primary neonatal SCs were transplanted into the basal forebrain in order to assess their ability to integrate within host tissue and to support axonal growth of a known neuronal phenotype, namely the cholinergic neurons of the septal cholinergic nuclei. This would provide important information on the ability of SC transplants to recruit axons from the nuclei of this well-characterised projection.

In the light of the results from the above studies, in particular, the desire to label the SC line for identification *in vivo*, a retroviral transfection system was set up to enable the transfection of GFP onto both the SC lines and primary SCs *ex vivo*. Such a method would not only allow accurate detection of transplanted cells *in vivo*, a feature crucial in any transplantation studies but, with a resident internal ribosome entry site or IRES, would also offer the potential to co-transfect genes of interest within the vector to accurately monitor any effects of the engineered cell type.

CHAPTER II

CHAPTER II – General Materials and Methods

2.1 Tissue culture

2.1.1 General

The medium for SC tissue culture was Dulbecco's Eagles Modified Medium (DMEM) + 10% Foetal Calf Serum (FCS) (both GIBCO BRL, UK), referred to together as DMEMF. Each 40ml volume of DMEMF was supplemented with 11.6mg glutamine (BDH, UK), 0.2 units penicillin, 0.2μg streptomycin (both GIBCO BRL, UK) and 440μg pyruvate (BDH, UK) and was filter-sterilised (0.2μm) prior to use.

All cell culture work was carried out in class I hoods, unless otherwise stated, and aseptic techniques were used throughout.

Poly-L-Lysine-coated dishes

Cell culture dishes were coated with poly-L-lysine (PLL) (Sigma Chemical Company Ltd., UK) by incubating the dishes in 1ml PLL at 0.1mg/ml for one hour at room temperature followed by 3 washes with distilled water. The dishes were air-dried prior to use.

Cell freezing media

Cells were frozen down in 1ml media containing 50% DMEM, 40% FCS and 10% Dimethylsulfoxide (DMSO, Sigma) in 1.8ml cryotubes (NUNC). The vials were slow-frozen by immersion in an isopropanol bath at $-80^{O}C$ overnight before storage in liquid nitrogen.

2.1.2 Preparation and isolation of neonatal Schwann cells

2.1.2.1 Dissection and isolation

Neonatal Schwann cells (NSCs) were prepared using a modified method of Brockes et al., 1979. Sciatic nerves were dissected from between 4-6 2 day-old (P2) locally bred AS rats, cut into 100μm sections using a McIlwain tissue chopper and the sections digested in 2ml 0.15% collagenase II (Sigma, UK) in DMEM and 200μl 1% trypsin (Lorne Laboratories Ltd., UK) before incubation in a water bath at 37^{O}C for 30 minutes. The reaction was stopped by adding 8ml DMEMF. The solution was spun at 1200rpm for 5 minutes in an Econospin Sorvall centrifuge, the supernatant removed and the cells were resuspended in 1.5ml DMEMF added and triturated using a fire-polished glass Pasteur pipette. The cells were then transferred to a NUNC cryotube, triturated three times using a 0.5 x 16mm hypodermic syringe needle and a 2ml syringe, transferred to an uncoated 35mm tissue culture plastic dish and incubated at 37^{O}C, 5% CO_2 for 48 hours.

2.1.2.2 Schwann cell purification

The cells were subsequently incubated in the presence of 10μM anti-mitotic cytosine arabinoside (araC) (Sigma, UK) for 2-3 days to reduce fibroblast contamination. The araC was removed and the cells were washed three times with DMEM before returning to the incubator with 1.5ml DMEMF per dish.

A complement-mediated killing of contaminant fibroblasts was carried out on the following day. The cells were trypsinised with trypsin solution: 4ml PBS, 200μl 1% trypsin and 20μl 100mM EDTA (Sigma, UK). This reaction was stopped with 5ml DMEMF and spun at 1200rpm for 5 minutes. Having removed the supernatant, the cells were resuspended in 100μl DMEM plus 25μl anti-Thy 1.1 IgM (Serotec,

UK) and incubated in a water-bath at 37°C for 40 minutes. After the incubation, a further 2ml DMEM was added, the cells were spun down and resuspended in 100µl DMEM plus 100µl guinea pig complement (Advanced Protein Products, UK) and incubated at 37°C for 40 minutes. The complement reaction was terminated with 5ml DMEMF, the cells were spun down and resuspended in DMEMF.

Cell density was measured using a haemacytometer (Weber Scientific International Ltd.) and cells were plated at 5-6 x 10^5 cells per 35mm PLL-coated dish in 1.5ml DMEMF. NSC cultures were maintained in twice-weekly changes of DMEMF.

2.2 Surgery

2.2.1 Extrusion transplantation of cells

NSCs were prepared at a density of 40-80 x 10^6/ml in DMEM containing 40% DNAse at 11,500 units/ml (Sigma, UK). Adult female AS rats (200-225g body weight) were anaesthetised intra-peritoneally using Avertin (2g 2,2,2-tribromoethanol (Aldrich Chem Co., USA), 2ml 2-methylbutan-2-ol (BDH, UK), 8ml absolute alcohol, and 100ml distilled water) at 1ml/100g body weight. Anaesthetised animals were positioned into the stereotaxic apparatus (made locally) and the bregma and surrounding area exposed. The cell suspension was microtransplanted at the designated stereotaxic co-ordinates using a pulsed air pressure system (Emmett *et al.*, 1990). The micropipette was made from siliconised glass with an internal diameter of approximately 130µm using a microelectrode puller (Palmer Bioscience, USA) and bevelled using a rotating sanding machine (made locally).

Animals were maintained with strict adherence to the Scientific Procedures Animals Act, 1986.

2.2.2 Perfusions

The animals were killed at the required time post-operatively using deep terminal dose pentobarbitone (Expiral; Sanofi Animal Health, UK). The thorax was opened, the heart exposed and the blood flushed out by transcardiac perfusion with 120ml PBS at room temperature. For cryostat immunostaining, the brain was dissected, snap-frozen in crushed dry ice and stored at $-70^{O}C$ until required. For vibratome and electron microscopy (EM) processing, the animal was perfused with 400ml appropriate fixative (see section 2.3.2.1), the brain dissected and stored in fixative solution at $4^{O}C$ until required. Perfusions were carried out using tungsten cannulas made locally.

2.3 Histology

2.3.1 Antibodies and reagents

The primary antibodies used were as follows: mouse monoclonal anti-p75 low affinity nerve growth factor receptor, IgG1 (clone 192, Boehringer Mannheim, UK) at 1:300; mouse monoclonal anti-panaxonal neurofilament, IgG1 (SMI 312, Sternberger Monoclonals Incorporated, USA) at 1:1000; goat polyclonal anti-choline acetyltransferase (ChAT) (#AB144P, Chemicon, UK) at 1:100; mouse monoclonal anti-glial fibrillary acidic protein, IgG1 (GFAP) (#MAB360, Chemicon, UK) at 1:500; mouse monoclonal anti-P0 (gift from Dr J. Archelos) at 1:500. The secondary antibodies were as follows: biotinylated anti-mouse and

biotinylated anti-goat IgG (Vector Laboratories, UK) at 1:700 and 1:500, respectively.

Primary antibodies were diluted in PBS with 0.1% Triton-X100 (TX-100) (Sigma, UK), except for anti-p75 antibody which was diluted in 0.25% TX-100. Secondary antibodies were diluted in PBS alone. Immunostaining was enhanced with an Avidin-Biotin complex (ABC) kit (Vectastain; Vector Laboratories, UK), prepared according to manufacturer's recommendations.

2.3.2 Staining

2.3.2.1 Fixatives

For vibratome sectioning, brains were perfused with 400ml 4% paraformaldehyde in 0.1M Phosphate Buffered Saline (PBS). For cryostat sectioning, frozen brains were cut and post-fixed in either 4% paraformaldehyde in 0.1M PBS or 5% acetic acid in 96% alcohol. For electron microscopy (EM), brains were perfused with 1% paraformaldehyde/1% glutaraldehyde containing 0.54% glucose, 0.002% $CaCl_2$.

2.3.2.2 Cryostat immunostaining

All incubations and washes were for 30 minutes at room temperature unless otherwise stated. 10-20μm coronal cryostat sections were cut (Reichart-Jung 2800 Fridgcut) and air-dried onto gelatin-coated glass slides over approximately 2 hours. Sections were fixed in either 4% paraformaldehyde (for anti-p75 immunostaining) or 5% acetic acid in 96% alcohol (for anti-GFAP or -P0 staining), washed thoroughly in PBS at 10 minute intervals over 30 minutes, blocked for non-specific protein binding with 1% dried skimmed milk solution (Marvel Milk Powder, UK) and incubated in the primary antibody overnight at $4^{O}C$. Sections were washed in

PBS for 30 minutes and then incubated with secondary antibody before a final series of washes and signal detection (see 2.3.3).

2.3.2.3 Vibratome immunostaining

All incubations were carried out for 1 hour at room temperature unless otherwise stated. 40-70μm free-floating vibratome sections were cut (Leica 1000S vibratome), washed in PBS, blocked with 10% dried skimmed milk solution for 30 minutes and incubated in primary antibody overnight at $4^{O}C$. On the following day sections were washed thoroughly at 15 minute intervals over 2 hours, incubated in secondary antibody, washed for 1.5 hours, incubated in ABC reagent for 45 minutes and washed for 1.5 hours before final signal detection (see 2.3.3).

2.3.3 Signal Detection

2.3.3.1 Horseradish Peroxidase-Diaminobenzidine (HRP-DAB)

Sections were taken after binding of the ABC complex and incubated in 50mg/100ml diaminobenzidine containing 0.006% hydrogen peroxide (both Sigma, UK). The brown-coloured reaction product was visible within approximately 3 minutes and sections were subsequently washed in PBS over 20 minutes before mounting.

2.3.3.2 Nickel enhancement

This intensified the HRP-DAB signal to produce a blue-black coloured reaction product. ABC-reacted sections were incubated in 1% nickel chloride (Sigma, UK) in distilled water for 3 minutes before incubation in the DAB solution; the sections were processed to completion as described above (2.3.3.1).

2.3.3.3 Nickel-Glucose Oxidase (Ni-GOD)

This provided an alternative sensitive method of detection to that of HRP-DAB and produced a black-coloured reaction product. Sections were taken after binding of the ABC complex and incubated in 0.1M acetate buffer pH 6, for 5 minutes. Reaction solution was prepared by adding 150mg β-D glucose (BDH, UK), 50mg DAB, 10μl glucose oxidase (15,150U/ml) (both Sigma, UK) to 100ml of filtered solution containing 0.1M acetate buffer, 0.04% ammonium chloride, 2.5% nickel ammonium sulphate and 0.25% β-D glucose (BDH, UK). Sections were incubated in the reaction solution for approximately 8 minutes to develop the signal and then washed in PBS over 5 minutes.

2.3.3.4 Tyramide Signal Amplification (TSA)

This provided a means to visualise an ABC-amplified signal with a fluorescent tag. The TSA system (NEN Life Science Products, USA) works by depositing tyramide residues at the site of the antigen/antibody complex on ABC-reacted sections, to which fluorophores subsequently bind either directly or indirectly. The 'TSA-direct' system was used in these experiments and involved the incubation of ABC-reacted sections in the TSA-fluorochrome reagent for 10 minutes followed by 30 minutes washing. Where double labelling was carried out, TSA-red or TSA-Cy3 was processed on the first antibody and TSA-green on the second antibody.

TSA reagents were used at the following dilutions: TSA-red at 1:250; TSA-Cy3 at 1:350; TSA-green at 1:250. Otherwise, protocols were followed according to manufacturer's recommendations. TSA-red is conjugated to Tetramethylrhodamine (TRITC); TSA-Cy3 to cyanine 3; TSA-green to Fluorescein (FITC).

2.3.3.5 Counterstaining

DAB- or Ni-GOD-stained sections were counterstained in thionin solution (Merck, UK) for 10 seconds, washed in distilled water, dehydrated through an ascending series of alcohols (70%, 96%, 100%) and cleared through Histoclear (National Diagnostics, UK) before mounting.

Fluorophore-stained sections were incubated in 4',6-diamidino-2-phenylindole (DAPI, Sigma, UK) diluted at 1:1000 in PBS for 10 minutes followed by 2 x 5 minute washes.

2.3.3.6 Mounting

Non-fluorescent sections were mounted with borosilicate glass coverslips (BDH, UK) and DePeX mounting reagent (Merck, UK). Fluorescent-labelled sections were mounted using an aqueous/glycergel mountant (Vectashield, Vector Laboratories, USA) and borosilicate coverslips and sealed in place with boat sealant (Ernest F. Fullam, USA).

2.4 Image Analysis

2.4.1 Confocal Imaging

Fluorescent double-labelled sections were visualised using the Leica TCS NT Multilaser Confocal System (UK) with an argon/krypton laser coupled to a Leica DMRBE microscope. Images were scanned using separate excitation filters to obtain specific signals in the TRITC/FITC range, that is, excitation/emission wavelengths of 550/570 and 494/517nm, respectively. Any bleed-through of the signals was eliminated by manipulation of incoming signal intensities and noise reduction. Otherwise, standard confocal operating procedures were followed.

2.4.2 Image Processing

Fluorescent-labelled images were scanned into the confocal imaging system and some images were processed further for contrast, brightness and superimposition with the use of Adobe Photoshop 5.0 (Windows 95).

All other photomicrographs were scanned into Adobe Photoshop with the use of a slide-scanner (Silverscan, Nikon COOLSCAN II).

CHAPTER III

CHAPTER III – Generation and Establishment of a Schwann Cell Line

3.1 Introduction

3.1.1 The importance of Schwann cells in nerve regeneration

The peripheral nerve grafting studies in the 1980s demonstrated not only that the environment of the peripheral nerve could support elongative growth of cut central axons, but that the active ingredient of these grafts was the presence of the peripheral myelinating glia, the Schwann cells (Scherer, 1997; Zorick and Lemke, 1996).

An important example of this is a study in which peripheral nerve was freeze-thawed prior to anastomosing onto transected optic nerve, thereby eliminating the cellular component of the graft and creating a peripheral transplant material devoid of SCs (Berry *et al.*, 1988). While the acellular grafts promoted some retinal ganglion cell (RGC) survival, they were poor at supporting elongative axonal growth. In contrast, normal grafts were able to support long axonal growth of a small number of RGC axons, in addition to providing trophic support to RGC cell bodies following the transection injury.

The results of a transgenic study revealed a mouse line with further evidence to support the importance of the SC in nerve regeneration (Kelly *et al.*, 1994; Rath *et al.*, 1995). The *Enr* mouse has a transgene-induced insertional mutation and neurons of the PNS in these mice displayed a poor capacity to regenerate. *In vivo* work later showed that the peripheral nerve was made up of abnormal SC-axon relationships and the defect was traced to problems in the early differentiation of

the SC. This work is an example of a direct link between the importance of a correctly functioning SC and successful nerve regeneration.

The increasing awareness of this importance led to a number of studies, both *in vitro* and *in vivo*, to better understand the mechanisms involved in successful nerve regeneration. However, the preparation of primary SCs for such studies is both time-consuming and limited in its yield. Several methods have been developed over recent years to improve the speed and yield of production, many based on a method developed nearly 20 years ago (Brockes *et al.*, 1979; Jirsová *et al.*, 1997; Levi *et al.*, 1995). However, while these methods have greatly improved both SC yield and purity, they continue to generate heterogeneous populations of SCs. The result is that each experiment which employs these cells carries with it the extra variable conferred by the cell population of the specific batch used.

For these reasons, some workers turned towards generating glial cell lines, including SC lines, which could retain the properties of primary cells but be produced in far greater numbers, with greater speed and moreover act as a homogeneous cell population for any subsequent studies.

3.1.2 Generation of SC Lines

SC lines have been created in recent years either by repeated passaging to generate a spontaneous cell line or by transfection of an oncogene to produce a transformed cell line (Boutry *et al.*, 1992; Chen *et al.*, 1987; Li *et al.*, 1996b; Peden *et al.*, 1989; Tennekoon *et al.*, 1987; Thi *et al.*, 1998; Watabe *et al.*, 1990). The value of the cell line is determined principally by the resultant phenotype. The phenotype should closely match that of primary SCs if the cell line is to serve as a valuable tool. In addition, the cell line should ideally expand quickly *in vitro* to generate large

numbers of cells, but differentiate when required to do so, either in a chosen system *in vitro* or when transplanted *in vivo*.

This level of 'control' has been supported in the past with the use of drug-inducible promoters, for example, with the use of zinc; the transforming oncogene is positioned downstream of the zinc-inducible promoter, such that removal of zinc from the media promotes arrest in cell proliferation and drives the cell to differentiate (Peden *et al.*, 1989).

The Simian virus (SV40) Large T antigen is an oncogene that has been used to create a number of cell lines including mixed glial cell lines, neuroepithelial lines and some SC lines (Goodman *et al.*, 1993; Marone *et al.*, 1995; Watabe *et al.*, 1990). Moreover, there currently exist a number of temperature-sensitive mutant alleles of the large T antigen (Loeber *et al.*, 1989). These are thermolabile proteins which are intact at a certain *permissive* temperature but morphologically altered and rendered non-functional at the higher *restrictive* temperature. Thus, a cell line transfected with such a protein would divide rapidly at the permissive temperature but differentiate at the higher restrictive temperature. This mechanism provides a means of easily regulating the cell line, and is further pertinent to transplantation studies where uncontrolled cell growth *in vivo* is to be avoided.

Temperature sensitive alleles have been used in the past to generate a neuroepithelial cell line (Marone *et al.*, 1995), an olfactory glial cell line (Franklin *et al.*, 1996) and SC lines (Chen *et al.*, 1987; Thi *et al.*, 1998). However, the value of such a line lies not only in its resemblance to the primary cell phenotype, but also in its ability to differentiate when required to do so.

A SC line which retained the primary cell phenotype would serve as a valuable tool for future studies in nerve regeneration. It would act as an abundant source of

SCs which could be rapidly generated to the required numbers for both *in vitro* and *in vivo* studies. In addition, it would serve as a basis for further transfections by which the effects of a particular gene of interest on the SC could be investigated.

3.1.3 Aims of the project

The thermosensitive allele of the large T antigen, tsA357 (Loeber *et al.*, 1989), was used to generate conditionally immortalised NSC lines. An expression vector harbouring the mutant allele was transfected into a population of NSCs using liposome-mediated transfection. Transfected cells, termed *STAG* (**S**chwann cell **T** **A**nti**G**en) cells, were selected and clonally expanded before undergoing extensive characterisation. Both primary NSCs and a population of spontaneously immortalised mouse SCs (Watabe *et al.*, 1995) were used as controls in the characterisation studies.

3.2 Materials and Methods

3.2.1 Generation of Schwann cell lines

3.2.1.1 Restriction digest of pCMV-T-neo

Digests were set up in 6 eppendorf tubes, each containing the following components: 6µl DNA at 0.5µg/ml, 3 units restriction enzyme with 5µl buffer (GIBCO BRL, UK), 1µl of BSA at 10ng/µl (Sigma, UK), 2µl of spermidine at 4mM (Sigma, UK) and 33µl of distilled water to give a total volume of 50µl. These were incubated in a 37^{O}C water bath (Grant Instruments, UK) for 1.5h.

A 0.7% agarose gel was made up using high quality agarose (NuSieve, FMC Bioproducts, UK) in 1 x Tris-acetate buffer (TAE) with ethidium bromide (Life Sciences, UK) at 0.5µg/ml. The melted agarose solution was poured into a casting plate with a slot former (10 x 1mm) and set at room temperature within 45 minutes. Approximately one-third of the volume of each restriction digest together with 2µl loading buffer (Life Sciences, UK) was loaded into the gel, the gel immersed in 1 x TAE buffer and electrophoresis was carried out at 50V for approximately 3 hours (Gene Power Supply 200/400, Pharmacia, UK).

3.2.1.2 Determining the G418 killing curve for P2 SCs at 33^{O}C

G418 antibiotic (GIBCO BRL, UK) was prepared in PBS to a working concentration of 50mg/ml. NSCs were generated as described before, plated out onto 6 x 35mm dishes at 5 x 10^5 cells per dish and incubated at 33^{O}C, 5%CO_2. 1.5ml DMEMF containing PDGF-BB at 20-25ng/ml (GIBCO BRL, UK) and forskolin at 2µM (Calbiochem, UK) was added to each of 6 x 10ml conical tubes, together with G418 at 50, 150, 300, 450, 600 and 750µg/ml in the 6 tubes,

respectively. This medium was used to replace the cell medium of the 6 dishes and the dishes were returned to the incubator at 33^{O}C for two weeks. On day 7, 1ml of the medium was replaced with 1ml fresh medium.

Assessment of cell death was carried out after 14 days. The number of cells surviving in each of 10 randomly chosen fields of view was recorded for each dish, all fields being at a magnification of x80 in a standard light microscope (Zeiss Axiovert 10, Germany).

After the initial experiment, a second killing curve was carried out using a narrower range of 4 antibiotic concentrations: 350, 450, 550 and 650μg/ml. This was carried out in duplicate in 8 x 35mm dishes using the same methods as described in the first experiment.

3.2.1.3 Optimisation of the lipofection protocol of P2 SCs with a β-gal reporter vector, pCMV-g

The plasmid, pCMV-g, contains the β-galactosidase reporter gene in the Simian CMV expression vector, pJ7 Ω (N. Mazarakis, unpublished data). NSCs were prepared, plated out onto 6 x 35mm dishes at 5 x 10^{5} cells per dish and incubated at 33^{O}C, 5% CO_2. Mitogens PDGF and forskolin were added to the cultures, as described earlier (3.2.1.2), 24h prior to transfection. Transfection medium was made up in 6 x 6ml polypropylene tubes (Becton Dickinson, UK) by adding 100μl Optimem, lipid reagent, LipoFECTIN, at 22.5, 30, 35, 40, 45 and 50μg in the six tubes, respectively (both GIBCO BRL, UK), a further 100μl Optimem and 14μg pCMV-g DNA (5μl at 2.8mg/ml). 14μg DNA had previously been determined as the optimal amount of DNA for transfection of this vector into NSCs (B.Watt, unpublished data). The solution was tapped-shaken and incubated for 15 minutes at

room temperature. 800µl fractions from a mitogen solution containing 4.8ml Optimem with PDGF and forskolin (3.2.1.2) were added to each of the 6 tubes containing transfection medium. The SC culture medium was subsequently replaced with the transfection medium and the dishes returned to 33°C, 5% CO_2 for an incubation period of 5 hours. The reaction was stopped by adding 1ml DMEMF containing 20% FCS to each dish.

Analysis of Transfection Efficiencies:

72h after transfection, each 35mm dish of cells was rinsed in PBS, fixed in 1ml 0.5% glutaraldehyde solution (BDH, UK) for 15 minutes, washed twice in PBS, and incubated overnight at 37°C in 1ml 5-bromo-4-chloro-3-indolyl-D-galactopyranoside (X-gal) solution (Sigma, UK) and covered in foil. After washing with PBS and adding 1ml 50% ethanol (BDH, UK), transfected cells were visualised under standard light microscopy as blue-coloured cells while non-transfected cells remained clear. The degree of transfection success was assessed by counting the relative numbers of blue cells versus clear cells in 20 randomly chosen fields at a magnification of x400, and with the use of a grid-marked ocular eye-piece in a standard light microscope (Zeiss Axiovert 10, Germany). The average 'transfection score' was calculated for each dish in this way.

3.2.1.4 Transfection of P2 SCs with pCMV-T-neo

SCs were transfected with pCMV-T-neo using the most favourable conditions obtained from the previous lipofection-optimising experiments. Experiments were repeated over several weeks to obtain a selection of transfected cultures. G418 selection was begun at 600µg/ml, as determined by the previous G418 killing curve

experiments, 48 hours after the initial transfection, and maintained at this level throughout all subsequent procedures.

The DMEMF/G418 (DMEMF/G) medium was refreshed weekly, initially with only half of the medium replaced on each occasion. Selection was maintained until the emergence of isolated clusters of G418-resistant cells. Transfected cells were subsequently termed *STAG* cells (**S**chwann Cell-Large **T** Anti**G**en).

3.2.2 Establishment of the STAG Lines

3.2.2.1 Expansion of Clones

Isolated $G418^R$ cell clusters emerged approximately 3 weeks after selection and were expanded in the following way. Clusters were marked on the underside of the 35mm dishes using a permanent fine black marker, the cells washed once in PBS and autoclaved 2mm plastic rings, made by cutting rings from the bases of 200µl pipette tips (L.Kay, UK), were positioned with a pair of fine forceps (FST, UK) using autoclaved vaseline (Vaseline, UK) over the marked area. The cluster of cells was trypsinised using 40µl trypsin medium, neutralised with equal volume DMEMF/G, and the whole volume triturated and transferred to an assigned 96-well plate (NUNC, UK). Cells were expanded through 48-well, 24-well, 6-well plates and into 60mm and 100mm plates before labelling and freezing down.

3.2.3 Characterisation of the STAG Lines

3.2.3.1 Morphology

Cells were observed under standard light microscopy (Zeiss Axiovert 10) and compared to primary NSC cultures. Photographs were taken using standard procedures with the attached integral camera.

3.2.3.2 Immunocytochemistry

The primary antibodies used were as follows: IgG1 mouse monoclonals anti-S100 (β-subunit, clone no. SH-B1), anti-laminin (clone no. LAM-89) and anti-CNPase (clone no. 11-5B) (all Sigma, UK) at 1:500; IgG1 mouse monoclonals anti-GFAP and anti-vimentin (code RPN1102) (both Amersham, UK) at 1:500; mouse monoclonal anti-p75 IgG1, clone 192 (Boehringer Mannheim, UK) at 1:200; mouse ascites anti-Thy 1.1 (gift from H. Jani) at 1:1000; mouse ascites anti-Ran-2 (gift from R.Mirsky) at 1:500; mouse monoclonal anti-P0 (gift from J.Archelos) at 1:1000; and mouse monoclonal anti-large T antigen IgG2a (clone no. PAb 101) (Pharmingen, USA) at 1:1000. All incubation steps were carried out at room temperature unless otherwise stated.

STAG line populations were grown on PLL-coated 13mm glass coverslips (Chance Propper Ltd., UK) to approximately 50% confluency before being processed for immunocytochemistry. Alternatively, 2 x 10^4 cells were seeded per well onto 8-chamber-well slides 24h prior to immunocytochemistry. Cells were washed in PBS and fixed in either 4% paraformaldehyde for 5 minutes (anti-p75 or anti-Ran-2) or 20 minutes (anti-S100), or in 5% glacial acid/ethanol at -20^{O}C for 10 minutes (antibodies to GFAP, laminin, vimentin, CNPase or T antigen).

After fixation, cells were washed 3 x 5 minutes in PBS, incubated in 10% dried skimmed milk solution (Marvel, UK) to reduce non-specific protein binding for 20 minutes, and incubated in primary antibody diluted in the blocking agent for 1 hour or at +4^{O}C overnight. After washing in PBS over 15 minutes, cells were incubated in the fluorochrome-conjugated secondary antibody, Cy3 anti-mouse IgG (code PA43002) (Amersham, UK) at 1:500 for 1 hour, washed over 15 minutes, post-fixed in 4% paraformaldehyde for 8 minutes, washed over 5 minutes and mounted

by inversion onto microscope glass slides using an aqueous/glycerol mountant (Permafluor, Immunotech, USA)

For Thy 1.1 staining, cells were first incubated in the primary antibody solution and subsequently post-fixed in 4% paraformaldehyde for 20 minutes.

Immunostained cells were observed using an inverted fluorescence microscope (Zeiss Axiophot, Germany), where any photos were also taken with the use of the attached camera.

3.2.3.3 Cell proliferation

This was carried out using 5-Bromo-2-deoxy-uridine (BrdU) in a system obtained from Boehringer Mannheim, UK (5-Bromo-2-deoxy-uridine Labelling and Detection Kit 1). The protocol is based on the ability of dividing cells to pick up labelled uridine which can then be identified using standard immunocytochemistry with a final FITC-conjugated secondary IgG antibody. Cells were stained on coverslips with the use of the supplied materials and the cells mounted and observed under fluorescence microscopy as described before (see 3.2.3.2). Cells which were green-fluorescent on excitation were recorded as those in division. Percentages of cells in division for each population tested were calculated based on the results of counts in 10 randomly chosen fields at a magnification of x200 (Zeiss Axiophot). The assay was carried out on 2 STAG lines and a population of primary NSCs.

3.2.3.4 Sodium dodecyl sulphate polyacrylamide gel electrophoresis (SDS-PAGE)

STAG lines were analysed for the presence of large T antigen protein using the SDS-PAGE/Western blotting technique. STAG cells from 2 x 100mm confluent

dishes were pelleted (Econospin Sorvall, UK) and stored at -70^{O}C until required. SDS-PAGE was carried out on these samples using a 1mm thick Atto mini-gel (Laemmli, 1970). Samples were denatured prior to this in 1.7% β-mercaptoethanol, 1% SDS, 3% glycerol, 1mM EDTA, 23mM Tris pH 6.8, 0.005% bromophenol blue (Sigma, UK) at 96^{O}C for 3 minutes. Samples were loaded at 40μg protein per well, as determined by a Bicinchoninic Acid Solution protein assay (Sigma, UK) with BSA as a standard, and run at constant current 15mA for approximately 3 hours. All gels were run in a discontinuous buffer system using 3% stacking gels.

Of 2 gels used per experiment, one was used for total protein Coomassie staining and the other for immunostaining. For protein staining, gels were shaken for 3 hours to overnight in 0.25% Coomassie Brilliant Blue (Sigma, UK), 15% acetic acid and 10% methanol (BDH, UK) and destained in the same solution without the Coomassie R250. The immunostaining procedure is described below.

3.2.3.5 Western blotting of proteins resolved on SDS-PAGE gels

Following SDS-PAGE, gels were electrophoretically transferred onto polyvinylidene difluoride membranes (Immobilon-PVDF, Millipore, UK) for 1 hour at 12^{O}C, 400mA, then 18 hours at 1500mA in 192 mM glycine, 25 mM Tris pH 8.3 (Towbin *et al.*, 1979) using the Hoefer TE62 Transphor II electrophoresis unit.

PVDF membranes were blocked for 1 hour in 5% non-fat milk (Marvel), incubated in the large T antigen primary antibody diluted at 1:1000 in the blocking agent for 3 hours on an orbital shaker (Denley, UK). After 3 washes in PBS over 15 minutes, the membranes were incubated for 1 hour in alkaline phosphatase-conjugated secondary IgG antibody (Calbiochem, UK) at 1:1000. The blots were

washed again before developing the signal in '1-Step' NBT/BCIP (Pierce, UK) developing solution. The reaction was stopped by rinsing in PBS and the blots were left to air dry.

All incubations were carried out at room temperature.

3.2.3.6 Reverse-Transcriptase-Polymerase Chain Reaction (RT-PCR)

STAG lines were reverse transcribed and then amplified using the PCR method in order to identify the messenger RNA of a number of growth factors and proteins typical of primary SCs. Cells were collected from 1 x 100mm confluent plates and total RNA was obtained using an RNA-extraction procedure (Qiagen, Germany). RNA quality was checked using spectrophotometry (Beckman DU 640B, UK) and agarose gel electrophoresis.

RNA was reverse transcribed and amplified using the RT-PCR method (Mocharla *et al.*, 1990) with a protocol which used Superscript II Reverse Transcriptase and Taq DNA Polymerase (GIBCO BRL, UK). First strand cDNA was synthesised from approximately 3μg RNA using random primers and 200U reverse transcriptase.

PCR primers were generated (Genosys Custom Biopolymers, USA) with sequences which were taken from a number of previous studies (Brunden *et al.*, 1992; Watabe *et al.*, 1995; Zaheer *et al.*, 1995).

PCR reactions were carried out using 10% of the first strand cDNA template in Taq DNA polymerase buffer, 200μM dNTP (GIBCO, UK), 1.5-3mM $MgCl_2$ (Perkin-Elmer, USA), 0.2μM of each primer and 5 U/μl Taq polymerase (Perkin-Elmer, USA) in a Peltier Thermal Cycler (PTC-200, MJ Research, USA) or Robocycler 96 (Stratagene, UK). PCR cycle times were as follows: initial template

denaturation at 96°C for 4 minutes; 35 cycles of denaturation at 96°C for 15s, annealing at 50-60°C for 30s, extension at 72°C for 1 minute; and a final extension step of 5 minutes, before maintaining at 4°C. PCR conditions were optimised for each primer pair; details of sequences and PCR conditions are given in Table 3.1.

Table 3.1 Primer Pair Sequences Used for PCR Amplification

Primer (species)	Sequence (5'-3')	Base pairs	Ref
NGF (human)	GTT TTG GCC AGT GGT CGT GCA G CCG CTT GCT CCT GTG AGT CCT G	498	[1]
BDNF* (human, rat)	ATG ACC ATC CTT TTC CTT ACT ATG GT TCT TCC CCT TTT AAT GGT CAA TGT AC	741	[1]
NT-3# (mouse)	ATG CAG AAC ATA AGA GTC AC AGC CTA CGA GTT TGT TGT TT	294	[2]
CNTF (rat)	GGC TAG CAA GGA AGA TTC GT TCC CTT GGA AGG TAC GGT AA	191	[2]
GDNF (rat)	ATG AAG TTA TGG GAT GTC GT CAG GGT CAG ATA CAT CCA CA	641	[2]
p75* (human, rat)	GAG CCG TGC AAG CCG TGC ACC CTC AGG CTC CTG GGT GCT GGG	438	[1]
P0 (mouse)	TTG GTG CTT CGG CTG TGG TC TGT TGC TGC TGT TGC TCT TC	427	[3]
TGF-B (human, rat, mouse)	GAA GCC ATC CGT GGC CAG AT GAC GTC AAA AGA CAG CCA CT	461	[1]

*PCR of p75 and P0 primers was carried out at 1.5mM $MgCl_2$; BDNF primers at 3mM $MgCl_2$; all others were carried out at 2mM $MgCl_2$

All primers were amplified successfully at annealing temperatures between 55-57°C, except those for NT-3 which annealed optimally at 50-53°C.

Refs:

1. (Zaheer *et al.*, 1995)
2. (Watabe *et al.*, 1995)
3. (Brunden *et al.*, 1992)

One-fifth of the PCR product was electrophoretically analysed on a 1.8% agarose gel containing ethidium bromide in 1 x TAE buffer (see 3.2.1.2 for details).

PCR experiments were routinely controlled by performing PCR without first using reverse transcriptase in first strand synthesis, by omitting one of the primers in the PCR or by running a PCR on water. In addition, a primer for the ubiquitous protein Ube1Y, which encodes a gene found on all mammalian X chromosomes (gift from J.Turner), was used to confirm correct first strand synthesis; the PCR product was 400bp.

3.2.4 Temperature Shift

All STAG lines were transferred to 39^{o}C and were assessed for changes in their immunophenotypic profile. The main criteria which were studied were cell morphology, expression of the large T antigen, cell division and expression of SC markers. These criteria were examined as described before (3.2.3). Cell phenotypes were observed for 1 month at the restrictive temperature.

3.3 Results

3.3.1 Generation of Schwann cell lines

3.3.1.1 Structure of pCMV-T-neo

pCMV-T-neo was constructed using the SV40 genome, a region of the multi-cloning site (MCS) of the Bluescript II KS +/- phagemid (Stratagene, UK), and the expression vector, pRc/CMV (Invitrogen, UK). Figure 3.1 shows schematically the method of construction. The vector was obtained at the end of step 2 with the entire linearised SV40 genome (1) cloned into the MCS of Bluescript phagemid (2) (P.Tegtmeyer, unpublished data). This was digested to excise the early genes of SV40 encoding the large T antigen sequence (3), and subsequently inserted into the gap, produced by a HindIII and NotI digest (4), in the polylinker of pRc/CMV (5). These subsequent cloning steps were carried out on site (N.Mazarakis, unpublished data).

3.3.1.2 Restriction digest pCMV-T-neo

pCMV-T-neo was mapped using a selection of restriction enzymes and the digested products can be seen in Figure 3.3. The band sizes compared well with the expected product sizes (see Fig. 3.4 for the precise locations of the 5 enzymes used in the digest): undigested DNA revealed the 3 conformations intact (lane 1); single digests with EcoR1 or Xba I produced 1 band representing the linearised plasmid at approximately 8kb (lane 3, 5); the digest of Pst I at 2 sites in the plasmid produced 2 products at approximately 6kb and 2kb (lane 2); digest with BamH1 at 3 sites produced 3 bands at approximately 5.7kb, 2kb and <702bp (lane 4, although this latter band is not easily visible).

Figure 3.1 Construction of the expression vector containing large T antigen, pCMV-T-neo. The entire linearised SV40 genome (1) was cloned into the MCS of Bluescript phagemid (2, P.Tegtmeyer, unpublished data). This was digested to excise the early genes of SV40 encoding the large T antigen sequence (3), and inserted into the gap, produced by a HindIII and NotI digest (4), in the polylinker of pRc/CMV (Invitrogen, UK) (5).

Figure 3.1 Construction of pCMV-T-neo

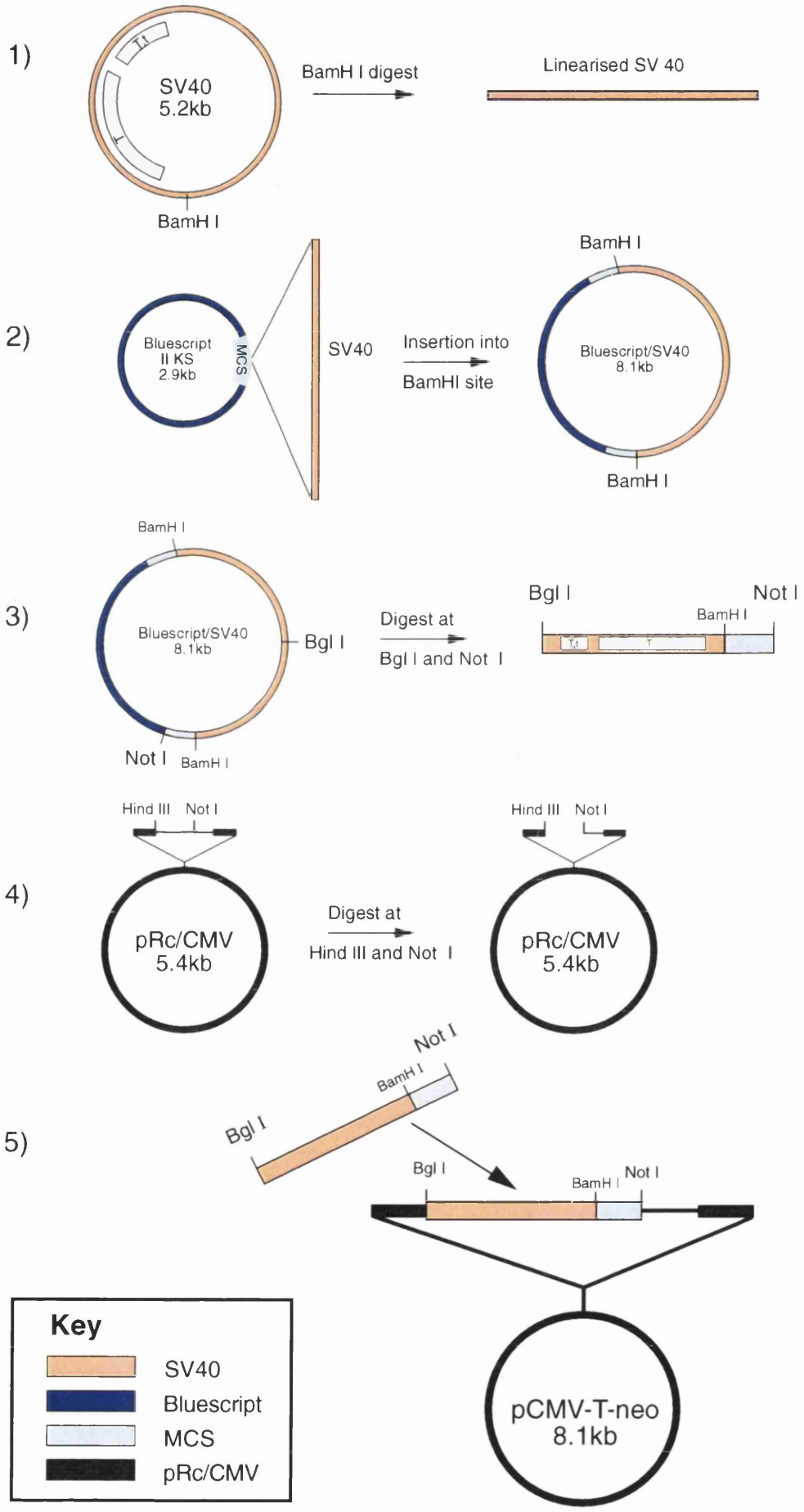

Figure 3.2 A schematic diagram of the method of liposome-mediated transfection. Plasmid DNA and a lipid-based reagent are combined to generate DNA containing liposomes. The liposomes are subsequently able to enter the host cell by endocytosis. *(taken from "Recombinant DNA, 2nd ed.," J. Watson et al., 1992; p222)*

Figure 3.2 A Schematic Diagram of the Method of Lipofection

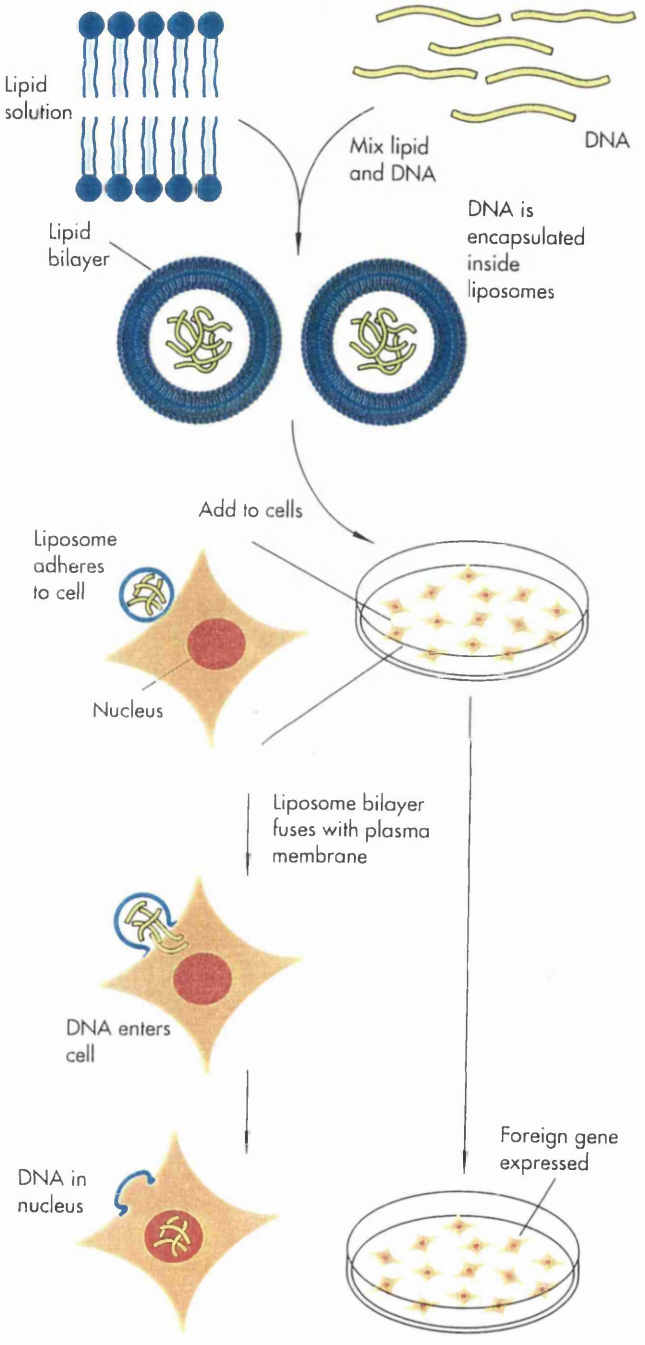

Figure 3.3. Restriction Digest of pCMV-T-neo. The lanes contain products of the following enzyme-digests: (1) undigested DNA, (2) Pst1, (3) EcoR1, (4) BamH1, (5) Xba1, (6) Not1. Lane 7 contains the lambda/BstE II molecular weight marker.

Figure 3.3 Restriction Digest of pCMV-T-neo

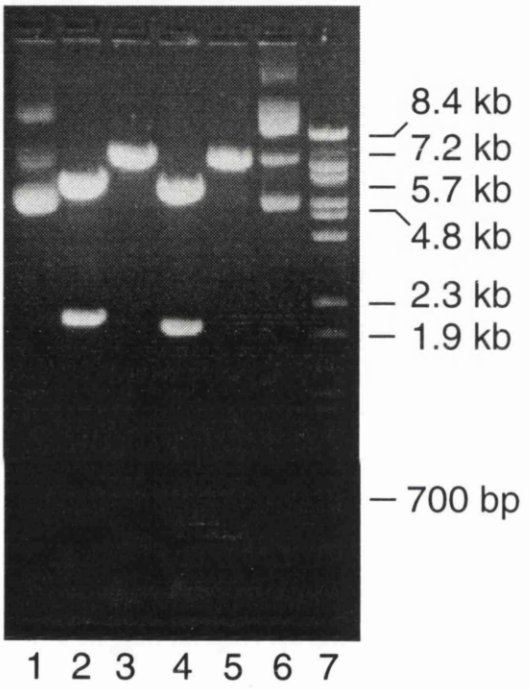

Figure 3.4. Location of the 5 Restriction Enzyme Sites Used in the Digest of pCMV-T-neo. The products of the digest in Figure 3.3 compare favourably with the expected sizes predicted from this restriction map.

Figure 3.4 Location of the 5 restriction enzyne sites used in the digest of pCMV-T-neo

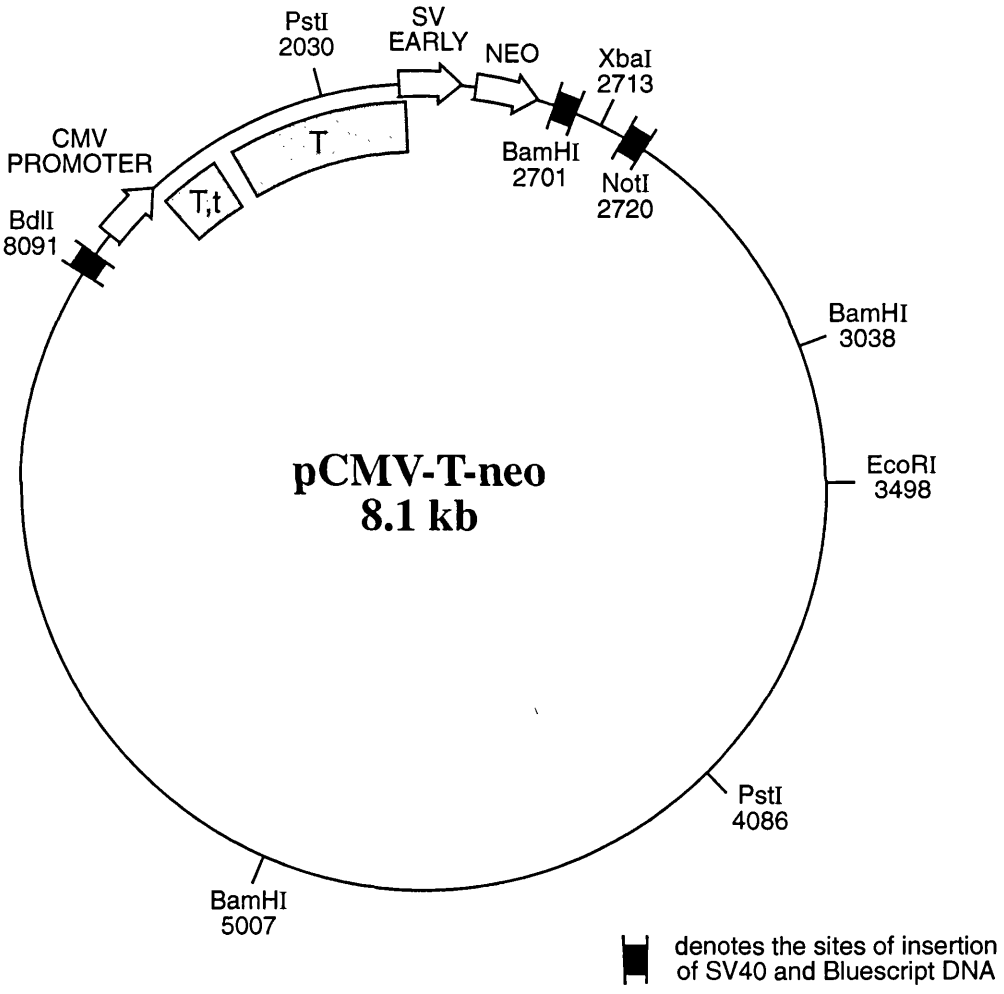

The Not1 digested products(6), however, ran similarly to undigested DNA and failed to result in correctly digested product sizes. This suggests that the Not1 site may have been altered in some way, but that it is a point mutation as the remaining digest products are unaffected.

3.3.1.3 G418 killing curve for NSCs at 33^{O}C

In the initial experiment, the number of cells viable at 14d after addition of G418 reduced with increasing concentration of the drug to complete cell death at 600μg/ml, although a few cells were found at 750μg/ml. In the second experiment using a narrower range of 350-650μg/ml, very few cells were found viable at 550μg/ml with none at 650μg/ml (Fig. 3.5; see appendix A2 for details). Cells from the control dish in the second experiment, in which G418 drug was omitted, showed some but not significant cell death and thousands of cells remained viable at day 14 (Fig. 3.5, appendix A1).

3.3.1.4 Lipofection of NSCs with pCMV-g

Liposome-mediated transfection involves the encapsulation of plasmid DNA into liposomes which are then endocytosed by the host cell (Fig. 3.2). There are a number of factors which determine the transfection efficiency of the system and require some optimisation, including the concentrations of plasmid DNA and lipid reagent.

Optimisation transfections were carried out with the use of the reporter vector, *pCMV-g*. Previous work had shown that the optimal amount of DNA to use in such lipofections with Lipofectin reagent and the plasmid, pCMV-g, was 14μg (B.Watt, unpublished data). In these experiments where the concentration of the Lipofectin

Figure 3.5 The G418 killing curve for neonatal SCs at 33°C

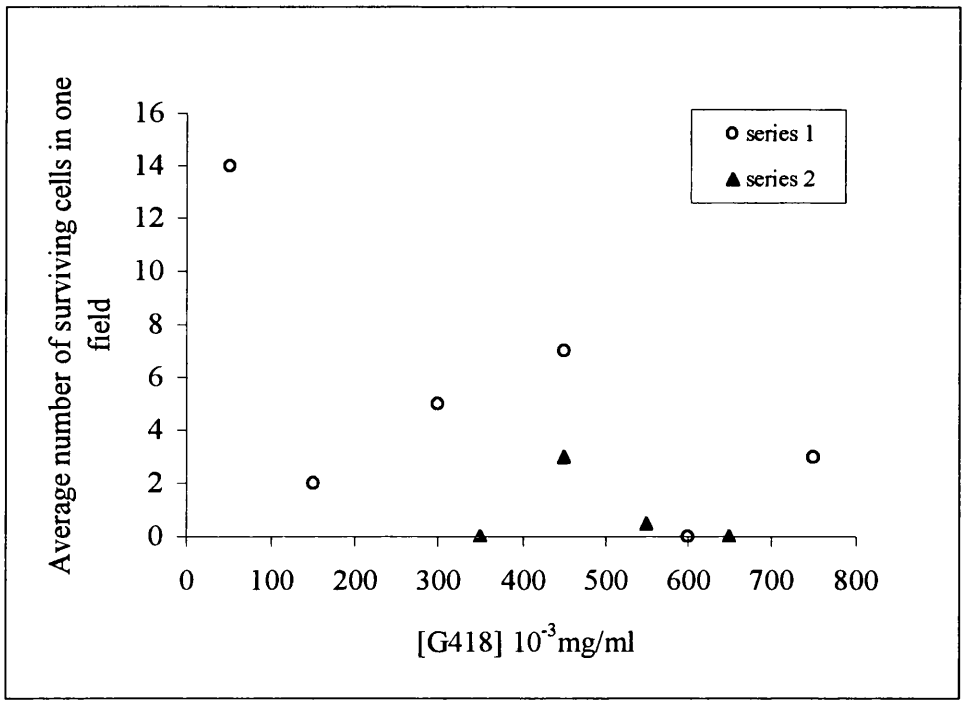

Note: Series 2 consists of the average scores of the results obtained from experiment 2.

Figure 3.6 Lipofection of NSCs at 33°C at 33°C with the reporter plasmid, pCMV-g

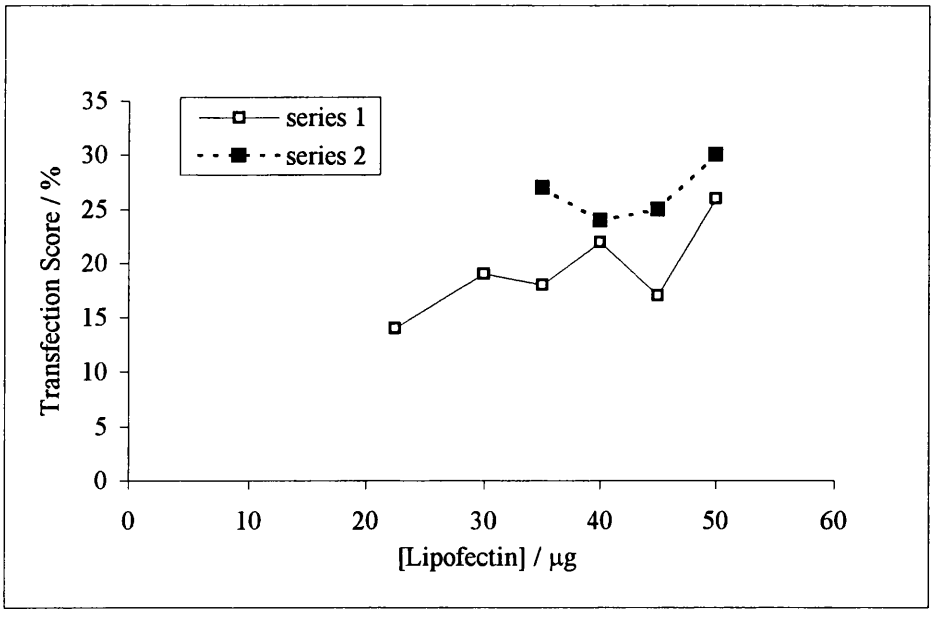

Note: for full cell counts, see Appendix A3.

reagent was varied, a good degree of transfection was obtained with the lipid reagent at 50μg. This produced a transfection score of 30% (Fig. 3.6, series 1).

Results from the first transfection experiment suggested that higher amounts of LipoFECTIN yielded higher transfection efficiencies. The transfection experiment was repeated using a narrower range of LipoFECTIN concentrations to more accurately determine the optimal concentration for transfection; LipoFECTIN was used at 35, 40, 45 and 50μg in 4 dishes, respectively. In the second experiment Lipofectin was used at 35-50μg and the same transfection protocol followed. This yielded improved transfection efficiencies overall with transfection peaking at 30% for Lipofectin at 50μg (Fig. 3.6, series 2; Fig. 3.7; Appendix A2).

The transfection results yielded from these two experiments suggested that this technique of lipofection was a viable means of obtaining cell lines by later transfection with the expression vector containing large T antigen, pCMV-T-neo.

3.3.1.5 Lipofection of NSCs with pCMV-T-neo

The semi-optimised protocol of lipofection was used to generate cultures of NSCs, transfected with the plasmid, pCMV-T-neo, over several weeks. G418 selection was applied to these cultures 48h after transfection at 600μg/ml and maintained throughout selection. There was considerable cell death over the first 2 weeks and an emergence of foci of cell growth during the subsequent weeks before these clusters were picked and expanded using cloning wells. This was the case for the bulk of the cultures transfected, although there was some variation on both the speed of cell death and the emergence and growth of resistant foci of cells.

Figure 3.7. Schwann cells transfected with β-galactosidase. 'A' shows an estimate of the numbers of cells transfected under optimal conditions; 'B' shows the expression of β-galactosidase throughout the cell body and process of a single cell. *(Scale bar: A, 10μm; B, 2.5μm)*

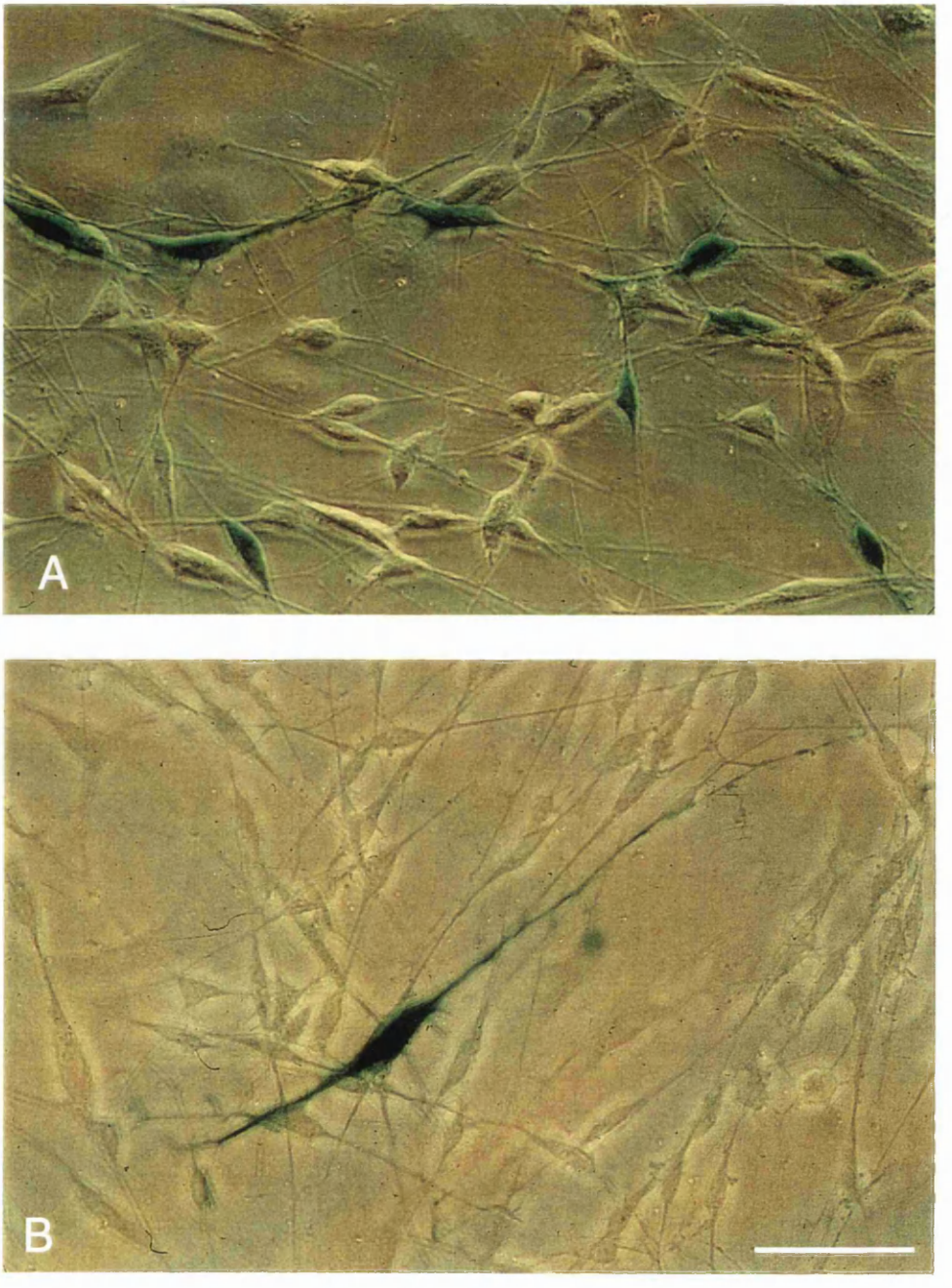
A
B

3.3.2 Establishment of the STAG cell lines

Morphology of transfected cells: Transfected cells showed a range of morphologies from the bipolar, spindle-shape typical of primary SCs to the broader, flattened morphology typical of primary fibroblasts.

Transfer of foci to cloning well plates: Cells were successfully transferred using cloning rings to either 96-well or 48-well plates where they were grown to confluence and passaged on to increasingly larger wells up to 100mm dishes. As the numbers of cells within each clone began to increase, it became clear that there existed differences in morphologies between clones that were apparent early after transfection. In addition, there were cells within some clones which displayed different morphologies. These may reflect either pleomorphism within the clone or alternatively indicate the presence of mixed clonal populations.

Re-cloning the cell lines: Following the emergence of mixed populations in some of the expanded clones, some cells were passaged at very low fractions and clusters that subsequently emerged were picked and transferred into cloning wells and expanded once more.

Initial transfection cultures were named SCT1-7, **S**chwann **C**ell **T**ransfectant, referring to the 7 transfections that were carried out. After expansion and any subsequent re-cloning, the cell lines were named **STAG** lines, **S**chwann cell-**L**arge **T** **A**nti**G**en lines, and all clones given individual numbering.

The major cell lines that were taken for subsequent characterisation were as follows:

1A1a	3Fao
1A1b	3Faii
3C2aii	3Fb
3C3	4B

3.3.3 Characterisation of the STAG cell lines

3.3.3.1 Morphology

The STAG cell lines taken for characterisation showed morphological features that ranged from the bipolar, spindle shape resembling primary SCs of 3C2aii, 3C3 and 3Faii to those of the broad-based, more flattened morphologies of 1A1 and 4B. Some cells within their population showed slightly different morphologies, for example the presence of some flattened cells in a population of otherwise bipolar, spindle-shaped cells of clone 3Faii. 4B contained exclusively flattened, rounded cells (see Figs. 3.8, 3.9).

3.3.3.2 Immunocytochemistry

Staining for large T antigen: all of the STAG lines tested were positive for large T antigen. The staining was nuclear and present in all the cells within each clone.

Staining for SC markers: the majority of the cell lines were positive for the markers, S100, GFAP, Ran-2, vimentin, A5E3, and negative for p75, P0 and CNPase.

Other markers: Thy1.1 – clone 4B was positive; a minority of cells within the clones 3C2aii, 3C3, 3Fao and 3Faii were positive; primary NSCs also contained positive cells.

(Figs. 3.10, 3.11A,B)

Figure 3.8. Emergence of the STAG Lines. Transfected cells displayed a range of morphologies. 3 weeks after selection, some cell clusters formed which showed an exaggerated elongated shape (A,B); morphologies across the clusters ranged from SC-like elongated (C) to semi-flattened (D) to flattened and rounded (E).

(Scale bar: A, 20μm; B-E, 10μm)

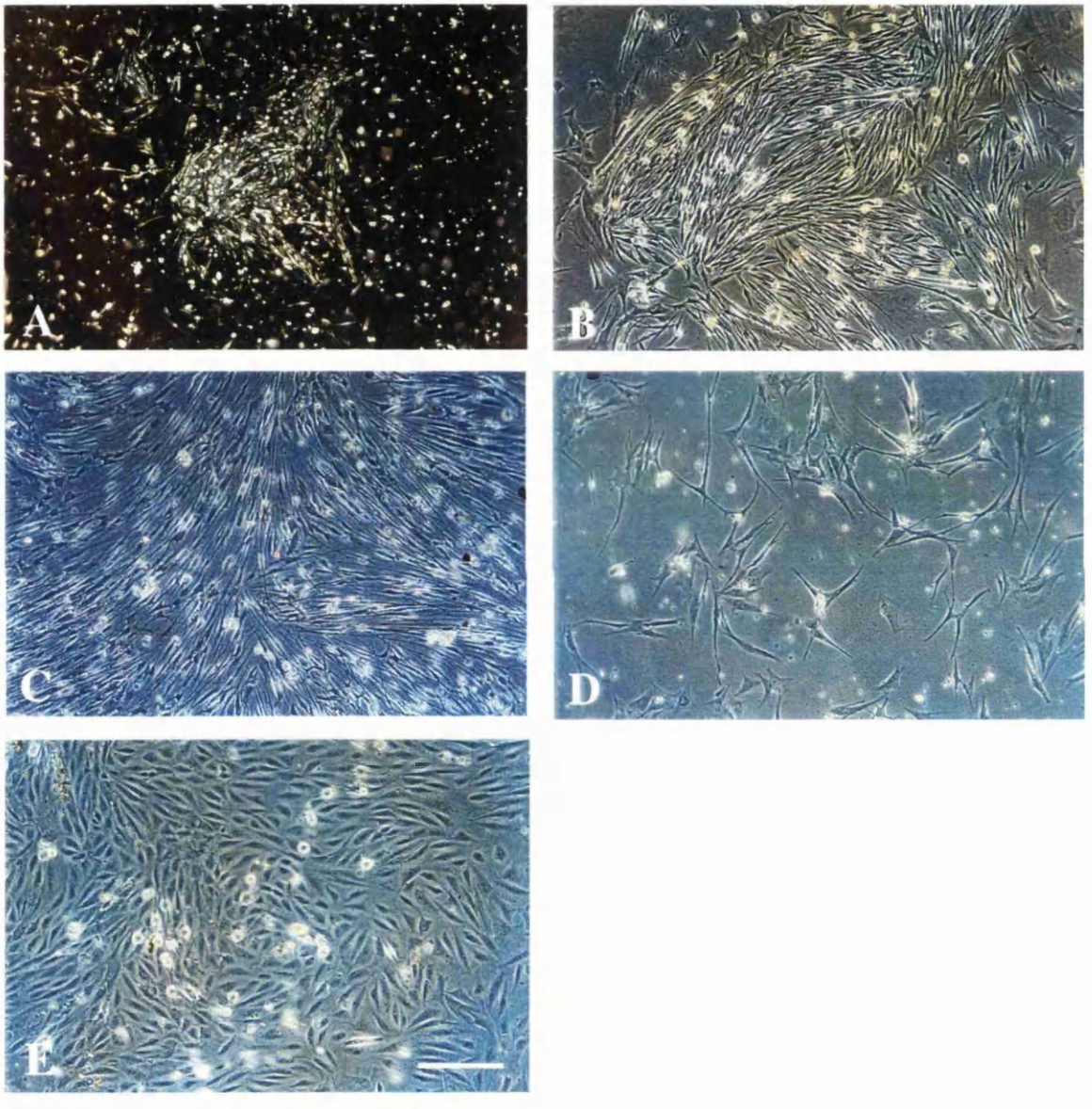
A
B
C
D
E

Figure 3.9. Morphology of the STAG Lines. The STAG lines display a range of morphologies which range from the largely bipolar, spindle shape typical of NSCs (A-C) to the flattened morphology reminiscent of typical fibroblasts (D, STAG 4B). Note also the whorls pattern that the STAG cells adopt when at high cell density (C, 3C2aii).

(Scale bar: A,C - 20μm; B, 5μm; D, 10μm)

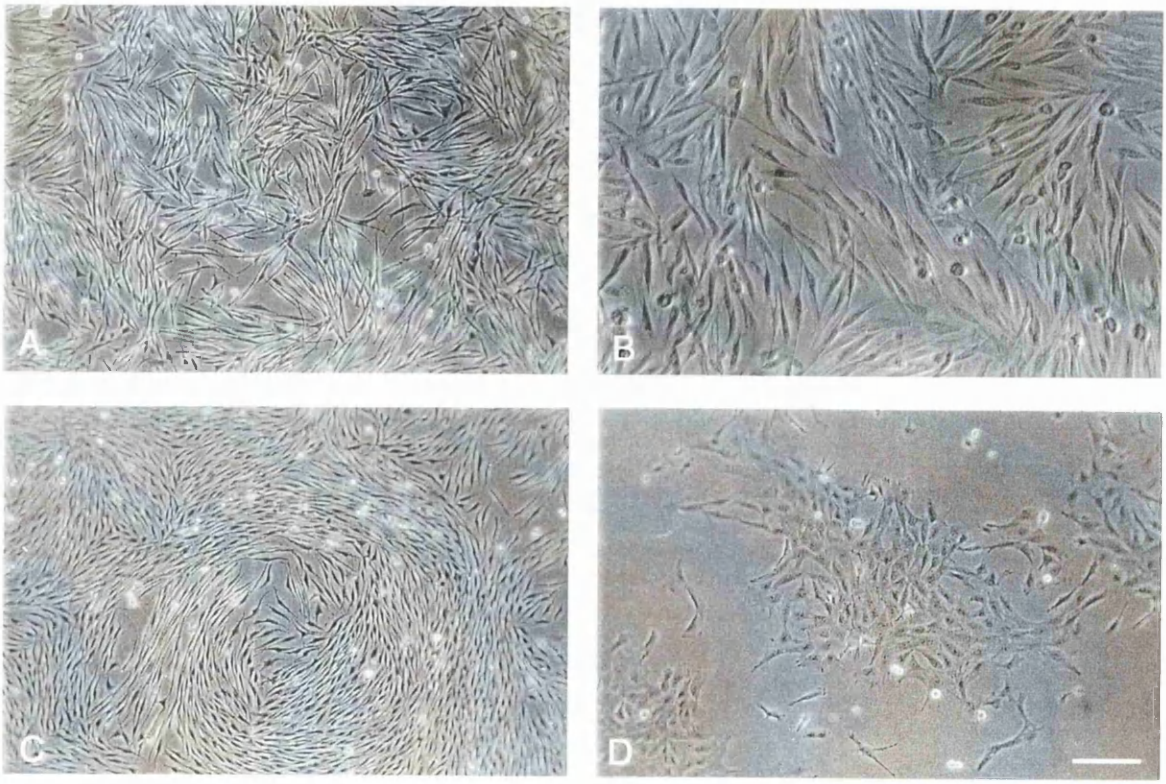
A
B
C
D

Figure 3.10. Immunocytochemistry of the STAG Lines. The STAG lines stain positively for the large T antigen and largely reproduce the immunophenotype of primary NSCs.

Figure 3.10 Immunocytochemistry of the STAG cell lines

Cell line	Antigenic Marker									
	Tag	S100	Thy1.1	p75	GFAP	Ran-2	A5E3	P0	Laminin	Vimentin
NSC	-	+	-/+	+	+	+	+	-	+	+
1A1a	+	+	-	-	+	+	+	-	+	+
1A1b	+	+	-	-	+	+	+	-	+	+
3C2aii	+	+	-/+	-	+	+	+	-	+	+
3C3	+	+	-/+	-	+	+	+	-	+	+
3Fao	+	+	-/+	-	+	+	+	-	+	+
3Faii	+	+	-/+	-	+	+	+	-	+	+
3Fb	+	+	-	-	+	+	+	-	+	+
4B	+	+	+	-	-	+	+	-	+	+

-/+ denotes a minority of positive cells

Figure 3.11A. Immunocytochemistry of the STAG Lines I. STAG 3Faii cells stain positively for the large T antigen (C, 3Faii – same section as in 'B'), and the markers S100, GFAP and Ran-2 as shown opposite. The staining is representative of all STAG lines.

(Scale bar: A, 20μm; B-F, 10μm)

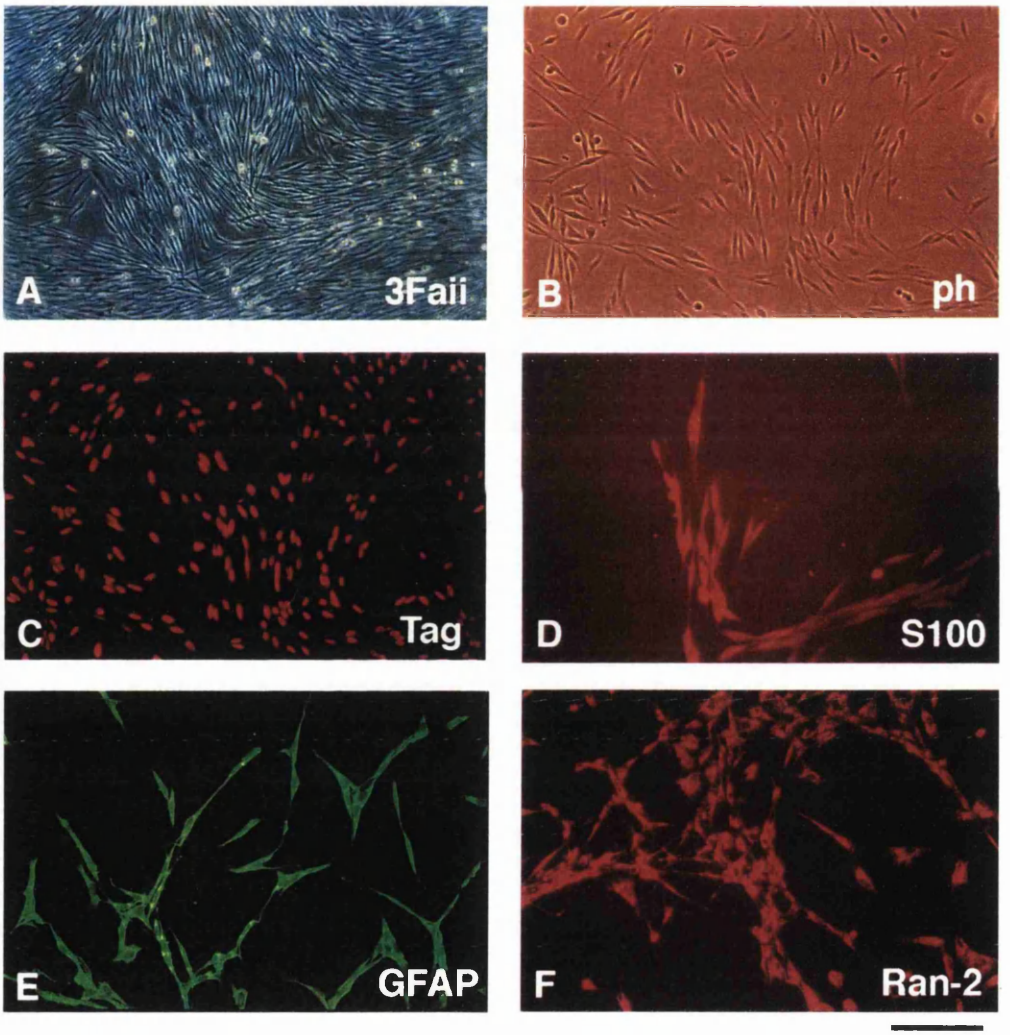
A
3Faii
B
ph
C
Tag
D
S100
E
GFAP
F
Ran-2

Figure 3.11B. Immunocytochemistry of the STAG Lines II . The 3Faii line stains positively for laminin and vimentin, but not p75; contrast with the primary neonatal SCs which stain positively for p75 (I). In addition, the 4B line is identified as a fibroblast cell line with all cells staining positively for Thy1.1 (L); 3Faii cells stain negatively for this antibody (K).

(Scale bar: G, I - 20μm; H, J-L - 10μm)

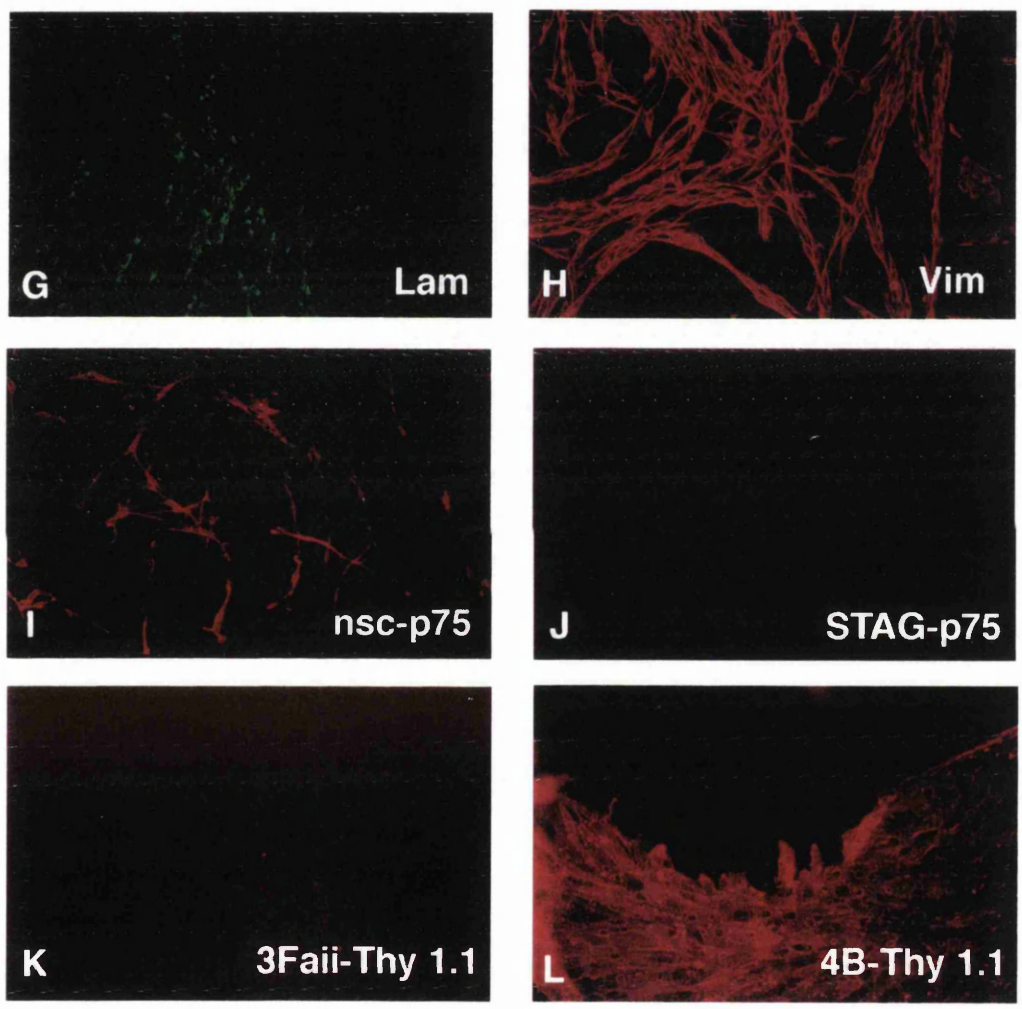
G
Lam
H
Vim
I
nsc-p75
J
STAG-p75
K
3Faii-Thy 1.1
L
4B-Thy 1.1

3.3.3.3 Cell proliferation

The 2 STAG lines tested, 1A1a and 3C3, showed cell division rates approximately 6-7 times higher than that of primary NSCs. NSCs gave a cell-fluorescence count of 6% of all cells in division, while 1A1a and 3C3 lines gave counts of 31% and 36%, respectively (Fig. 3.12; Appendix A4).

Figure 3.12. Mean Percentages of NSCs and STAG Cells in Proliferation*

	Cells in proliferation / %
NSC	6
1A1	31
3C3	36

*see appendix A3 for full cell count

3.3.3.4 Western blotting for the large T antigen

Western blots carried out on all the STAG cell lines stained positively for the large T antigen protein, with the product corresponding to the appropriate molecular weight of approximately 85kDa (Fig. 3.13). The 3T3-Tag cell line also stained positively, although weakly so, while the spontaneously immortalised cell line, IMS32, was negative for the protein. The corresponding Coomassie-stained gel shows approximately equal amounts of total loaded protein (Fig. 3.13B).

In addition to the product seen at 85kDa, there was a second smaller product at approximately 80kDa. As an element of small t antigen was cloned into the original expression vector used to transfect the primary SCs, it was thought that the smaller-sized product might represent this element. Consequently, the blotting was repeated with a new antibody, specific to the C-terminal epitope found within the last 190 amino acids of large T antigen only.

Immunostaining of this second blot reproduced the positive band at 85kDa, but also produced an additional smaller product of lower intensity, this time at approximately 70kDa. The lower-molecular weight product was not equivalent to the size of small t antigen, and was taken to be the result of proteolysis of the large T antigen protein or of non-specific binding. The corresponding total protein-stained gel showed equally loaded lanes (not shown).

3.3.3.5 RT-PCR of STAG Lines

RT-PCR of the STAG lines demonstrated the presence of messenger RNA (mRNA) for a number of neurotrophic and other growth factors normally found in primary SCs (Fig. 3.15). STAG lines were positive for mRNA encoding BDNF, NT-3, CNTF, GDNF (in most but not all lines), TGF-β and the peripheral myelin protein, P0. The most notable difference, however, was the absence of the low-affinity nerve growth factor receptor, p75, in most of the STAG cells and that of NGF in all of the STAG lines tested.

Figure 3.15 RT-PCR of the STAG Lines

Cell line	Primer							
	NGF	BDNF	NT-3	CNTF	GDNF	p75	TGF-β	P0
IMS32	+	(+)	+	+	+	+	+	(+)
1A1a	-	+	+	+	-	(+)	+	+
1A1b	-	+	+	+	+/-	+/-	+	+
3C2aii	-	+	+	+	-	-	+	(+)
3C3	-	+	+	+	+	-	+	+
3Faii	-	+	+	+	+	-	+	+
4B	-	+	+	-	+	-	+	+
PC12	-	+	+	+	-	+	+	+

(+) denotes weak positive product
+/- denotes mixed results

Figure 3.13. Western blot of the STAG lines for the large T antigen protein. The large T antigen protein is approximately 85kDa in molecular weight and is recognised by the positive bands in all STAG line lanes at this weight; IMS32, a spontaneous SC line, and 3T3-Tag, are used as negative and positive controls respectively, although the 3T3-Tag stains only weakly positive (A). The corresponding Coomassie gel shows equal loading proteins (B).

Figure 3.13 Western Blot of 7 STAG Lines Staining for the Large T Antigen

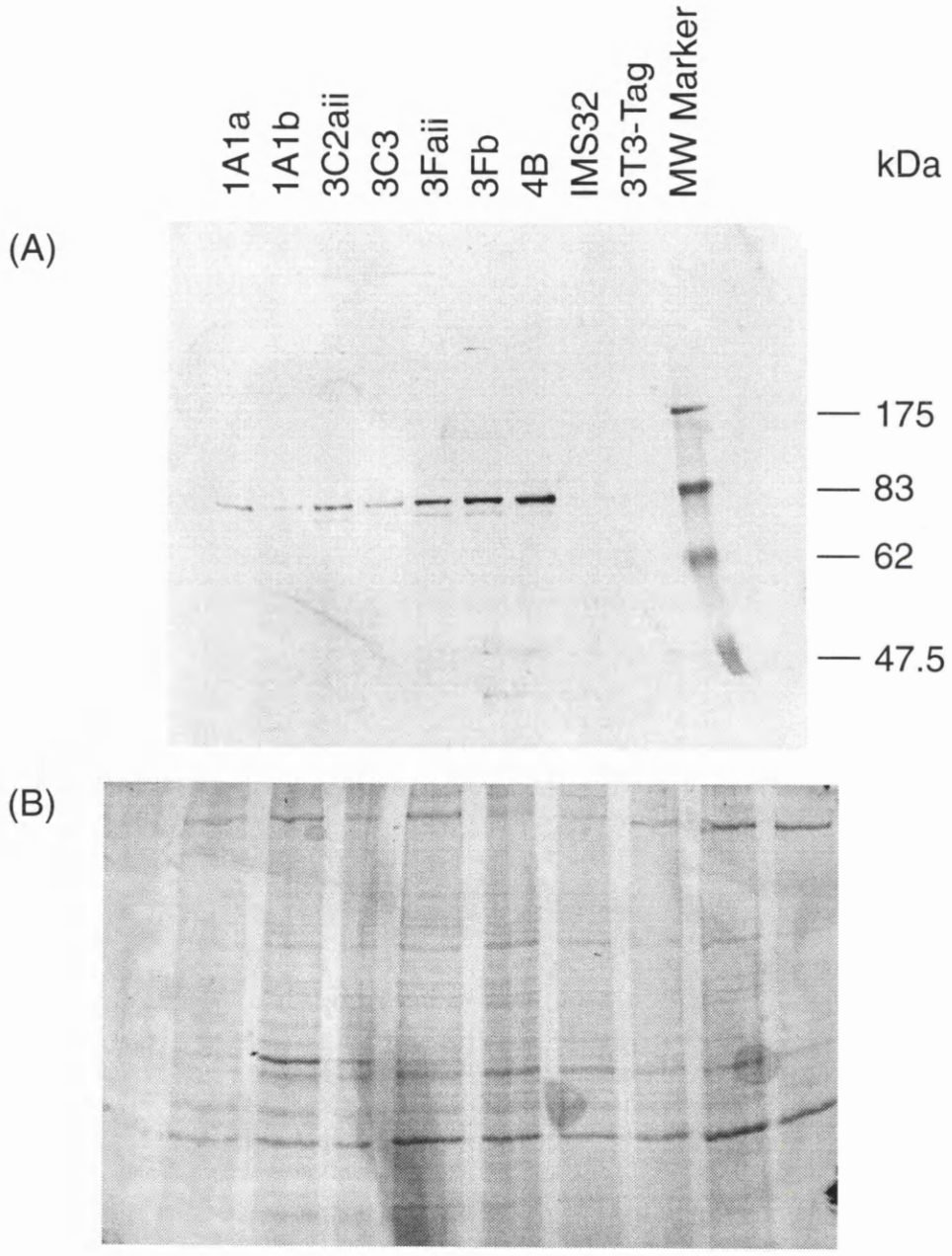

Figure 3.14. Western blot of the STAG lines using a large T antigen-specific antibody. Immunostaining shows persistence of the positive band at approximately 85kDa and of the secondary band at 60-70kDa; the latter product does not represent small t antigen and may be product of proteolysis.

Figure 3.14 Western Blot of 7 STAG Lines Using a Large T Antigen-specific Antibody

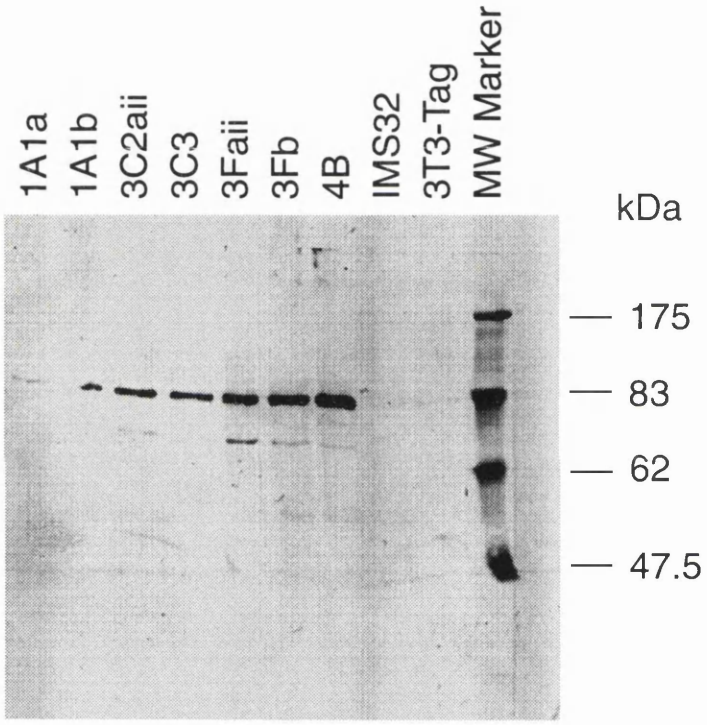

Figure 3.16. Reverse Transcriptase-Polymerase Chain Reaction (RT-PCR) of the STAG lines. (molecular weight marker in lane 1 of A-D is 100bp ladder, with the bright band at 500bp) Annealing temperatures were optimised for each primer pair; 'A' shows the gradual increase in signal of the BDNF PCR product (741bp) from IMS32 cDNA with increases in temperature from $55^{O}C$ (lane 2) to $62^{O}C$ (lane 9) in $1^{O}C$ intervals. STAG line cDNAs were subsequently screened for the BDNF product and all lines show positive bands at approximately 741bp (B); the location of the cell lines is as follows: IMS32 (lane 2 - weak positive band); 1A1a (3), 1A1b (4), 3C2aii (5), 3C3 (6), 3Faii (7) and 4B (8).

'C' shows the result of screening for the GDNF PCR product (641bp). Lanes 2-8 contain the same cell lines as described above for 'B', and show mixed results for the GDNF product; lane 9 contains PC12 cDNA and is negative for the product. Lanes 10-14 contain the same cDNAs run in lanes 2-6, respectively, screened for the ubiquitous primer product, Ube1Y (400bp); all cell lines show appropriately sized PCR products indicative of successful PCR.

'D' shows the PCR products amplified with primers for the myelin protein, P0, and represent cell line cDNAs as follows: 1A1a (1), 3C2aii (2), 3C3 (4), 4B (5), PC12 (6), control water (7).

A

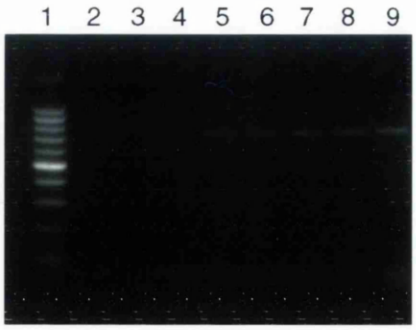

B

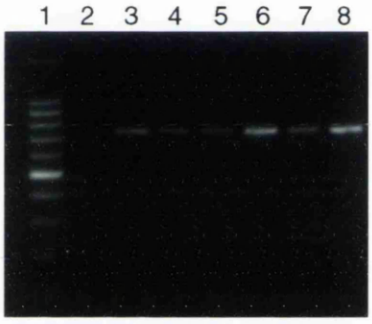

C

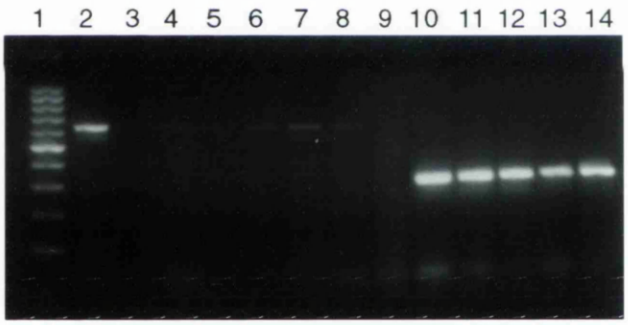

D

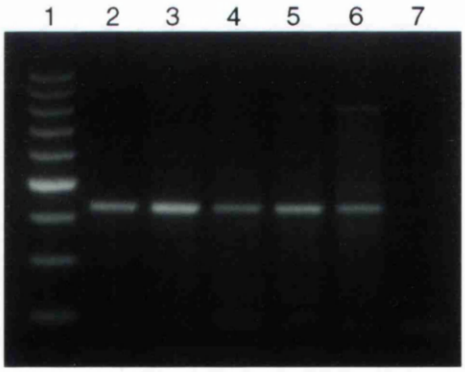

3.2.4 Temperature shift

The STAG lines were transferred to the restrictive temperature of 39^{O}C for a period of 1 month and assessed for changes in their phenotype. The majority of the lines reacted to the temperature shift with significant reductions in their rates of cell division and reduced immunoreactivity to the large T antigen. The phenotypes are described in more detail below.

Morphology

Most STAG lines displayed a change in cell morphology within a few days of transferring to the restrictive temperature. In most cases, the cells' morphology changed from the bipolar, elongated cell body seen at 33^{O}C to one with a rounded cell body with long, fine extended processes. 3C3 was an example of a cell line which demonstrated this phenomenon (Fig. 3.17). In contrast, STAG line 4B showed no significant change in morphology but continued to display the rounded flattened shape seen at 33^{O}C (not shown). This was still evident at 1 month.

Cell proliferation and expression of the large T antigen

All of the STAG lines tested demonstrated a clear reduction in the rate of cell proliferation when transferred to incubation at 39^{O}C (Fig. 3.17). However, the length of the incubation period before which a significant reduction could be seen was variable across the lines and ranged from 2-3 days (STAG-3Fb) to 1 month (STAG-4B). Indeed, although 4B cells had shown a significantly reduced rate of cell division by 1 month, they continued to show moderate-high rates of division at this time-period (data not shown).

The levels of expression of large T antigen similarly decreased when the cells were transferred to 39^{o}C, as determined by immunocytochemical staining. The majority of cell lines showed a noticeable decrease in signal, which was formerly a strong nuclear signal (see Fig. 3.11A), within a few days of the temperature shift. STAG 1A1a was a typical example of this effect and immunostaining for the large T antigen at 8d after the shift can be seen in Fig. 3.17(E, F). Other lines such as the 4B line showed a slower down-regulation of large T antigen protein and continued to express low levels after 1 month at the restrictive temperature (not shown).

Expression of other SC markers

Expression of the markers GFAP and p75 had not significantly changed when the STAG lines were transferred to the restrictive incubation temperature. In contrast, expression of P0 may have been upregulated. Several STAG lines displayed a moderate immunoreactivity to the P0 antibody, but although above the signal of 4B-staining, a putative fibroblast cell line, this may have represented non-specific protein binding (Fig. 3.18).

In order to test whether immunoreactivity to the P0 antibody was significantly above non-specific, background levels, a number of controls were set up. In addition to binding of non-specific proteins with a 10% non-fat milk solution, STAG cells were also immunostained for the neuron-specific enolase (NSE) and pan-neurofilament antibodies. Immunostaining for these 2 neuron-specific markers, in fact, produced some positive staining for both antigens in the STAG cell lines.

All STAG cell lines stained positively for the pan-axonal neurofilament marker, showing the strongest signal in the nucleus. As a result, primary SCs were prepared

and immunostained for the neurofilament marker and were also found to stain positively (not shown).

Immunostaining for the NSE antigen, proposed to be a neuron-specific antigen, also produced immunoreactivity in the some of the STAG cell lines. While the signal was weak, it was above that observed in control wells which contained no primary antibody, and approximately equal to that observed in cells stained for the P0 antigen. With equal levels of staining for both NSE and P0, it was taken that the observed immunoreactivity to the P0 antibody in the STAG lines was a product of non-specific protein binding.

The immunostaining of STAG cells for the remainder of the markers demonstrated no change in immunoreactivity from that observed at 33^{O}C (data not shown).

Figure 3.17 Temperature shift of the STAG lines. STAG 3C3 lines were incubated in parallel at 33^{O}C and 39^{O}C. Cell division dropped significantly within a few days of the temperature shift, and by 8d, those cells at 33^{O}C have already been passed confluency and been passaged onto a new dish (A, B), while those at 39^{O}C have shown a dramatic decrease in cell division and have reached approximately 25% confluency in the original dish (C, D). Expression of the large T antigen also decreased although less rapidly; the 3C2aii line shows a decrease to near undetectable levels, also by 8d after the temperature shift (E, F).

(Scale bar: A,C - 20μm; B,D - 10μm; E,F - 5μm)

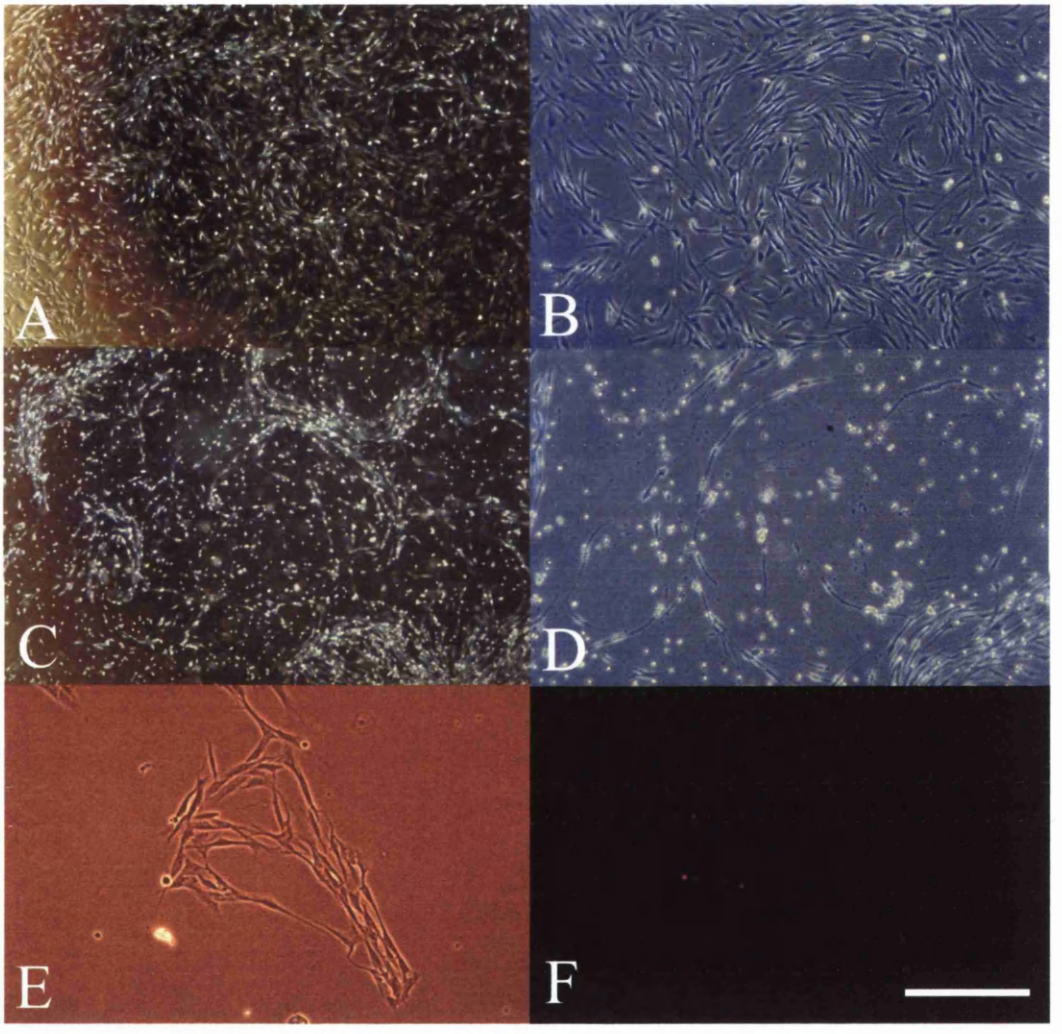
A
B
C
D
E
F

Figure 3.18 Immunostaining of STAG lines for the P0 protein. Immunostaining for the P0 protein showed moderate immunoreactivity to the antibody in several STAG lines, including 1A1a (A). In contrast, the putative fibroblast line, 4B, showed only weak immunoreactivity (B).

(Scale bar, 5μm)

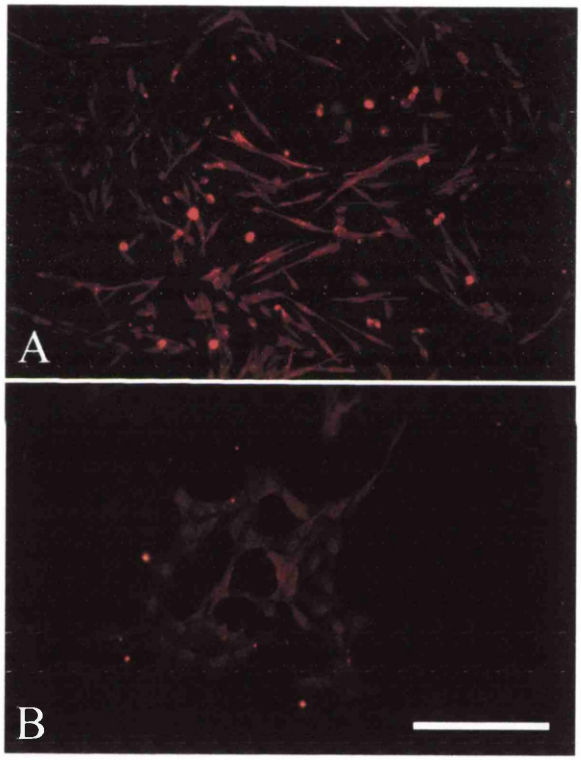
A
B

3.4 Discussion

3.4.1 Generation of conditionally immortalised SC lines

Conditionally immortalised SC lines have been generated in the present study by transfection with an expression vector encoding the thermosensitive allele of the large T antigen, tsA357 (Loeber *et al.*, 1989). The cell lines, known as STAG lines, divide at rates of approximately 6 times that of primary neonatal SCs (NSCs) (Brockes *et al.*, 1979), they express typical SC markers such as S100, laminin and vimentin, and they express messenger RNA (mRNA) for a number of nerve growth factors, as well as for the peripheral myelin protein, P0. Evidence of the incorporation of the large T antigen has been shown by positive Western blotting in addition to positive staining in immunocytochemistry.

Several aspects of the STAG lines will now be discussed in turn.

3.4.2 Presence of fibroblasts in some STAG cell lines

Immunostaining for the Thy1.1 antigen, a cell surface marker unique to fibroblasts and not SCs, indicated that some STAG lines were not composed of pure SCs but contained small numbers of fibroblasts. In these cell lines, the Thy1.1-positive cells were always in the minority and did not reach more than 5% of the cell population at any time.

The STAG line, 4B, was identified as a pure fibroblast cell line with the cells showing a broad, flattened morphology and positive staining for the Thy1.1 antigen. As a fibroblast cell line, the 4B line is a useful control cell line when assaying the phenotype of the SC lines.

The presence of fibroblasts is a normal component of primary SC cultures and is unlikely to compromise the growth-promoting properties of a STAG line which

contains low numbers of them. However, there are a number of methods which could be employed to eliminate the fibroblasts completely from these STAG lines.

The ability to effectively differentiate fibroblasts from SCs on immunostaining for the Thy1.1 antigen, and not solely on their morphologies, makes FACS-sorting the first choice method of separation. After immunostaining for the Thy1.1 antigen, the cell culture would be taken for FACS-separation of Thy1.1-negative SCs from the Thy1.1-positive fibroblasts. Given that these cells are rapidly dividing cell lines, the FACS-sorting could be easily repeated in a second round to ensure that the sorted cell culture contained no fibroblasts.

Alternatively, mixed STAG cultures could be subcloned by passage at a greatly reduced cell density to encourage the clonal expansion of isolated cell clusters. Individual clusters could then be expanded and characterised to produce pure SC-lines.

3.4.3 STAG cell lines express a SC-like immunophenotype

The STAG lines express a number of properties which resemble those of primary neonatal SCs (NSCs) *in vitro*. Most of the lines display the bipolar, spindle-shaped morphology with extended processes typical of primary SCs *in vitro* and *in vivo* (Schwann, 1847). The STAG lines express SC markers S100, laminin and vimentin *in vitro* (Brockes *et al.*, 1979; Cornbrooks *et al.*, 1983; McGarvey *et al.*, 1984; Yen and Fields, 1981), as well as the markers of non-myelinating SCs, GFAP, Ran-2 and A5E3 (Jessen and Mirsky, 1984).

In contrast to neonatal SCs, the STAG cells do not express the low affinity nerve growth factor receptor. Furthermore, they do not express the myelin proteins, P0,

GalC or MAG in culture under normal conditions. These two aspects will now be discussed in turn.

Expression of the low-affinity nerve growth factor receptor

STAG lines do not show immunoreactivity to p75 protein which is typically expressed by SCs *in vitro* and *in vivo* (DiStefano and Johnson, 1988). However, this is consistent with observations which show that primary NSCs can lose their immunoreactivity to p75 within a few weeks of isolated cell culture (Morgan *et al.*, 1991), an observation which has been confirmed here (data not shown). Down-regulation of the protein is believed to be the consequence of extended removal of the SCs from axonal contact, and is also observed in some but not all other SC lines (Boutry *et al.*, 1992; Watabe *et al.*, 1990). After the initial up-regulation of p75 on SCs after injury in the PNS, there follows a period where expression and production of the receptor is gradually reduced to background levels as the reinnervation of cut axons progresses (You *et al.*, 1997).

RT-PCR of the STAG lines demonstrated that p75 mRNA could be detected in a small number of the cell lines, while, p75 protein was never detected in immunocytochemical studies. Other SC lines, both transformed and non-transformed, have also been reported to have lost expression of p75 (Boutry *et al.*, 1992; Thi *et al.*, 1998; Watabe *et al.*, 1994).

The functional significance of p75-expression on SCs with respect to the induction of elongative axonal growth is not clear. The combination of the production of NGF and the expression of its receptor, p75, may be important in the regeneration of peripheral axons after injury (Heumann *et al.*, 1987a; Taniuchi *et al.*, 1986). It may also be important in the induction of central cholinergic axonal

growth by SCs which have been transplanted into the CNS (Kromer and Cornbrooks, 1985). However, the mouse SC line generated by Boutry et al., (1992) which does not appear to express the p75 receptor on cells in culture, remains able to remyelinate demyelinated axons when transplanted into the spinal cord.

It is further possible that the expression of p75 is linked to that of the transforming oncogene, large T antigen. The results from the Western blots suggest that the cell lines, 1A1a and 1A1b, which have been shown to be positive for p75 mRNA, also show low levels of the large T antigen protein. Immunostaining of the Western blot in the remainder of the cell lines suggest higher levels of the large T antigen in the other cell lines, in particular, in STAG-4B.

Expression of the nerve growth factor

RT-PCR carried out on the STAG lines in the present study showed the absence of mRNA encoding nerve growth factor (NGF), a neurotrophic factor which is produced by primary SCs (Assouline *et al.*, 1987). Although most other SC lines previously created have not been tested for the expression of nerve growth factors, one study which has investigated the expression of a range of growth factors has demonstrated positive expression of NGF in the spontaneously immortalised SC line, IMS32 (Watabe *et al.*, 1995).

The loss absence of NGF expression in the STAG lines may be a reflection of the RT-PCR protocol rather than of the true loss of NGF in the STAG lines. Given that primary SCs secrete NGF in the media, a biological assay using STAG line-conditioned media was carried out to investigate the production of biologically active NGF.

The pheochromocytoma cell line (PC12) is a sympathetic neuronal cell line and differentiates in the presence of NGF; the differentiation of PC12 cells can be observed in culture by the extension of small neuritic processes (Connolly *et al.*, 1979). Conditioned media from SCs containing active NGF, therefore, induces the differentiation of PC12 cells and the extension of long neurites.

This assay of NGF production was undertaken for the STAG cells using the IMS32 line as a positive control (Watabe *et al.*, 1995). Preliminary results showed that while conditioned media taken from the STAG 3Faii cell line did induce some extension of PC12 processes, this was observed in very low numbers of PC12 cells (data not shown). The media taken from the IMS32 line induced the extension of a similar number of neuritic processes, although this was not to the extent that was recorded in the original report of this assay (Watabe *et al.*, 1995). Greater analysis of the PC12 neurites in this assay would be required to determine whether the numbers of extended neurites was significant and whether the STAG cells produce biologically active NGF.

Alternatively, commercially available ELISA kits can provide a means of assessing and quantifying the amounts of secreted growth factors in samples of conditioned media.

Expression of the myelin phenotype

The STAG cells in culture demonstrate a non-myelinating cell phenotype as determined by positive staining for the markers GFAP, Ran-2 and A5E3 (Jessen *et al.*, 1990). The lack of positive immunostaining of the myelin markers in the STAG cells is consistent with results from previous studies which demonstrate a loss of

expression by isolated SCs with time *in vitro* (Brockes *et al.*, 1980; Mirsky *et al.*, 1980).

However, recent reports have shown that the major peripheral myelin protein, P0, is in fact, constitutively expressed by SCs (Cheng and Mudge, 1996; Lee *et al.*, 1997). RT-PCR studies have suggested that the myelin phenotype of SCs is largely determined by extrinsic signals, both positive and negative, which act on myelin protein expression around pre-existing basal levels of expression (Lee *et al.*, 1997; Morgan *et al.*, 1994).

RT-PCR studies of the STAG lines in the present study confirm that P0 mRNA can be identified in the cell lines, despite negative immunostaining for the protein. Thus, the ability to myelinate axons may not be lost in the STAG cells, but require sufficient and appropriate signalling to induce the myelin phenotype.

In addition, the expression of P0 has been linked to the expression of the large T antigen (Bharucha *et al.*, 1994). This report suggests that in conjunction with the transcription factor, c-Jun, large T antigen acts to suppress P0 expression by binding to the P0 promoter. In the present study, this may be another mechanism of down-regulation of P0 protein in the cell lines.

A biological assay of myelination was undertaken for 2 STAG lines with the use of a dorsal root ganglia (DRG) myelination assay. In the presence of ascorbic acid, cultured DRG neurons are myelinated by co-cultured primary SCs when incubated over approximately 1 month (Eldridge *et al.*, 1987). This assay was used to investigate the myelinating capacity of STAG cell lines, 3C2aii and 3Faii. However, these lines continued to divide rapidly when transferred to the incubation temperature of $37^{O}C$ and co-culture with DRG neurons, and were subsequently not able to myelinate the DRG neurons (data not shown).

The STAG cells in this assay were taken from their normal incubation temperature of 33°C and transferred onto DRG neurons at 37°C. The results suggest that the cell lines did not respond sufficiently quickly to either the raised temperature of 37°C or to the presence of the neuronal signals to reduce their cell division and subsequently differentiate.

The DRG myelination assay had been carried out before any extensive analysis of the behaviour of the cell lines at higher restrictive temperatures. Later studies of the behaviour of the STAG lines at 39°C showed a significant reduction in cell division at this temperature for all the lines tested. However, these changes in cell division took place over the first week, and the change was less significant for the 3Faii cell line, one of the cell lines which had been used unsuccessfully in the DRG-myelination assay described above.

Given that other STAG cell lines, such as the 3Fb line, responded more quickly to the increase in temperature, it may now be appropriate to repeat the myelination assay with the 3Fb cell line. Whether these STAG lines would show an equally significant reduction in cell division at 37°C, and thereafter adopt a myelin phenotype in the presence of appropriate axonal signals, has not been further studied.

3.4.4 STAG cell lines are conditional on the temperature of incubation

The rate of cell division in the majority of the STAG lines had decreased significantly within 3 days at the restrictive incubation temperature of 39°C; immunostaining for the large T antigen was markedly reduced by 1-2 weeks at this temperature. Thus, the STAG lines displayed a cell line status which was conditional on the temperature of incubation.

Most of the STAG lines showed a decrease in cell division which was significant within 3 days of incubation at the higher temperature, and also demonstrated a rounding of the cell body and extension of fine processes during this time. The 3C3 and 3Faii cell lines showed slightly less sensitivity to the change in incubation temperature, although they had nearly ceased to divide completely by 1 month at the higher temperature. The 4B cell line showed the least temperature sensitivity of all the STAG lines and continued to require passaging after 1 month at 39^{O}C, although at a much reduced frequency.

The differences in the response to incubation at the restrictive temperature are likely to reflect the nature of the incorporation of the large T antigen into the different STAG lines. In a recent study which also used a thermosensitive allele of the large T antigen to generate SC lines (Thi *et al.*, 1998), the cell line with the lower copy number of the large T antigen of 1-2 copies, demonstrated a more sensitive reaction to the temperature-shift to the restrictive temperature; these cells showed a near arrest in cell division. In contrast, the second cell line which contained 2-5 copies of the oncogene showed continued cell division, although at a much reduced rate.

In addition, the rates of cell division can be correlated to some extent with the levels of expression of the large T antigen that have been found in the STAG lines, as determined by Western blotting. The cell line which shows the least resistance to a reduction in cell division, STAG-4B, also shows the greatest signal of protein staining in the Western blot. Similarly, the cell lines 1A1a and 1A1b which show lower levels of the T antigen protein respond significantly to incubation at the restrictive temperature.

Some of the STAG lines, including the 3C3 and 3Faii lines, were returned to 33°C after 1 week at 39°C, and were found to have subsequently regained their normal rate of cell division (data not shown). The conditions for growth would thus appear to be reversible between these temperatures.

At the immunocytochemical level, the immunophenotype of the STAG cells is unchanged from that at the permissive temperature of 33°C with all major SC markers expressed by the STAG lines. With respect to P0 staining, there was suspected to be some immunoreactivity to the protein. However, while this was above the signal from cells incubated without the primary antibody, the signal was similar to that when the cells were incubated in neuron-specific antibodies, pan-neurofilament and neuron-specific enolase (NSE).

Although the STAG cells stain positively for the pan-neurofilament antibody (the signal was concentrated around the nucleus), primary SCs in the present study were also found to stain positively when screened in parallel experiments (also reported by colleagues in the lab). Staining for NSE, however, was very weak and usually similar in intensity to the P0 staining. Although not a common marker of glial cells, NSE-immunoreactivity has been demonstrated for differentiating oligodendrocytes, reactive astrocytes and reactive and neoplastic SCs (Filie *et al.*, 1996; Sensenbrenner *et al.*, 1997). The presence of NSE, a glycolytic enzyme, in these cells is suggested to be a product of the high energy demands of these cell types.

Given the possibility of true staining of NSE in the STAG cell lines, it is not clear from these immunostaining results whether there is any significant up-regulation of P0 protein in STAG cells at the non-permissive temperature. Western

blotting methods may be able to demonstrate more conclusively the presence of P0 protein.

3.4.5 STAG cell lines are not easily identifiable *in vivo*

Given that the STAG lines did not express the low affinity nerve growth factor receptor, they could not be identified by immunostaining for this marker when transplanted into the brain. Although a number of alternative markers were used to identify STAG cells *in vivo*, the STAG cell transplants in the basal forebrain remained difficult to identify specifically against other host glia. Transplants of the STAG 1A1a line, which had showed a positive PCR product for p75, showed some immunoreactivity to the p75 antibody *in vivo* when transplanted into the septal cholinergic nuclei. However, when perfused at 12d, staining of the transplants was weak and not clear as a means of identifying the STAG cell population.

Thionin-staining demonstrated the presence of cell material in the line of the injection track, but the graft was not as wide as had been seen with similar primary SC transplants (see 4.3), although only 2 animals had been stained in this way. Similarly, immunostaining for the astrocytic marker GFAP suggested that the transplant which had formed was not as pronounced as had been evident in primary SC transplants. Further immunostaining suggested that although small numbers of neurofilament-positive fibres could be seen within the region of the transplant, this was difficult to interpret in the light of the poorly visible transplant.

It is possible that the STAG lines had lost the ability to form columnar transplants in the way that primary SCs are able to. The formation of columnar SC-transplants, as seen in both the thalamus (Brook *et al.*, 1994) and the basal forebrain (4.3), requires the alignment of SC processes in a tight and ordered fashion, a

process which is already well-developed by 72h of transplantation (4.3). This may involve the expression of both local environmental and intrinsic cues, the latter complement of which may be incomplete in the transformed STAG cell lines. Loss of such cell-cell contact expression may be the result of the extended time in culture in isolation, or the result of integration of the large T antigen.

Alternatively, it is possible that the STAG cell transplants are able to form columnar transplants, but that the small numbers of animals used and poor immunostaining has made it difficult to clearly identify these columns. With the STAG cells difficult to identify *in vivo*, it remains difficult to accurately quantify their ability to survive and promote axonal growth in the CNS.

Finally, it is important to note that on no occasion has a tumour been found in the animals which have had STAG cell transplants. This is in contrast to the finding from the DRG co-culture study, where the 3C2aii and 3Faii lines overgrew their cell cultures at 37^{O}C. Immortalised cells grafted into the CNS can continue to divide and form tumours (Horellou *et al.*, 1990; Shimohama *et al.*, 1989), however, no signs of excessive cell growth were ever found in STAG cell transplants. Aside from the temperature sensitivity of the STAG cell lines in *in vitro* studies, this finding suggests that there must be sufficient communication of the cells with the local environment that they eventually cease to divide and differentiate appropriately *in vivo*.

3.4.6 Summary

Primary NSCs have been immortalised with an expression vector encoding the large T antigen. Characterisation of these 'STAG' cell lines demonstrates that they retain the immunophenotype of primary SCs in vitro, although they do not express the low-

affinity nerve growth factor receptor, p75. RT-PCR studies show that they contain the mRNA for several growth factors and also for the peripheral myelin protein. The lack of an effective marker of these cells *in vivo* has made it presently difficult to assess their phenotype *in vivo*.

CHAPTER IV

CHAPTER IV – Extrusion Transplants of Neonatal Schwann Cells into the Basal Forebrain System

4.1 Introduction

4.1.1 Peripheral nerve grafts can stimulate elongative growth of cut central axons

In contrast to the CNS, the PNS is able to support elongative axonal growth after injury. The reasons for this are likely to be complex but are believed to involve the presence of both growth-permissive and inhibitory factors (Olson, 1997; Pollock, 1995).

Given the more successful regenerative ability of the peripheral nervous system, workers sought to transplant peripheral nerve components into the CNS in an attempt to further stimulate central axonal growth. The concept of peripheral nerve grafting was initially described by Ramón y Cajal (Ramon y Cajal, 1928). In more recent times, Aguayo and co-workers published an important study of peripheral nerve grafts in the adult rat spinal cord (Richardson *et al.*, 1980). In this study, they transplanted a piece of autologous peripheral nerve into a small gap excised from the thoracic spinal cord, and several months later observed significant central axonal growth within the graft of up to 10mm in length.

The demonstrations that adult central axons retain the intrinsic ability to extend long distances offers promise for future repair strategies. Later peripheral nerve studies not only confirmed the early findings of long axonal growth but also suggested that the extent of this ability was determined largely by the distance between the neuronal cell body and the site of axonal injury (Benfey and Aguayo, 1982; Richardson *et al.*, 1984).

4.1.2 Peripheral nerve grafting experiments

Several important peripheral nerve grafting experiments followed these initial findings. In a study of the retinotectal system, Vidal-Sanz et al. (1987) transected the optic nerve and grafted a piece of tibial nerve over the surface of the brain to examine whether lesioned retinal ganglion cells could regenerate through the graft and onto their target cells in the tectum. They demonstrated with the use of tracers that not only could retinal ganglion cell axons be identified throughout the length of the graft, but that some of these axons had indeed formed terminal arborisations within the superior colliculus, the tectal target of normal retinotectal axons. This not only provided further evidence that peripheral nerve grafts could induce elongative growth of cut central axons, but further suggested that these axons could re-synapse onto their original, intended terminal field in the CNS. A similar grafting method later used in the adult hamster indicated that these synapses were electrophysiologically functional, as determined by the restoration of light-induced reflexes (Carter *et al.*, 1989; Keirstead *et al.*, 1989).

In general, however, while central axons show long axonal growth in entering and extending within peripheral nerve grafts, they do not show this growth beyond the graft when re-entering the CNS.

4.1.3 The Importance of Schwann cells in peripheral nerve grafts

Schwann cells (SC) constitute the major glial cells of the peripheral nervous system and produce an abundance of molecules including growth factors, cell adhesion molecules, extracellular matrix components and immunoeffector molecules (Mirsky and Jessen, 1996; Zorick and Lemke, 1996). As the myelinating glia of the PNS, its

role is crucial to successful regeneration of lesioned peripheral axons (Brecknell and Fawcett, 1996).

Berry et al., investigated the importance of the SC in the observed effect of peripheral nerve grafts in the CNS (Berry *et al.*, 1988). They freeze-thawed peripheral nerves, thereby destroying the cellular element of the grafts (predominantly SCs and fibroblasts), and anastomosed them to optic nerve and demonstrated that both retinal ganglion cell survival and axonal growth was greater in normal than in acellular grafts. Although the latter did provide some trophic support, axonal growth was more significant in the presence of viable cells. Similar results were obtained from another study which examined the effectiveness of peripheral nerve grafts devoid of SCs (Smith and Stevenson, 1988).

Molecular studies further support the notion that SCs are crucial for successful nerve regeneration. The *Enervated* (*Enr*) mouse exhibits a transgene-induced insertional mutation in the SC and has been shown to undergo impaired peripheral nerve regeneration (Rath *et al.*, 1995). Ultrastructural studies following peripheral nerve injury demonstrated abnormal SC-axon relationships and poor myelination of axons, the primary cause of which was attributed to a problem in early SC differentiation. This study is an example of a direct link between an abnormal SC and impaired peripheral nerve regeneration.

4.1.4 Transplantation of SCs into the CNS

While SCs in peripheral nerve grafts are known to be able to induce long axonal growth, there is less information about the ability of SCs, in isolation, to recruit central axons. In addition, there are few studies which have described the recruitment of central axons of a known phenotypic class and which document any

specificity of axonal growth that SCs may confer. It is possible that the ability of SCs to induce central axonal growth is limited to only a certain number of neuron subclasses (Benfey *et al.*, 1985).

In recent years, there have been a variety of models which introduce suspensions of SCs into the CNS in an attempt to stimulate elongative growth of central axons (Montero-Menei *et al.*, 1992; Montgomery *et al.*, 1996; Xu *et al.*, 1995). These studies have shown that SC grafts can mediate long axonal growth within them.

The technique of micro-transplantation of cell suspensions has been used in recent years as a means to deposit small volumes of transplant material into defined locations within the CNS (Emmett *et al.*, 1990; Leanza *et al.*, 1996; Nikkah *et al.*, 1995). The technique was used in this laboratory to deposit suspensions of neonatal SCs within the adult thalamus (Brook *et al.*, 1994). Pure populations of SCs were obtained using a method based on that of Brockes et al., 1979. When extruded using a pulsed air pressure system into the thalamus, these cells were found to form aligned and ordered columnar transplants which integrated well with the host tissue. These SC columns induced significant elongative axonal growth within them, and demonstrated that appropriately aligned SCs could induce elongative growth of central axons.

This minimally traumatic procedure provides a clean and relatively simple means of depositing SCs into the CNS. The source of axons recruited by the SC transplants in this study could not be precisely identified but were thought to be those of the thalamic reticular nucleus, an idea supported by the results of whole peripheral nerve transplants into the thalamus (Benfey *et al.*, 1985; Zhang *et al.*, 1995a; Zhang *et al.*, 1995b).

4.1.5 The basal forebrain cholinergic system

The cholinergic neurons of the septum and diagonal band of Broca which project to the hippocampus form the 'septohippocampal pathway' and are part of the basal forebrain cholinergic system (Dutar *et al.*, 1995). This projection is a well-defined and well-characterised pathway with specific histological markers, and is severely affected in Alzheimer's disease, although the disease differentially affects several cholinergic-innervated regions of the brain (Geula and Mesulam, 1996; Henderson, 1995). It is also well-documented to be responsive to NGF, both *in vitro* and *in vivo*. The latter studies involve both the exogenous delivery of NGF to the cholinergic neurons after lesions in the pathway (Hagg *et al.*, 1990a; Hefti, 1986), and also the use of peripheral nerve grafts to restore the lesioned pathway (Hagg *et al.*, 1990b; Kromer and Cornbrooks, 1985; Wendt *et al.*, 1983).

SCs are well-known to produce NGF and express the low-affinity receptor to NGF, NGF-R or p75 (Assouline *et al.*, 1987; Assouline and Pantazis, 1989; DiStefano and Johnson, 1988). Moreover, both NGF and its receptor are up-regulated in an acute response to peripheral nerve injury, a phenomenon which may contribute to successful nerve regeneration (Heumann *et al.*, 1987a; Heumann *et al.*, 1987b).

In addition, cholinergic neurons have been shown to be responsive to elevated levels of NGF, provided by skin fibroblasts engineered to produce the growth factor (Kawaja and Gage, 1991; Kawaja *et al.*, 1992). The suggestion from these studies is that NGF is sufficient to induce cholinergic axonal growth and that the resultant growth is mediated by astrocytic processes. Given that astrocytes have often been attributed with an inhibitory role in central axonal regeneration (Ridet *et al.*, 1997), the study re-examines that role in the context of cholinergic axonal growth.

Thus, the cholinergic neurons of the septohippocampal projection seem an ideal candidate for recruitment by SC transplants. Previous studies of SC suspensions in the basal forebrain cholinergic system suggest that SCs can indeed support cholinergic axonal growth *in vivo* (Montero-Menei *et al.*, 1992; Stichel *et al.*, 1996).

4.1.6 Aims of the project

I have used the extrusion transplantation method to study whether primary NSCs are able to induce elongative axonal growth from the nuclei of cholinergic neurons in the basal forebrain. This would provide an important example of suspensions of SCs supporting central axonal growth of a known phenotype. This technique allows the close examination of transplanted cells with host glia and axons, and the relatively atraumatic nature of the procedure means that the development of the gliotic reaction to host tissue invasion is kept to a minimum. It would provide information on the role of host glia in the context of such transplants, and further, on the behaviour of SCs in the CNS, an aspect which is important in any repair strategy that would involve the use of SCs.

4.2 Materials and Methods

4.2.1 Preparation of neonatal Schwann cells for transplantation

Neonatal Schwann cells (NSCs) were prepared at 50 x 10^6/ml in DMEM containing 40% DNAse at 11,500 U/ml and maintained on ice thereafter. The cells were resuspended prior to each transplantation procedure.

4.2.2 Transplants of NSCs into the septal cholinergic nuclei

Locally-bred adult AS rats were used for transplantation and were anaesthetised and prepared as described in 2.2.1. A pulsed air pressure system (Emmett *et al.*, 1990) was used to deposit the cells into the brain at stereotaxic co-ordinates measured from the bregma, with the head held in the flat skull position, of 0.6mm rostral, 0.5mm lateral, 8.5mm ventral. Approximately 5µl containing 2.5 x10^5 cells was deposited at 0.5µm intervals through a bevelled siliconised glass micropipette (approximately 130µm internal diameter) along a 3mm vertical track (Fig. 4.1). The micropipette was washed with PBS between transplants.

4.2.3 Histology

4.2.3.1 Perfusions

Animals were perfused at 3-165d post-operation (po) with either 4% paraformaldehyde (vibratome/cryostat processing), 1% glutaraldehyde/1% paraformaldehyde (EM processing), or with PBS alone for later post-fixation (cryostat processing), as described in 2.2.2.

Figure 4.1. Extrusion transplantation of NSCs into the septal cholinergic nuclei. 'A' is a diagram of a stereotaxis, used to microtransplant the cells into the brain at specific co-ordinates: (N) needle, (P) platform, (V1, V2) valves 1 and 2. Air is pulsed through the system in the direction of the open arrows to push the cell suspension out of the needle, N, and into the desired co-ordinates. 'B' is a schematic diagram which shows the placement of the SC column (red) into the septal cholinergic nuclei (green). The labels are as follows: corpus callosum (cc), cholinergic nuclei of septum and band of Broca (cho), cortex (cx), lateral ventricle (lv), striatum (str), SC transplant (tra).

A

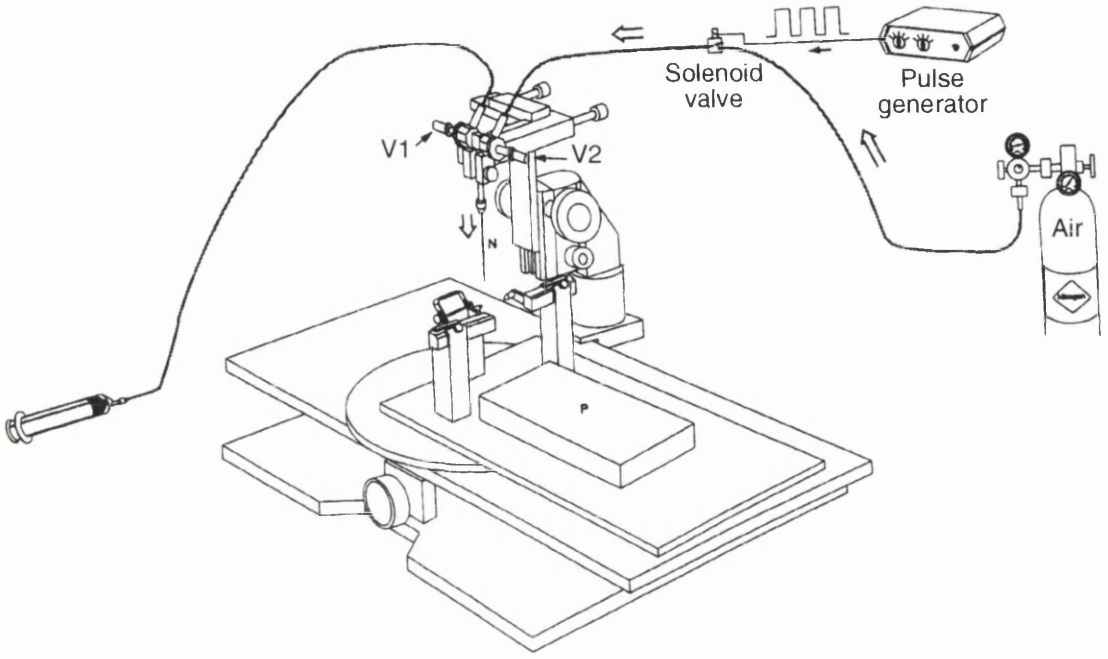
Solenoid valve
Pulse generator
V1
V2
N
P
Air

B

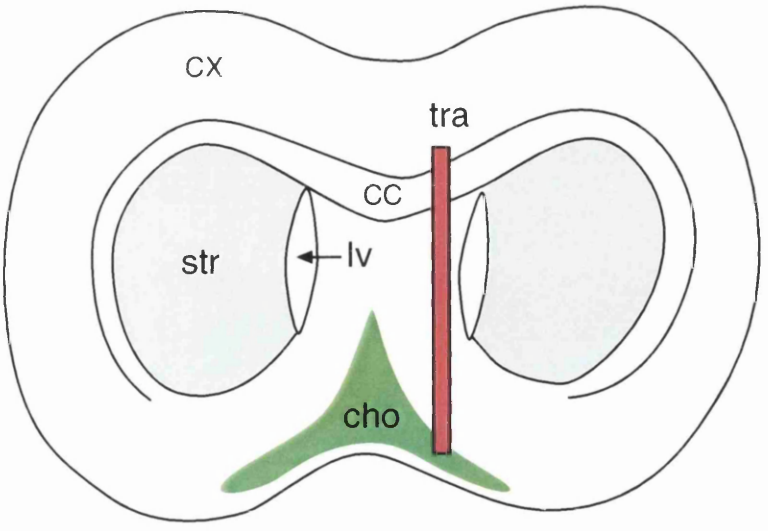
CX
tra
CC
str
lv
cho

4.2.3.2 Immunohistochemistry

Immunohistochemistry was carried out as described in 2.3. Chromogenic-stained sections were recorded using standard light microscopy with an integral camera (Zeiss Axioskop). Fluorescence-stained sections were scanned into the confocal imaging system where permanent records could be kept. Slides of these sections were stored in a cool place and re-analysed when required.

4.2.3.3 Electron microscopy

Fixation and Embedding

EM-perfused brains were sectioned on the vibratome at 150-200μm thickness. After washing thoroughly in washing solution (0.1M PB containing 0.002% $CaCl_2$, 8% glucose), the sections were post-fixed in 1% osmium tetroxide in 0.1 M PB for 1.5 hours and subsequently processed in the following protocol with the use of an automated tissue processor (Lynx-el Microscopy Tissue Processor): sections were washed in the washing solution for 10 minutes, dehydrated in an ascending series of ethanols (50, 70%, 80%, 95% and 100%; three changes of 5 minutes for each step) and acetone (BDH, UK) (two changes of 20 minutes), immersed in 1:1 acetone and resin (TAAB, UK) for 1 hour and 100% resin overnight for resin infiltration. All the above steps were carried out at room temperature. The sections were then flat embedded in resin on glass slides coated with mould-releasing compound (Formen-Trenmittal Hobby Fluid, Hobby Wholesale, UK) and the resin was polymerised by incubation at $60^{O}C$ for 48 hours.

Sectioning

Sections were cut out from the resin slips and fixed using Superglue (Bostik, UK) onto resin blocks. Semi-thin sections at 1-2μm thickness were cut using a glass knife (Leica, UK) in an ultramicrotome (Reichart-Jung, UK) and mounted onto gelatin-coated slides; sections were placed onto droplets of water which evaporated when placed onto a hotplate. Ultra-thin sections at 80nm were obtained using a diamond knife on the ultramicrotome and collected on copper grids.

Staining

Semithin sections were immersed in an equal mixture of 1% methylene blue in distilled water and 1% Azur II in 1% disodium tetraborate for 30 seconds, rinsed with distilled water and the solution dried on a hot plate ($70^{O}C$).

Copper grids holding the ultra-thin sections were immersed in 0.3% uranyl acetate in methanol for 7 minutes, washed three times in methanol and air dried. They were then immersed in Reynolds lead citrate solution for 7 minutes, rinsed three times in distilled water and air dried. Reynold's lead citrate was made up using the following method: 1.33g of lead nitrate and 1.76g sodium citrate.$2H_2O$ (BDH, UK) were added consecutively to 30mls of distilled water and dissolved in 8ml of 1 N NaOH (BDH, UK); distilled water, which had been boiled and cooled in a sealed container to decrease the amount of O_2, was added to make the total volume up to 50ml.

4.3 Results

4.3.1 Preparation of NSCs for transplantation

NSC cultures obtained at the end of the preparation method showed over 95% purity although fibroblast contamination became more significant with subsequent time *in vitro*. Consequently, NSC cultures were used immediately or soon after the complement-mediated kill to minimise the contribution of the fibroblasts.

NSCs displayed a bipolar or tripolar, spindle-shaped morphology and extended fine processes *in vitro* (Fig. 4.2). Further SC purification from the contaminant fibroblasts was possible by the nature of their differential adhesion to the cell culture dish; SCs lifted first when lightly trypsinised and tapped-shaken.

4.3.2 Immunostaining of NSC transplants in the basal forebrain

Suspensions of NSCs extruded into the septal cholinergic nuclei of the basal forebrain survived the transplantation procedure and formed tight and ordered columnar transplants which integrated well with host tissue. Animals which held the transplants were behaviourally indistinguishable from normal littermates within hours of the procedure and did not appear to show any adverse reactions to the transplants.

Several aspects of the SC transplants will now be discussed in turn.

4.3.2.1 Formation and integration of NSC columns which arise from the nuclei of the septal cholinergic neurons

NSC transplants were observed cleanly by staining with a monoclonal antibody to the low-affinity nerve growth factor receptor, p75. The transplants extended dorsally from the nuclei of the septal cholinergic neurons in the basal forebrain to the

Figure 4.2. Primary neonatal SCs (NSCs) in culture. NSCs display bi- and tripolar morphologies with fine extended processes. Relatively pure cultures of NSCs may still contain some fibroblasts.

(Scale bar: A, 20μm; B, 5μm)

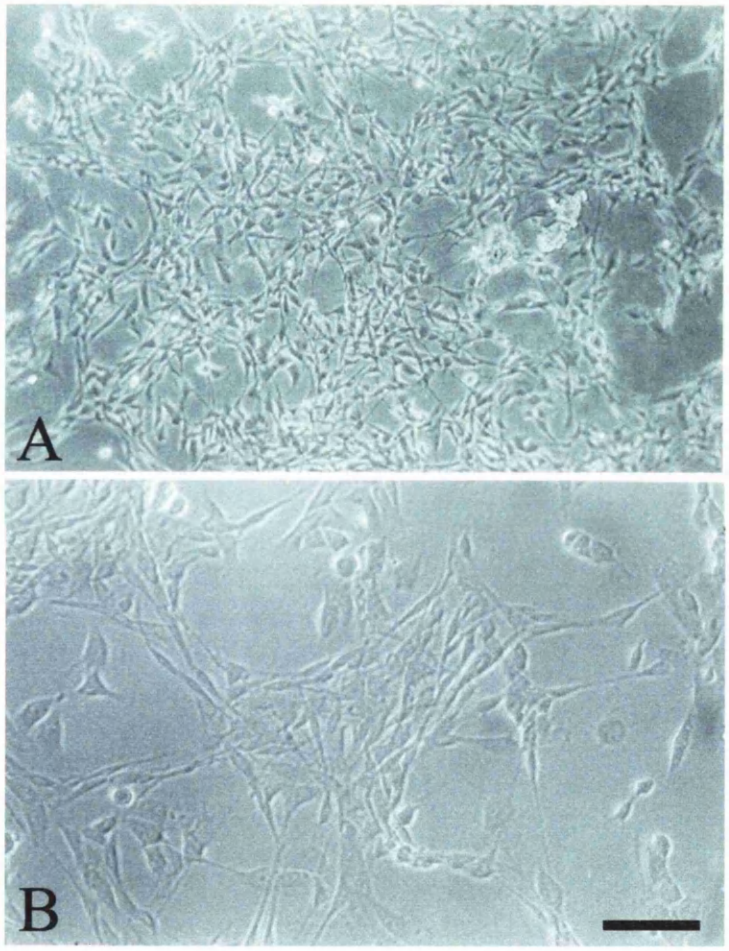
A
B

white matter tract, the corpus callosum (Fig. 4.3); in some cases, the transplants formed bridges which ran across the corpus callosum (n=5) (Fig. 4.4C).

When fully formed the columnar transplants measured approximately 3mm in dorso-ventral length and 0.5mm in antero-posterior depth; the width of the transplants varied from approximately 200μm at their bases to 30μm at the narrower points of the column. Confocal images of coronal sections taken at intermediate levels through the transplant can be seen in Fig. 4.4.

The columns were made up of SC processes which had aligned along the length of the transplant, and which were tightly packed within an ordered and well-defined structure (Fig. 4.3, 4.5). Alignment of SC processes had taken place within 72 hours (n=2), was well-developed by 7d post-operation (po) (n=3) and changed little thereafter up to 47d po, the latest time tested (n=20) (Fig. 4.6).

The location of the SCs was generally confined to the ordered structure of the transplant, although flares of migrating SCs could be seen which branched off the main body of the transplant (Fig. 4.3C). In these cases, SC migration could be seen within 5d of the transplantation. The major route of migration was along the blood vessel network; SCs, themselves, are able to induce new blood vessel formation and this was seen regularly in the transplants (data not shown).

4.3.2.2 Astrocytic processes align along the length of the transplant

There was a limited and localised astrogliotic reaction to the transplant as indicated by the increased GFAP immunoreactivity in the region of the transplant (Fig. 4.7). Astrocytes were initially absent from the body of the transplant by 3d po (n=2) and began to infiltrate the transplant from approximately 7d po (n=3) (Fig. 4.8).

Figure 4.3 SC-transplants are identified cleanly by p75-immunostaining (DAB method; coronal sections, all transplants are at 12d). SCs form aligned processes to form a columnar transplant (sc) (A), the base of which lies in the p75-positive nuclei of the septal cholinergic neurons (scn) (B). 'C' shows flares of SCs (f) migrating from the dorsal aspect of the transplant.

(Scale bar: A - 200μm; B - 100μm; C - 50μm)

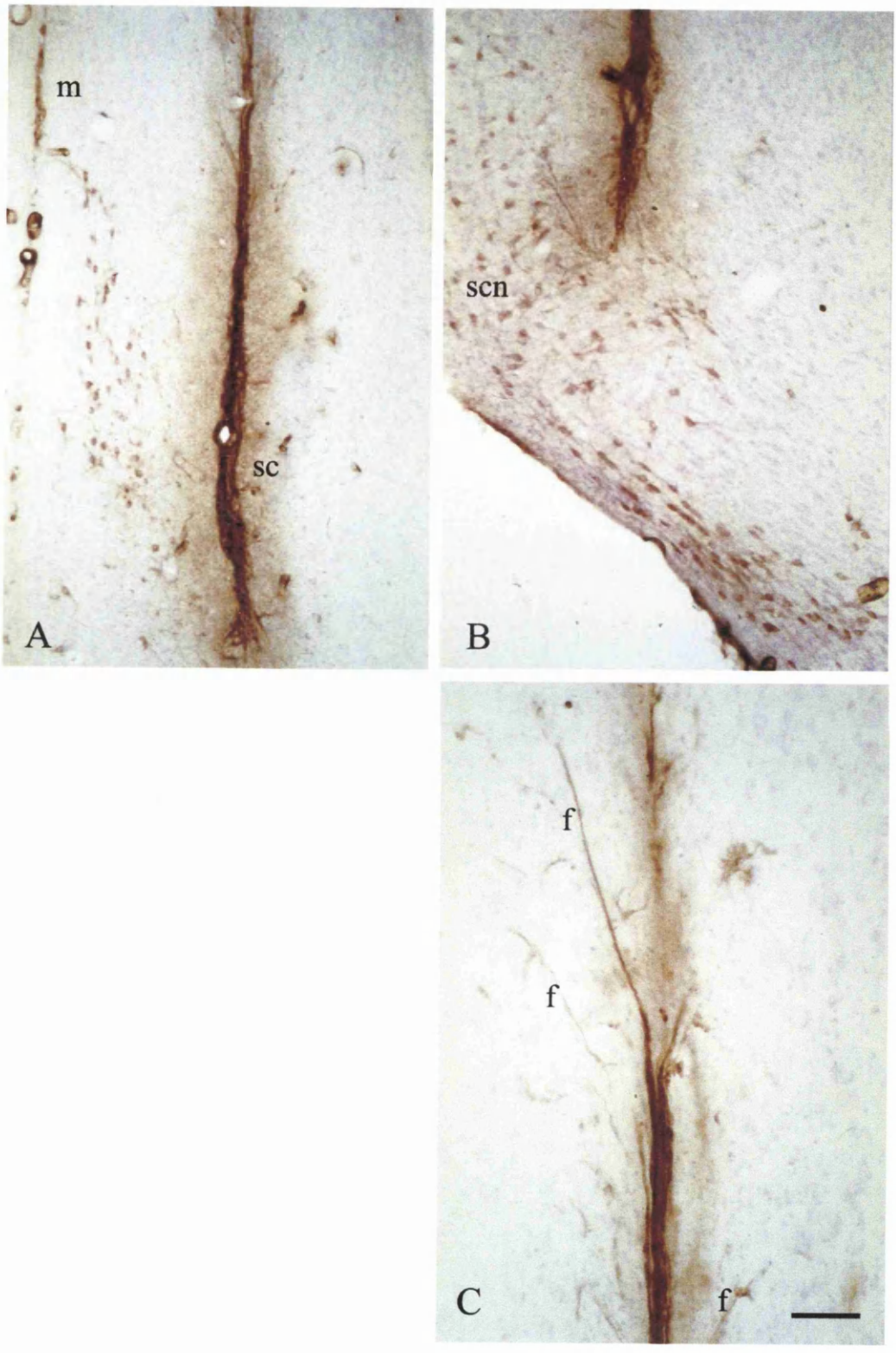
m
sc
A
scn
B
f
f
f
C

Figure 4.4A Intermediate coronal sections taken through a single transplant. (A-F are montages of projected confocal images which were taken of p75-immunostained sections (TSA method); the animal was perfused at 3d. Each montage series of images A-F represents a depth of 40μm taken through the section; the location of each section in the transplant is given in μm relative to the transplant in section C.) Extruded SCs form a columnar transplant with a wide base and narrow length; the dorsal aspect of the column may extend to the corpus callosum (cc), as is seen here (C). Figure 4.4B shows the 3 subsequent sections posterior to section C. (lateral ventricle, LV)

(Scale bar, 200μm)

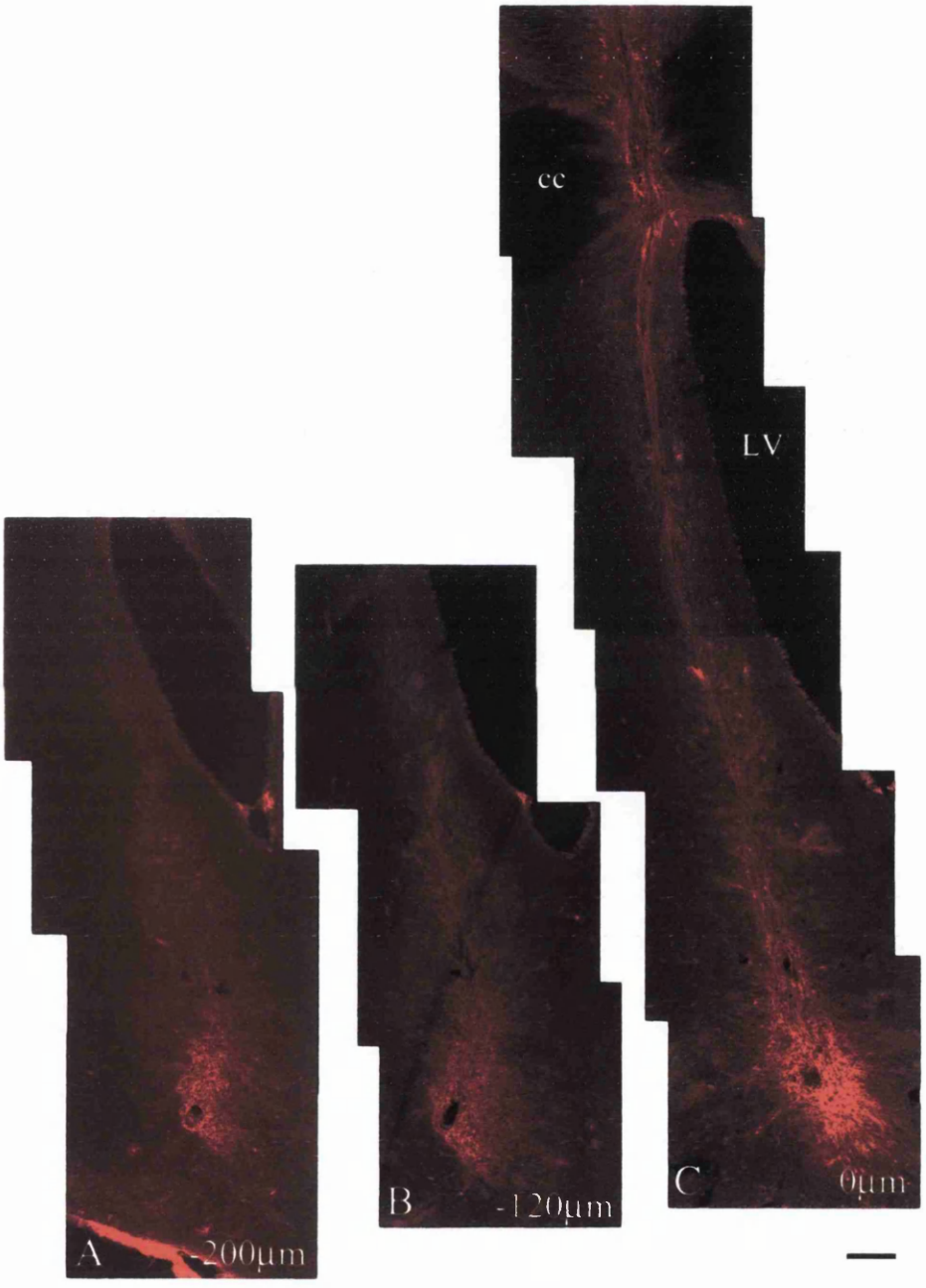
cc
LV
A
-200µm
B
-120µm
C
0µm

Figure 4.4B Intermediate coronal sections taken through a single transplant (see Fig. 4.4A for details) Sections are posterior to that in 'C' as indicated in μm. (lateral ventricle, LV)

(Scale bar, 200μm)

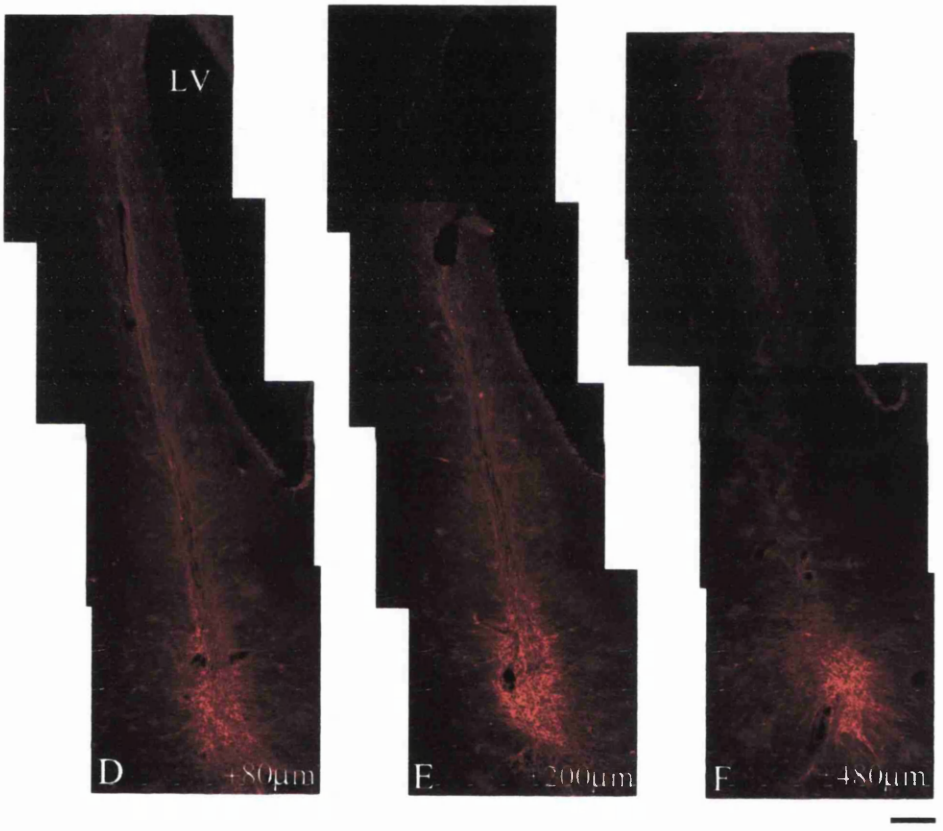
LV
D
+80μm
E
+200μm
F
+480μm

Figure 4.5 Alignment of SC processes. At high magnification, p75-staining (DAB, Ni-enhanced; coronal sections) shows that the column transplants are composed of tight and ordered bundles of dorso-ventrally aligned SC processes (A,B); in some regions, individual SCs can be discerned (arrow in C).

(Scale bar: A - 50μm; B, C - 25μm)

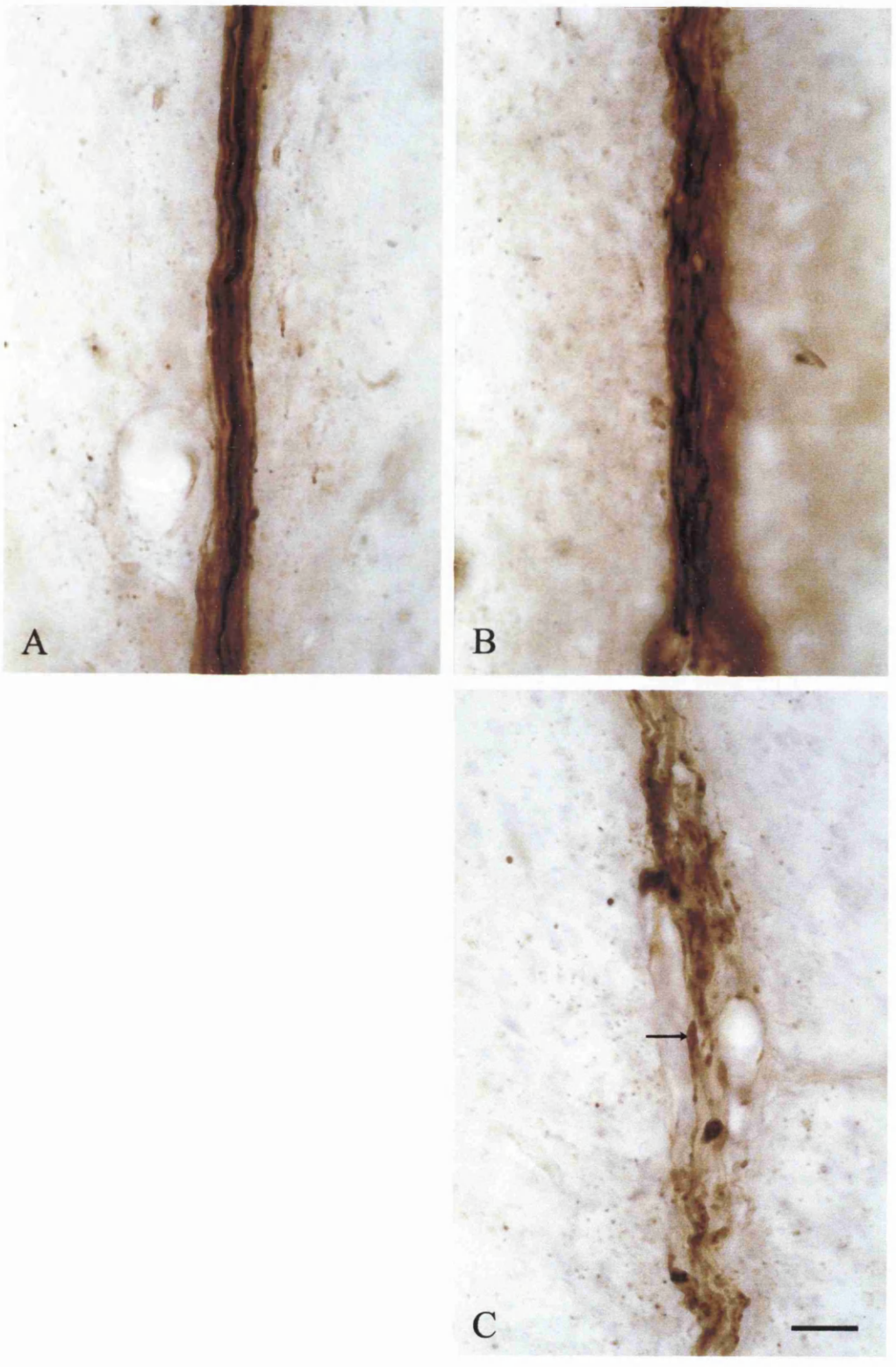
A
B
C

Astrocytic processes had aligned along the length of the transplant by 14d po (n=3), and this persisted in the long-term transplants which were analysed.

4.3.2.3 Astrocytes are intimately associated with the SCs within the transplant

Double-labelled sections of GFAP and p75 demonstrated that the SC and astrocytic processes within the transplant columns were intimately associated with each other (Fig. 4.9, 4.10). The close association was not observed until 1 week, at which time the astrocytes began to extend their processes within the transplants. The association persisted in all transplants up to 45d po, the latest time analysed (n=12) (Fig. 4.9), and is likely to persist in longer-term transplants although SCs could not be easily identified *in vivo* beyond 45d.

4.3.2.4 Oligodendroctyes increase their APC immunoreactivity and some are included within the columnar transplants

Oligodendrocytes were identified by immunostaining for the Adenomatous Polyposis Coli (APC) antigen, originally associated with colorectal cancer but recently identified in oligodendrocytes in the adult rat brain (Bhat *et al.*, 1996). Immunostaining showed that there was a local increase in immunoreactivity of the APC antigen in the region of the transplant; this was also observed at other regions which were in line with the injection track (n=8) (Fig. 4.11A,B).

Sections which were double-labelled with APC and GFAP suggest that while astrocytes eventually extend aligned processes within the columnar transplants, the oligodendrocytes do not integrate so readily (n=8), although some can be located within the transplant (Fig. 4.11C,D).

Figure 4.6 Alignment of SCs in the transplants. (A-C are projected confocal images of coronal p75-immunostained sections, stained with the TSA method). Alignment of SC processes along the length of the transplants has already taken place by 3d (A), and does not change significantly over subsequent weeks; (B) represents the transplant in an animal perfused at 7d, (C) at 5 weeks. (lateral ventricle, LV)

(Scale bar: A, 50μm; B, 32μm; C, 8μm)

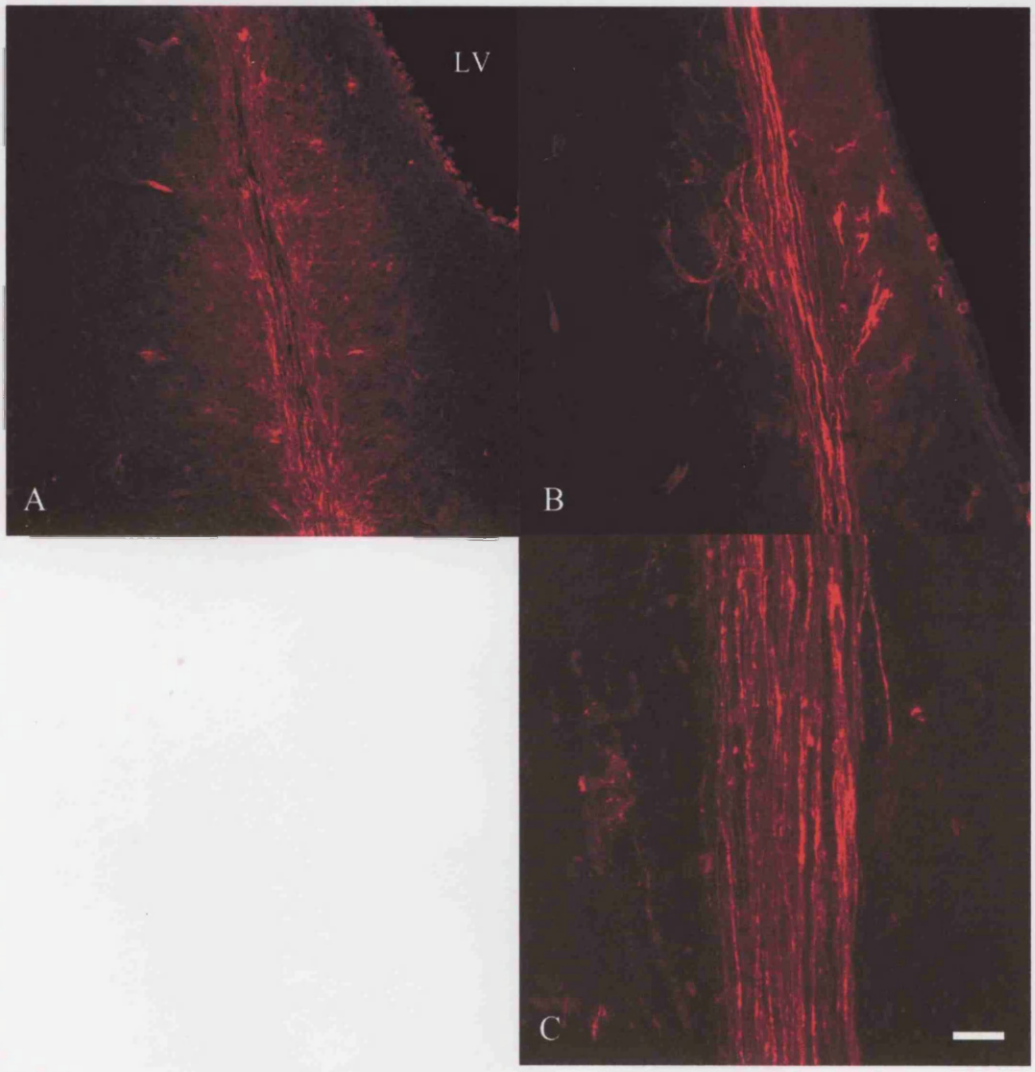
LV
A
B
C

Figure 4.7 Astrocytic gliosis at the transplant site (coronal sections immunostained with GFAP (Ni-GOD method), taken at 4 months). A small, localised gliotic reaction to the transplant (A), seen at higher magnification, shows some alignment of astrocytic processes within the transplant.

(*Scale bar: A - 250μm; B - 60μm*)

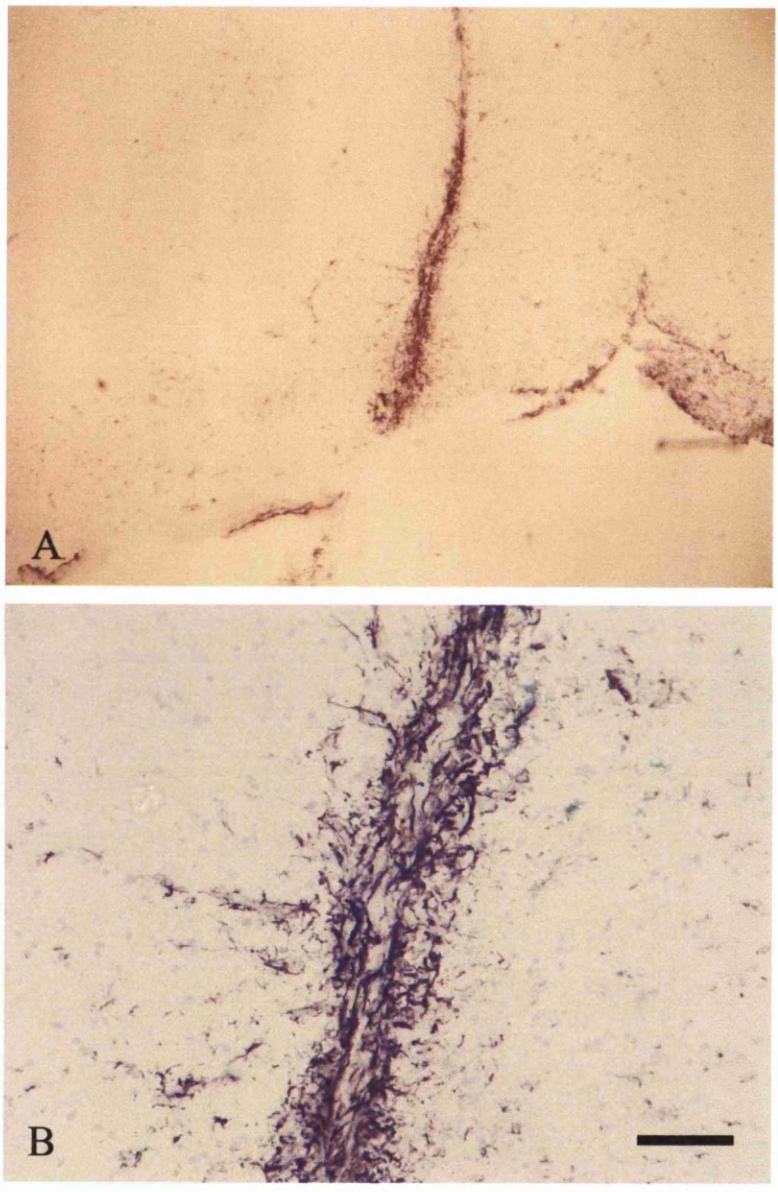
A
B

Figure 4.8 Development of the astrocytic invasion of the transplant. (coronal sections immunostained with GFAP (TSA method); A-D are projected confocal images, taken from approximately 30μm in depth) Astrocytic processes are absent from the base and length of the transplant (tra) by 3d (A,B). Aligned GFAP-positive processes infiltrate the transplant over approximately 2 weeks (C, 7d; D, 14d.

(Scale bar, 50μm)

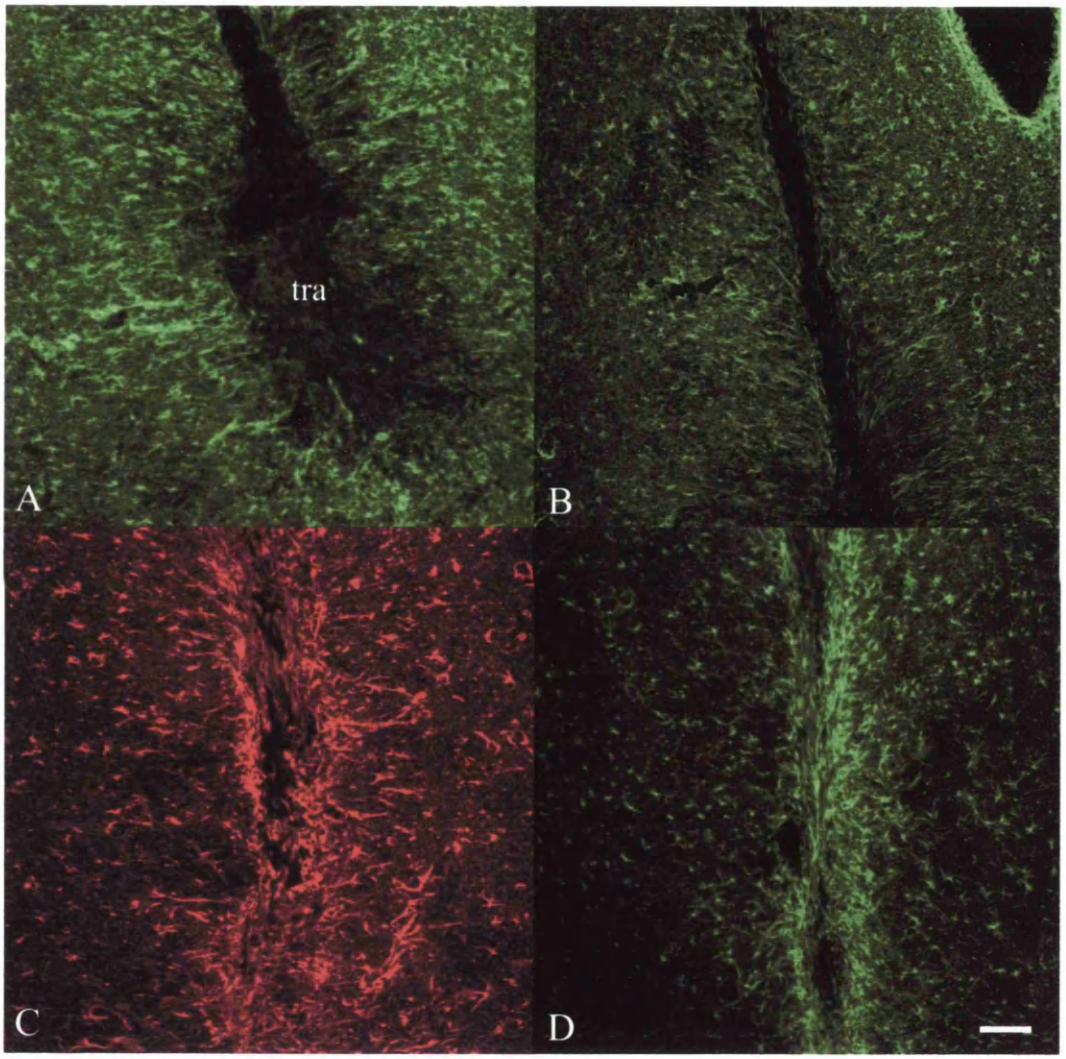
tra
A
B
C
D

Figure 4.9 Aligned SC and astrocytic processes. (coronal sections double-stained with p75/GFAP (TSA method) at 45d; A-C are projected confocal images taken through a depth of 35μm) SCs (red) and astrocytes (green) show a similar staining pattern within a transplant (A,B); the combined image shows the close association of the 2 cell types within the transplant (C).
(Scale bar, 50μm)

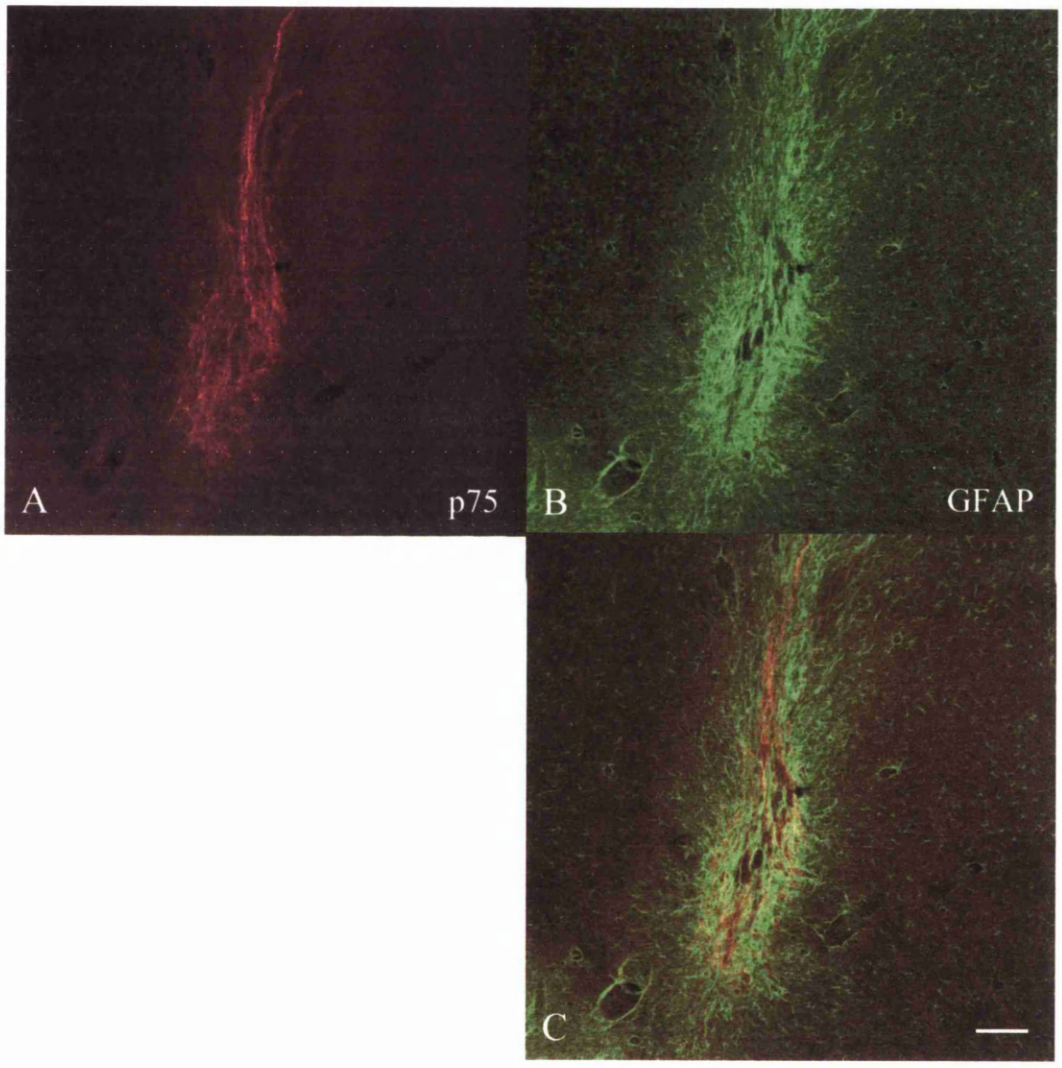
A
p75
B
GFAP
C

Figure 4.10 High power image of aligned SC and astrocytic processes. (projected confocal image of a p75/GFAP double-labelled coronal section from a transplant taken at 14d; sections are taken through a depth of 30μm) SCs (p75, red) and astrocytes (GFAP, green) are intimately associated along the length of the transplant.

(Scale bar, 50μm)

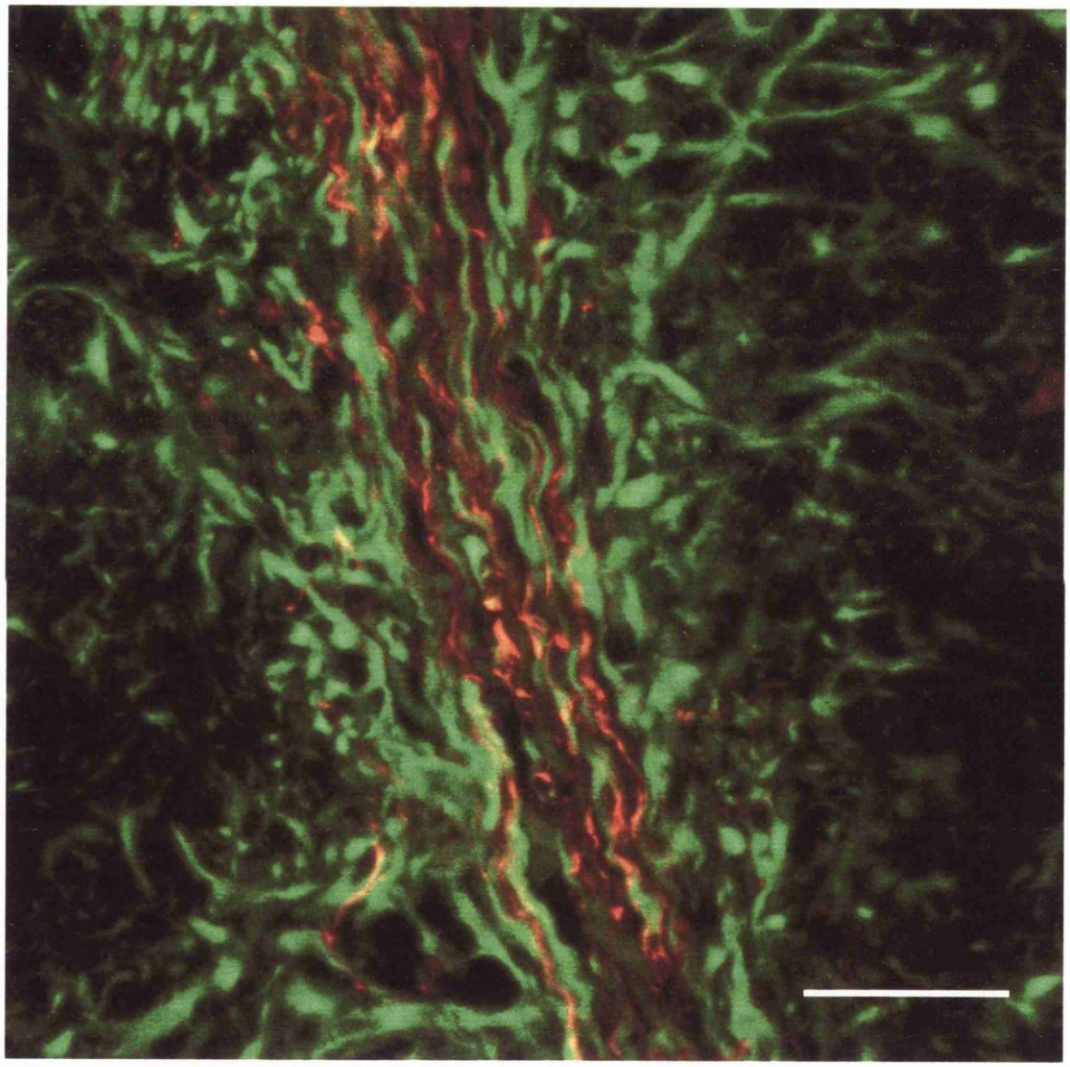

Figure 4.11 Oligodendrocytes at the transplant site (coronal sections immunostained with APC (red) and GFAP (green) (TSA method); projected confocal images are taken through a depth of 25-40μm.) Immunostaining with anti-APC shows an up-regulation of this marker in the region of the transplant column (asterisk) (A) at 3d, and also more dorsally across the corpus callosum (cc) at the site of the injection track (B). Sections double-labelled with APC/GFAP (C,D) show alignment of astrocytes and some oligodendrocytes within the columns. (lateral ventricle, LV)

(Scale bar: A-C, 50μm; D, 20μm)

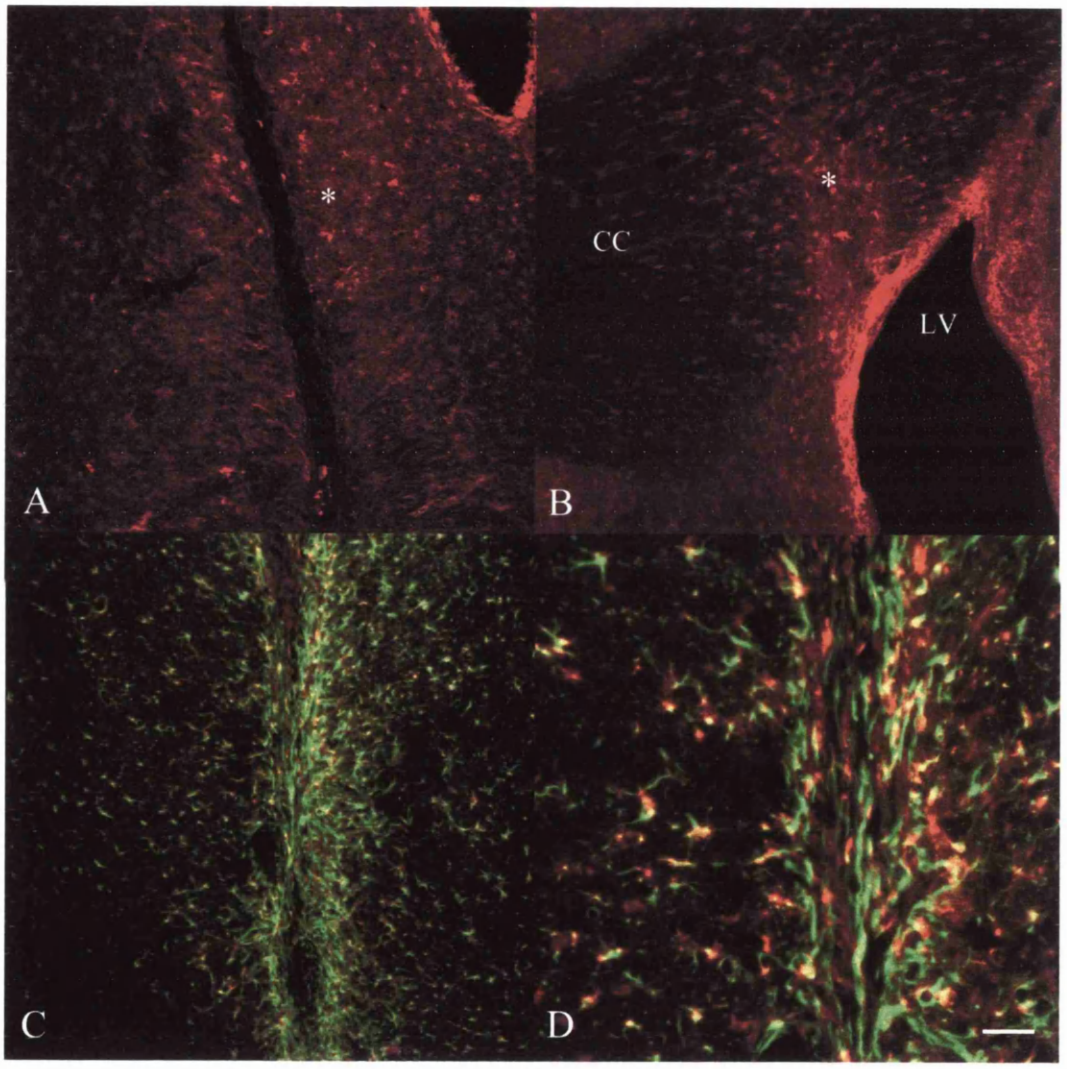
A
B
CC
LV
C
D

4.3.2.5 Modest numbers of neurofilament-reactive fibres are recruited into the columnar transplants

Neurofilament-reactive (NF-positive) fibres were seen within the transplants by 3d po (n=3). At this time-point, the fibres showed varicosities along their lengths and were seen at both the bases of the transplants in the septal cholinergic nuclei, and at the dorsal aspects of the column close to the corpus callosum.

At later time-periods, NF-positive fibres were identified along the length of the transplant and they displayed elongative, unbranched axonal growth with few varicosities (n=10) (Fig. 4.12).

NF-positive fibres were also seen in transplants into other regions of the brain where NSC transplants had been deposited away from the intended target of the septal cholinergic neurons. These regions included the medial edge of the lateral ventricle, the inferior edge of the anterior commissure and the cortex above the corpus callosum (Fig. 4.13). The morphology of the NF-positive fibres in these locations was as found in the columns originating in the basal forebrain.

Immunostaining for the peripheral myelin protein, P0, showed that the axons within the SC columns of the basal forebrain had not been myelinated by the SCs. This was carried out on animals which had transplants that were at least 4 weeks po (n=3) (data not shown).

4.3.2.6 p75- and ChAT-immunostaining of septal cholinergic neurons

Cholinergic neurons of the basal forebrain are immunoreactive for both p75 and ChAT antigens. Given that NSCs also express p75, an immunostaining protocol was required which could give specific staining of the two antigens. Fig. 4.14 shows the result of specific staining in the nuclei of the septal cholinergic neurons; the punctate

Figure 4.12 Neurofilament-positive fibres are recruited within the transplants (coronal sections stained with pan-axonal neurofilament, DAB method). Neurofilament-positive fibres can be seen running along the length of the transplant (A), and display a long, unbranched morphology with few varicosities; some fibres are seen running directly from the base of the brain (B).

(Scale bar, 40μm)


A
B

Figure 4.13 Neurofilament recruitment by SC columns in the brain. Recruitment of neurofilament-positive axons (green) by SC columns (red) in 2 aberrantly placed transplants, 'A' lateral to the basal cholinergic neurons close to the ventral border of the striatum (str), and 'B' in the cortex (cx) ('A' and 'B' are both projected confocal images of double-labelled sections stained using TSA). Neurofilament-positive axons could also be identified in transplants situated at the medial border of the lateral ventricle (LV) (A) and at the ventral border of the anterior commissure (ac) (B); immunoreactive axons were identified using DAB staining.

(Scale bar: white, (A,B) 30μm; black, (C,D) 50μm)

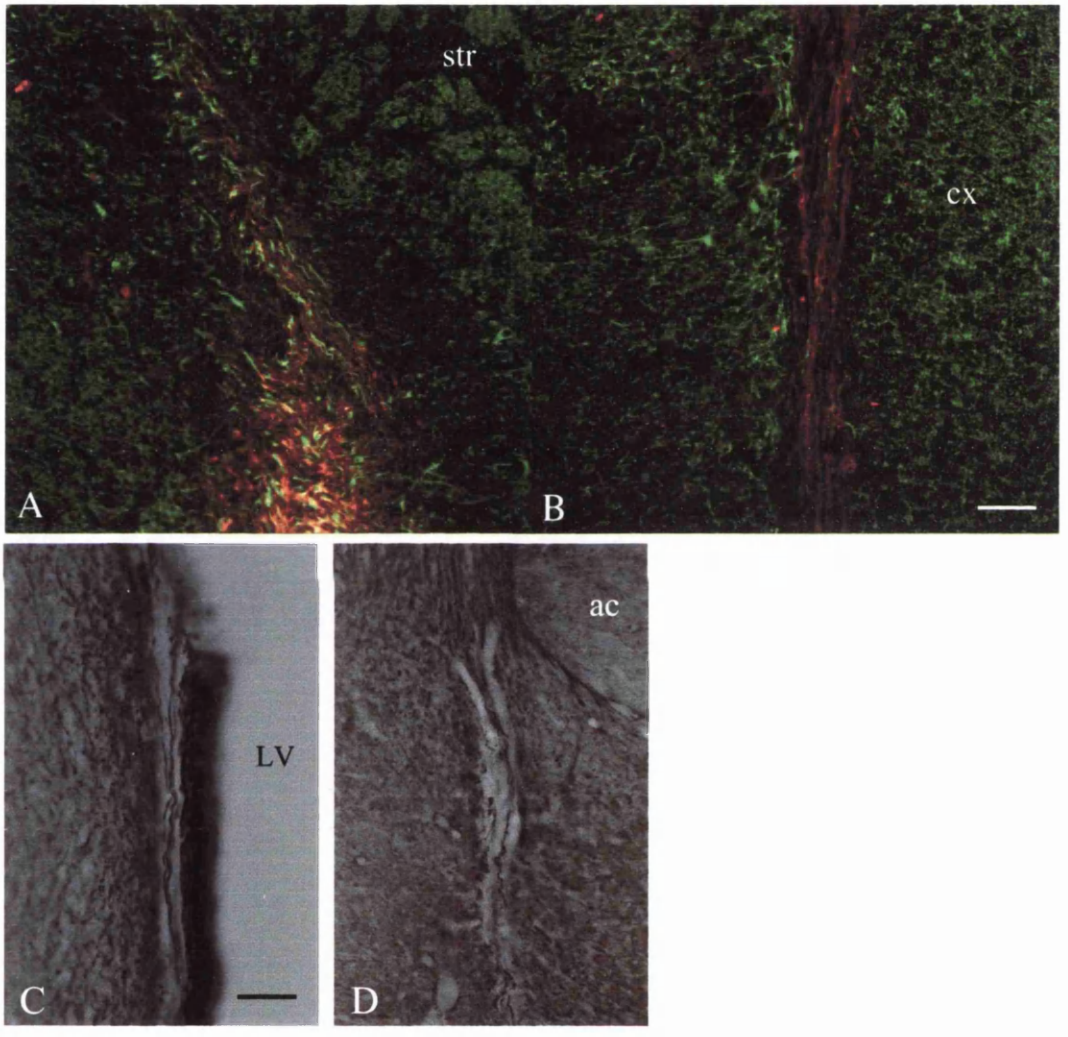
str
cx
A
B
LV
C
ac
D

staining of the p75 receptor antigen is in contrast to the stronger cytoplasmic staining of the ChAT enzyme; the combined image shows co-localisation of the two antigens.

However, while immunostaining with p75 and ChAT identifies the cholinergic nuclei, only ChAT is also able to clearly identify axons in the region of the transplant. At no time were p75-positive processes found within the region of the transplant in normal animals or on the contralateral side of animals with transplants (data not shown). The p75-positive processes which were found within the transplant area were therefore taken to be those of the SCs.

4.3.2.7 Recruitment of ChAT-positive fibres by the SC transplants

ChAT activity was markedly increased in the cell bodies and the processes of the basal septal cholinergic neurons by 3d after transplantation (n=2). ChAT-immunoreactive (ChAT-IR) fibres displayed varicosities in the region of the base of the transplant, as found with NF-immunostaining, and at several points along the column (Fig. 4.15). At later time-periods, staining revealed ChAT-IR axons within the columns, although this was not obvious at low power magnification, and was often overwhelmed by the stronger p75-staining of transplanted SCs.

ChAT-IR fibres could be seen entering the base of the transplant by 3d (Fig. 4.16) and double labelling showed a close association with p75-positive SCs (4.17) (n=2). This was evident at later time-points up to 34d po, where double-staining of the full length of the transplant column showed co-localisation of the SCs and recruited ChAT axons, as seen in Figure 4.18; ChAT-positive fibres were identified entering the base of the p75-positive transplant and were visible along the length of the column, although in moderate numbers only.

A higher magnification of the dorsal aspect of the same column can be seen in Figure 4.19; SCs were identified by immunostaining using ABC and the TSA-red conjugate (2.3.3.4), ChAT-IR fibres were identified with TSA-green. SCs in this region have migrated in flares off the main body of the transplant (F) and the immunostaining pattern of the two antigens demonstrates that there is an associated elongative growth of cholinergic axons within these flares. Given that the red signal, representing the SCs, extends beyond that of the green ChAT signal, it suggests that migrating SCs have induced elongative growth of cholinergic axons behind them.

In addition, in all cases where the SCs at the superior end of the columns had crossed the corpus callosum, small numbers of either NF-positive or ChAT-positive fibres were found extending with them (n=4). These fibres were seen within 3d of the transplantation, and showed varicosities and no branches in growth (Fig. 4.20).

4.3.2.8 ChAT-IR fibres enter the transplant before astrocytic process invasion

Double-staining of ChAT with GFAP at early time points shows that ChAT-IR axons are recruited into the base of the transplant and extend dorsally within the transplant by 3d, prior to astrocytic process invasion and alignment (n=2) (Fig. 4.21). ChAT-positive axons can be seen entering the transplant past GFAP-positive processes and then extending dorsally within the transplant. Some ChAT-IR fibres are associated with astrocytic profiles at the border of the transplant (Fig. 4.21B). This is in contrast to the frequent close association of SCs and ChAT-positive axons evident in adjacent sections (Fig. 4.17).

Figure 4.14 Septal cholinergic neurons (projected confocal images of coronal sections immunostained with p75 and ChAT (TSA method) in normal animals). Sections of neuronal cell bodies show positive cytoplasmic staining for ChAT antigen (A), and punctate staining for the p75 receptor antigen in the same section (B); the combined image in C shows co-localisation of the two antigens (p75-red, ChAT-green) in the nuclei. Immunostaining for the ChAT antigen produced intense staining in the septal cholinergic nuclei, with all dendrites and axons cleanly visible (D).

(Scale bar: A-C, 20μm; D, 12μm)

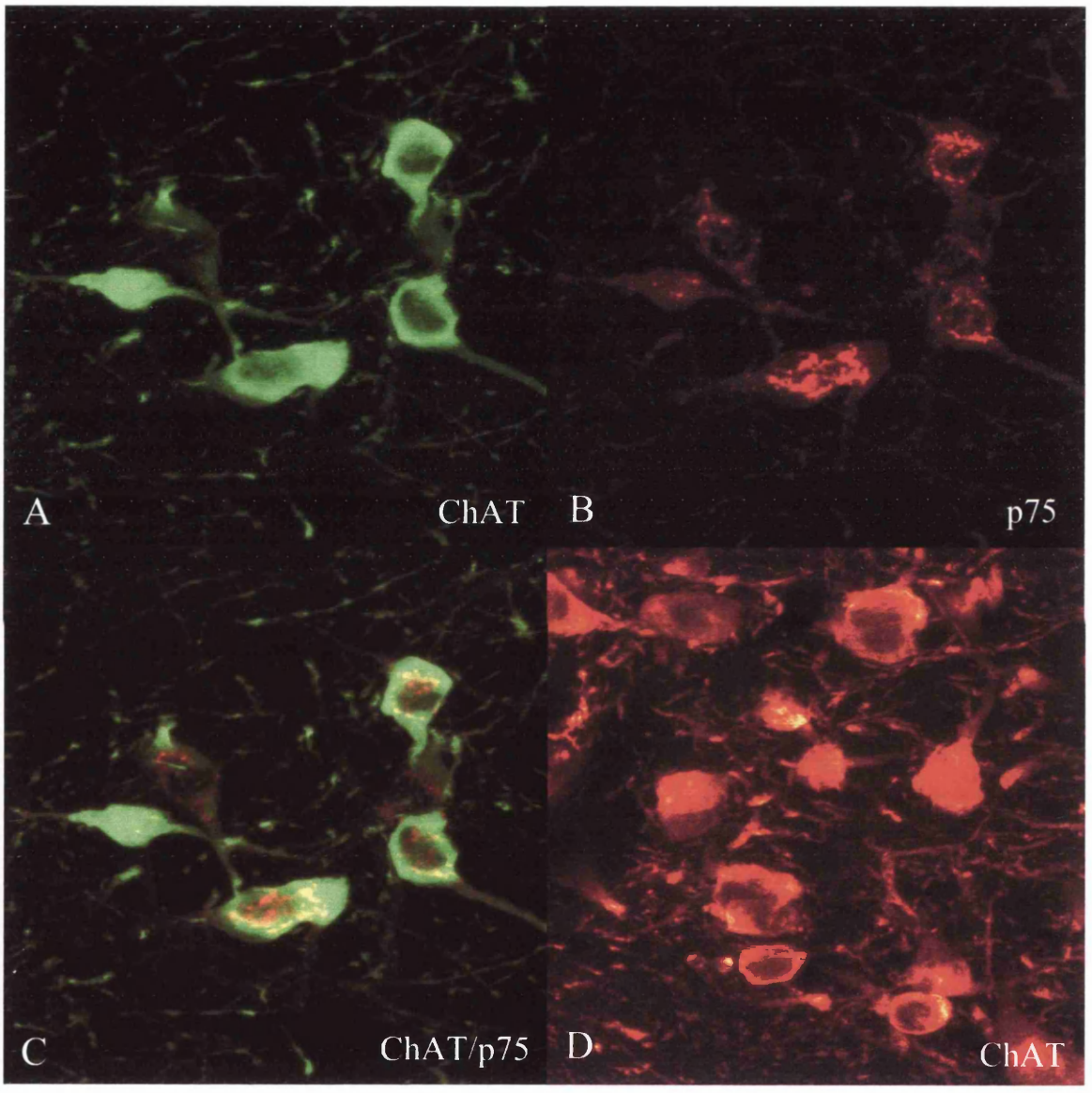
A
ChAT
B
p75
C
ChAT/p75
D
ChAT

Figure 4.15 ChAT-positive fibres in a full length transplant (montage of projected confocal images of coronal sections stained for the ChAT antigen; optical sections were taken through a 40μm depth through the transplant) ChAT-positive fibres are recruited from the septal cholinergic neurons (scn) at the base of the transplant, and can be seen at intermediate points dorsally through the transplant. Perfusion is at 7d.

(Scale bar, 80μm) (lateral ventricle, LV)


LV
scn

Figure 4.16 ChAT-IR fibres are recruited within 72h (projected confocal images of coronal sections, stained with the TSA method). There is significant ChAT-immunoreactivity at the base of the transplant by 72h which is directed towards the base of the transplant (A). In another animal at the same time period, individual axons can be seen running directly into the base of the transplant; the axons show straight, elongative axonal growth (arrows in B and C). 'D' shows ChAT-positive fibres recruited into the transplant at 7d po.

(Scale bar: A,B,D - 60μm; C, 25μm)

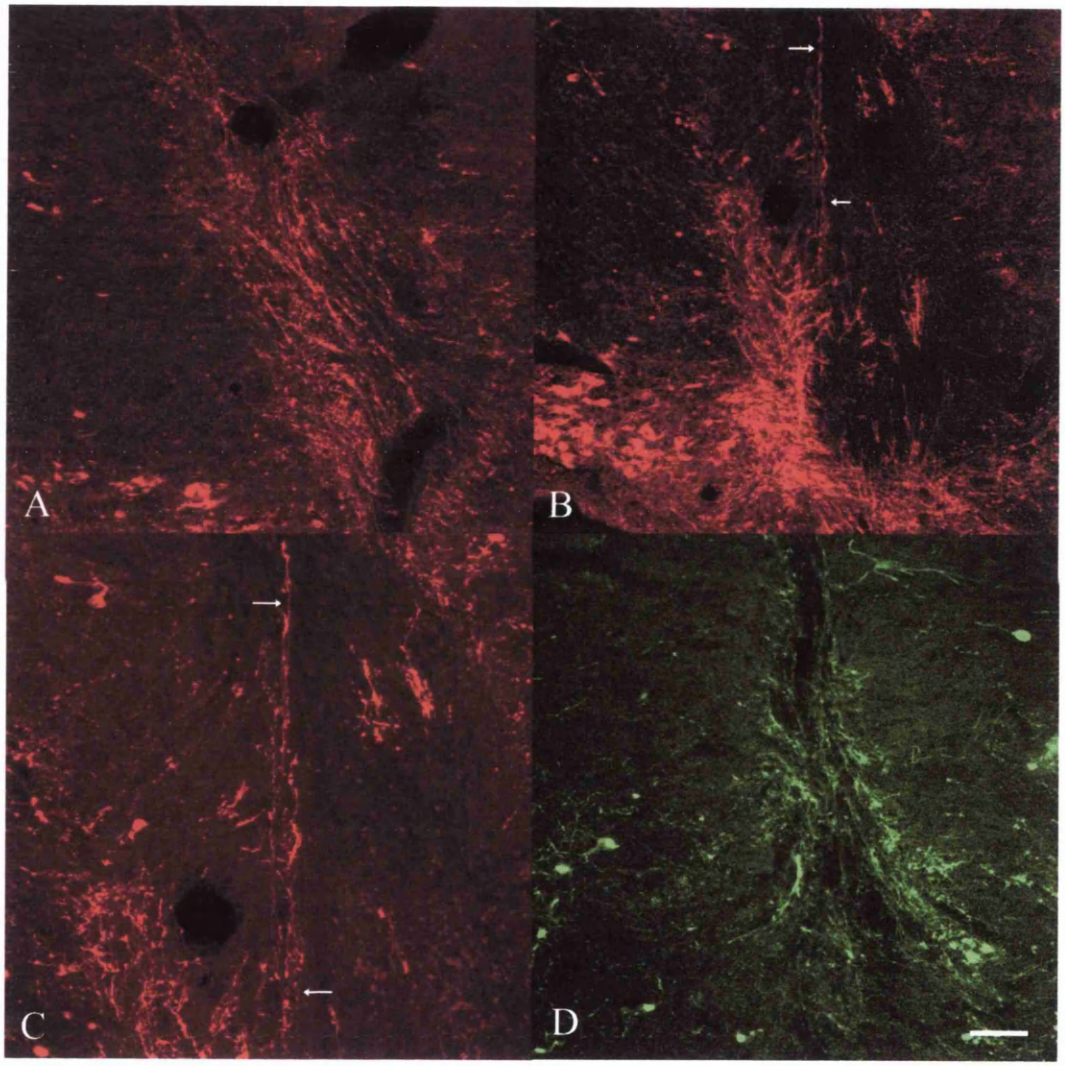
A
B
C
D

Figure 4.17 Co-localisation of SCs and recruited ChAT-axons (projected confocal images of a p75/ChAT double-stained coronal section of a transplant at 72h, stained using the TSA method). ChAT-IR fibres (green) can be seen recruited into the base of the transplant (A), which co-localise with p75-positive SCs (red) in the same section (B, asterisk in C). Dorsal and ventral aspects of the transplant in this section can be seen at higher power in 'C' and 'D', respectively; note, in particular, the intimate association of one pair of SCs (red) and ChAT axon(s) (green) defined by the arrowheads in D.

(Scale bar: A,B - 60μm; C,D - 15μm)

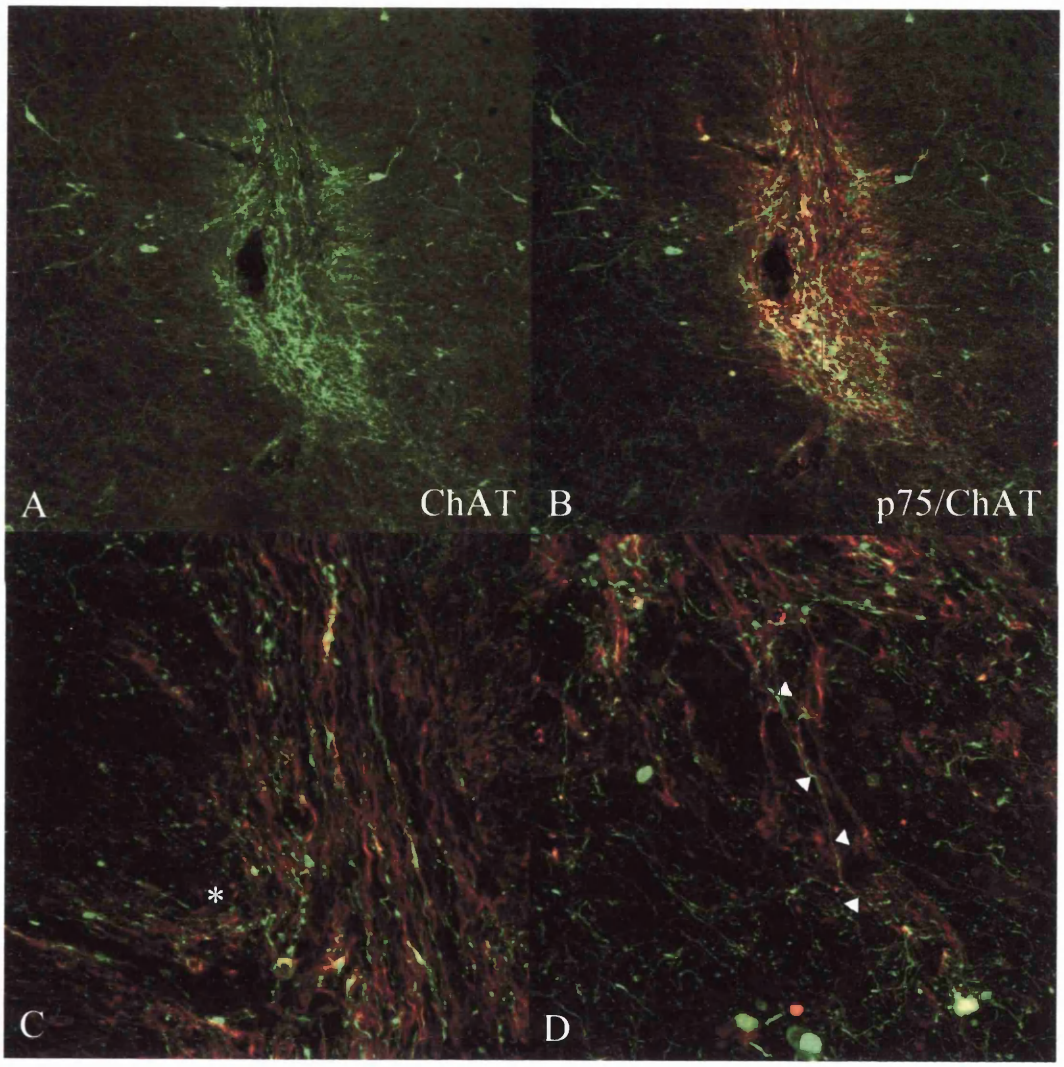
A
ChAT
B
p75/ChAT
C
D

Figure 4.18 Full length column double-stained for p75 and ChAT antigens (A and B are montages of projected confocal images, each of which consist of optical sections taken through a 50μm depth throughout the length of the transplant; p75 (red) and ChAT (green) were stained with the TSA method; C is the overlay image). Taken from a transplant at 34d, these images show a fully formed transplant (tra) and associated recruitment of ChAT-positive fibres within the column. Note especially the ChAT-IR fibres entering at the base of the transplant (asterisk). The dorsal aspect of the transplant (marked 'f') can be seen at higher magnification in Fig. 4.19. (septal cholinergic nuclei (scn); lateral ventricle (LV))

(Scale bar, 90μm)

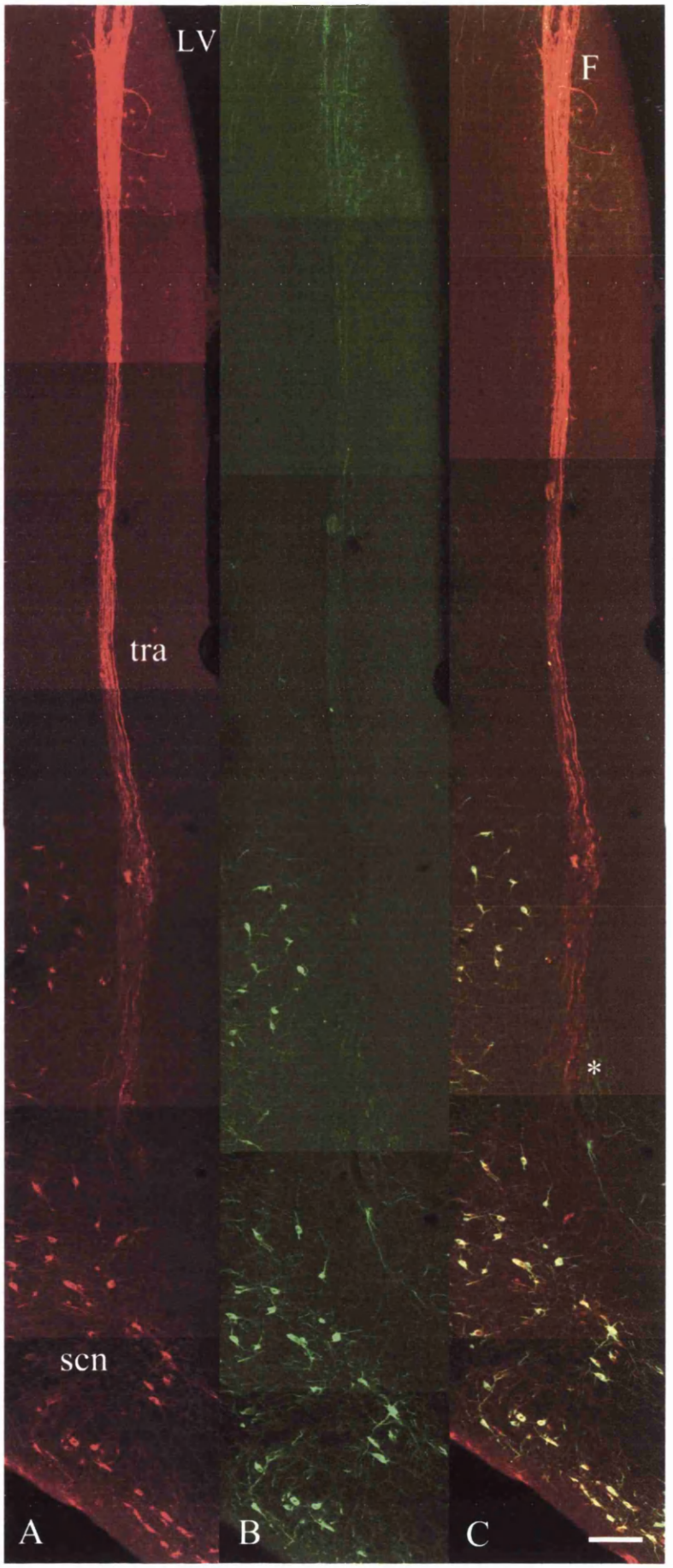
LV
F
tra
*
scn
A
B
C

Figure 4.19 Dorsal aspect of a transplant showing co-localisation of SCs and ChAT-positive fibres (high magnification image taken of the dorsal aspect of the column seen in Figure 4.18). SC processes (red) co-localise with ChAT-IR fibres (green) in the transplant; one major flare (F) of migrating SCs can also be seen, co-localising with ChAT-IR fibres.

(Scale bar, 50μm)

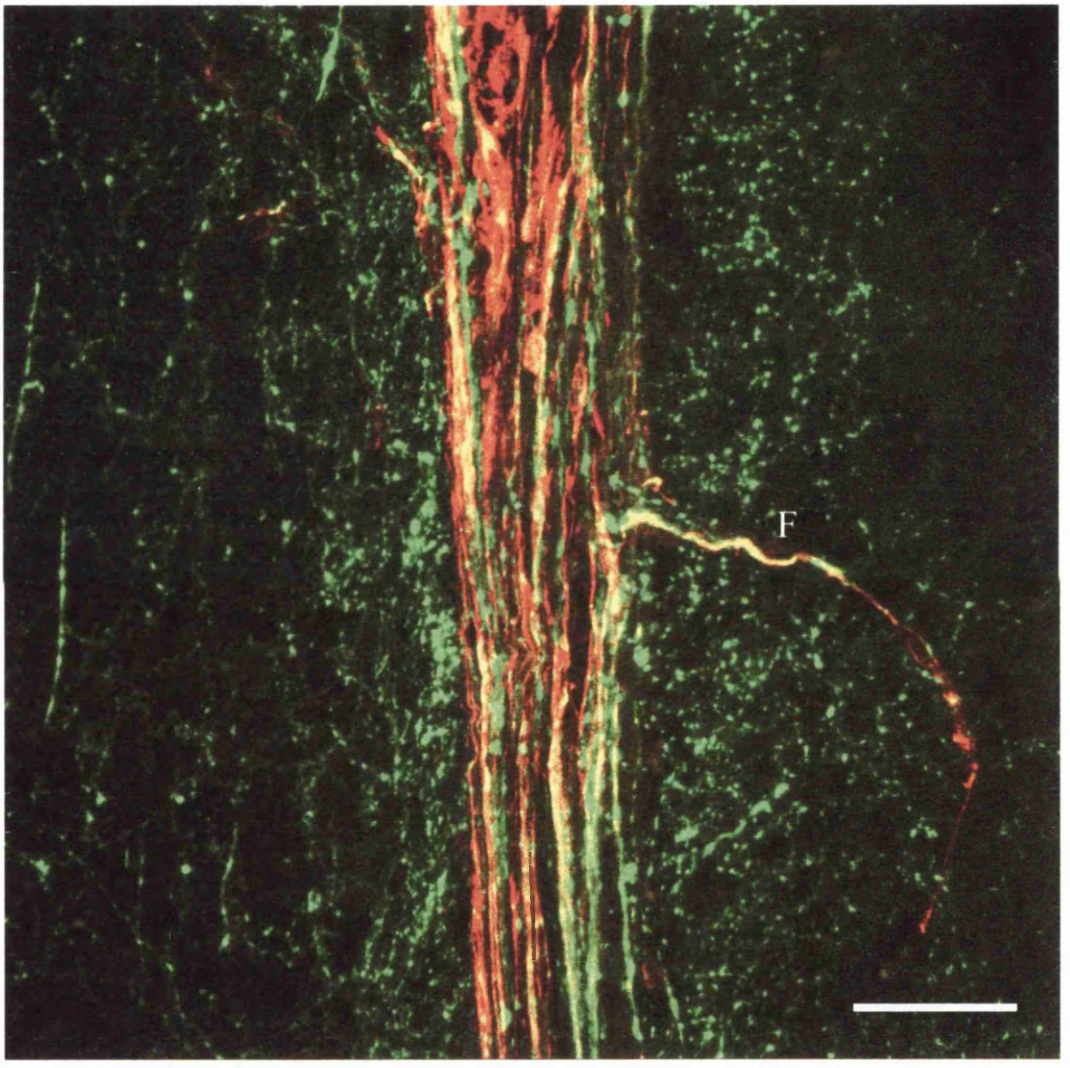
F

Figure 4.20 ChAT-fibre recruitment across the corpus callosum (coronal sections stained with ChAT (red) and GFAP (green) (TSA method); projected confocal images of the dorsal aspect of the transplants, adjacent to the corpus callosum). ChAT-fibres can be identified at low (A,C) and high (B,D) magnification of the same section, crossing the corpus callosum (cc) at 3d (A,B) and 7d (C,D); ChAT-immunoreactivity is increased on the supracallosal (sf) fibres (A). C,D are additionally stained with GFAP to show the associated astroglial reaction; the arrowheads in 'D' delineate closely associated ChAT-IR fibres with GFAP-IR astrocytic fibres (asterisk represents tear in tissue; striatum (str), lateral ventricle (LV)).

(Scale bar: A,C - 50μm; B,D - 13μm)

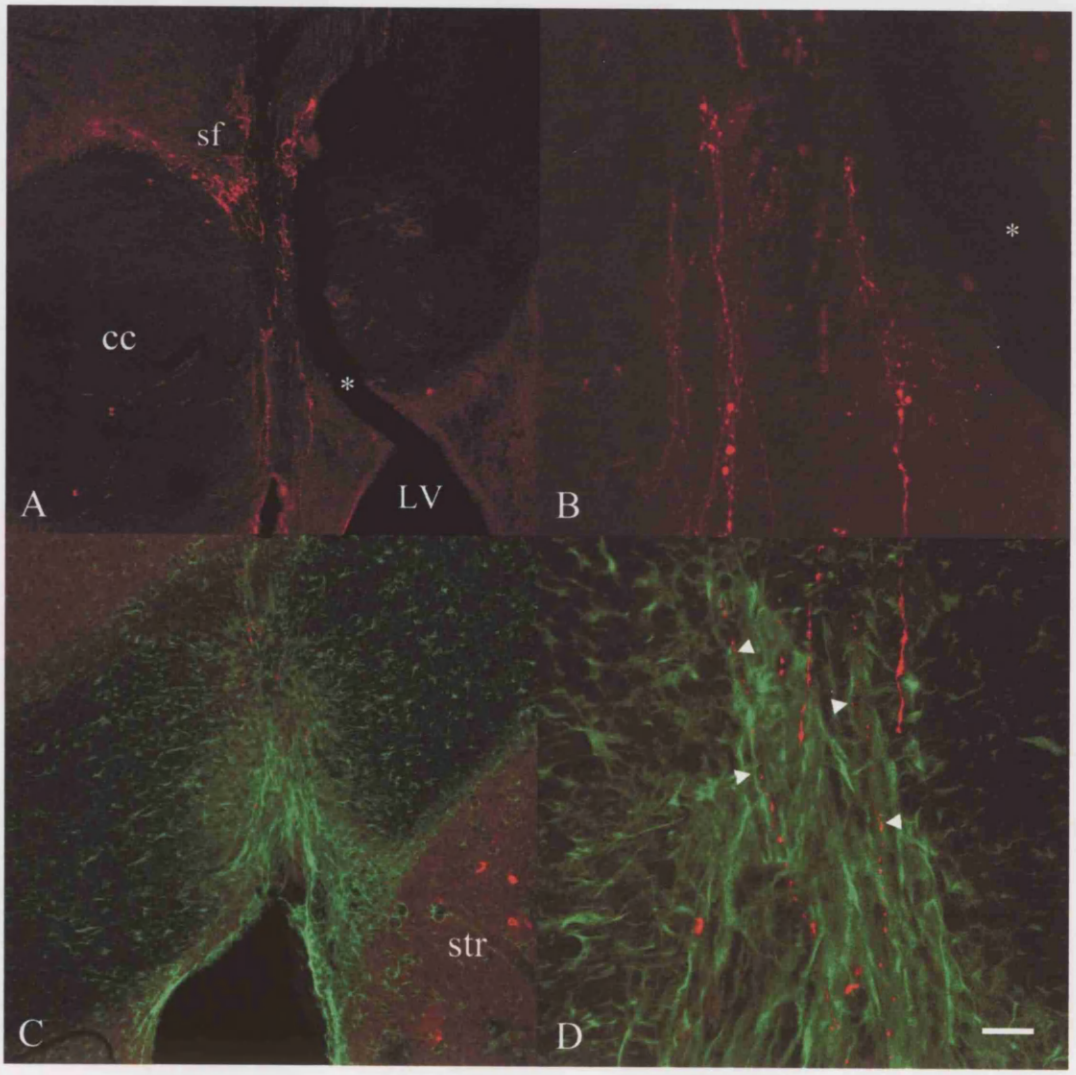
sf
cc
*
LV
A
B
*
str
C
D

Figure 4.21 ChAT recruitment is prior to astrocytic process invasion (projected confocal images of a ChAT/GFAP double-stained coronal section, taken through a 35μm depth; animal perfused at 3d) ChAT-positive (red) axons can be seen entering the body of the transplant which is absent of GFAP-positive (green) processes (A). Higher magnification of 'A', shows axons (red) entering the transplant and turning dorsally within the transplant (B); note also the association of some ChAT-immunoreactive axons with GFAP-astrocytic profiles (arrowheads in B). (septal cholinergic neurons, scn) *(Scale bar: A, 50μm; B, 13μm)*

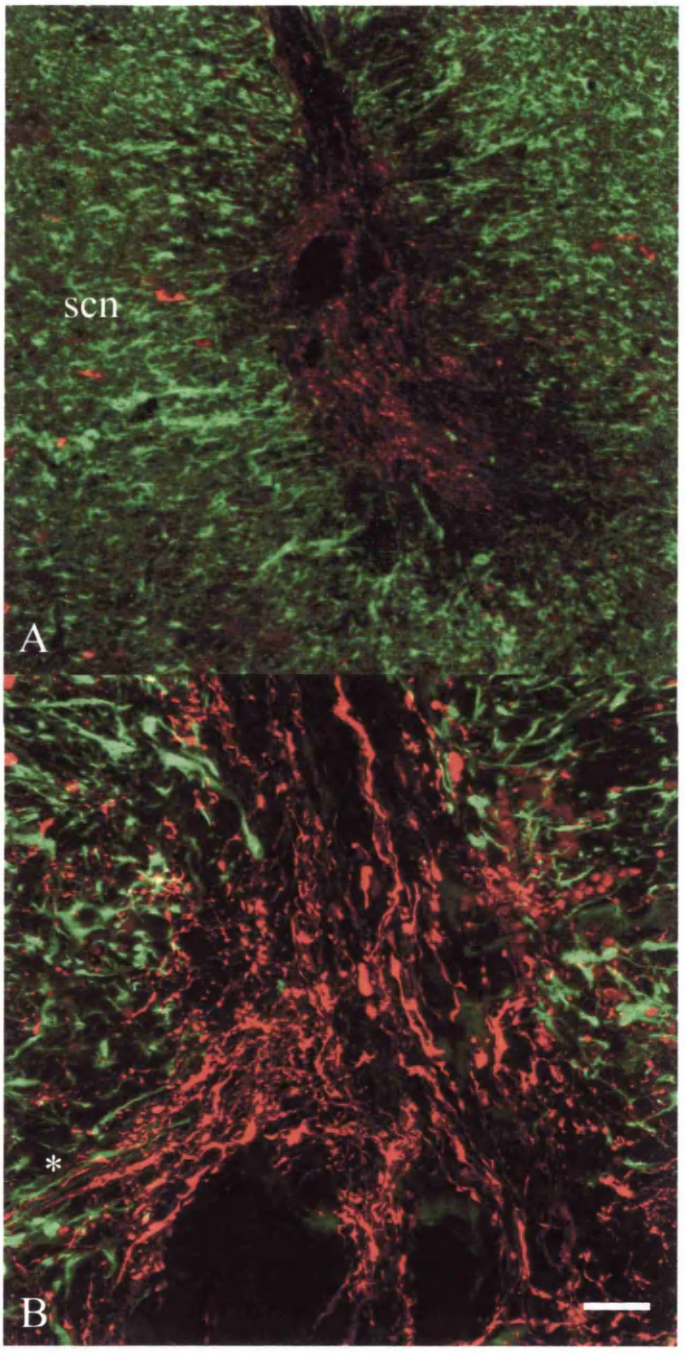
scn
A
*
B

4.3.2.9 Some but not all recruited axons are cholinergic in phenotype

Although some fibres recruited into the SC transplants were ChAT-IR, other axons were identified which were tyrosine-hydroxylase (TH)-reactive, and others which were NF-reactive but not ChAT-IR (n=3) (Fig. 4.22). However, although some increase in TH activity was observed in the region of the transplant at 3d and 7d po (n=3), elongative growth could not be identified within the columns at later time points (not shown).

4.3.2.10 Control sections and transplants

All immunostaining was carried out with control sections in parallel where the primary antibody was omitted and these demonstrated no end-staining (not shown). Controls were also used to develop specific double-staining protocols (Fig. 23A,B).

In addition, animals were transplanted with DMEM alone, in the absence of SCs, as an additional control (n=2). These reproduced the gliotic reaction surrounding the injection track (data not shown), but demonstrated an absence of both p75-and ChAT-IR fibres within the column (Fig. 4.23C,D).

Figure 4.22 Non-ChAT-IR axons within the transplant (projected confocal images of TH-red/ChAT-green (A,B) and NF-red/ChAT-green (C) double-labelled sections of transplants stained using TSA signal detection, and taken at 3d (A,C) and 7d (B)). Transplants showed ChAT-IR axonal recruitment into the SC columns although some transplants also showed stimulation of tyrosine hydroxylase-immunoreactive fibres (A,B). Other transplants demonstrated that many neurofilament-reactive axons were not also ChAT-immunoreactive (C).

(Scale bar: A,B - 60μm; C, 24μm)

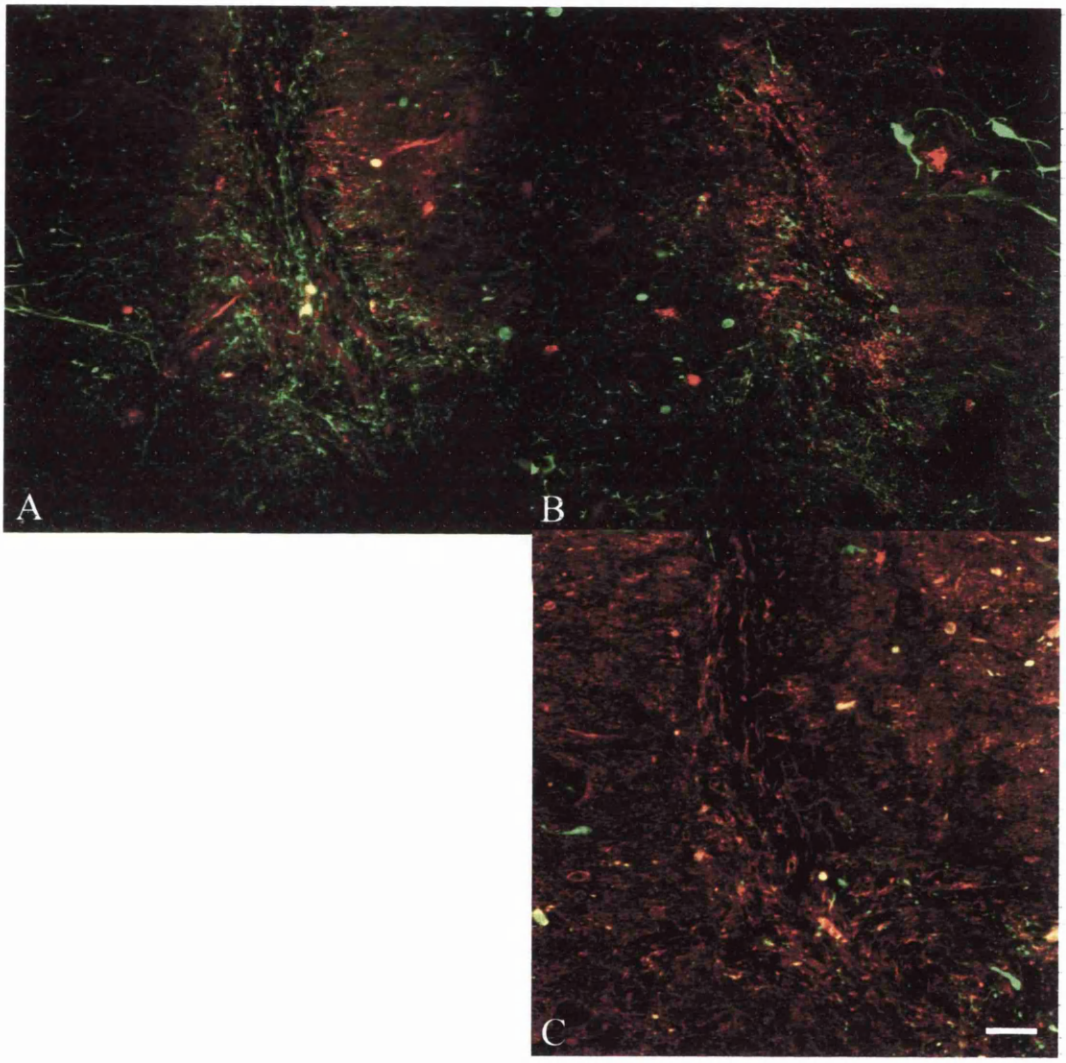
A
B
C

Figure 4.23 Control sections (projected confocal images of dorsal striatum of normal, unoperated animals (A,B), and basal forebrain of animals with a control DMEM transplant (without cells) perfused at 4 months (C,D). 'A' shows specific staining of ChAT-positive neurons (red) in the dorsal striatum (str) with ubiquitous GFAP-positive astrocytes (green); B shows ChAT-positive striatal neurons (green) against a tyrosine hydroxylase-positive striatum (red).

Control transplants of DMEM alone into the basal cholinergic neurons (scn) demonstrate no up-regulation or recruitment of ChAT-IR (green) fibres into the base of the transplant (C) or more dorsally within the column (D). (corpus callosum, cc; lateral ventricle, LV)

(Scale bar, 50μm)

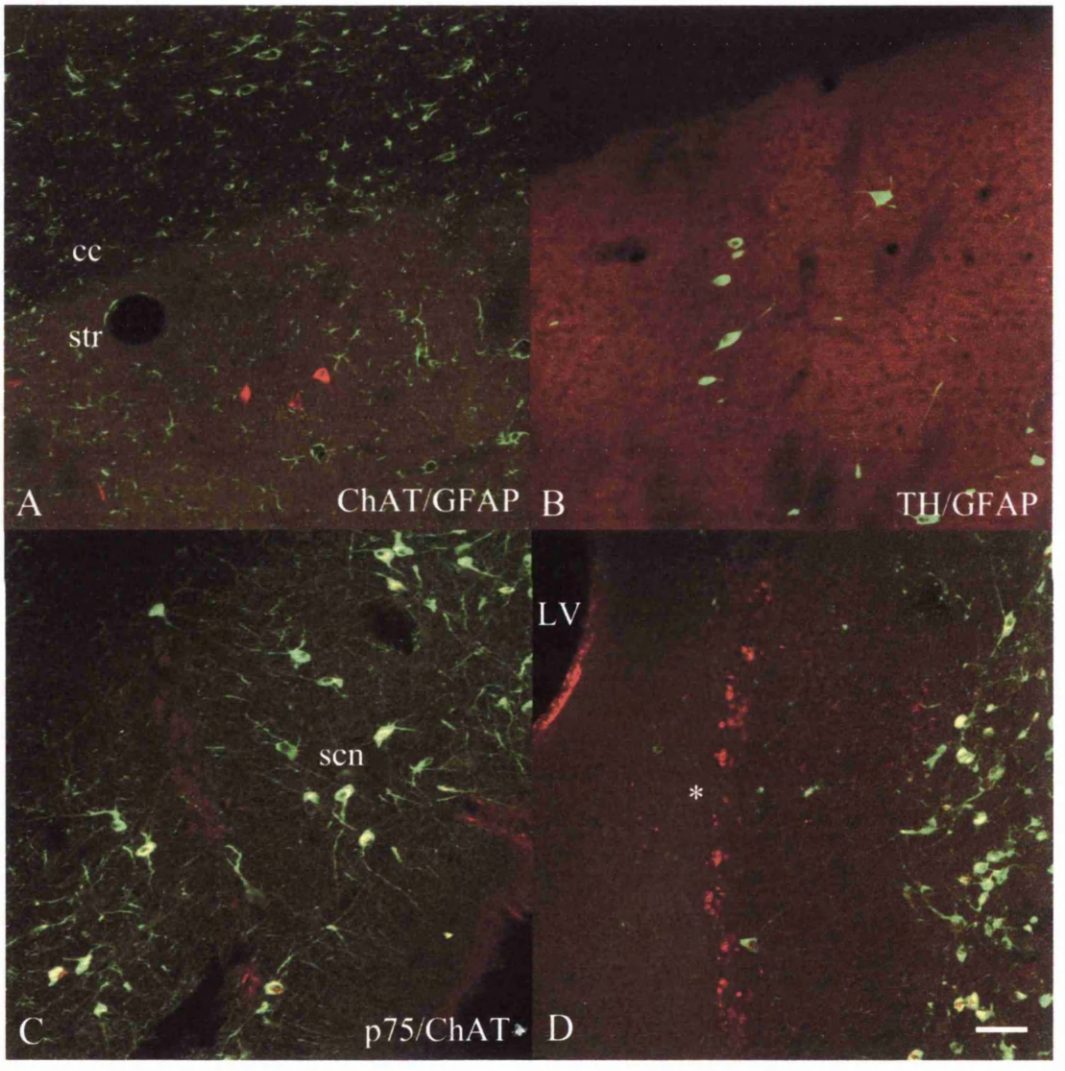
cc
str
A
ChAT/GFAP
B
TH/GFAP
scn
C
p75/ChAT
LV
*
D

4.4 Discussion

When extruded into the nuclei of the septal cholinergic neurons, suspensions of neonatal SCs form tight and ordered columnar transplants which readily integrate with host glia. These SC columns are able to recruit cholinergic axons from the base of the transplant into the columns, through which they are able to show elongative axonal growth for several millimetres. Several aspects of the SC columns will now be discussed in turn.

4.4.1 Formation of SC columnar transplants within the basal forebrain

Extruded SC columns consist of aligned SC processes

The SC columns are well-developed by 72h of the injection of the SCs, and consist of aligned processes which lie discretely in the trajectory of the injection track. This phenomenon has been observed before with extruded SCs in the thalamus (Brook *et al.*, 1994). The alignment of processes is likely to be the result of the extrusion transplantation procedure where cells are deposited at intermittent points along the vertical track, and of the cell-cell communication of the transplanted SCs. The ability to form columnar transplants, however, is not exclusive to SCs since at least fibroblasts transplanted in this way are also able to form similarly aligned transplants (Brook *et al.*, 1994; Kawaja *et al.*, 1992). In contrast, there is no associated axonal extension within normal fibroblast transplants.

In previous studies of SC suspension transplants in the brain, the cells have generally been deposited in a bolus at the intended site, although they might subsequently show some migration and alignment within nearby white matter tracts (Montero-Menei *et al.*, 1992; Stichel *et al.*, 1996). SCs transplanted directly into the corticospinal tract have also been found aligned along the longitudinal axis of

the white matter fibre tracts (Li and Raisman, 1997). However, as with the initial extrusion transplants described by Brook et al., (1994), the SCs in the present study form an aligned columnar transplant which is shaped by the transplantation procedure rather than by the interaction with the local environment. Although the host glia are later involved in the cellular make-up of the transplant, the basis of the transplant is the formation of aligned SC processes.

The SC columns are stable up to at least 45d po. Identification with the p75 antibody is not effective beyond this time, perhaps due to down-regulation of the receptor after ensheathment of the axons (Heumann *et al.*, 1987b). Ultrastructural studies have shown that the transplanted SCs can still be identified in the columns at 5 months po.

SCs in the transplant integrate with host glia

Astrocytic processes can be seen entering the transplant from 1 week post-operation and continue to extend aligned processes within the body of the transplant over the next 3 weeks. The identification of oligodendrocytes in the transplant has been less clear; the use of the APC antibody (Bhat *et al.*, 1996) in this context has led to clearer recognition of the cell bodies than that of their processes. However, aligned APC-immunoreactive processes could be recognised within the transplant, and double-labelling with the GFAP antigen demonstrated the presence of adjacent astrocytic processes. The extent of oligodendrocyte process alignment was slight, as determined by APC-immunoreactivity, and not as pronounced as that of the astrocytes.

The presence of aligned astrocytic processes is a structural feature of normal white matter tracts in the CNS; processes of astrocytes and oligodendrocytes lie in

the longitudinal axis of the normal adult rat fimbria and, together with the remaining host glia in the tracts, form neatly arranged and ordered rows through which axons can extend (Suzuki and Raisman, 1994). The composition of the extrusion transplants shows some resemblance to the normal white matter tract anatomy described above in that SC and astrocytic processes extend aligned, interdigitated processes along the length of the transplant. The presence of transverse processes, as described in the fimbria in the above study, is less obvious in the extruded transplants of the present study and is perhaps a function of the narrower transplant width in the present study.

The time period of astrocyte infiltration into the transplant is also shorter in the present suspension transplants than in other more solid grafts, in which astrocyte penetration does not take place until 3 weeks post-transplant (Kawaja and Gage, 1991; Xu *et al.*, 1995). This may have an impact on the subsequent composition of the grafts if astrocytes are absent from them for several weeks, and also on the subsequent local environment for induction of central axonal growth (Kawaja and Gage, 1991).

Astrocytic processes are intimately associated with those of SCs

Although there is a host glial reaction to the SC transplant that is typical of host tissue invasion (Bignami and Dahl, 1976), the resultant increase in GFAP immunoreactivity in the present study is minimal. From approximately 1 week po, astrocytes begin to extend aligned processes into the transplant and double-labelled sections show the close association of the SCs with the astrocytic processes which develops with subsequent time post-operation. SC and astrocytic processes are frequently observed in direct apposition.

It is important to note that although SCs may express GFAP in culture (Jessen *et al.*, 1990), axonal contact *in vivo* induces a differentiated SC phenotype and with it, down-regulation of GFAP. As a result, the GFAP immunoreactivity *in vivo* can be attributed solely to the astrocyte population. The observation that there is no overlap of the signals of p75 and GFAP in p75/GFAP double-labelled sections is consistent with this idea (Figs. 4.9, 4.10).

Studies of glial cell transplants into the X-irradiated, demyelinated spinal cord have shown an exclusion of SCs by astrocytes under certain conditions (Blakemore and Franklin, 1991; Blakemore and Patterson, 1978); the migration of SCs and their remyelination of host axons is limited by the astrocytes in favour of central remyelination. A similar restriction of SC migration has been described for SC transplants in the neonatal *shiverer* brain (Baron Van Evercooren *et al.*, 1992); the transplantation of cells, rather than as part of a peripheral nerve fragment, led to an absence of SC myelination and the gradual exclusion of the SCs in favour of the resident astrocytes.

These studies suggest an incompatibility of SCs with astrocytes in the CNS and that in the context of axonal regeneration, the presence of astrocytes might compromise the ability of SCs to induce central axonal growth. Further *in vitro* and *in vivo* studies have sought to characterise the astrocyte-SC interactions which may underlie this behaviour, and implicate chondroitin sulphate proteoglycan as a candidate mediator of this behaviour (Ghirnikar and Eng, 1994; Ghirnikar and Eng, 1995; Guenard *et al.*, 1994).

In the present study, however, SCs and astrocytes are observed together in an intimate relationship and in the presence of central axonal growth. The nature of the transplantation procedure may be a contributing factor to the close association

that results between the SCs and host glia; the absence of a solid graft containing multiple components affords a closer, more immediate interaction of the SC suspension transplant with host glia. In contrast to the above studies, the SCs are not excluded from their site of transplantation and appear to show a compatible relationship with resident astrocytes.

4.4.2 Recruitment of cholinergic axons within the SC transplants

ChAT-axons are recruited at the base and dorsal extent of the columns

Recruited neurofilament-immunoreactive fibres can be seen at the base of the transplant, where ChAT-immunoreactive (ChAT-IR) fibres are identified entering the transplant and extending dorsally within the column, and at the dorsal aspect where ChAT-IR fibres can be identified crossing the corpus callosum. As ChAT-IR axons are not normally seen in these regions of the SC transplant in adult life, it can be taken that these axons represent new growth; that they are fine in morphology and show varicosities is consistent with this idea.

The normal septohippocampal pathway in the adult rat consists of axons which project rostrally and dorsally through the fimbria-fornix and supracallosal pathways, and then caudally to innervate distal cortical and hippocampal targets (Dutar *et al.*, 1995). In the present study, ChAT-IR axons are extended dorsally from the septal nuclei such that they extend in a plane which is posterior and nearly parallel to the normal projection. This type of induction of axonal growth appears to be the first example of ChAT-IR axons extending directly from the nuclei of the septal cholinergic neurons, and in a direction and a pathway which they would never take in normal life.

Given the normal projection of the septohippocampal pathway, it is likely that axons of the supracallosal striae, *en route* to cortical and hippocampal targets, are recruited into the dorsal aspects of the SC columns. While it is possible that those axons recruited from the septal nuclei at the base of the brain extend dorsally through the column to reach the dorsal-most extent of the transplants, a number of features suggest that this is not the case. Firstly, single axons could not be traced for the full length of the column; secondly, there was a strong ChAT-IR of the supracallosal fibres which was observed end-on in the coronal sections; finally, the short time-period of 3d post-operation is not likely to provide sufficient time for the basal septal axons to reach the dorsal extent of the column transplants.

Cholinergic axonal growth within the transplants is associated with SCs

Double-immunostaining shows that the cholinergic axons recruited by the transplants are associated with p75-IR SC processes. The induction of cholinergic axonal growth by SCs or SC-containing grafts has been observed using a number of other methods (Hagg *et al.*, 1990b; Kromer and Cornbrooks, 1985; Montero-Menei *et al.*, 1992; Stichel *et al.*, 1996). The mechanisms underlying the induction of axonal growth by SCs may involve many processes in concert. SCs possess a number of features which may enable them to support axonal regeneration (Ide, 1996).

Firstly, SCs produce and secrete a well-established profile of growth factors. These include the original nerve growth factor, NGF, BDNF and CNTF (Acheson *et al.*, 1991; Assouline *et al.*, 1987; Sendtner *et al.*, 1991). The role of NGF, in particular, may be a key component of the growth-promoting effect on septal cholinergic neurons as observed in the present study; that exogenous NGF has long

been known to stimulate the growth and survival of lesioned cholinergic fibres is consistent with this idea (Hefti, 1986; Rosenberg *et al.*, 1988). A recent paper has shown that septal cholinergic neurons may also be responsive to the fibroblast growth factor, FGF-2 (Fagan *et al.*, 1997).

SCs also produce a number of cell adhesion and extracellular matrix molecules which have found to be important in axonal growth *in vitro* (Bixby *et al.*, 1988; Seilheimer and Schachner, 1988). A peripheral nerve transplant study carried out in the adult rat thalamus studied this *in vivo* and correlated the expression of L1, NCAM (Neural Cell Adhesion Molecule) and NCAM-PSA (the embryonic, polysialylated form of NCAM) with regenerating axons (Zhang *et al.*, 1995a); the up-regulation of L1 was particularly significant in the neurons of the thalamic reticular nucleus (Benfey *et al.*, 1985). An accompanying study of the same model further showed the immunoreactivity of tenascin-C on regenerating thalamic axons extending through the SC graft (Zhang *et al.*, 1995b); the presence of a putative tenascin-C receptor on the axons was suggested to have mediated the growth-promoting effect of the peripheral nerve graft-derived tenascin-C.

A more recent study has reported the expression of L1 and NCAM-PSA in the fimbria-fornix of the basal forebrain system (Aubert *et al.*, 1998). Transection of the fimbria-fornix transection was followed by the assessment of the subsequent sprouting in the hippocampal formation (Crutcher and Marfurt, 1988) together with that of the expression of NCAM-PSA and L1 on the projecting septohippocampal fibres; the assessment was carried out in the presence of NGF- versus control β-galactosidase-producing fibroblasts. Analysis of multiple-labelled sections showed that both L1 and NCAM-PSA were up-regulated on regenerating ChAT-IR axons seen in the NGF-producing fibroblast grafts. Given that SCs produce NGF, it is

possible that the SCs in the present study are acting in a similar way to promote extension of the septal cholinergic axons.

The association of cholinergic axonal growth with SC processes in the present study suggests that the expression of cell adhesion molecules is involved in the induction of growth. SCs express both L1 and NCAM (Zhang *et al.*, 1995a), and may mediate extension of the septal axons through binding of these molecules, and so carry the axons through the otherwise inhibitory CNS tissue.

Another mechanism contributing to the action of the SCs on the septal cholinergic neurons in the present study might involve the neuregulins, a large group of structurally related polypeptide factors, and their receptors, four transmembrane protein-tyrosine kinases of the ErbB family and its receptors (Carraway and Burden, 1995; Gassmann and Lemke, 1997). Expression studies have shown that neuregulin is expressed in selective areas of the adult rat CNS, including the basal forebrain (Chen *et al.*, 1994). Given that SCs express the neuregulin receptors ErbB-2 and ErbB-3 (Dong *et al.*, 1995; Meyer and Birchmeier, 1995), reciprocal cell-cell interactions between the SCs and the cholinergic neurons may play a role in the observed axonal extension.

A recent study describes the induction of expression of neuregulins on peripheral nerves and the erbB receptors on SCs during Wallerian degeneration (Carroll *et al.*, 1997). The response to injury described here involved the stimulation of SC proliferation through their erbB receptors, rather than the cell contact-mediated induction of axonal growth *per se*, although there may be an additional role in the present study outside that of glial cell proliferation (Corfas *et al.*, 1995; Goodearl *et al.*, 1995). Carroll and colleagues (1997) further describe how SCs may act via autocrine as well as the paracrine routes to induce their own

proliferation in the response to nerve injury, and indeed, this may act indirectly in the present study to promote axonal growth. In fact, SCs in the present study may additionally have an impact on astrocytes, which also express neuregulin, through their close association *in vivo* (Pinkas-Kramarski *et al.*, 1994).

Cholinergic axons associate with astrocytic processes at the periphery of the transplant

The identification of ChAT-IR processes associating with astrocytic processes at the periphery of the SC transplants was observed as early as 3d post-operatively. In these sections, ChAT-IR processes could be seen entering the base of the transplant close to astrocytic processes, and when into the cavity of the transplant, ChAT axons turned and extended dorsally within the column.

The association of astrocytes and axonal regeneration is not a common event in the lesioned adult rat CNS. Astrocytes have been shown to support central axonal growth *in vitro* (Baehr and Bunge, 1990; Noble *et al.*, 1984). However, mature astrocytes, in contrast to immature astrocytes, have long been described *in vivo* as a non-permissive substrate for adult axonal growth and as an active inhibitor of central axonal regeneration (Silver, 1994).

In the presence of NGF, cholinergic neurons of the basal forebrain system have been shown on several occasions to associate and extend along the surfaces of astrocytic processes (Aubert *et al.*, 1998; Eagle *et al.*, 1995; Kawaja and Gage, 1991). As mentioned above, Kawaja et al., 1991 introduced grafts of fibroblasts, genetically engineered to produce NGF, into the striatum and showed in ultrastructural studies that axons extended along astrocytic processes within the graft. Axons were not found on astrocytic surfaces covered with basal lamina, but

were always found on glial surfaces, including on the surfaces of small numbers of endogenous SCs that had entered the grafts. In addition, given the appearance of the in-growing astrocytic processes prior to that of the axons (which were found to arise from the nucleus basalis), the authors suggested that it was the axons which had penetrated the grafts along the astrocytic surfaces and not vice versa.

Later studies suggested that it was the presence of cell adhesion molecules associated with astrocytic and cholinergic processes which mediated the successful axonal growth in the presence of NGF (Chalmers *et al.*, 1996). The identification of nerve growth factor-inducible large glycoprotein (NILE) on sprouting cholinergic axons, and the expression of NCAM on astroglial processes may in this case have combined to enable cholinergic axonal fasciculation and growth along astrocytic processes. As with the earlier studies (Kawaja and Gage, 1991), the axons in this study were those of the striatum and the transplant was composed of fibroblasts engineered to produce NGF. Cholinergic neurons did not express NILE in control transplants of normal non-engineered fibroblasts.

In the present study, astrocytic processes can be seen at the periphery of the transplants, and most clearly at the transplant bases, which were associated with ChAT-IR fibres. This is consistent with the idea that in the presence of NGF, ChAT-axons can extend along the surfaces of reactive astrocytes. These astrocyte-ChAT axon associations were not generally observed in the body of the transplant. However, given that by 3d post-operation, ChAT-IR axons and not astrocytic profiles were found within the transplant, if astrocytes did mediate the crossing of axons into the transplant, then they did not appear to play any further part within the transplant.

Some studies have shown the enhancement of the ability of astrocytes *in vitro* to support axonal growth in the presence of cell adhesion molecules, including that of L1 (Mohajeri *et al.*, 1996; Neugebauer *et al.*, 1988; Yazaki *et al.*, 1996). Other studies have shown that cytokines IL-1 with bFGF improve the ability of astrocytes to support neuritic growth, and that these effects do not correlate with the astrocytic expression of such molecules as NCAM and laminin (Fok-Seang *et al.*, 1998). Given that SCs are able to express many of these adhesion molecules, the interaction of astrocytes with SCs to promote cholinergic axonal extension seems more plausible.

Some but not all recruited axons are cholinergic in phenotype

The proportion of ChAT-positive axons from all axons which were recruited by the transplants was not formally assessed. However, double-labelled sections showed that while few axonal fibres within the transplants were tyrosine-hydroxylase positive, there was a significant number of recruited axons which were neurofilament-positive but ChAT-negative.

Non-ChAT-IR axons recruited by the transplants may be of the GABAergic class, a neuronal phenotype which forms a major complement of the axons in the septohippocampal pathway (Kohler *et al.*, 1984). SC transplants have already been documented in previous studies to recruit axons of this latter phenotype through peripheral nerve transplants in the thalamus (Benfey *et al.*, 1985; Vaudano *et al.*, 1995; Zhang *et al.*, 1995a).

The remainder of the population of septohippocampal neurons may contain a number of different neuropeptides, including in particular, galanin and *N*-acetyl-aspartyl-glutamate (NAAG) (Forloni *et al.*, 1987; Senut *et al.*, 1989). The induction

of axon growth by these classes of neurons has not previously been associated with SCs in the CNS, although some immunoreactive fibres have been associated with SCs in the normal PNS (Kuramoto *et al.*, 1996; Papka and McNeill, 1993).

4.4.3 Summary

Neonatal SCs extruded into the septal cholinergic nuclei are able to survive, form aligned cellular processes along the length of the column and integrate with the host glia. Host astrocytes penetrate the transplant from approximately 1 week and subsequently begin to extend aligned processes closely associated with SCs. These SC transplants are able to induce the extension of cholinergic axons into and within the columns for several millimetres; cholinergic axons are also recruited from the supracallosal fibres at the dorsal aspect of the transplants.

Several mechanisms may underlie the induction of elongative axonal growth within the transplants. SCs express a number of cell adhesion molecules and growth factors which are known to be growth-permissive. One of these might involve the cell adhesion molecule, L1, which has previously been associated with the growth of cholinergic axons in the presence of NGF, and which would be one target for future studies.

CHAPTER V

CHAPTER V - Retroviral Transfection of the Green Fluorescent Protein

5.1 Introduction

5.1.1 Identification of transplanted cells *in vivo*

In studies which employ the transplantation of cells *in vivo*, one must be confident that the same cells can be accurately and specifically identified at a later chosen date. The emergence of monoclonal antibodies and antibody technology as a whole has facilitated such studies. When cells are transplanted into a particular region they can be recognised by an antibody specific to that cell type, a process made easier when the cell is foreign to that tissue site. However, when the tissue site already contains cells of the transplant cell type, for example when neurons are transplanted into the brain or spinal cord, then these cells become more difficult to identify.

In such an example, one may use a marker specific to the neuron subclass being transplanted. However, if the use of such a specific antibody is either not practical, as dictated by some fixatives, or ineffective in achieving optimal detection, then alternatives need to be found.

5.1.2 Pre-labelling of transplanted cells

The use of mouse donor cells in a rat host is an example where the transplanted cells can be identified by applying a species-specific antibody (Davies *et al.*, 1994). Sex-specific differences can be utilised in transplanting male-derived cells into a female host, and exploiting the unique Y chromosomes of the male-derived

transplanted cells (O'Leary and Blakemore, 1997). However, the use of such methods can remain either impractical or produce sub-optimal staining.

An alternative method of labelling is to use dyes to label the cells *in vitro* prior to their transplantation. PKH2 is a commercially available fluorescent cell linker which incorporates into the cell membrane and thereby acts as a cell tracker molecule (Horan and Slezak, 1989); transplanted cells pre-labelled with this marker can be visualised *in vivo* on appropriate excitation. These cells do not require any further immunostaining to be visualised and also offer the potential of double labelling by staining for a second antigen.

However, in transplants carried out in this lab where cells have been labelled with PKH2 or with the nuclear dye, Hoechst 33342 (Baron-Van Evercooren *et al.*, 1991), the signal that one receives from these cells *in vivo* does not extend far out of the cell bodies (G.Brook, unpublished data); this is more significant with cells which extend long processes. In addition, the signal is not exclusive to the transplanted cells but can also be seen in host cells, a factor which is important in the subsequent analysis of transplanted cells. This has been found for both SCs transplanted into the brain (A.Soekarno, pers. comm.) and olfactory ensheathing cells transplanted into the corticospinal tract (Y.Li, pers. comm.). It has been observed in these studies that host cells have either phagocytically taken up the cell label together with the transplanted cell or they have simply picked up fluorescent cell debris. In either case, the accuracy of the identification of transplanted cells is compromised. Finally, the loss of fluorescence after each cell division means that long-term tracking of transplanted cells cannot be easily achieved (studies have utilised this very feature to investigate the rates of cell growth (Ashley *et al.*, 1993))

and in a cell such as the Schwann cell, where cell division is high on transplantation into the brain (Stichel *et al.*, 1996), this loss with time is significant.

5.1.3 Green Fluorescent Protein

Green Fluorescent Protein (GFP) is a naturally fluorescent protein isolated from the jellyfish, *Aequorea victoria*, and since its isolation it has proved to be an invaluable tool in the field of developmental biology and in cell tracking studies (Pines, 1995; Prasher, 1995). It has been significantly enhanced in both its ease of excitation and the intensity of the signal with which it fluoresces (Cormack *et al.*, 1996), and its emission spectrum has been shifted such that it can be detected more easily with existing FITC-filters.

The use of GFP to genetically label cells prior to transplantation would offer a very useful strategy in uniquely identifying those cells at a later stage. GFP is non-toxic to cells, can be expressed throughout the cell compartments and can be observed in conjunction with other fluorescent markers. However, transfection of mammalian cells can be both arduous and inefficient and long-tem expression of the gene may be difficult to achieve.

5.1.4 Retroviral-mediated transfection of Green Fluorescent Protein

Viral-mediated transfection exploits the natural ability of the virus to introduce foreign genes into host cells. The development of viral vectors in recent years has led to a number of transfection systems which have been improved in both their safety of use and their efficiency (Goff and Shenk, 1993; Robbins *et al.*, 1998).

The major systems which are currently in use today include adeno- or adeno-associated viruses, retroviruses, herpes simplex viruses, and also poxviruses and

alphaviruses. Although these viral groups show many features in common, they each possess certain elements which give them specific advantages and disadvantages for any given transfection; adenoviruses are able to infect non-dividing cells and are encountered in everyday life; retroviruses infect dividing cell populations with long-term expression of the gene of interest; and herpes simplex viruses show latency and can therefore offer stable, long-term expression (Breakefield, 1993; Carroll and Moss, 1997; Tubulekas *et al.*, 1997).

Retroviral transfection involves the insertion of the retroviral genes into the host cell genome, and thereby induces long-term, stable expression of the foreign gene of interest (Marin *et al.*, 1997; Yoshimoto *et al.*, 1995). Transfection with this method can yield over 95% transfection efficiency in a dividing cell population. However, for such high efficiencies to be reached, retroviral cell lines need to yield high-titre virus. *Packaging cell lines* provide the packaging function necessary for viruses which have been depleted of essential *gag, pol* and *env* genes to produce infectious *virions*. When these specialised cell lines are transfected with the crippled retroviral construct, infectious packaged viral particles are released into the media and can subsequently be used to infect or *transduce* a chosen target cell population. As the target cells lack the necessary packaging function for further propagation of the virus, the infection is single and there is no further passage of virus; the cultures are devoid of functional 'helper' virus and are termed *helper-free* (Fig. 5).

However, there remains the potential hazard of recombination of packaging cell and viral vector DNA. One important consequence of this may be the return to virulence of the retrovirus. Thus, packaging cell lines are created which minimise the functional consequences of any genetic recombination, and which require

Figure 5 A schematic diagram of the method of retroviral-mediated transfection.

(taken from "Recombinant DNA", 2nd ed., 1992, Scientific American Books, p227)

Figure 5 A schematic diagram of the method of retrovirus transfection

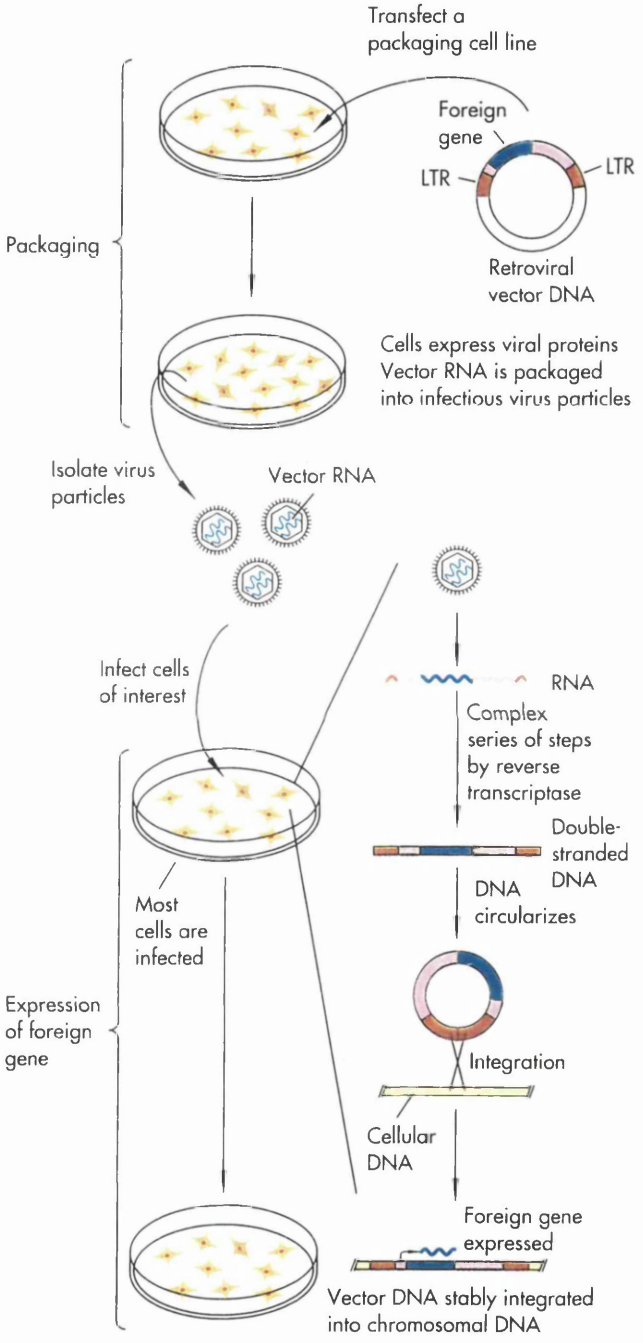

multiple separate components to recombine for a virus to regain its virulence (Danos and Mulligan, 1988). While the chances of recombination at each of several sites is remote, this remains a potential hazard.

A recently developed system uses a new third-generation packaging cell line, termed the 'Phoenix line' (fNX), engineered to overcome some of the problems associated with previous generation packaging cell lines (Kinsella and Nolan, 1996; Pear *et al.*, 1993). The fNX cell lines are based on the 293T cell line, a human embryonic kidney cell line transfected with the large T antigen (DuBridge *et al.*, 1987; Graham *et al.*, 1977), they carry strong promoters to support high expression of genes and they contain fewer original retroviral loci which could interfere with infectious viral assembly and release.

The introduction of the gene encoding GFP into such a retroviral system was carried out very recently and used with success in a study of T lymphocytes (Heemskerk *et al.*, 1997). Moreover, this retroviral GFP-plasmid contains an 'Internal Ribosome Entry Site' (IRES) element which enables the translation of 2 open-reading frames from a single messenger RNA strand (Jang *et al.*, 1990). Hence, one would see the expression of GFP co-incident with that of the second gene of interest (Dash *et al.*, 1996; Grignani *et al.*, 1998).

5.1.5 Aims of the project

I have used the fNX packaging cell line to set up a retroviral transfection system to efficiently label cells with GFP prior to transplantation into the adult rat CNS. This requires firstly, the optimisation of transfection of the fNX line with the disabled retroviral plasmid, and then optimisation of the transduction of target cells with infectious viral particles containing the recombinant GFP gene. Finally, the

transduced target cells would need to retain their green fluorescence when transplanted *in vivo*.

This system would facilitate the identification of transplanted cells *in vivo*. The STAG cell lines, in particular, would be an ideal candidate for transfection using this system as they are currently difficult to visualise *in vivo*.

In addition, the presence of the IRES element within the retroviral construct provides the opportunity to transfect an additional gene of interest easily and efficiently into the desired cell type and monitor more accurately its effect *in vivo*.

5.2 Materials and Methods

5.2.1 General

Phoenix cells (fNX) (Pear *et al.*, 1993) were maintained in Iscoves Modified Dulbecco's Medium (IMDM, GIBCO BRL, UK) containing 10% FCS and 0.2μg streptomycin and 0.2U penicillin per 40ml volume, referred to as IMDMF. fNX cells were cultured on tissue culture-treated flasks (Becton Dickinson, UK). The fNX-A line is an amphotrophic packaging cell line engineered on the backbone of the 293T line, a human embryonic kidney cell line transfected with the SV40 Large T antigen, with additional features which make it effective at high transient episomal expression of foreign genes (Kinsella and Nolan, 1996).

The retroviral construct which was used in conjunction with the packaging cell line, named LZRSpBMN-IRES-EGFP, is a 12.4kb plasmid with 2 'Long Term Repeats' (LTR), and containing within them an IRES element with a multi-cloning site upstream and the gene encoding the brighter, red-shifted mutant of GFP, EGFP (Zhang *et al.*, 1996), downstream from it (Heemskerk *et al.*, 1997). The plasmid I have used is also known as S001, reflecting specific endonuclease sites within the construct, and contains the gene for puromycin resistance (Fig. 5.1).

All tissue culture work involving this retroviral system was carried out in a class II containment facility and stringent safety measures were employed throughout.

5.2.2 Transfection of the fNX line with the retroviral plasmid, S001

5.2.2.1 Calcium phosphate-mediated transfection

The calcium phosphate ($CaPO_3$) mediated transfection was carried out using a protocol based on standard procedures (Sambrook *et al.*, 1989). The $CaPO_3$ precipitate was made up by adding a calcium solution with both salmon sperm

Figure 5.1 Restriction endonuclease map of the retroviral plasmid, S001. Plasmid amplification in bacteria followed by restriction digest was carried out to confirm the structure of the plasmid (data not shown).

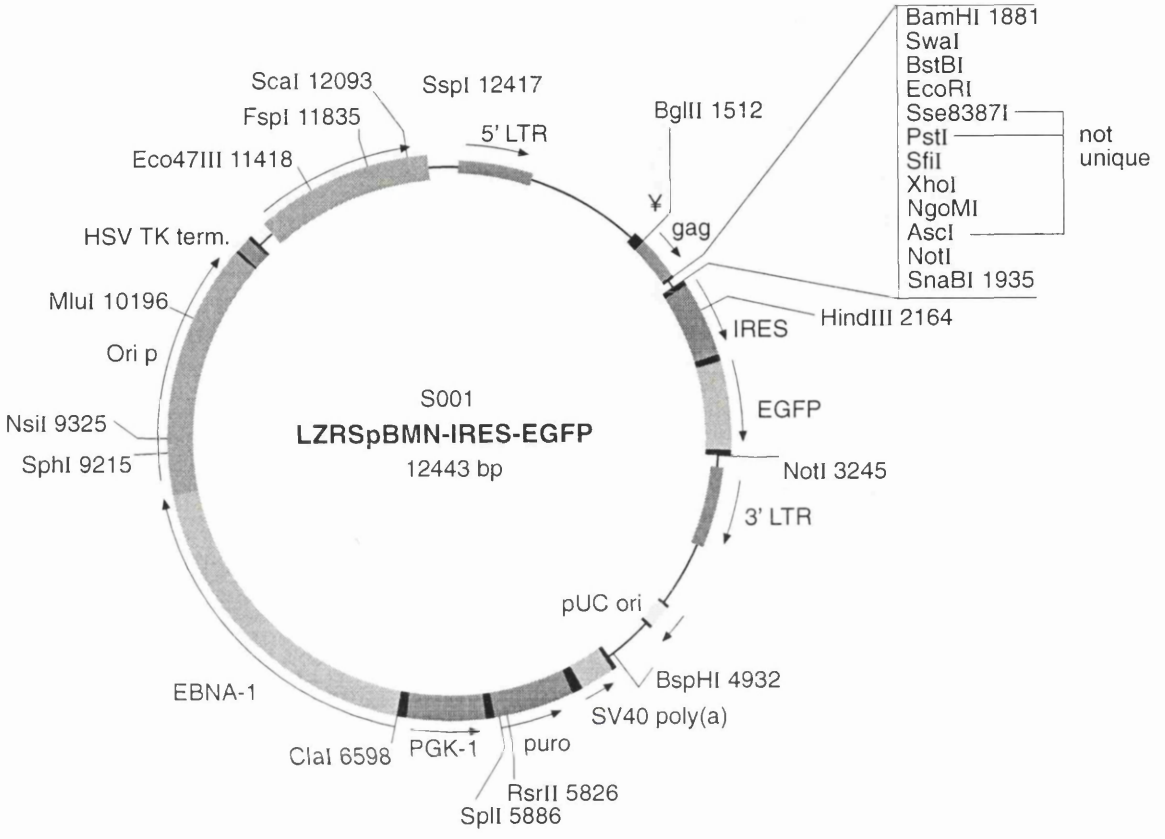
S001
LZRSpBMN-IRES-EGFP
12443 bp
BamHI 1881
SwaI
BstBI
EcoRI
Sse8387I
PstI
SfiI
XhoI
NgoMI
AscI
NotI
SnaBI 1935
not unique
HindIII 2164
BglII 1512
ScaI 12093
SspI 12417
FspI 11835
Eco47III 11418
5' LTR
HSV TK term.
MluI 10196
Ori p
NsiI 9325
SphI 9215
gag
IRES
EGFP
NotI 3245
3' LTR
pUC ori
BspHI 4932
SV40 poly(a)
puro
RsrII 5826
SpII 5886
PGK-1
ClaI 6598
EBNA-1

carrier DNA and plasmid DNA, the latter of which required some optimisation, to one containing phosphate in Hepes-Buffered Saline (HBS) (GIBCO BRL, UK). In the crucial step of the formation of the $CaPO_3$ precipitate, the DNA solution was added drop-wise to the phosphate buffered solution *whilst* bubbling air through the phosphate solution with the use of a peristaltic pump. The precipitate was incubated for a 20 minutes at room temperature and then added drop-wise to the plate of fNX cells which contained fresh IMDMF with chloroquine at 30μM, and incubated overnight at 37^{O}C, 5% CO_2 (approximately 16h). The precipitate was removed from the cells the following morning and replaced with fresh IMDMF media.

5.2.2.2 Effectene-mediated transfection

The 'Effectene' reagent, a lipid-based commercially available transfection reagent (Qiagen, UK), was used according to manufacturer's recommendations and required the incubation of the Effectene reagent, the plasmid and an 'Enhancer' reagent, designed to package the DNA more efficiently. Briefly, an incubation of these components for 10 minutes at room temperature was followed by the addition of the resultant Effectene/DNA complexes onto the cells for an incubation period of 5h at 37^{O}C, 5% CO_2 (Qiagen, UK). The reaction was stopped by the replacement of normal media with IMDMF media.

5.2.2.3 Analysis of transfection efficiencies

Transfections were carried out with the use of multi-well plates (Becton Dickinson, UK) and later with PLL-coated 100mm dishes (NUNC, UK). fNX cells were seeded at $6x10^5$ cells per well of a 6 well-plate (6wp) or $4x10^6$ cells per 100mm

dish 24h prior to transfection. Cells transfected through either method were observed under fluorescence microscopy (Zeiss Axiophot) at 24h and 48h post-transfection and assessed for transfection efficiency.

Puromycin selection of transfected cells was carried out using puromycin (Clontech, UK) at 2μg/ml.

5.2.3 Transduction of target cells

5.2.3.1 Virus collection

At 24h post-transfection of the fNX cells, the media on the cell cultures was replaced with 7ml fresh Iscoves media and the cells were returned to the incubator. At 48h post-transfection, this media was harvested as viral supernatant. The supernatant was passed through a 0.45μm filter (Schleicher & Schuell (FP 030/2), Germany) to remove cellular material and debris, snap-frozen by placing in either liquid nitrogen or dry ice, and stored subsequently at $-80^{O}C$.

For viral harvest at later time-points, fNX cell media was replaced with 7ml fresh media 24h prior to the harvest time and collected as described above. Where transfected fNX cell cultures reached confluency in the initial 100mm dishes, they were passaged onto 75cm flasks; 1ml aliquots were collected from overnight cultures containing 15ml IMDMF media and stored as described above for long-term viral transduction experiments.

5.2.3.2 Transduction of 3T3 cells

3T3 cells (gift of C. Magnus, NIMR) were plated onto 24wp wells at a density of 2-4 x 10^4 cells/ml/well 24h prior to transfection. Two methods of transduction were

used; one method used 'Dotap', a lipid transfection reagent (Boehringer Mannheim, UK), and the other used polybrene (Sigma, UK).

The dotap method: 1ml virus was thawed, diluted where required in IMDMF, and dotap added at 10μg/ml. After a 10 minute incubation on ice, the viral cocktail was re-suspended and used to replace the existing 3T3 media for a period of 4-16h at $37^{O}C$, 5% CO_2. After the incubation, the cells were washed once in PBS and incubated in fresh media. The cells were observed using fluorescence microscopy (Zeiss Axiophot) at 48h and analysed thereafter (5.2.4.3).

The polybrene method: 1ml virus was thawed, polybrene was added to it at 4μg/ml and the resultant viral media was used to infect the 3T3 cells as described above. There was no incubation of the virus with the polybrene prior to incubation with the 3T3 cells.

5.2.3.3 Analysis of transduction efficiency

Transduced target cells were analysed with a 'Fluorescence-Activated Cell Sorter' (FACS), carried out in a separate lab as an on-site facility (C.Atkins; FACStar Plus, Becton Dickinson, UK); the FL1 emission channel was used to monitor green fluorescence. 48h after transfection with the virus, the 3T3 cells were trypsinised, collected in 300μl total volumes and taken in FACS-polypropylene tubes (Becton-Dickinson, UK) to the FACS lab for analysis. Approximately 5000 cells were sorted from each sample and the percentage of sorted cells was taken as the transfection efficiency for that well. FACS analysis data was recorded in a

spreadsheet from which subsequent graphical and statistical data could be extracted (Microsoft Excel 97, Win. 95).

5.2.4 Transduction of STAG lines

Viral infections of STAG lines were carried out with the STAG-3Faii line using the protocol described above (5.2.4). 3Faii cells were seeded onto 24wp wells at 3 x 10^4/ml/well 24h prior to transfection.

5.2.5 Transplantation of GFP-transfected STAG cells into the adult rat brain

5.2.5.1 Transfection and transplantation of STAG-3Faii-GFP cells

STAG-3Faii cells were transfected using the retroviral transfection method described above and FACS-analysed for transfection efficiency. Transfected cell cultures were subsequently prepared for transplantation at 50 x 10^6 cells/ml and transplanted into either the septal cholinergic nuclei (stereotaxic co-ordinates, AP +0.6, L +0.5, D 8.5-5.5), as carried out previously with primary NSCs (see 4.2.1 and 4.2.2 for details), or into the dorsal striatum using a similar extrusion technique at the stereotaxic co-ordinates, AP –0.2, L +2.9, D 4.5-1.5 (Fig. 5.2).

5.2.5.2 Processing of STAG-3Faii-GFP transplants

Animals were perfused with either 4% paraformaldehyde or with PBS flushing as described before (2.2.2). Vibratome and cryostat sections were examined under fluorescence microscopy immediately after cutting. For 2 transplants, 1 for each of the transplant sites, vibratome sections were further processed for immunostaining of neurofilament, TH and ChAT antigens, as described before (2.3.1).

Figure 5.2 Schematic diagram of the transplantation of STAG-GFP cells into the dorsal striatum. The STAG-GFP cell suspension (tra) was extruded from the dorsal striatum (str) through the corpus callosum (cc) and into the inferior layers of the cortex (cx). (lateral ventricle, LV)

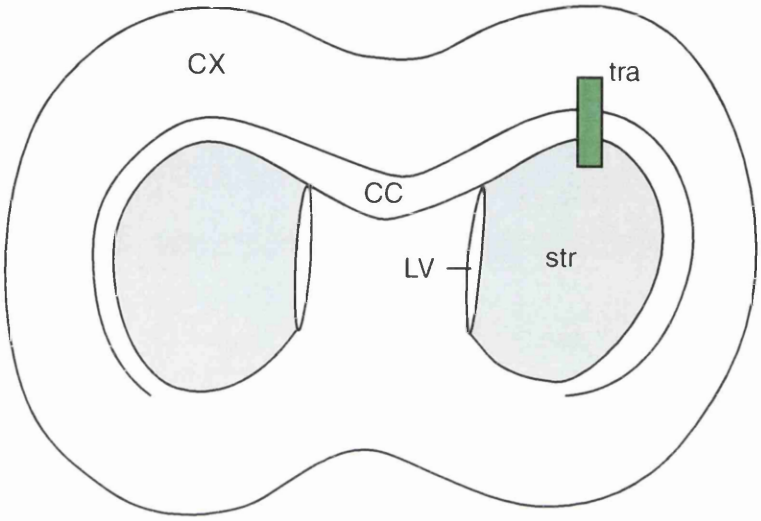
CX
tra
CC
LV
str

5.2.6 Transduction of primary glial cells

Primary neonatal Schwann cells (NSCs) and olfactory ensheathing cells (OECs) were prepared as described before (for NSCs, see 2.1.2; for OECs, see (Li *et al.*, 1997), and viral infections were carried out as described above for both populations of cells. In addition, the cells were incubated in mitogens for the period of the transfection; NSCs were given forskolin and PDGF-BB as described previously (3.2.1.3); OECs were incubated in bovine pituitary extract (BPE) at 12μg/ml (Chuah and Au, 1993).

5.3 Results

5.3.1 fNX cell culture

fNX cells show a flattened cell morphology with irregularly shaped cell bodies and some extension of small processes. They displayed contact-inhibition of growth but were maintained by passage of cells prior to confluency and at low fractions. Tissue culture-treated culture-ware of Becton Dickinson, UK provided the most favourable substrate for fNX cells, however, PLL+ coated dishes were used as an effective alternative.

5.3.2 Transfection of fNX cells with S001

2 methods of transfection were studied to obtain the most efficient means of transfection of the fNX cells with the retroviral plasmid, S001. One method used calcium phosphate-mediated transfection, the other used 'Effectene', a relatively new lipid-based reagent which was claimed to transfect with high efficiency (Qiagen, UK). Given that the fNX cell line is reported to be a highly transfectable cell line (Pear *et al.*, 1993), a transfection protocol was required which would consistently produce at least 50% transfection efficiency.

5.3.2.1 Analysis of transfection efficiency

In the early experiments, transfection outcomes were rated by simple observations and estimates of transfection percentages. A system of counting using a 3 line x 3 line grid scratched onto the underside of each well was later developed to attempt to compare more quantitatively the differences in transfection efficiency across the wells. The total number of GFP-positive cells was counted in the visible field at x200 magnification over each of the 9 crossed-points formed by the grid. The total

number of GFP-positive cells per well at these 9 points was then calculated and averaged to give a 'Transfection Score' for each well (Fig. 5.5A).

However, the numbers of transfected cells in subsequent transfection experiments had so increased that this grid-counting system was no longer practical or viable. At this point, records of estimates of transfection efficiency were resumed and transfection scores were rated to the nearest 20%.

5.3.2.2 $CaPO_3$- vs. Effectene-mediated transfection

As reported in previous studies, fNX cells were highly transfectable producing maximal transfection efficiencies of approximately 70%. The results of the 2 methods of transfection that were investigated are described below; a summary of the results of these transfections can be found in figure 5.3; full details are in Appendix B1, B2.

Effectene can transfect up to 20% fNX cells at 48h

Effectene transfections (ET) were carried out as described previously (5.2.2.2). Transfections ET-1 and ET-2 were carried out on STAG-3Faii cells due to the unavailability of fNX cells at the time of transfection, and demonstrated that low numbers of STAG cells could be transfected using the Effectene reagent. The numbers of GFP+ cells in ET-2 were greater than could be counted in total. Therefore, it was decided to stop subsequent transfections at 24h, when there would be fewer numbers of transfected cells, and thereby enable total cell counts to be carried out and comparisons to be made across the wells.

ET-3, carried out on fNX cells, showed that at 24h post-transfection there were in fact, no GFP-+ fNX cells visible in any field of view. This may have been the

expression of the GFP. The results of ET-4 and ET-5, taken at 48h post-transfection, confirmed that fNX cells could be transfected successfully using this method but that green fluorescence may not be visible until 24-48h after the transfection.

With the use of total cell counts in ET-4, 0.4μg DNA was observed to be optimal for transfections in 6wp wells (Fig. 5.3; Appendix B1). ET-5 produced a higher transfection efficiency than previous transfections, and total cell counts were substituted for estimates of transfection efficiency percentages. The optimally transfected cells of ET-5 were scored as 20%.

Optimised $CaPO_3$ transfections can transfect up to 70% fNX at 48h

The initial calcium phosphate transfection, CP1, demonstrated that hundreds of GFP+ cells could be seen as early as 24h after transfection with S001 and estimated at 20%. The result of CP1 coincided with that of ET-5 where the transfection efficiency had been rated at 20% at 48h. Given the high transfection efficiency of the wells of CP1 at only 24h after transfection, and the high economical cost of the lipid reagent, Effectene, it was decided to continue subsequently with the calcium phosphate protocol (Fig. 5.4).

3 elements of the CP transfection protocol were subsequently studied with respect to their significance within the protocol: i) the amount of DNA used per transfection, ii) the incubation of the $CaPO_3$ precipitate prior to transfection, and iii) the use of chloroquine (CQ), an agent which inhibits DNAse and is proposed to improve transfection efficiency. In addition, CP transfections were repeated to confirm that high transfection efficiencies could consistently be obtained.

Transfections were carried out with the use of 6 well plates (wp) and eventually in 100mm dishes (Fig. 5.3).

The results of CP2, taken at 48h, confirmed the greater transfection efficiency over the Effectene-method; approximately 40% fNX cells were GFP-positive. The wells where the $CaPO_3$ precipitate had been incubated at room temperature for the prescribed 20 minutes prior to incubation on the cells did not show a significant difference in transfection efficiency from those wells in which the precipitate was added immediately onto the cells.

Given the success of the earlier transfections, CP3 was carried out in a 100mm dish and the supernatant collected as virus for titration experiments; TEF was estimated at 40%. This demonstrated that moderate numbers of fNX cells could be transfected at the 100mm dish level. In addition, supernatant from CP3 was collected over several days as virus stock for later titration and infection experiments (5.3.4).

CP4 was terminated early due to the excessive cell density of fNX cells prior to transfection. CP5 was carried out on STAG cells and is described in 5.3.5.

CP6-9 were carried out to assess the amount of plasmid DNA necessary for high transfection efficiency. The results suggested that 10μg DNA was significantly more effective than 5μg, but that there was no further advantage in using 20μg than 10μg.

CP6 and CP8 were further used to investigate the importance of chloroquine (CQ) in the transfection protocol. In both transfections, the significance of the use of CQ on transfection outcome was equivocal and its use was maintained in all subsequent transfection protocols.

In CP7, the significance of the incubation of the $CaPO_3$ precipitate was assessed (first assessed in CP2), and the result again suggested that this step was not essential for high transfection efficiency. Incubation of the precipitate was therefore omitted from subsequent transfections and the precipitate was added immediately to fNX cell cultures. Subsequent transfections, CP8-10, yielded high TEFs of 40-60% and were consistent with the decision to omit the incubation step.

In the revised protocol, the $CaPO_3$ precipitate incubation step was omitted, the use of CQ was maintained, and 10μg DNA was used in the transfection. CP11-15 were carried out using this protocol to yield virus for viral titrations and subsequent target cell transfections. These transfections continued to yield high transfection efficiencies of up to 70% by 48h (not shown). An example of a typical fNX cell transfection at this stage can be seen in figure 5.4E.

5.3.3 Puromycin killing curve for fNX cells

Given both the high percentage of transfected fNX cells at 48h after transfection of the retroviral plasmid and the high levels of expression of the plasmid, virus can be taken from this time-point and used to infect target cells with high efficiency (Grignani *et al.*, 1998). An alternative strategy involves the selection of exclusively transfected cells with the use of puromycin antibiotic, the gene of resistance for which is found within the retroviral construct (Fig. 5.1). For this latter strategy, a puromycin killing curve (PKC) was established to determine the concentration at which all cells lacking the resistant gene would be killed, thereby selecting for transfected cells only.

Normal fNX cells were seeded onto 4 wells of a 12wp at a density of 4×10^5 cells/ml/well. 1ml IMDMF containing puromycin at concentrations of 0.5, 1.0, 2.0

Figure 5.3 Summary table of the fNX cell transfections. ET- and CP-transfections produced good percentages of transfected cells; CP-transfections were further optimised to obtain reproducibly high transfection efficiencies of up to 70% (see Appendix B1 for details of ET-4).

Figure 5.3 Transfection of fNX cells with S001 - Comparison of transfection efficiency (TEF) in Effectene vs. calcium phosphate transfections

Expt.	Dish size	Variables	TEF %	Results
ET-1*	24wp	pilot transfection; [DNA] 0.1-0.3μg, EF 2.5-10μl	5	EF is a viable transfection method
ET-2*	12wp	[DNA] 0.2-0.7μg (EF, 5μl)	5-10	Scores of GFP+ cells; need to count lower nos. at 24h or develop counting system
ET-3	6wp	EF 0-15μl (DNA, 0.4μg)	0	No GFP+ cells at 24h, reaction stopped
ET-4	6wp	[DNA] 0.2-0.7μg (EF, 10μl)	5-10	[DNA] optimal at 0.4μg
ET-5	6wp	EF 0-10μl (DNA, 0.4μg)	10-20	Hundreds of GFP+ cells; counting system not practical; EF optimal at 10μl
CP-1	6wp	pilot CP, 6μg total DNA	10-20	Hundreds of GFP+ cells at 24h, reaction stopped
CP-2	6wp	Incubation of $CaPO_3$ ppt. (DNA at 6μg)	20-40	Good TEF at 48h; incubation ppt. not significant
CP-3	100mm	pilot 100mm dish (DNA at 6μg)	40	viral supernatant collected for infections
CP-5*	100mm	pilot transfection for STAG line, DNA at 6μg	10	Low numbers of STAG-GFP+ cells
CP-6	100mm	[DNA] 5μg vs. 10μg; CQ vs. no CQ	20-40	TEF significantly higher at 10μ than 5μg; incubation ppt. not significant
CP-7	100mm	[DNA] 5μg vs. 10μg; incubation of $CaPO_3$ ppt.	40	10μg DNA may give higher TEF; incubation ppt. not signficant
CP-8	100mm	[DNA] 5μg vs. 10μg; CQ vs. no CQ	40-60	TEF significantly higher at 10μ than 5μg; use of CQ not significant; TEF up to 70%
CP-9	100mm	[DNA] 10μg vs. 20μg	60	TEF not significantly different with DNA at 20μg
CP-10	100mm	virus collection, DNA set at 10μg	60	High TEF at 60-70%, virus collection is begun

EF = Effectene transfections
CP = calcium phosphate transfections
*transfection of STAG-3Faii cells
CP-4 was discontinued
CQ = chloroquine

Figure 5.4 Transfection of fNX cells with the GFP (fNX cells are photographed in a phase/FITC-filter mix). fNX cells show an irregularly shaped cell body with small, extended processes; green fluorescent cells can be clearly distinguished from non-transfected cells (A). Comparisons of early transfected cell cultures were usually clear to make; for example, an ET-transfection, ET5, seen in 'B' at 48h shows significantly reduced numbers of fluorescent cells compared to a CP-transfection, CP2, seen in 'C' also at 48h. Typical CP-transfections after optimisation produced high transfection efficiencies, seen in phase/FITC-filter mix (D) and dark field (E); 'D' and 'E' are CP11 cells at 48h after transfection.

(Scale bar: B, C – 20μm; A, D-E – 10μm)

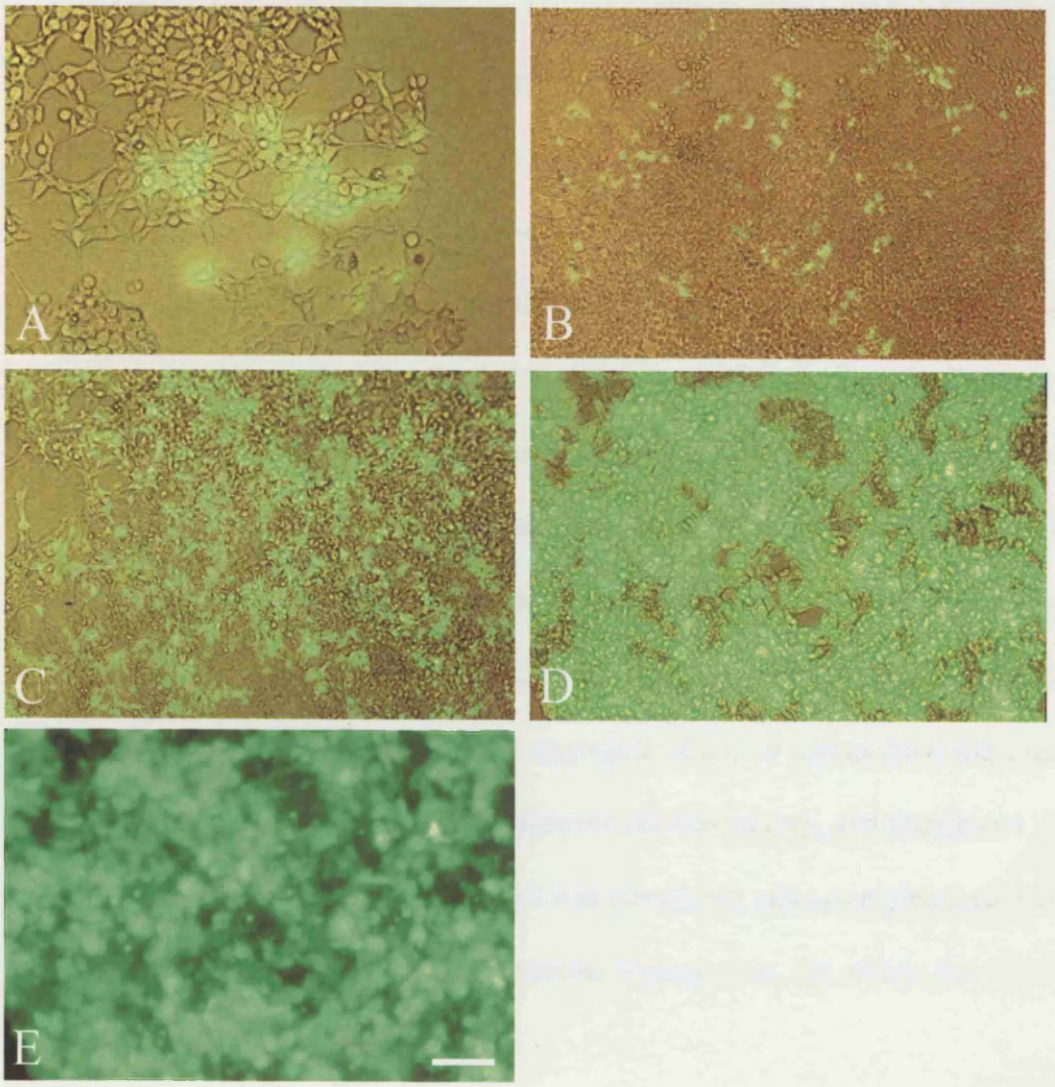
A
B
C
D
E

and 3.0μg/ml was added to wells 1-4, respectively, 24h after seeding. Cells were monitored over 2 weeks under standard light microscopy with a 10x10 square grid-ocular lens piece and with the following counting system.

A 3 line x 3 line grid was scratched onto the underside of each well with a diamond knife, as described for the early transfection experiments (Fig. 5.5A; section 5.3.2.1). The 10x10 grid seen through the lens piece (Fig. 5.5B) was positioned consecutively over each of the 3 diagonal points of the 9 points resulting from the scratched grid. At each of the 3 points and with the use of further sub-divisions seen shaded in Figure 5.3B for each quadrant, a score of 1-4 was given for each shaded area, made up of 4 smaller squares, depending on the number of individual squares which showed *any* healthy cells within them. For example, if 3 of the 4 individual squares in the shaded area showed viable cells within them but the 4th did not, then that area would be given a score of 3. This was carried out for the 4 shaded areas in each quadrant of the grid, and at each of the 3 diagonal points in the scratched grid. Finally, the aggregate of all the scores from the 3 diagonal points was used to obtain an average score per shaded area, and designated the PKC score for that well. The experiment was terminated when complete cell death was observed at any one of the concentrations of puromycin, the criteria for which was a PKC score of less than 1.

In the first experiment, PKC-1, significant cell death was observed within the first week of application of the puromycin in wells containing 2-3μg/ml (Fig. 5.6A; Appendix B2). The PKC score dropped to below 1 after 13d in wells containing 2-3μg/ml; the wells showed complete cell death at this time-point.

In PKC-2, the experiment was repeated with puromycin at 2μg/ml to confirm that normal fNX cells would undergo complete cell death at this concentration. 4 x

12wp wells were set up with fNX cells approaching confluency, reproducing the approximate cell density that would exist 48h after transfection of fNX cells. Puromycin was added to wells 1-2 at 2μg/ml, and was omitted in wells 3-4 which were used as control wells.

The PKC score showed a gradual decrease in wells 1-2 over the first week in puromycin and subsequently dropped to below 1 by day 10 (Fig. 5.6B,C). Complete cell death was observed in these wells and the result confirmed that all untransfected fNX cells would be killed by 10d in puromycin at 2μg/ml. The control wells showed confluency throughout the time period tested. The full cell counts for PKC-2 and PKC-1 can be seen in Appendix B2.

5.3.4 Viral titration and FACS analysis

Transduced 3T3 cells were analysed by 'Fluorescence-Activated Cell Sorting' (FACS) due to its ease of analysis and the ability to carry out quantitative assessment. Briefly, the technique charges fluorescent cells from a fine but steady stream of cell droplets, untransfected cells are uncharged and fall in a vertical path, charged cells are diverted from their normal course and collected in a second tube positioned in line with the diverted course. The percentage of diverted or 'sorted' cells can be calculated automatically.

Virus obtained from the calcium phosphate transfections was used to infect target 3T3 cells to assess the efficiency of transduction. In general, transduction efficiency was high and optimally close to 90%. Viral titration experiments were termed 'VT' and usually involved the collection of virus at 48-72h after fNX cell-transfection, unless stated otherwise. Details of these experiments can be seen in Appendix B3.

Figure 5.5 Cell counting in the PKC experiments. 'A' shows the grid drawn on the underside of the dish and the 3 marked points (closed circles) at which the cells were counted. 'B' shows the 10 x 10 lens eyepiece grid used to count the cells; cells were counted as described in 5.2.3 using standard light microscopy and at a magnification of x200.

A

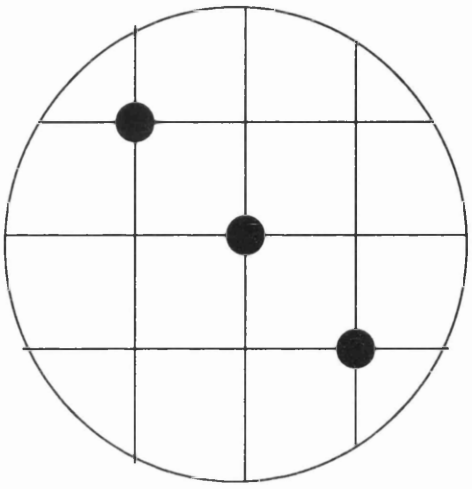

B

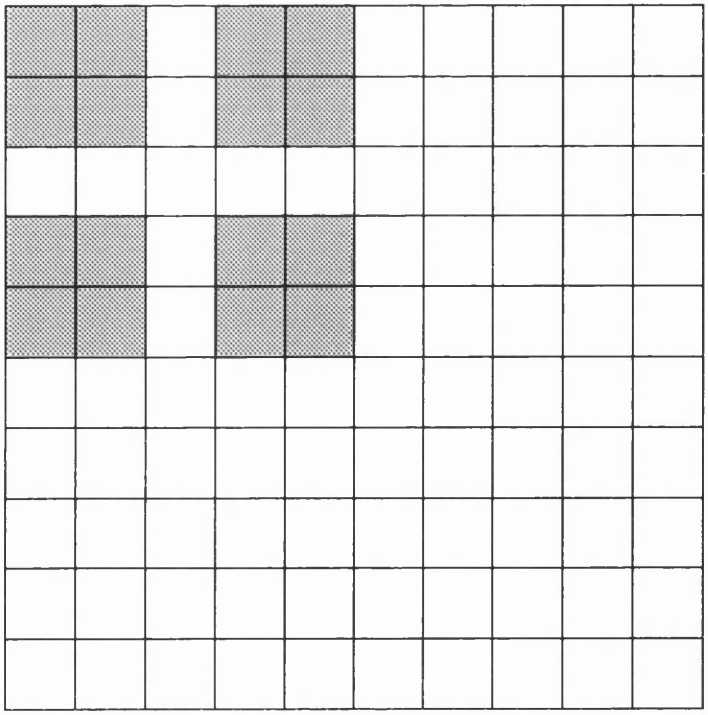

Figure 5.6 Puromycin killing curve data of fNX cells. The PKC scores of PKC-1 (A) and PKC-2 (B) show that complete cell death of the fNX cells was observed by 14d at a puromycin concentration of 2μg/ml. 'C' represents the average PKC scores taken from the 2 wells which contained puromycin at 2μg/ml in PKC-2 (B); there is significant cell death after 1 week in puromycin at this concentration and complete cell death by 10d (see Appendix B2 for full cell counts).

A Puromycin killing curve of fNX cells, PKC-1

DAY	PUROMYCIN µg/ml			
	0.5	**1**	**2**	**3**
1	3.6	2.9	3.0	2.8
2	3.5	2.8	1.5	1.5
5	3.7	2.8	1.3	1.2
6	4.0	2.6	1.8	1.3
7	3.9	1.9	0.4	0.8
8	4.0	2.8	0.6	0.8
9	4.0	1.9	0.9	0.9
12	4.0	1.5	1.3	1.3
13	4.0	1.9	0.8	0.5
14	4.0	1.6	0.9	0.5

B PKC-2

DAY	PUROMYCIN µg/ml			Average score at
	0	**2**	**2**	2µg/ml
1	4.0	4.0	4.0	4.0
2	4.0	4.0	4.0	4.0
3	4.0	4.0	3.0	3.5
4	4.0	3.9	3.2	3.6
7	4.0	2.4	3.6	3.0
8	4.0	2.9	1.3	2.1
10	4.0	0.3	0.4	0.4

C

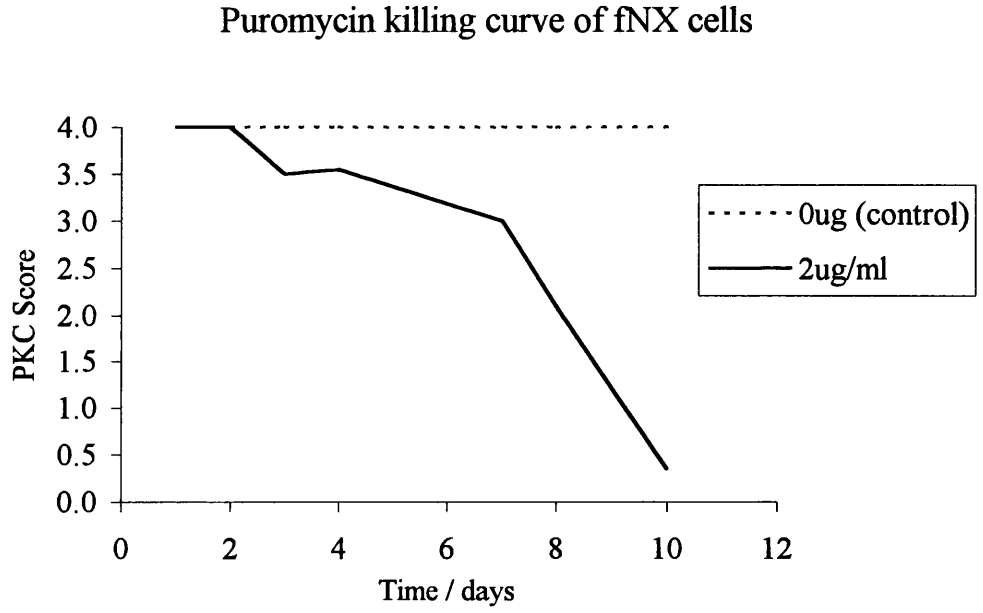

5.3.4.1 Transduction efficiency of virus

A number of aspects of the transduction system were analysed by comparison of the transduction efficiency of 3T3 cells by virus under different circumstances. These are described below.

Viral titration

VT1 was carried out to determine the infection competency of the virus. 3T3 cells were infected with virus at a range of dilutions of up to 1:33. 3T3 cells analysed at 48h after transfection showed a decrease of transduction with dilution of virus, with 1ml stock virus producing a mean transduction efficiency of 79.3% (Fig. 5.7A; Appendix B3). Given that 3 x 10^4 cells were initially seeded, the viral titre from this titration is calculated at approximately 2.5 x 10^4 infectious units per ml virus.

Storage and use of virus

The transduction competency of a series of virus samples stored at $-80^{O}C$ was compared to that of another series of the same samples which had been thawed and then re-frozen prior to transduction of 3T3 cells (Fig. 5.7B; Appendix B3, VT2(1-6)). FACS-analysis demonstrated that virus which had undergone a second freeze-thaw cycle had a considerably reduced transduction efficiency ($p=0.06$). The size of the reduction ranged from 13% to 29% in the 3 samples that were tested.

Time of viral harvest post-fNX cell transfection

Virus was collected from the fNX cell-transfection, CP3, over a number of days post-transfection of the cells and was used to examine the effect on transduction efficiency with the time of viral harvest. These initial results suggested that viral

Figure 5.7A Viral titrations I. Transduction efficiency of 3T3 cells with dilution of virus. FACS-analyses show a reduction in transduction efficiency with dilution of virus. Viral stocks were used to obtain 3 series (CP5A-C) of viral dilutions vs. transduction efficiency (see Appendix B3; VT1[1-12]). The 3 series show 4 sets of data each (01-04; 05-08; 09-12 represent CP5A, B and C, respectively) which demonstrate a reduction in transduction efficiency with dilution of viral stock.

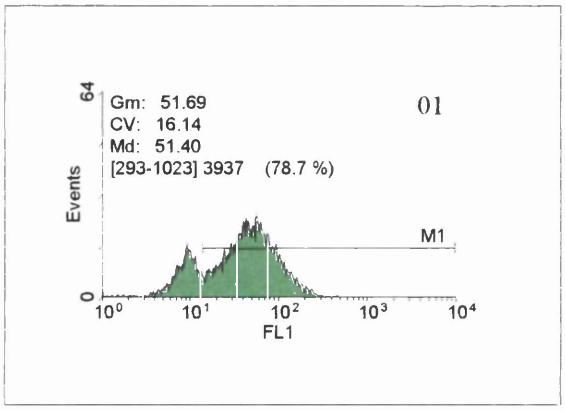
Gm: 51.69
CV: 16.14
Md: 51.40
[293-1023] 3937 (78.7 %)
01
M1
Events
FL1

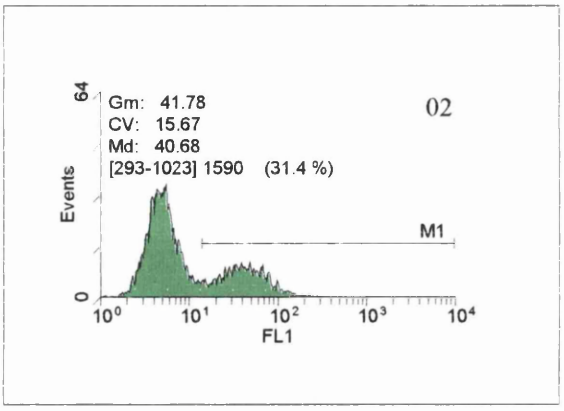
Gm: 41.78
CV: 15.67
Md: 40.68
[293-1023] 1590 (31.4 %)
02
M1
Events
FL1

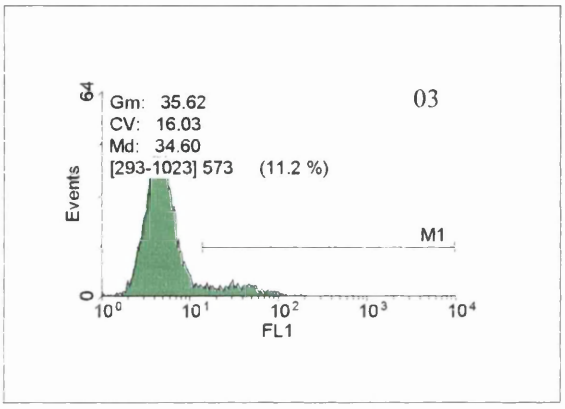
Gm: 35.62
CV: 16.03
Md: 34.60
[293-1023] 573 (11.2 %)
03
M1
Events
FL1

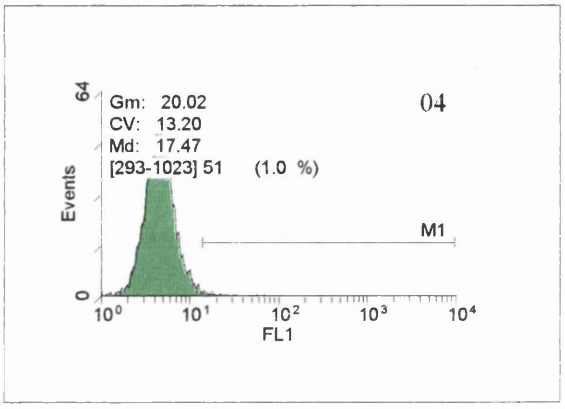
Gm: 20.02
CV: 13.20
Md: 17.47
[293-1023] 51 (1.0 %)
04
M1
Events
FL1

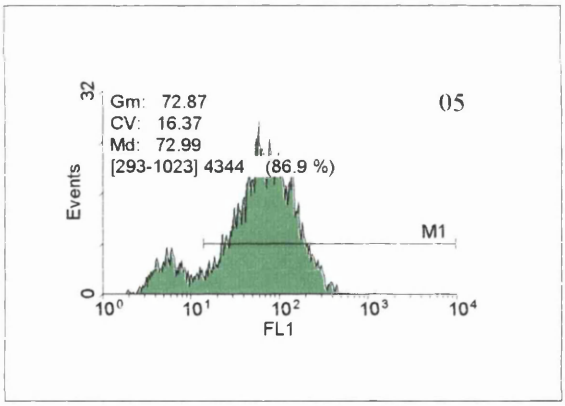
Gm: 72.87
CV: 16.37
Md: 72.99
[293-1023] 4344 (86.9 %)
05
M1
Events
FL1

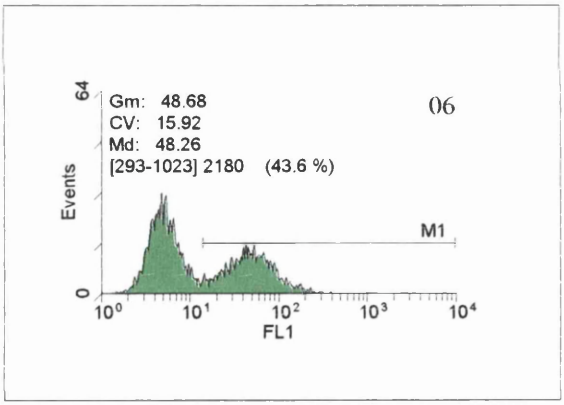
Gm: 48.68
CV: 15.92
Md: 48.26
[293-1023] 2180 (43.6 %)
06
M1
Events
FL1

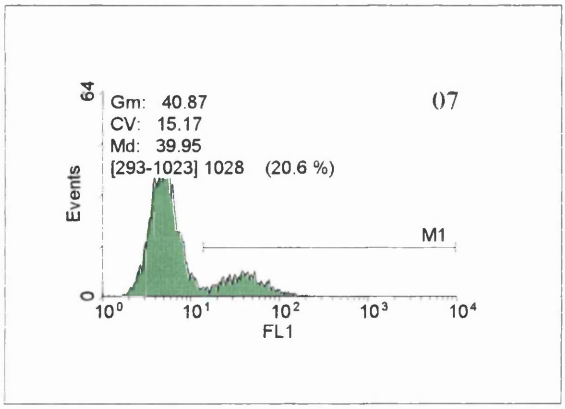
Gm: 40.87
CV: 15.17
Md: 39.95
[293-1023] 1028 (20.6 %)
07
M1
Events
FL1

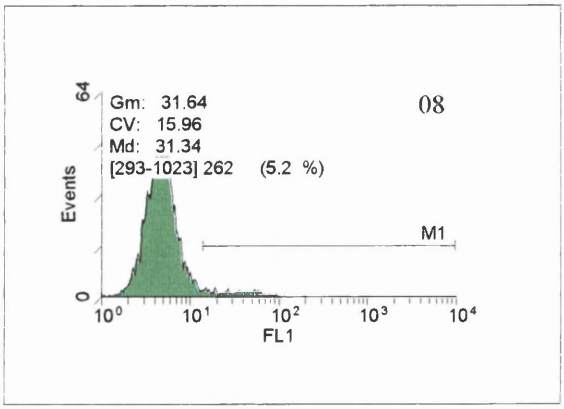
Gm: 31.64
CV: 15.96
Md: 31.34
[293-1023] 262 (5.2 %)
08
M1
Events
FL1

Figure 5.7B Viral titrations II. Transduction efficiency with dilution of virus (see Fig. 5.7A for details).

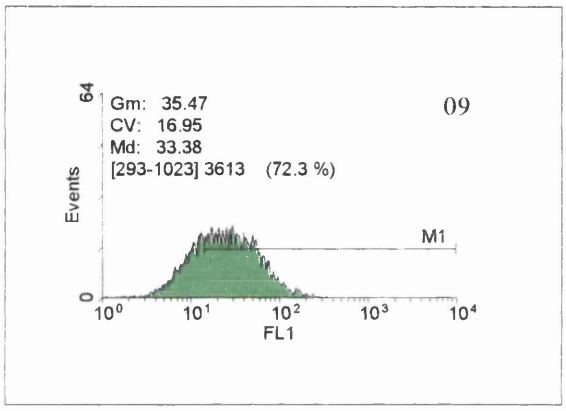
09
Gm: 35.47
CV: 16.95
Md: 33.38
[293-1023] 3613 (72.3 %)
M1
Events
64
0
10^0 10^1 10^2 10^3 10^4
FL1

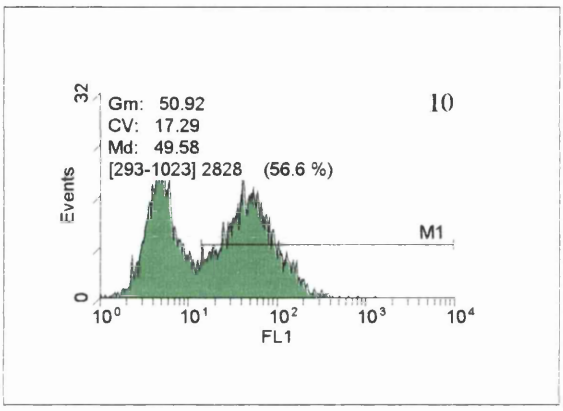
10
Gm: 50.92
CV: 17.29
Md: 49.58
[293-1023] 2828 (56.6 %)
M1
Events
32
0
10^0 10^1 10^2 10^3 10^4
FL1

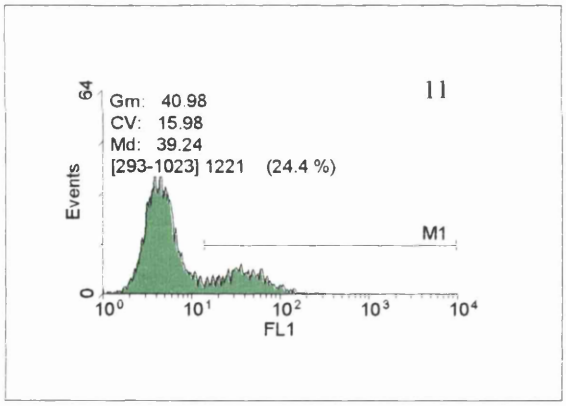
11
Gm: 40.98
CV: 15.98
Md: 39.24
[293-1023] 1221 (24.4 %)
M1
Events
64
0
10^0 10^1 10^2 10^3 10^4
FL1

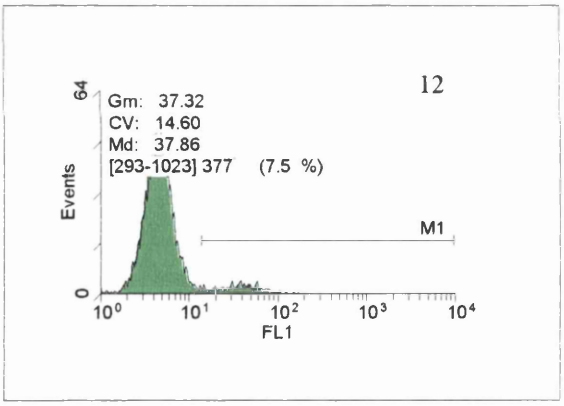
12
Gm: 37.32
CV: 14.60
Md: 37.86
[293-1023] 377 (7.5 %)
M1
Events
64
0
10^0 10^1 10^2 10^3 10^4
FL1

Figure 5.8 Viral titrations II. The effect on transduction efficiency with dilution of virus (A, see Fig. 5.7 for details) and by repeated freeze-thaw cycles (B).

A

Transduction of 3T3 cells: Efficiency with dilution of virus

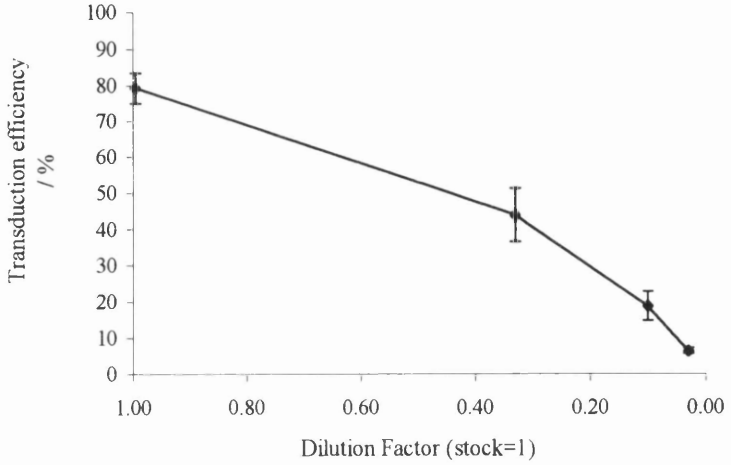

B

Effect of the freeze-thaw process on the efficiency of transduction of 3T3 cells

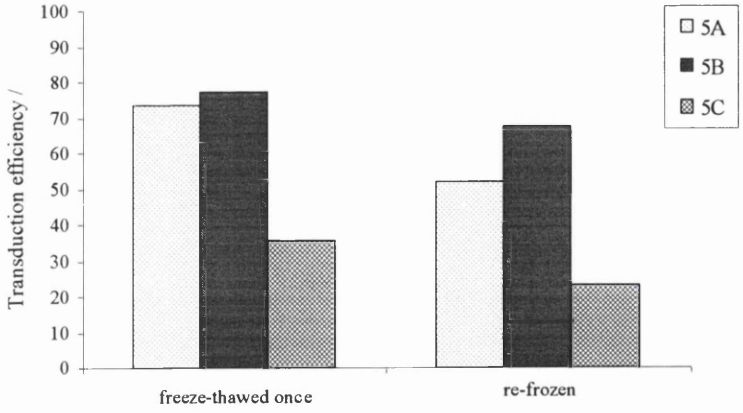

transduction efficiency was moderate-high in the first 3 days after fNX cell-transfection, but by 1 week this had decreased considerably (Appendix B3; VT2[7-11]).

However, the decline in transduction efficiency with virus taken from the CP3 cell culture at 8d post-transfection, was not observed in parallel experiments which had been carried out to assess the variability of transduction efficiency and FACS analyses. In these latter experiments, 6ml stock virus, harvested 8d after the fNX cell-transfection, was used to transduce 3T3 cells in 6 identical wells (Appendix B3; VT2[13-18]). The result was a transduction efficiency average of 74% and a range from 67.8-77.1%. Hence, the observed rapid decline in transduction efficiency with time seen in some CP3 samples was not consistent with other experiments run in parallel which demonstrated an average transduction efficiency of 74% at the same time-point. Moreover, 1ml (fresh) virus taken from the CP3 culture at 12d post-transfection demonstrated a transduction efficiency of 62%.

Although further experiments were carried out to repeat the analysis of transduction efficiency with time of viral harvest post-transfection, this was not successfully completed; one possible cause of the failures of subsequent transduction experiments may have been an underlying contamination of the 3T3 cell batch which was used. Transduction with a second batch obtained from a different source (B. Thomas, NIMR) and a subsequent return to high transduction efficiencies (Appendix B3; VT9) suggested that this may have been a factor, although cell density of 3T3 cells may also have been an important factor. Cells should be in a mitotic state to maximise their chances of incorporating the virus, and some failed transductions were in cells which had reached confluency within 24h of the transduction step.

Transduction with dotap vs. polybrene

The use of polybrene created several problems in the transduction of target cells. The initial use of polybrene overnight in the viral transduction, alongside wells in which dotap was used, showed massive cytotoxicity in those wells containing polybrene and not in those containing dotap (Appendix B3; VT2[20-23]).

The incubation period of polybrene was subsequently reduced to 4h to prevent the cytotoxicity that was observed with the overnight incubations. Although reduced from the overnight levels of toxicity, the 4h incubations continued to induce significant cell death.

In contrast, dotap was not toxic on 3T3 cells when incubated for up to 24h and induced no significant cell death when incubated overnight.

5.3.5 Transduction of STAG lines

5.3.5.1 Low percentage of STAG-GFP cells after viral infection

Virus obtained from CP3 was used for the first transduction carried out on a 70% confluent 100mm dish of 3Faii cells. At 24h, although the cells remained healthy-looking there were no GFP-positive cells visible in the dish, as were found in transduced 3T3 cells (not shown). The cause of the poor result was not known but was attributed to the lower temperature of incubation of the STAG 3Faii line of $33^{O}C$; whether the lower temperature was important in the transduction reaction giving rise to small numbers of infected cells, or in the delayed expression of the green fluorescent protein subsequent to transduction was not clear.

The experiment was repeated with 2 x 35mm dishes of STAG 3Faii cells, with all steps at $33^{O}C$, and the dishes were monitored over 7d. At 24h and 48h, no GFP-positive cells were seen in either of the dishes. By 6d, however, moderate numbers

of green-fluorescent cells could be found within the dishes (not shown). An estimate of 20% of all cells were found to be expressing the GFP. FACS analysis on day 7 showed that the 2 dishes in fact contained 12% and 17% GFP-positive cells, respectively (not shown). Although this demonstrated that STAG 3Faii cells could be successfully transfected with GFP but showed delayed expression of the protein, the numbers of transduced cells remained low at less than 20%.

In addition, the virus used in this second infection was taken 12d after transfection of fNX cells (CP3), and may have been another factor in the low percentage of GFP-positive cells.

5.3.5.2 Raising the incubation temperature of the viral infection to 37^{O}C increases the transduction efficiency of STAG cells

A third STAG 3Faii line infection experiment was set up, this time with the infection step carried out at 37^{O}C to determine whether the increased temperature would give rise to a higher transfection efficiency. The 3Faii cells were maintained at 33^{O}C before and after incubation with the virus. In addition, the virus used for the infection was obtained from an earlier time-point post-transfection of fNX cells (CP8, 48h PT).

72h after transduction, moderate numbers of GFP-positive cells could be seen, estimated at 40%, a feature which had not been apparent with previous infections at 33^{O}C. An aliquot of these cells, termed *3Faii-GFP-1* cells (Fig. 5.9), was frozen down.

FACS analysis of a separate aliquot of the same cell population at 2 weeks post-infection demonstrated that 42% of the cells were GFP-positive. These GFP+ cells were subsequently FACS-sorted to obtain a population of pure GFP+ 3Faii cells.

However, these cells acquired a bacterial contamination 2d after the FACS-sort and were eventually discarded. A second FACS-sort was carried out on the original transfected cells (Fig. 5.10) and on the following day, the sorted cells appeared healthy and viable; fluorescence microscopy showed that all the cells visible were green fluorescent (not shown). These cells were termed *3Faii-GFP-1S* (Sorted) cells.

The pre- and post-sorted cells, 3Faii-GFP-1 and –1S, respectively, were later used for transplantation into the adult rat brain (5.3.6).

5.3.6 Transplantation of STAG-GFP cells into the adult rat brain

STAG cells were transplanted into the adult rat brain to determine whether expression of GFP was retained *in vivo*. This would enable the detection of the STAG cell lines *in vivo*, which had previously been difficult, and furthermore, would allow the study of the phenotype of the STAG cell lines *in vivo*.

Pre- and post-sorted 3Faii-GFP cells were collected as described before (5.3.5.2). Immunostaining of the STAG-GFP cells showed that these cells retained the phenotype of normal STAG cells (not shown), as described before (Fig. 3.11). STAG-GFP cells were subsequently transplanted into the adult rat septal cholinergic nuclei or the dorsal striatum; 2 transplants of pre-sorted cells, where GFP+ expression was present in approximately 40% of the cells (Fig. 5.10), were deposited into the septal cholinergic nuclei and 4 into the dorsal striatum. In addition, 4 animals were transplanted with STAG-GFP post-sorted cells, one day after the FACS-sort, where green fluorescence had been observed on all cells *in vitro* prior to transplantation (not shown).

Figure 5.9 STAG cells transduced with GFP (3Faii cells in culture, photographed with the fluorescein (FITC)-filter). 3Faii cells show expression of the GFP at 6d post-transduction, seen at low power (A) and high power magnification (B); note that expression is seen throughout the cell body and process.

(Scale bar: A, 20μm; B, 10μm)

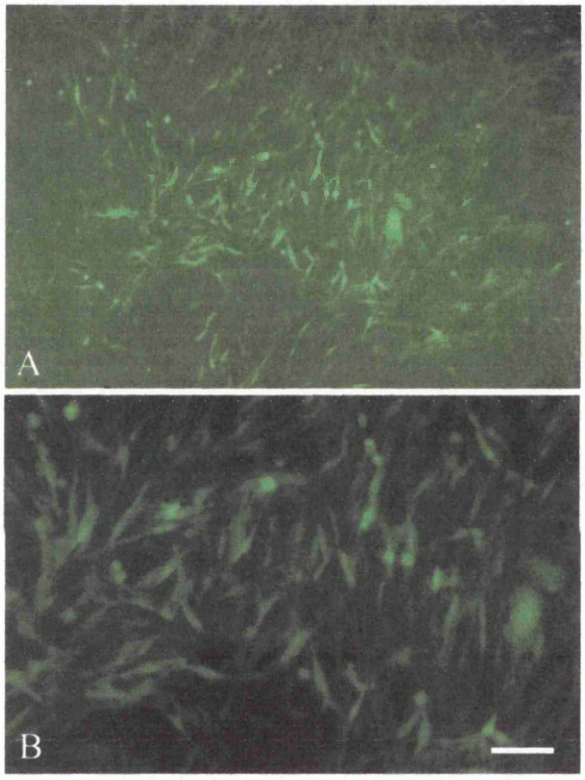
A
B

Figure 5.10 FACS-sorting of STAG cells transduced with GFP. STAG 3Faii cells transfected with GFP were taken for sorting 7d post-infection; FACS-analysis showed that approximately 40% of all cells were expressing the GFP, and clearly separated in this field from non-GFP expressing cells, and these were purified from non-transfected cells. ('M1' represents those cells purified for subsequent transplantation – see 5.3.6)

FACS sort of STAG-3Faii-GFP-1S

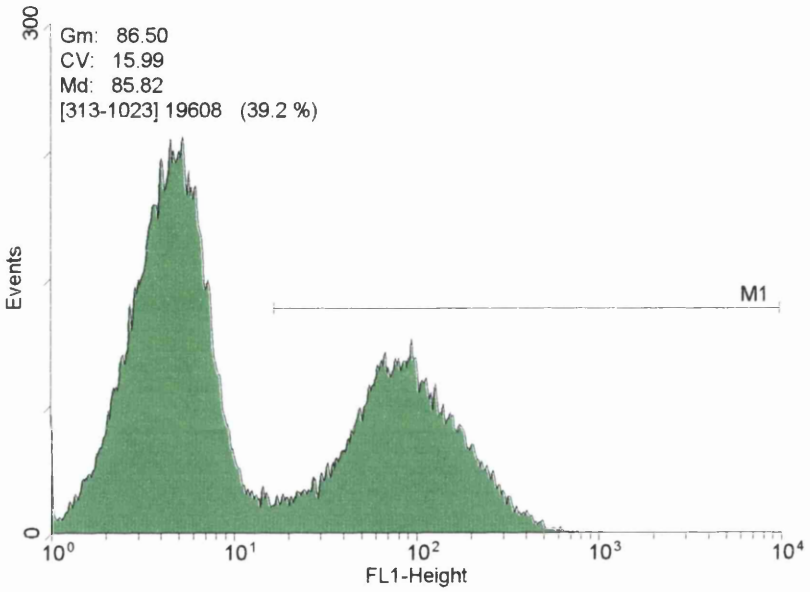

Retention of GFP in vivo

Unstained coronal vibratome sections taken at 2d post-operation (po) revealed the presence of GFP+ cells in the region of the dorsal striatum and the corpus callosum (n=2) (Fig. 5.11). This demonstrated that target cells transduced with GFP-virus could retain expression of the GFP after 2d *in vivo*.

GFP-expression was observed in a large number of cells which displayed an elongated cell morphology which was typical of STAG 3Faii cells *in vitro*. However, there was also a large area in the vicinity of the transplant which fluoresced, although this yellow-green signal was typical of background, non-specific fluorescence rather than of the characteristic green fluorescence of GFP-expressing cells. These cells, which were localised to the transplant area, were presumed to be those STAG cells which were not expressing the GFP when transplanted into the striatum.

Vibratome sections of transplants of pre-sorted STAG-3Faii-GFP cells into the striatum at 7d showed continued expression of transplanted cells in the region of the transplant (n=3). The presence of non-specific fluorescence remained in the region of the transplant (Fig. 5.11). However, the transplants which had been deposited into the septal cholinergic nuclei could not be visualised in fluorescence (n=2). At high magnification, small numbers of GFP-positive cells could be seen at the base of the transplant, however, the columnar transplant that had been seen for primary SC transplants was not observed.

In addition, analysis of 4 transplants containing post-sorted STAG-GFP cells transplanted into the septal cholinergic nuclei also demonstrated the complete absence of GFP-expressing cells at the transplant site. This may have been the product of bacterial contamination through tissue culture.

Processing of STAG-GFP transplants

Vibratome sections containing transplants in the dorsal striatum demonstrated expression of GFP when observed under fluorescence microscopy immediately after sectioning (Fig. 5.11, 5.12). In contrast, the cryostat sections from one animal, which contained pre-sorted STAG-GFP cells also in the striatum, did not reveal GFP-positive cells at the transplant site (not shown). The apparent loss of expression may have been the result of the snap-freeze of the brains containing the transplant prior to sectioning and so denaturing the structure and fluorescence of GFP. However, a small amount of fluorescence was seen in the region of the transplant and this may suggest a poor transplant rather than loss of expression of GFP in the cells of the transplant.

Immunostaining for the neurofilament and GFAP antigens was carried out for the vibratome sections containing striatal STAG-GFP transplants. In addition to the GFAP reaction around the transplant typical of reactive astrocytes, there was some immunoreactivity to the neurofilament antibody at the transplant site (n=2) (not shown). These findings would need to be verified with further experiments.

STAG-3Faii-GFP cells in the dorsal striatum and corpus callosum

STAG-3Faii-GFP cells survived transplantation into the dorsal striatum, formed aligned cellular processes, as is often seen for primary SCs *in vivo*, and showed extensive migration within the corpus callosum (Fig. 5.11, 5.12); STAG-GFP cells could be further identified by their bipolar spindle-shaped cell morphology at high magnification (Fig. 5.12B). GFP+ cells could be seen extending within the corpus callosum for several millimetres lateral to the injection site within 48h (n=2).

Figure 5.11 Transplantation of STAG-3Faii-GFP cells into the dorsal striatum (montage of photomicrographs of coronal sections recorded immediately after vibratome-sectioning). Aligned STAG-GFP cells can be seen in the transplant column within the cortex (cx), and where this meets the corpus callosum (asterisk), STAG-GFP cells can be identified extending both along the corpus callosum (cc) and within the dorsal striatum (str). This animal was perfused at 7d post-operation. *(Scale bar, 15μm)*

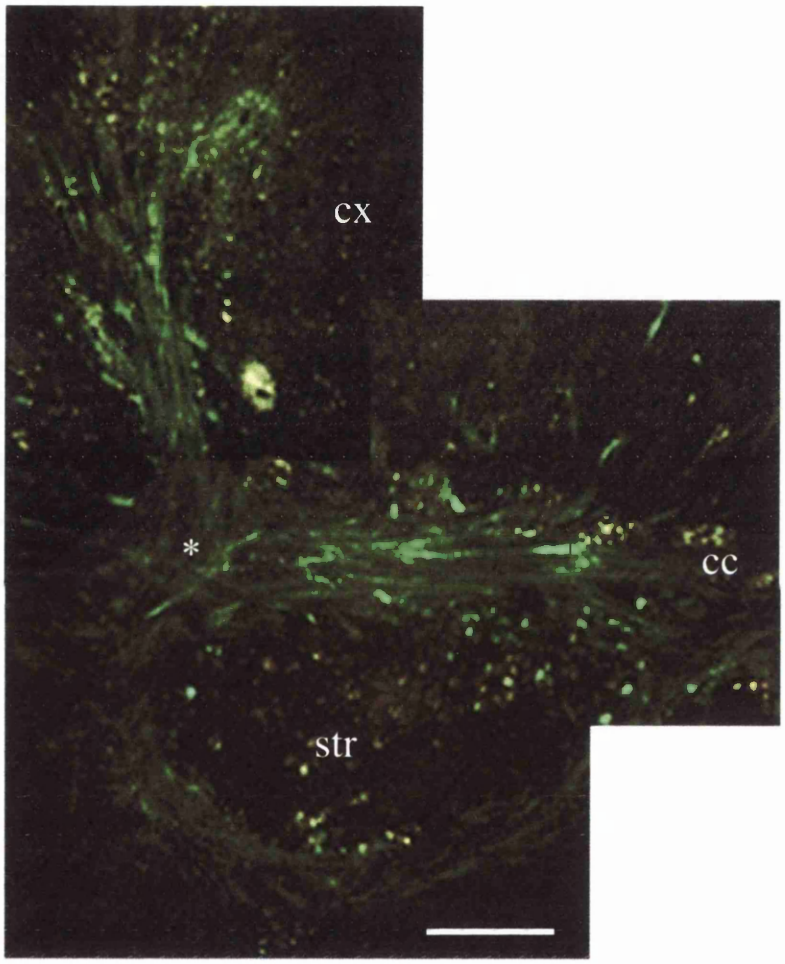
cx
*
cc
str

Figure 5.12 STAG-GFP cells within the corpus callosum (photomicrographs of coronal sections). STAG-GFP cells can be identified within the tract of the corpus callosum (cc), several millimetres lateral to the injection site (A). Higher magnification of the GFP-expressing cells within the axis of the corpus callosum demonstrates the bipolar, spindle shape typical of the STAG line *in vitro*.

(Scale bar: A, 10μm; B, 5μm)

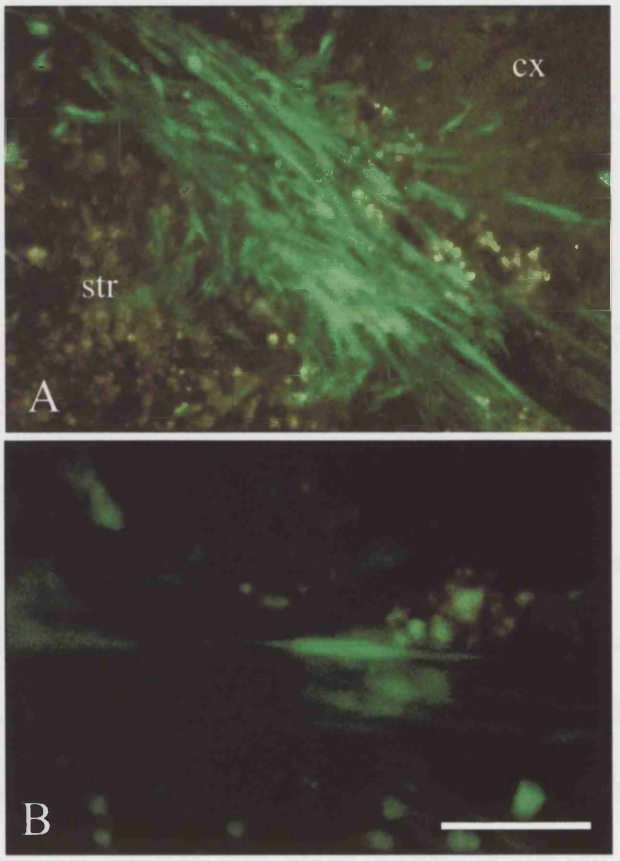
cx
str
A
B

5.3.7 Transduction of primary neonatal SCs and olfactory ensheathing cells

Primary glial cells may have a useful role in aiding the repair of cut central fibre tracts (Franklin and Barnett, 1997; Li *et al.*, 1997). The study of primary neonatal SCs (NSCs) and olfactory ensheathing cells (OECs) in the CNS would benefit if they could be labelled with GFP prior to transplantation. Therefore, transduction experiments were begun using these 2 cell types.

Given that both cell populations do not readily divide under normal conditions, primary NSCs and OECs were stimulated with mitogens in order to encourage high transfection efficiencies with the retrovirus. Mitosis was observed in both cell cultures within 24h of the use of forskolin and PDGF-BB for SCs, and bovine pituitary extract (BPE) for OECs, typically characterised by the formation of whorls of aligned cell processes (not shown).

The initial series of transductions was carried out on 4 x 35mm dishes, 2 each for NSCs and OECs at a cell density of 5 x 10^5 cells/dish. 1ml virus obtained from an optimised fNX-cell transfection was used to infect 3 of the dishes overnight in dotap; 1 x NSC dish was maintained as a control and the cells were incubated in normal DMEMF media overnight. Analysis of the cells at 24h and 48h showed low numbers of GFP-expressing cells, although by 6d, moderate numbers of GFP cells could be seen in the OEC cultures (Fig. 5.13). FACS-analysis at 6d demonstrated that the 2 x OEC cultures contained 26% and 41% GFP-positive cells, respectively, while the remaining infected NSC culture showed 16.7%; the control NSC culture showed no green fluorescent cells (not shown).

These results demonstrated that moderate numbers of OECs could be transfected in this way, and that with optimisation of conditions, large transduction

efficiencies might be attainable. The NSC transduction would need to be repeated. Primary OECs and NSCs were subsequently plated onto 24wp wells at 4 x 10^4/ml/well 24h prior to infection and infected with virus. In these experiments, the timing of mitogens was examined, and primary cells were incubated in mitogens for the entire length of the experiment up to 48h post-infection, and compared to cells in which the mitogens were removed at the end of the infection step. Preliminary results suggest that mitosis during and after the infection step are crucial for high transduction efficiency, although more experiments would need to be carried out to confirm this.

Figure 5.13 Transduction of primary glial cells *in vitro*. Olfactory ensheathing cells (OECs) were transduced with GFP in culture, although with only moderate efficiency (A, note the non-GFP-expressing cells around those which have been successfully transduced). Where OECs are transduced with the GFP, they display expression throughout the cell body and processes (B).

(Scale bar: A, 20μm; B, 10μm)

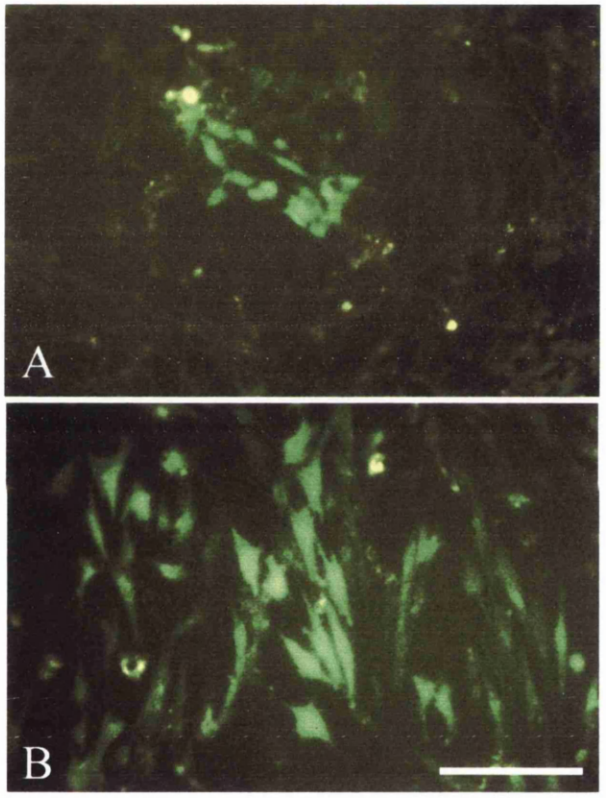
A
B

5.4 Discussion

5.4.1 Transfection of the fNX packaging cell line with GFP

Comparisons of Effectene-transfections with calcium phosphate transfections showed that not only was calcium phosphate a more economical means of transfecting the fNX packaging cell line, but it was more effective. In optimised transfections, the $CaPO_3$ method was able to transfect approximately 70% of fNX cells by 48h. A high percentage transfection efficiency is necessary if virus is to be taken at this early stage for successful transduction of target cells.

For safety reasons, transfected fNX cells could not be FACS-analysed to determine more precise percentages of transfection efficiency. The cell counting system which was initially developed for assessment of transfection efficiency, where total numbers of cells in 9 fields of view were counted, soon became impractical as thousands of GFP-expressing cells were visible within the fields of view. The use of simple estimation of transfection efficiency was resumed and this appeared to be satisfactory, given that by CP10, high efficiency transfections could consistently be produced.

The incubation of the $CaPO_3$ precipitate prior to addition to the fNX cells was not found necessary in the present study. Other studies also show an omission of this step (Kinsella and Nolan, 1996). With regards the use of chloroquine in the transfection of fNX cells, this was not found crucial for high transfection efficiency. Other studies do describe the use of chloroquine in transfection of the fNX cells (Kinsella and Nolan, 1996; Staal *et al.*, 1996). Given that in the present study, its inclusion in the protocol was not apparently detrimental to the cells, its use was continued in all subsequent transfections.

The transfection efficiency of fNX cells obtained in the present study compares favourably with previous reports of the same cell line (Grignani *et al.*, 1998; Pear *et al.*, 1993).

Puromycin selection of transfected fNX cells

The concentration of puromycin required to kill all untransfected fNX cells was calculated in the present study at 2μg/ml. In the second PKC experiment, the high starting cell density was closer to that which would exist in the fNX cell transfections at 48h after transfection, from which time the selection process, if required, would begin. Significant cell death was observed from approximately 7d of selection with puromycin at 2μg/ml.

Selection of a transfected fNX-cell culture for 12d in puromycin at 2μg/ml showed a moderate level of cell death over this time-period. Analysis of the selected cell population after 12d in puromycin showed that all cells displayed green fluorescence, although some showed low levels of fluorescence (not shown), and the cell population was subsequently frozen down. However, on later retrieval of the cells for viral collection, the culture rapidly acquired a bacterial contamination and underwent complete cell death within 48h. Virus from this puromycin-selected culture could not therefore be used for analysis of transduction efficiency.

Selection of transfected fNX cells is likely to further increase the viral titre, although this has yet to be tested in the present study. Previous reports have demonstrated an increase of approximately 30% in viral titre, as determined by the increase in colony-forming units per millilitre of virus; transfected fNX cells in this study were selected with puromycin at 1μg/ml (Grignani *et al.*, 1998).

5.4.2 Viral titration and transduction of 3T3 cells

Virus taken from 48h after transfection of fNX cells with the retroviral plasmid, was able to transduce up to 90% of 3T3 cells under optimal conditions, as determined by FACS analysis. 3T3 cells expressed GFP within 24h of infection with the virus, with greater numbers of GFP-expressing cells by 48h; green fluorescence was observed throughout the cell body and processes.

Several aspects of the viral infections will now be discussed in turn.

Titration of virus

Transduction with the supernatant of transfected fNX cell cultures was able to infect approximately 75% of 3T3 cells, as determined by the expression of GFP 48h after infection. Given the conditions of the 3T3 cell transduction, and that infections of 3T3 cells are single infections resulting from single infectious viral particles, the transfected fNX cell cultures tested using this assay can be calculated to produce approximately 2.5×10^4 infectious units per ml. As the virus used for this titration assay was obtained form an early fNX-cell transfection, the current optimised fNX transfections should provide infectious virus units at a greater concentration that this value.

Previous reports of the fNX cell transfection system can produce approximately 10^6 infectious units per ml. Although, in the present study, the titre is considerably lower than this, infectious titres could be easily increased by reducing the volume of the media which the virus is harvested from. In addition, further optimisation of the transfection and transduction processes may yield higher titres.

Transduction with time of viral harvest

Although one experiment suggested that the titre of infectious virus fell rapidly in the first week after transfection of fNX cells, this finding was not substantiated with several other transduction results using the same original fNX cell culture.

In the original analysis of transduction with time of viral harvest, although efficiency was moderate-high up to 72h post-transfection, virus taken at 8d and 12d post-transfection showed only 15-20% transduction efficiency. In parallel analyses, however, 6 identical cultures of 3T3 cells transduced with virus taken also at 8d post-transfection, demonstrated an average of 74% transfection efficiency.

Although previous reports have suggested that the intensity of green fluorescence of the fNX packaging cells may diminish with time, probably as a function of decreasing episomal plasmid copy number, the efficiency of virus taken up to 30d post-transfection remains high (Grignani *et al.*, 1998; Pear *et al.*, 1993).

Given that in the present study, a later analysis of virus taken 12d after transfection of fNX cells (the same culture as that described above) showed a transfection efficiency of 62%, the original analysis of transfection with time of viral harvest is not likely to be representative of viral transduction efficiency with time of viral harvest.

These experiments would need to be repeated to confirm that viral infection competency in the present system remained high beyond 1 week post-fNX cell transfection. Given that infection efficiency has been shown to be high from at least 2-12d, the present system already provides ample time to produce large quantities of virus for subsequent transduction of target cells.

Inconsistency of transduction efficiency of 3T3 cells

The 3T3 cells used in the initial series of transduction analyses were replaced with a batch of 3T3 cells from a different source due to the long lifetime of the former batch. However, after screening of the second batch later identified an underlying Mycoplasma contamination, the original 3T3 cell line was reintroduced for subsequent transductions.

It is possible that the reduction in observed transfection efficiency of the second batch of 3T3 cells with several viral stocks was, at least in part, due to the underlying Mycoplasma infection. On re-introducing the original 3T3 cell line, high transfection efficiencies were again obtained on virus samples that had previously produced poor transfection efficiencies.

In addition, the cell density of the 3T3 cells at the time of transfection was found to be important in the subsequent transduction efficiency of the cells. Those 3T3 cells which showed confluency within 24h of the viral infection were unlikely to show high transfection efficiency when FACS-analysed at 48h. Although cell division during the period of viral incubation is an important pre-requisite for uptake of the viral GFP, the presence of cell division subsequent to this also appears to be important for efficient transduction.

5.4.3 Transduction of STAG cells with GFP

Transduction of the STAG 3Faii cell line was not efficient when carried out at the normal STAG cell incubation temperature of 33^{O}C. However, the transfection efficiency improved when the temperature of the viral incubation was changed to 37^{O}C. Although there remained a delayed expression of the GFP *in vitro*, approximately 40% of cells were found to express GFP by 7d after transduction.

Given that the STAG 3Faii cells constitute a rapidly dividing cell line, transduced cells can be quickly purified by FACS-sorting of GFP-positive cells. This was carried out with one population of transfected STAG 3Faii cells and yielded approximately 2 x 10^6 GFP+ cells within 2h of FACS-sorting (not shown). Confirmation of GFP-expression in all cells was obtained when visualised under fluorescence microscopy.

When FACS-sorting was carried out on a GFP-transduced 3Faii cell culture, on 3 of the 4 occasions a rapid and lethal bacterial contamination developed within 72h of the sort. The contamination after FACS-sorting may have developed in the process of the sorting procedure, itself, or may have been the precipitation of an underlying level of contamination originating from the viral source; transfected fNX-cell cultures were regularly observed in a different lab for fluorescence and occasionally acquired a bacterial contamination in the process of transporting the cells between the labs.

As an alternative to FACS-sorting, STAG cells could in future be transduced with multiple cycles of viral infections. This has been described successfully in a recent report which utilises the fNX cell lines (Grignani *et al.*, 1998), where haematopoietic progenitor cells underwent up to 4 cycles of infection over approximately 12h. The transfected cells were subsequently FACS-sorted to obtain pure populations of GFP-expressing progenitor cells, which themselves, were later shown to share those clonogenetic and differentiative properties of the unfractionated progenitor cell population. This provides further evidence to show that incorporation of the GFP is unlikely to have an effect on the normal phenotype of the cells which take it up (see also Heemskerk *et al.*, 1997).

In the above and other similar studies, several transduced cell lines have shown approximately 95% transfection efficiency (Grignani *et al.*, 1998; Muldoon *et al.*, 1997), demonstrating that retroviral transfection can optimally transfect the vast majority of a target cell population. The optimal percentages of transduced cells may vary across cell lines and primary cell types. However, the technique of FACS enables pure populations of transduced cells to be collected, and in the context of the present study, can provides a pure GFP-tagged population for transplant studies.

5.4.4 Transplantation of STAG-GFP cells into the adult rat brain

STAG-3Faii-GFP cells were transplanted into the adult rat brain and were shown to retain the expression of GFP when *in vivo*. Although relatively small numbers of these transplants have so far been carried out, several aspects of these transplants will now be discussed in turn.

Processing of GFP-transplants

The presence of GFP+ cells in 4% paraformaldehyde-perfused vibratome sections and not cryostat sections may have been a product of the low numbers of transplants involved, rather than a reflection of the loss of expression on freezing. The structure and therefore the detection of GFP can be severely disrupted by a number of conditions, including certain chemical reagents and extremes in pH conditions (Bokman and Ward, 1981; Ward and Bokman, 1982). Indeed, this may consequently render visualisation of tissue which requires acid-alcohol fixation difficult.

However, the expression of GFP in the cryostat sections is unlikely to have been lost solely on freezing. For example, in the present study, a population of

transfected fNX cells was frozen down in liquid nitrogen but retained fluorescence when thawed and observed under fluorescence microscopy several weeks later.

In those transplants which showed the presence of GFP-positive cells, the background fluorescence level of the sections was exceptionally low.

Expression of GFP *in vivo*

While STAG-GFP cells could be clearly identified *in vivo* with their elongated, bipolar cell morphology, there are two important issues which should be addressed when using this technique to identify transplanted cells *in vivo*. Firstly, are all the transplanted cells expressing GFP, and secondly, are all those cells which are expressing GFP *in vivo* originally transplanted cells?

In answer to the first question, the present transplants into the dorsal striatum were not all GFP-positive; pre-transplant FACS-analysis showed that approximately 40% of these cells were expressing GFP at significant levels. The hue of yellow-green fluorescence background which was observed in the vicinity of the transplant site, can thus be attributed to transplanted STAG 3Faii cells which were either negative for the GFP, or were expressing GFP at very low levels. If STAG-GFP cultures could be successfully FACS-sorted prior to transplantation, then this should provide expression of GFP in 100% of the transplanted cells, a feature which can be verified by FACS prior to transplantation.

With regards to the second issue of whether all fluorescent cells *in vivo* are transplanted (STAG) cells, the answer is more difficult to ascertain. Target cells, such as the STAG 3Faii line in the present study, do not contain the packaging signal present in the original fNX packaging cell line. Transfections of the target cells should therefore be single transfections with no further propagation of the

virus. Moreover, the present fNX packaging cell line is designed with fewer original retroviral loci so as to further reduce the risk of a return to viral potency (Pear *et al.*, 1993). Therefore, the chance that a host cell in the adult rat brain has acquired the GFP through a series of recombination events is remote.

Given the potential risk of recombination events involving viral sequences, media from the transduced cells was regularly collected for analysis of helper virus. None of the samples tested positive for the presence of infectious virus, as determined by the inability to transduce 3T3 cells (data not shown).

Finally, another possible cause of non-STAG-GFP cells expressing GFP *in vivo* is through phagocytosis of a STAG cell. Both macrophages and astrocytes are able to phagoctyose cells in the CNS (Al-Ali and Al-Hussain, 1996; Aldskogius and Kozlova, 1998). However, no cells expressing the morphology of these two cell types were ever seen in the STAG cell transplants carried out in the present study. Indeed, contact with the acidic contents of the lytic lysosomes after the process of phagocytosis is likely to irreversibly denature the GFP, and thereby destroy the fluorescence.

Double-labelling immunohistochemistry and ultrastructural studies would further be able to identify the presence of GFP-containing host cells

STAG 3Faii cells *in vivo*

STAG-3Faii-GFP cells in the striatum

When transplanted into the CNS, STAG-3Faii-GFP formed aligned processes at the transplant site. When transplanted into the striatum, GFP-positive cells were found at the base of the transplant in the dorsal striatum, across the corpus callosum perpendicularly and within the corpus callosum for several millimetres lateral to the

injection site. Given that this was seen within 48h of the transplant procedure, this suggests extensive migration of the STAG 3Faii cells within the corpus callosum by this time point.

Immunostaining of these transplants showed that a second antigen could be identified in these sections additional to that of GFP-expressing STAG cells. Immunostaining for the GFAP antigen showed the localised astrocytic reaction around the striatal transplant present at 2d and at 7d, the 2 time-points tested. Neurofilament-immunoreactivity at the transplant site suggested that axons were being recruited into the STAG cell transplants in the striatum, and indeed into the corpus callosum, although, this would need to be substantiated with further experiments. The signal of ubiquitous neurofilament in the present study overwhelmed that of the GFP-expressing STAG cells. Nevertheless, multiple immunostaining of GFP-expressing transplants can be achieved with further optimisation.

STAG-3Faii-GFP cells in the basal forebrain

A population of STAG-3Faii-GFP cells was FACS-sorted to obtain a pure population of GFP-expressing cells which was confirmed by fluorescence microscopy. These GFP-sorted cells were transplanted into the septal cholinergic nuclei of 4 animals, as had been previously carried out for neonatal Schwann cells (SCs). However, at time-points from 7d to 1 month, no GFP-positive cells were observed within the brains of these animals.

There are a number of possible explanations which may underlie this result. Although SCs are known to be able to migrate within the CNS, it is unlikely that all the transplanted STAG cells migrated away from the transplant site such that they

were missed altogether. In addition, STAG-GFP cells were previously observed in the striatum at 7d, and were therefore, unlikely to have lost GFP-expression when examined in the basal forebrain at the same time-point.

An important difference in the striatal transplants and the 4 basal forebrain transplants described above was the nature of the STAG cells which had been transplanted; pre-sorted cells were transplanted into the striatum but post-sorted STAG-GFP cells were transplanted into the basal forebrain. Given that in the 2 FACS-sorts of STAG-GFP cells previously carried out, the sorted cells had acquired a bacterial contamination and undergone complete cell death within 48h subsequently, it was highly likely that the sorted cells used for transplantation into the basal forebrain had also acquired a contamination and died *in vivo*.

The sorted cells which were used for transplantation had appeared viable at the time of preparation, 48h after the FACS-sort. However, a subsequent FACS-sort of a population of GFP-transduced 3Fb cells also resulted in contamination and complete cell death, this time after 96h of the sort, and having appeared relatively healthy at 48h. Given the results of the second sort, it is further likely that the transplanted cells had died *in vivo* in the first week after transplantation, prior to perfusion at 7d.

5.4.5 Transduction of primary SCs and olfactory ensheathing cells

The early transduction experiments of primary SCs and olfactory ensheathing cells (OECs) suggested that if sufficient numbers of cells remained in mitosis throughout the length of the procedure, then moderate-large numbers of cells could be successfully transfected with GFP. Although these cells are not fast-dividing cell lines, they can be stimulated with mitogens to show significant rates of cell

division. The stimulation of cell division of OECs is less well characterised than that of SCs (Chuah and Au, 1993; Levi *et al.*, 1995).

Preliminary transfections showed that up to 41% of OECs were transduced with GFP-virus under the present conditions. Optimisation of the transfection conditions could significantly increase this value, and also that of primary SCs. In addition, the use of multiple cycles of viral infection as described earlier and as reported in a recent study (Grignani *et al.*, 1998), together with the use of FACS-sorting, provide the opportunity to obtain large and pure populations of GFP-expressing cells which can be utilised in cell transplant studies.

5.4.6 Summary

The fNX retroviral transfection system is able to provide a high efficiency transfection method for labelling cell transplant material with the GFP. 3T3 cell lines have been used to optimise the conditions for transduction of target cells with infectious virus containing GFP. Although infectious titres could be further increased with more optimisation, the system currently provides the opportunity to infect large cell populations prior to transplantation, which if FACS-purified, could enable pure GFP-expressing cells to be transplanted into the central nervous system.

The transfection system has been used to trace suspension transplants of STAG cells, which had previously been difficult to identify *in vivo*. Preliminary studies have shown that the STAG-GFP cells retain the immunophenotype of pre-transduced STAG cells *in vitro*, and when transplanted into the dorsal striatum, they form aligned processes within the column and are able to migrate extensively within the corpus callosum.

CHAPTER VI

CHAPTER VI – General Discussion

This project has raised a number of issues regarding the study of transplanted material into the central nervous system (CNS). These include, in particular, the use of immunohistochemistry to identify cells transplanted into the host CNS, and the application of similar 'bridging' transplant techniques to encourage repair in the CNS.

There are several advantages to creating a cell line. In the present study, the Schwann cell (SC) line was generated with the intention of providing an abundant source of SCs, cells which are presently in great demand as an aid to stimulating regeneration in the CNS (Levi *et al.*, 1995). As with other cell lines, this SC line would provide a theoretically limitless source of cells and require little preparation and tissue culture management as compared to fresh SCs isolated from peripheral nerve. If the cell line so created was phenotypically comparable to the original primary cell type then it could be used as a tool for the assessment of SC behaviour both *in vitro* and *in vivo*. In addition, the cell line could be used as a basis for further genetic manipulation in order to assess the potential of individual transfected gene products, for example, cell adhesion molecules and growth factors, in the context of promoting CNS regeneration (Tuszynski *et al.*, 1998).

However, there are a number of considerations which must be made when using such cell lines. One of the most important of these is that the cell line has been generated by a gene transfection step, the site of integration of which is essentially random. Consequently, any 'useful' properties of the cell line may not be able to be reproduced.

Associated with the random integration of the gene encoding the large T antigen is the issue of antigen expression stability in that cell line; there may be a de-activation or re-activation of neighbouring gene expression close to the site of large T antigen integration. This may be relevant in the present STAG lines where there is down-regulation of the receptor to the nerve growth factor.

There will also be a number of cells within the STAG lines which have mutated since the initial transfection and therefore that cell line will lose its homogeneity cell status with increasing time in culture. This may be a feature of the STAG lines, as determined by some altered cell morphologies within some cell lines, although this may also be a product of cloning originally from small clusters of cells rather than from a single cell.

Therefore, the generation of a SC line provides principally a tool for the study of relevant cell biology, and as a basis for subsequent transfections of genes of interest to study their significance *in vivo*.

In the present study of primary SC-transplants in the basal forebrain, the phenomenon of antigen expression stability is again important. Although this is important in a cell line as described above, it is also relevant to primary cells characterised *in vitro* and later observed *in vivo*. An example of this in the present study is the expression of the low-affinity nerve growth factor receptor, p75, by the SCs. While it is well-documented that primary SCs can express p75 *in vitro*, on myelinating axons *in vivo* the SCs down-regulate expression of p75 and up-regulate expression of the myelin proteins (Morgan *et al.*, 1991). Although the transplanted SCs in the present study do not appear to be myelinating axons *in vivo*, it is not clear what percentage of the SCs continue to express the p75 protein *in vivo*, and

therefore, what percentage of the cells are identified by immunohistochemistry. Similarly, primary SCs can express the intermediate filament protein, GFAP, *in vitro*, but down-regulate expression of this protein when brought into contact with axons (Mirsky and Jessen, 1996); in the present study this is used to identify astrocytes (GFAP-positive) but not SCs *in vivo*.

The use of electron microscopy (EM) would make it possible to analyse the ultrastructural make-up of the transplants and avoid some of the above-mentioned problems in light immunohistochemistry. Although EM-processed sections were begun in the present study, these would need to be repeated to substantiate the observations so far made at the light microscope level.

Given the loss of expression of p75 on the immortalised STAG cell lines a new marker was required to identify these cells *in vivo*. The STAG cell lines were rat cell lines and so donor/host species differences could not be exploited in this case as has been described in previous studies (Lund *et al.*, 1985). Although a nuclear fluorescent dye such as Hoechst could have been used, this would have provided only nuclear labelling and would not have been able to identify the long processes of labelled cells. In addition, the Hoechst dye would have been diluted with each cell division making identification of the STAG cells more difficult with time *in vivo* (Stichel *et al.*, 1996). The expression of large T antigen by the STAG lines at this raised temperature *in vivo* was also so reduced that identification of STAG cells using antibodies to this marker was not possible.

Given the recent development of Green Fluorescent Protein (GFP), this offered a useful label with which to mark the STAG cells. Labelled cells could be later identified without the need for fixation and the associated time-consuming

immunohistochemistry; transplants of the labelled cells could be labelled further with host glial and axonal markers to obtain multiple-labelled sections; and the nature of the bicistronic vector used to transfect the GFP label onto the STAG cells could allow later incorporation of an additional gene of interest and enable simultaneous cell tracking. Preliminary transfections with GFP and transplants of GFP-transfected cells into the brain in the present study suggest that this indeed, is a useful means of tracking a cell type *in vivo*.

The use of cell-labels of any kind requires that the label does not alter the phenotype of the cell which is labelled and that the system is non-toxic to the system in which it is used. Although still relatively new, the use of GFP-labelling to track a specific cell population has proved to be relatively safe in these respects; one example of this is a study in which GFP-transfected haematopoietic progenitor cells were analysed for their clonogenetic and differentiative properties and found to be indistinguishable from non-transfected progenitor cells derived from the same original cell population (Grignani *et al.*, 1998).

Although no obvious toxicity was observed in the brains of those animals containing STAG-GFP transplants in the present study no formal assessment of the host response was made. Blood samples could be extracted to assay the T and B cell response of the host immune system, while antibodies for various lymphocytic cell surface markers could be used to assess the *in situ* response to GFP-expressing transplants.

Future work with the use of GFP-transfected SCs may help to not only track transplanted cells within the brain, and thereby, give a greater appreciation of SC behaviour and migration in the CNS, but, given the make-up of the bicistronic

vector, further allow the accurate tracking of SCs transfected with additional genes of interest. One candidate gene would be that encoding the cell adhesion molecule, L1. In this way, the transplantation of new trophic and tropic molecules presented on the 'right' cell type may provide sufficient permissive cues to enable functional regeneration of lesioned CNS pathways.

Furthermore, the nature of the extrusion transplantation system used in the present study enables one to transplant suspension material into the brain with minimally traumatic consequences, a procedure which would benefit any therapeutic strategies in CNS-injured patients. With the use of a modified stereotaxic apparatus to provide oblique angle injections, one could use the system to access and 'bridge' a wide range of white matter tracts situated within the brain, if the appropriate cocktail of cell transplant material could first be elucidated for the given tract.

Given that a cell transplantation-based strategy might be found to promote regeneration of lesioned CNS pathways, it is important to consider the host (patient) response to the procedure. Where cells foreign to the patient are used, the patient would certainly require immunosuppressive (and cytotoxic) drugs to minimise any immune reaction directed against the transplant material. Where the cell was taken from the patient, himself, this would greatly minimise the chances of transplant rejection. Indeed, the ideal method of repair in a CNS-injured patient might involve the extraction of a particular cell type from the patient's own body, expansion and appropriate manipulation *ex vivo*, and then transplantation back into the patient. However, the use of recombinant DNA/proteins in humans may yet hold much to our ignorance and the development of such gene therapy is presently still short of its promise (Group, 1996).

Given that studies in CNS regeneration are ultimately focused towards treating brain and spinal cord injuries in humans, it is worth considering that the patient may greatly enjoy the consequences of even a slight improvement in regenerating central fibres; to many spinal cord-injured patients, the quality of life is already significantly improved by a recovery of some independence. The psychosocial implications of spinal cord-injury and such debilitating conditions as multiple sclerosis can be more profound than the loss of motor function, itself, and the recovery of basic functions such as urinary continence cannot be underestimated. Indeed, if science is able to significantly improve the capacity of central neurons to regenerate but remains unable to recover an entire population of injured neurons, then this may remain a concern more of academics than of patients.

References

Acheson, A., Barker, P. A., Alderson, R. F., Miller, F. D., and Murphy, R. A. (1991). Detection of brain-derived neurotrophic factor-like activity in fibroblasts and Schwann cells: inhibition by antibodies to NGF. *Neuron* **7,** 265-75.

Al-Ali, S. Y., and Al-Hussain, S. M. (1996). An ultrastructural study of the phagocytic activity of astrocytes in adult rat brain. *J Anat* **188,** 257-262.

Aldskogius, H., and Kozlova, E. N. (1998). Central neuron-glial and glial-glial interactions following axon injury. *Prog Neurobiol* **55,** 1-26.

Aschner, M. (1998). Astrocytes as mediators of immune and inflammatory responses in the CNS. *Neurotoxicology* **19,** 269-81.

Ashley, D. M., Bol, S. J., Waugh, C., and Kannourakis, G. (1993). A novel approach to the measurement of different in vitro leukaemic cell growth parameters: the use of PKH GL fluorescent probes. *Leuk Res* **17,** 873-82.

Assouline, J. G., Bosch, P., Lim, R., Kim, I. S., Jensen, R., and Pantazis, N. J. (1987). Rat astrocytes and Schwann cells in culture synthesize nerve growth factor-like neurite-promoting factors. *Brain Res* **428,** 103-18.

Assouline, J. G., and Pantazis, N. J. (1989). Detection of a nerve growth factor receptor on fetal human Schwann cells in culture: absence of the receptor on fetal human astrocytes. *Brain Research. Dev Brain Res* **45,** 1-14.

Aubert, I., Ridet, J. L., Schachner, M., Rougon, G., and Gage, F. H. (1998). Expression of L1 and PSA during sprouting and regeneration in the adult hippocampal formation [In Process Citation]. *J Comp Neurol* **399,** 1-19.

Baehr, M., and Bunge, R. P. (1990). Growth of adult rat retinal ganglion cell neurites on astrocytes. *Glia* **3,** 293-300.

Baron Van Evercooren, A., Clerin Duhamel, E., Lapie, P., Gansmuller, A., Lachapelle, F., and Gumpel, M. (1992). The fate of Schwann cells transplanted in the brain during development. *Dev Neurosci* **14,** 73-84.

Baron-Van Evercooren, A., Gansmuller, A., Clerin, E., and Gumpel, M. (1991). Hoechst 33342 a suitable fluorescent marker for Schwann cells after transplantation in the mouse spinal cord. *Neurosci Lett* **131,** 241-4.

Benfey, M., and Aguayo, A. J. (1982). Extensive elongation of axons from rat brain into peripheral nerve grafts. *Nature* **296,** 150-153.

Benfey, M., Bunger, U. R., Vidal-Sanz, M., Bray, G. M., and Aguayo, A. J. (1985). Axonal regeneration from gabaergic neurons in the adult rat thalamus. *J Neurocytol* **14,** 279-296.

Berkemeier, L. R., Winslow, J. W., Kaplan, D. R., Nikolics, K., Goeddel, D. V., and Rosenthal, A. (1991). Neurotrophin-5: a novel neurotrophic factor that activates trk and trkB. *Neuron* **7,** 857-866.

Berry, M., Rees, L., Hall, S., Yiu, P., and Sievers, J. (1988). Optic axons regenerate into sciatic nerve isografts only in the presence of schwann cells. *Brain Res Bull* **20,** 223-231.

Bharucha, V. A., Peden, K. W. C., and Tennekoon, G. I. (1994). SV40 Large T Antigen with c-jun Down-regulates Myelin P0 Gene Expression: A Mechanism for Papovaviral T Antigen-Mediated Demyelination. *Neuron* **12,** 627-637.

Bhat, R. V., Axt, K. J., Fosnaugh, J. S., Smith, K. J., Johnson, K. A., Hill, D. E., Kinzler, K. W., and Baraban, J. M. (1996). Expression of the APC tumor suppressor protein in oligodendroglia. *Glia* **17,** 169-74.

Bixby, J. L., Lilien, J., and Reichardt, L. F. (1988). Identification of the major proteins that promote neuronal process outgrowth on Schwann cells in vitro. *J Cell Biol* **107,** 353-61.

Blakemore, W. F., and Franklin, R. J. (1991). Transplantation of glial cells into the CNS. *Trends Neurosci* **14,** 323-7.

Blakemore, W. F., and Patterson, R. C. (1978). Suppression of remyelination in the CNS by X-irradiation. *Acta Neuropathol (Berl)* **42,** 105-13.

Bokman, S. H., and Ward, W. W. (1981). Renaturation of Aequorea gree-fluorescent protein. *Biochem Biophys Res Commun* **101,** 1372-80.

Boutry, J. M., Hauw, J. J., Gansmuller, A., Di Bert, N., Pouchelet, M., and Baron Van Evercooren, A. (1992). Establishment and characterization of a mouse Schwann cell line which produces myelin in vivo. *J Neurosci Res* **32,** 15-26.

Breakefield, X. O. (1993). Gene delivery into the brain using virus vectors [news; comment]. *Nat Genet* **3,** 187-9.

Brecknell, J. E., and Fawcett, J. W. (1996). Axonal regeneration. *Biol Rev Camb Philos Soc* **71,** 227-55.

Bregman, B. S., Kunkel Bagden, E., Schnell, L., Dai, H. N., Gao, D., and Schwab, M. E. (1995). Recovery from spinal cord injury mediated by antibodies to neurite growth inhibitors [see comments]. *Nature* **378,** 498-501.

Brockes, J. P., Fields, K. L., and Raff, M. C. (1979). Studies on cultured rat Schwann cells I. Establishment of pure populations from purified nerve. *Brain Res* **165,** 105-118.

Brockes, J. P., Raff, M. C., Nishiguchi, D. J., and Winter, J. (1980). Studies on cultured rat Schwann cells. III. Assays for peripheral myelin proteins. *J Neurocytol* **9,** 67-77.

Brook, G. A., Lawrence, J. M., Shah, B., and Raisman, G. (1994). Extrusion transplantation of Schwann cells into the adult rat thalamus induces directional host axon growth. *Exp Neurol* **126,** 31-43.

Brunden, K. R., Ding, Y., and Hennington, B. S. (1992). Myelin protein expression in dissociated superior cervical ganglia and dorsal root ganglia cultures. *J Neurosci Res* **32,** 507-515.

Burden-Gulley, S. M., Pendergast, M., and Lemmon, V. (1997). The role of cell adhesion molecule L1 in axonal extension, growth cone motility, and signal transduction. *Cell Tissue Res* **290,** 415-22.

Carbonetto, S. (1991). Facilitatory and inhibitory effects of glial cells and extracellular matrix in axonal regeneration. *Curr Opin Neurobiol* **1,** 407-413.

Caroni, P., and Schwab, M. E. (1988). Two membrane fractions from rat central myelin with inhibitory properties for neurite growth and fibroblast spreading. *J Cell Biol* **106,** 1281-1288.

Carraway, K. L., 3rd, and Burden, S. J. (1995). Neuregulins and their receptors. *Curr Opin Neurobiol* **5,** 606-12.

Carroll, M. W., and Moss, B. (1997). Poxviruses as expression vectors. *Curr Opin Biotechnol* **8,** 573-7.

Carroll, S. L., Miller, M. L., Frohnert, P. W., Kim, S. S., and Corbett, J. A. (1997). Expression of neuregulins and their putative receptors, ErbB2 and ErbB3, is induced during Wallerian degeneration. *J Neurosci* **17,** 1642-1659.

Carter, D. A., Bray, G. M., and Aguayo, A. J. (1989). Regenerated retinal ganglion cell axons can form well-differentiated synapses in the superior colliculus of adult hamsters. *J Neurosci* **9,** 4042-50.

Chalfie, M., Tu, Y., Euskirchen, G., Ward, W. W., and Prasher, D. C. (1994). Green fluorescent protein as a marker for gene expression. *Science* **263,** 802-5.

Chalmers, G. R., Peterson, D. A., and Gage, F. H. (1996). Sprouting adult CNS cholinergic axons express nile and associate with astrocytic surfaces expressing neural cell adhesion molecule. *J Comp Neurol* **371,** 287-299.

Charlton, H. M., Barclay, A. N., and Williams, A. F. (1983). Detection of neuronal tissue from brain grafts with anti-Thy-1.1 antibody. *Nature* **305,** 825-7.

Chen, G. L., Halligan, N. L. N., Lue, N. F., and Chen, W. W. (1987). Biosynthesis of myelin-associated proteins in Simian virus 40 (SV40)-transformed rat Schwann cell lines. *Brain Res* **414,** 35-48.

Chen, J. K., Yao, L. L., and Jenq, C. B. (1991). Mitogenic response of rat Schwann cells to fibroblast growth factors is potentiated by increased intracellular cyclic AMP levels. *J Neurosci Res* **30,** 321-327.

Chen, M. S., Bermingham-McDonogh, O., Danehy, F. T., Jr., Nolan, C., Scherer, S. S., Lucas, J., Gwynne, D., and Marchionni, M. A. (1994). Expression of multiple neuregulin transcripts in postnatal rat brains. *J Comp Neurol* **349,** 389-400.

Cheng, H., Cao, Y., and Olson, L. (1996). Spinal cord repair in adult paraplegic rats: partial restoration of hind limb function [see comments]. *Science* **273,** 510-513.

Cheng, L. L., and Mudge, A. W. (1996). Cultured schwann cells constitutively express the myelin protein P_0. *Neuron* **16,** 309-319.

Chuah, M. I., and Au, C. (1993). Cultures of ensheathing cells from neonatal rat olfactory bulbs. *Brain Res* **601,** 213-20.

Connolly, J. L., Greene, L. A., Viscarello, R. R., and Riley, W. D. (1979). Rapid, sequential changes in surface morphology of PC12 pheochromocytoma cells in response to nerve growth factor. *J Cell Biol* **82,** 820-7.

Corfas, G., Rosen, K. M., Aratake, H., Krauss, R., and Fischbach, G. D. (1995). Differential expression of ARIA isoforms in the rat brain. *Neuron* **14,** 103-115.

Cormack, B. P., Valdivia, R. H., and Falkow, S. (1996). FACS-optimized mutants of the green fluorescent protein (GFP). *Gene* **173,** 33-8.

Cornbrooks, C. J., Carey, D. J., McDonald, J. A., Timpl, R., and Bunge, R. P. (1983). In vivo and in vitro observations on laminin production by Schwann cells. *Proc Natl Acad Sci U S A* **80,** 3850-4.

Crowley, C., Spencer, S. D., Nishimura, M. C., Chen, K. S., Pitts-Meek, S., Armanini, M. P., Ling, L. H., MacMahon, S. B., Shelton, D. L., Levinson, A. D., and et al. (1994). Mice lacking nerve growth factor display perinatal loss of sensory and sympathetic neurons yet develop basal forebrain cholinergic neurons. *Cell* **76,** 1001-11.

Crutcher, K. A., and Marfurt, C. F. (1988). Nonregenerative axonal growth within the mature mammalian brain: ultrastructural identification of sympathohippocampal sprouts. *J Neurosci* **8,** 2289-302.

Danos, O., and Mulligan, R. C. (1988). Safe and efficient generation of recombinant retroviruses with amphotropic and ecotropic host ranges. *Proc Natl Acad Sci U S A* **85,** 6460-4.

Dash, R., Lawrence, M., Ho, D., and Sapolsky, R. (1996). A Herpes simplex virus vector overexpressing the glucose transporter gene protects the rat dentate gyrus from an antimetabolite toxin. *Exp Neurol* **137,** 43-48.

Davies, S. J., Field, P. M., and Raisman, G. (1994). Long interfascicular axon growth from embryonic neurons transplanted into adult myelinated tracts. *J Neurosci* **14,** 1596-1612.

Davies, S. J., Fitch, M. T., Memberg, S. P., Hall, A. K., Raisman, G., and Silver, J. (1997). Regeneration of adult axons in white matter tracts of the central nervous system. *Nature* **390,** 680-683.

DiStefano, P. S., and Johnson, E. M., Jr. (1988). Nerve growth factor receptors on cultured rat Schwann cells. *J Neurosci* **8,** 231-41.

Doevendans, P. A., Becker, K. D., An, R. H., and Kass, R. S. (1996). The utility of fluorescent in vivo reporter genes in molecular cardiology. *Biochem Biophys Res Commun* **222,** 352-358.

Dong, Z., Brennan, A., Liu, N., Yarden, Y., Lefkowitz, G., Mirsky, R., and Jessen, K. R. (1995). Neu differentiation factor is a neuron-glia signal and regulates survival, proliferation, and maturation of rat Schwann cell precursors. *Neuron* **15,** 585-596.

Dong, Z., Dean, C., Walters, J. E., Mirsky, R., and Jessen, K. R. (1997). Response of Schwann cells to mitogens in vitro is determined by pre- exposure to serum, time in vitro, and developmental age. *Glia* **20,** 219-30.

DuBridge, R. B., Tang, P., Hsia, H. C., Leong, P. M., Miller, J. H., and Calos, M. P. (1987). Analysis of mutation in human cells by using an Epstein-Barr virus shuttle system. *Mol Cell Biol* **7,** 379-87.

Dutar, P., Bassant, M. H., Senut, M. C., and Lamour, Y. (1995). The septohippocampal pathway: structure and function of a central cholinergic system. *Physiol Rev* **75,** 393-427.

Eagle, K. S., Chalmers, G. R., Clary, D. O., and Gage, F. H. (1995). Axonal regeneration and limited functional recovery following hippocampal deafferentation. *J Comp Neurol* **363,** 377-388.

Eckenstein, F. P. (1994). Fibroblast growth factors in the nervous system. *J Neurobiol* **25,** 1467-80.

Eldridge, C. F., Bunge, M. B., Bunge, R. P., and Wood, P. M. (1987). Differentiation of axon-related Schwann cells in vitro. I. Ascorbic acid regulates basal lamina assembly and myelin formation. *J Cell Biol* **105,** 1023-34.

Emmett, C. J., Jaques Berg, W., and Seeley, P. J. (1990). Microtransplantation of neural cells into adult rat brain. *Neuroscience* **38,** 213-222.

Fagan, A. M., Suhr, S. T., Lucidi-Phillipi, C. A., Peterson, D. A., Holtzman, D. M., and Gage, F. H. (1997). Endogenous FGF-2 is important for cholinergic sprouting in the denervated hippocampus. *J Neurosci* **17,** 2499-2511.

Filie, A. C., Lage, J. M., and Azumi, N. (1996). Immunoreactivity of S100 protein, alpha-1-antitrypsin, and CD68 in adult and congenital granular cell tumors. *Mod Pathol* **9,** 888-92.

Fok-Seang, J., DiProspero, N. A., Meiners, S., Muir, E., and Fawcett, J. W. (1998). Cytokine-induced changes in the ability of astrocytes to support migration of oligodendrocyte precursors and axon growth. *Eur J Neurosci* **10,** 2400-15.

Forloni, G., Grzanna, R., Blakely, R. D., and Coyle, J. T. (1987). Co-localization of N-acetyl-aspartyl-glutamate in central cholinergic, noradrenergic, and serotonergic neurons. *Synapse* **1,** 455-60.

Franklin, R. J., and Blakemore, W. F. (1997). Transplanting oligodendrocyte progenitors into the adult CNS. *J Anat* **190,** 23-33.

Franklin, R. J., Gilson, J. M., Franceschini, I. A., and Barnett, S. C. (1996). Schwann cell-like myelination following transplantation of an olfactory bulb-ensheathing cell line into areas of demyelination in the adult CNS. *Glia* **17,** 217-24.

Franklin, R. J. M., and Barnett, S. C. (1997). Do olfactory glia have advantages over Schwann cells for CNS repair? *J Neurosci Res* **50,** 665-672.

Fu, S. Y., and Gordon, T. (1997). The cellular and molecular basis of peripheral nerve regeneration. *Mol Neurobiol* **14,** 67-116.

Gassmann, M., and Lemke, G. (1997). Neuregulins and neuregulin receptors in neural development. *Curr Opin in Neurobiol* **7,** 87-92.

Gehrmann, J., Matsumoto, Y., and Kreutzberg, G. W. (1995). Microglia: intrinsic immuneffector cell of the brain. *Brain Res - Brain Res Rev* **20,** 269-87.

Geula, C., and Mesulam, M. M. (1996). Systematic regional variations in the loss of cortical cholinergic fibers in Alzheimer's disease. *Cereb Cortex* **6,** 165-77.

Ghirnikar, R. S., and Eng, L. F. (1994). Astrocyte-Schwann cell interactions in culture. *Glia* **11,** 367-77.

Ghirnikar, R. S., and Eng, L. F. (1995). Chondroitin sulfate proteoglycan staining in astrocyte-Schwann cell co-cultures. *Glia* **14,** 145-152.

Goff, S., and Shenk, T. (1993). Viral genetics. *Curr Opin in Genetics & Dev* **3,** 163-98.

Goodearl, A. D., Yee, A. G., Sandrock, A. W., Jr., Corfas, G., and Fischbach, G. D. (1995). ARIA is concentrated in the synaptic basal lamina of the developing chick neuromuscular junction. *J Cell Biol* **130,** 1423-34.

Goodman, M. N., Silver, J., and Jacobberger, J. W. (1993). Establishment and neurite outgrowth properties of neonatal and adult rat olfactory bulb glial cell lines. *Brain Res* **619,** 199-213.

Götz, R., Koster, R., Winkler, C., Raulf, F., Lottspeich, F., Schartl, M., and Thoenen, H. (1994). Neurotrophin-6 is a New Member of the Nerve Growth Factor Family. *Nature* **372,** 266-268.

Graham, F. L., Smiley, J., Russell, W. C., and Nairn, R. (1977). Characteristics of a human cell line transformed by DNA from human adenovirus type 5. *J Gen Virol* **36,** 59-74.

Grignani, F., Kinsella, T., Mencarelli, A., Valtieri, M., Riganelli, D., Lanfrancone, L., Peschle, C., Nolan, G. P., and Pelicci, P. G. (1998). High-efficiency gene transfer and selection of human hematopoietic progenitor cells with a hybrid EBV/retroviral vector expressing the green fluorescence protein. *Cancer Res* **58,** 14-9.

Group, A. C. T. S. (1996). A double-blind placebo-controlled clinical trial of subcutaneous recombinant human ciliary neurotrophic factor (rHCNTF) in amyotrophic lateral sclerosis. ALS CNTF Treatment Study Group. *Neurol* **46,** 1244-1249.

Guenard, V., Aebischer, P., and Bunge, R. P. (1994). The astrocyte inhibition of peripheral nerve regeneration is reversed by Schwann cells. *Exp Neurol* **126,** 44-60.

Hagg, T., Vahlsing, H. L., Manthorpe, M., and Varon, S. (1990a). Nerve growth factor infusion into the denervated adult rat hippocampal formation promotes its cholinergic reinnervation. *J Neurosci* **10,** 3087-92.

Hagg, T., Vahlsing, H. L., Manthorpe, M., and Varon, S. (1990b). Septohippocampal cholinergic axonal regeneration through peripheral nerve bridges: quantification and temporal development. *Exp Neurol* **109,** 153-63.

Heemskerk, M. H., Blom, B., Nolan, G., Stegmann, A. P., Bakker, A. Q., Weijer, K., Res, P. C., and Spits, H. (1997). Inhibition of T cell and promotion of natural killer cell development by the dominant negative helix loop helix factor Id3. *J Exp Med* **186,** 1597-602.

Hefti, F. (1986). Nerve growth factor promotes survival of septal cholinergic neurons after fimbrial transections. *J Neurosci* **6,** 2155-62.

Henderson, Z. (1995). Responses of Basal Forebrain Cholinergic Neurons to Damage in the Adult Brain. *Prog Neurobiol* **48,** 219-254.

Heumann, R., Korsching, S., Bandtlow, C., and Thoenen, H. (1987a). Changes of nerve growth factor synthesis in nonneuronal cells in response to sciatic nerve transection. *J Cell Biol* **104,** 1623-31.

Heumann, R., Lindholm, D., Bandtlow, C., Meyer, M., Radeke, M. J., Misko, T. P., Shooter, E., and Thoenen, H. (1987b). Differential regulation of mRNA encoding nerve growth factor and its receptor in rat sciatic nerve during development, degeneration, and regeneration: role of macrophages. *Proc Natl Acad Sci* **84,** 8735-9.

Hohn, A., Liebrock, J., Bailey, K., and Barde, Y. A. (1990). Identification and Characterisation of a Novel Member of the Nerve Growth Factor Family. *Nature* **344,** 339-341.

Horan, P. K., and Slezak, S. E. (1989). Stable cell membrane labelling. *Nature* **340,** 167-8.

Horellou, P., Brundin, P., Kalen, P., Mallet, J., and Bjorklund, A. (1990). In vivo release of dopa and dopamine from genetically engineered cells grafted to the denervated rat striatum. *Neuron* **5,** 393-402.

Hortsch, M. (1996). The L1 family of neural cell adhesion molecules: Old proteins performing new tricks. *Neuron* **17,** 587-593.

Howe, D. G., and McCarthy, K. D. (1998). A dicistronic retroviral vector and culture model for analysis of neuron-Schwann cell interactions [In Process Citation]. *J Neurosci Methods* **83,** 133-42.

Ide, C. (1996). Peripheral nerve regeneration. *Neuroscience Res* **25,** 101-21.

Jang, S. K., Pestova, T. V., Hellen, C. U., Witherell, G. W., and Wimmer, E. (1990). Cap-independent translation of picornavirus RNAs: structure and function of the internal ribosomal entry site. *Enzyme* **44,** 292-309.

Jessen, K. R., and Mirsky, R. (1984). Nonmyelin-forming Schwann cells coexpress surface proteins and intermediate filaments not found in myelin-forming cells: a study of Ran-2, A5E3 antigen and glial fibrillary acidic protein. *J Neurocytol* **13,** 923-34.

Jessen, K. R., and Mirsky, R. (1991). Schwann cell precursors and their development. *Glia* **4,** 185-94.

Jessen, K. R., and Mirsky, R. (1997). Embryonic Schwann cell development: the biology of Schwann cell precursors and early Schwann cells. *J Anat* **191,** 501-5.

Jessen, K. R., Morgan, L., Stewart, H. J., and Mirsky, R. (1990). Three markers of adult non-myelin-forming Schwann cells, 217c(Ran-1), A5E3 and GFAP: development and regulation by neuron-Schwann cell interactions. *Development* **109,** 91-103.

Jirsová, K., Sodaar, P., Mandys, V., and Bär, P. R. (1997). Cold jet: a method to obtain pure Schwann cell cultures without the need for cytotoxic, apoptosis-inducing drug treatment. *J Neurosci* **78,** 133-137.

Kawaja, M. D., and Gage, F. H. (1991). Reactive astrocytes are substrates for the growth of adult CNS axons in the presence of elevated levels of nerve growth factor. *Neuron* **7,** 1019-30.

Kawaja, M. D., Rosenberg, M. B., Yoshida, K., and Gage, F. H. (1992). Somatic gene transfer of nerve growth factor promotes the survival of axotomized septal neurons and the regeneration of their axons in adult rats. *J Neurosci* **12,** 2849-64.

Keirstead, H. S., Hasan, S. J., Muir, G. D., and Steeves, J. D. (1992). Suppression of the onset of myelination extends the permissive period for the functional repair of embryonic spinal cord. *Proc Natl Acad Sci U.S.A.* **89,** 11664-11668.

Keirstead, S. A., Rasminsky, M., Fukuda, Y., Carter, D. A., Aguayo, A. J., and Vidal-Sanz, M. (1989). Electrophysiologic responses in hamster superior colliculus evoked by regenerating retinal axons. *Science* **246,** 255-7.

Kelly, D., Chancellor, K., Milatovich, A., Francke, U., Suzuki, K., and Popko, B. (1994). Autosomal recessive neuromuscular disorder in a transgenic line of mice. *J Neurosci* **14,** 198-207.

Kinsella, T. M., and Nolan, G. P. (1996). Episomal vectors rapidly and stably produce high-titer recombinant retrovirus. *Hum Gene Ther* **7,** 1405-13.

Kohler, C., Chan-Palay, V., and Wu, J. Y. (1984). Septal neurons containing glutamic acid decarboxylase immunoreactivity project to the hippocampal region in the rat brain. *Anat Embryol* **169,** 41-4.

Kramm, C. M., Chase, M., Herrlinger, U., Jacobs, A., Pechan, P. A., Rainov, N. G., Sena-Esteves, M., Aghi, M., Barnett, F. H., Chiocca, E. A., and Breakefield, X. O. (1997). Therapeutic efficiency and safety of a second-generation replication-conditional HSV1 vector for brain tumor gene therapy. *Hum Gene Ther* **8,** 2057-68.

Kromer, L. F., and Cornbrooks, C. J. (1985). Transplants of Schwann cell cultures promote axonal regeneration in the adult mammalian brain. *Proc Natl Acad Sci USA* **82,** 6330-4.

Kuramoto, H., Kato, Y., Sakamoto, H., and Endo, Y. (1996). Galanin-containing nerve terminals that are involved in a dual innervation of the striated muscles of the rat esophagus. *Brain Res* **734,** 186-92.

Laemmli, U. K. (1970). Cleavage of structural peptide during the assembly of the head of bacteria phage T4. *Nature* **227,** 680-685.

Lai, K. O., Fu, W. Y., Ip, F. C., and Ip, N. Y. (1998). Cloning and expression of a novel neurotrophin, NT-7, from carp. *Mol Cell Neurosci* **11,** 64-76.

Leanza, G., Nikkhah, G., Nilsson, O. G., Wiley, R. G., and Björklund, A. (1996). Extensive reinnervation of the hippocampus by embryonic basal forebrain

cholinergic neurons grafted into the septum of neonatal rats with selective cholinergic lesions. *J Comp Neurol* **373,** 355-357.

Lee, M., Brennan, A., Blanchard, A., Zoidl, G., Dong, Z., Tabernero, A., Zoidl, C., Dent, M. A., Jessen, K. R., and Mirsky, R. (1997). P0 is constitutively expressed in the rat neural crest and embryonic nerves and is negatively and positively regulated by axons to generate non-myelin-forming and myelin-forming Schwann cells, respectively. *Mol Cell Neurosci* **8,** 336-50.

Levi, A. D., Bunge, R. P., Lofgren, J. A., Meima, L., Hefti, F., Nikolics, K., and Sliwkowski, M. X. (1995). The influence of heregulins on human Schwann cell proliferation. *J Neurosci* **15,** 1329-1340.

Levi-Montalcini, R. (1987). The Nerve Growth Factor 35 Years Later. *Science* **237,** 1154-1162.

Levi-Montalcini, R., and Hamburger, V. (1952). Selective Growth-Stimulating Effects of Mouse Sarcoma on the Sensory and Sympathetic Nervous System of the Chick Embryo. *J Exp Zool* **116,** 321-361.

Li, R., Chen, J., Hammonds, G., Phillips, H., Armanini, M., Wood, P., Bunge, R., Godowski, P. J., Sliwkowski, M. X., and Mather, J. P. (1996a). Identification of Gas6 as a growth factor for human Schwann cells. *J Neurosci* **16,** 2012-2019.

Li, R. H., Sliwkowski, M. X., Lo, J., and Mather, J. P. (1996b). Establishment of Schwann cell lines from normal adult and embryonic rat dorsal root ganglia. *J Neurosci* **67,** 57-69.

Li, Y., Field, P. M., and Raisman, G. (1997). Repair of adult rat corticospinal tract by transplants of olfactory ensheathing cells [see comments]. *Science* **277,** 2000-2002.

Li, Y., and Raisman, G. (1993). Long axon growth from embryonic neurons transplanted into myelinated tracts of the adult rat spinal cord. *Brain Res* **629,** 115-27.

Li, Y., and Raisman, G. (1994). Schwann cells induce sprouting in motor and sensory axons in the adult rat spinal cord. *J Neurosci* **14,** 4050-4063.

Li, Y., and Raisman, G. (1995). Sprouts from cut corticospinal axons persist in the presence of astrocytic scarring in long-term lesions of the adult rat spinal cord. *Exp Neurol* **134,** 102-111.

Li, Y., and Raisman, G. (1997). Integration of transplanted cultured Schwann cells into the long myelinated fiber tracts of the adult spinal cord. *Exp Neurol* **145,** 397-411.

Liebrock, J., Lottspeich, F., Hohn, A., Hofer, M., Hengerer, B., Masiakowwski, P., Thoenen, H., and Barde, Y. A. (1989). Molecular Cloning and Expression of Brain-Derived Neurotrophic Factor. *Nature* **341,** 149-152.

Lin, L. H., Doherty, D. H., Lile, J. D., Bektesh, S., and Collons, F. (1993). GDNF: A Glial Cell Line-Derived Neurotrophic Factor for midbrain dopaminergic neurones. *Science* **260,** 1130-1132.

Loeber, G., Tevethia, M. J., Schwedes, J. F., and Tegtmeyer, P. (1989). Temperature-sensitive mutants identify crucial structural regions of Simian virus 40 large T antigen. *J Virol* **63,** 4426-4430.

Lund, R. D., Chang, F. L., Hankin, M. H., and Lagenaur, C. F. (1985). Use of a species-specific antibody for demonstrating mouse neurons transplanted to rat brains. *Neurosci Lett* **61,** 221-6.

Lund, R. D., and Hankin, M. H. (1995). Pathfinding by retinal ganglion cell axons: transplantation studies in genetically and surgically blind mice. *J Comp Neurol* **356,** 481-9.

Manthorpe, M., Skaper, S., Adler, R., Landa, K., and Varon, S. (1980). Cholinergic neuronotrophic factors: fractionation properties of an extract from selected chick embryonic eye tissues. *J Neurochem* **34,** 69-75.

Marin, M., Noel, D., and Piechaczyk, M. (1997). Towards efficient cell targeting by recombinant retroviruses. *Mol Med Today* **3,** 396-403.

Marone, M., Quiñones-Jenab, V., Meiners, S., Nowakowski, R. S., Ho, S. Y., and Geller, H. M. (1995). An immortalized mouse neuroepithelial cell line with neuronal and glial phenotypes. *Dev Neurosci* **17,** 311-323.

Matyszak, M. K., and Perry, V. H. (1995). Demyelination in the central nervous system following a delayed-type hypersensitivity response to bacillus Calmette-Guerin. *Neuroscience* **64,** 967-77.

McGarvey, M. L., Baron-Van Evercooren, A., Kleinman, H. K., and Dubois-Dalcq, M. (1984). Synthesis and effects of basement membrane components in cultured rat Schwann cells. *Dev Biol* **105,** 18-28.

McKeon, R. J., Schreiber, R. C., Rudge, J. S., and Silver, J. (1991). Reduction of neurite outgrowth in a model of glial scarring following CNS injury is correlated with the expression of inhibitory molecules on reactive astrocytes. *J Neurosci* **11,** 3398-3411.

Meyer, D., and Birchmeier, C. (1995). Multiple essential functions of neuregulin in development [see comments]. *Nature* **378,** 386-390.

Midha, R., Fehlings, M. G., Tator, C. H., Saint-Cyr, J. A., and Guha, A. (1987). Assessment of spinal cord injury by counting corticospinal and rubrospinal neurons. *Brain Res* **410,** 299-308.

Mirsky, R., and Jessen, K. R. (1996). Schwann cell development, differentiation and myelination. *Curr Opin Neurobiol* **6,** 89-96.

Mirsky, R., Winter, J., Abney, E. R., Pruss, R. M., Gavrilovic, J., and Raff, M. C. (1980). Myelin-specific proteins and glycolipids in rat Schwann cells and oligodendrocytes in culture. *J Cell Biol* **84,** 483-94.

Mocharla, H., Mocharla, R., and Hodes, M. E. (1990). Coupled reverse transcription-polymerase chain reaction (RT-PCR) as a sensitive and rapid method for isozyme genotyping. *Gene* **93,** 271-5.

Mohajeri, M. H., Bartsch, U., van der Putten, H., Sansig, G., Mucke, L., and Schachner, M. (1996). Neurite outgrowth on non-permissive substrates in vitro is enhanced by ectopic expression of the neural adhesion molecule L1 by mouse astrocytes. *Eur J Neurosci* **8,** 1085-97.

Montero-Menei, C. N., Pouplard Barthelaix, A., Gumpel, M., and Baron Van Evercooren, A. (1992). Pure Schwann cell suspension grafts promote regeneration of the lesioned septo-hippocampal cholinergic pathway. *Brain Res* **570,** 198-208.

Montgomery, C. T., Tenaglia, E. A., and Robson, J. A. (1996). Axonal Growth into Tubes Implanted within Lesions in the Spinal Cords of Adult Rats. *Exp Neurol* **137,** 277-290.

Morgan, L., Jessen, K. R., and Mirsky, R. (1991). The effects of cAMP on differentiation of cultured Schwann cells: progression from an early phenotype (04+) to a myelin phenotype (Po+, GFAP-, N-CAM-, NGF-receptor-) depends on growth inhibition. *J Cell Biol* **112,** 457-467.

Morgan, L., Jessen, K. R., and Mirsky, R. (1994). Negative regulation of the P0 gene in Schwann cells: suppression of P0 mRNA and protein induction in cultured Schwann cells by FGF2 and TGF beta 1, TGF beta 2 and TGF beta 3. *Development* **120,** 1399-409.

Muldoon, R. R., Levy, J. P., Kain, S. R., Kitts, P. A., and Link, C. J., Jr. (1997). Tracking and quantitation of retroviral-mediated transfer using a completely humanized, red-shifted green fluorescent protein gene. *Biotechniques* **22,** 162-7.

Neugebauer, K. M., Tomaselli, K. J., Lilien, J., and Reichardt, L. F. (1988). N-cadherin, NCAM, and integrins promote retinal neurite outgrowth on astrocytes in vitro. *J Cell Biol* **107,** 1177-87.

Nikkah, G., Cunningham, M. G., Cenci, M. A., McKay, R. D., and Björklund, A. (1995). Dopaminergic microtransplants into the substantia nigra of neonatal rats with bilateral 6-OHDA lesions. I. Evidence for anatomical reconstruction of the nigrostriatal pathway. *J Neurosci* **15,** 3548-3561.

Noble, M., Fok-Seang, J., and Cohen, J. (1984). Glia are a unique substrate for the in vitro growth of central nervous system neurons. *J Neurosci* **4,** 1892-903.

Okabe, M., Ikawa, M., Kominami, K., Nakanishi, T., and Nishimune, Y. (1997). 'Green mice' as a source of ubiquitous green cells. *FEBS Lett* **407,** 313-9.

O'Leary, M. T., and Blakemore, W. F. (1997). Oligodendrocyte precursors survive poorly and do not migrate following transplantation into the normal adult central nervous system. *J Neurosci Res* **48,** 159-167.

Olson, L. (1997). Regeneration in the adult central nervous system: experimental repair strategies. *Nature Medicine* **3,** 1329-35.

Pallini, R., Fernandez, E., and Sbriccoli, A. (1988). Retrograde degeneration of corticospinal axons following transection of the spinal cord in rats. A quantitative study with anterogradely transported horseradish peroxidase [see comments]. *J Neurosurgery* **68,** 124-8.

Papka, R. E., and McNeill, D. L. (1993). Light- and electron-microscopic study of synaptic connections in the paracervical ganglion of the female rat: special reference to calcitonin gene-related peptide-, galanin- and tachykinin (substance

P and neurokinin A)-immunoreactive nerve fibers and terminals. *Cell Tissue Res* **271,** 417-28.

Pawliuk, R., Bachelot, T., Raftopoulos, H., Kalberer, C., Humphries, R. K., Bank, A., and Leboulch, P. (1998). Retroviral vectors aimed at the gene therapy of human beta-globin gene disorders. *Ann NY Acad Sci* **850,** 151-62.

Pear, W. S., Nolan, G. P., Scott, M. L., and Baltimore, D. (1993). Production of high-titer helper-free retroviruses by transient transfection. *Proc Natl Acad Sci U S A* **90,** 8392-6.

Peden, K. W. C., Charles, C., Sanders, L., and Tennekoon, G. I. (1989). Isolation of Rat Schwann Cell Lines: Use of SV40 T Antigen Gene Regulated by Synthetic Metallothionein Promoters. *Exp Cell Res* **185,** 60-72.

Pines, J. (1995). GFP in mammalian cells. *Trends Genet* **11,** 326-7.

Pinkas-Kramarski, R., Eilam, R., Spiegler, O., Lavi, S., Liu, N., Chang, D., Wen, D., Schwartz, M., and Yarden, Y. (1994). Brain neurons and glial cells express Neu differentiation factor/heregulin: a survival factor for astrocytes. *Proc Natl Acad Sci U S A* **91,** 9387-91.

Pollock, M. (1995). Nerve regeneration. *Curr Opin Neurol* **8,** 354-8.

Prasher, D. C. (1995). Using GFP to see the light. *Trends Genet* **11,** 320-3.

Prendergast, F. G., and Mann, K. G. (1978). Chemical and physical properties of aequorin and the green fluorescent protein isolated from Aequorea forskalea. *Biochemistry* **17,** 3448-53.

Ramiro, A. R., De Yebenes, V. G., Trigueros, C., Carrasco, Y. R., and Toribio, M. L. (1998). Enhanced green fluorescent protein as an efficient reporter gene for retroviral transduction of human multipotent lymphoid precursors. *Hum Gene Ther* **9,** 1103-9.

Ramon y Cajal, S. (1928). "Degeneration and regeneration of the nervous system (May, R.M, transl.)." Hafner, New York.

Rath, E. M., Kelly, D., Bouldin, T. W., and Popko, B. (1995). Impaired peripheral nerve regeneration in a mutant strain of mice (Enr) with a Schwann cell defect. *J Neurosci* **15,** 7226-7237.

Richardson, P. M., Issa, V. M., and Aguayo, A. J. (1984). Regeneration of long spinal axons in the rat. *J Neurocytol* **13,** 165-182.

Richardson, P. M., McGuinness, and Aguayo, A. J. (1980). Axons from CNS neurones regenerate into PNS grafts. *Nature* **284,** 264-265.

Ridet, J. L., Malhotra, S. K., Privat, A., and Gage, F. H. (1997). Reactive astrocytes: cellular and molecular cues to biological function [published erratum appears in Trends Neurosci 1998 Feb;21(2):80]. *Trends Neurosci* **20,** 570-7.

Ridet, J. L., and Privat, A. (1995). Gene therapy in the central nervous system: Direct versus indirect gene delivery. *J Neurosci Res* **42,** 287-293.

Robbins, P. D., Tahara, H., and Ghivizzani, S. C. (1998). Viral vectors for gene therapy. *Trends Biotechnol* **16,** 35-40.

Rosenberg, M. B., Friedmann, T., Robertson, R. C., Tuszynski, M., Wolff, J. A., Breakefield, X. O., and Gage, F. H. (1988). Grafting genetically modified cells to the damaged brain: restorative effects of NGF expression. *Science* **242,** 1575-8.

Rudge, J. S., Li, Y., Pasnikowski, E. M., Mattsson, K., Pan, L., Yancopoulos, G. D., Wiegand, S. J., Lindsay, R. M., and Ip, N. Y. (1994). Neurotrophic factor receptors and their signal transduction capabilities in rat astrocytes. *Eur J Neurosci* **6,** 693-705.

Sambrook, J., Fritsch, E., and Maniatis, T. (1989). "Molecular Cloning, a laboratory manual." Cold Spring Harbour Laboratory Press, New York.

Scherer, S. S. (1997). The biology and pathobiology of Schwann cells. *Curr Opin Neurol* **10,** 386-97.

Schnell, L., and Schwab, M. E. (1990). Axonal regeneration in the rat spinal cord produced by an antibody against myelin-associated neurite growth inhibitors. *Nature* **343,** 269-272.

Schwann, T. (1847). Microscopical researches into the accordance in the structure and growth of animals and plants. Sydenham Society, London.

Seilheimer, B., and Schachner, M. (1988). Studies of adhesion molecules mediating interactions between cells of peripheral nervous system indicate a major role for L1 in mediating sensory neuron growth on Schwann cells in culture. *J Cell Biol* **107,** 341-51.

Selmaj, K., Raine, C. S., Farooq, M., Norton, W. T., and Brosnan, C. F. (1991). Cytokine cytotoxicity against oligodendrocytes. Apoptosis induced by lymphotoxin. *J Immunol* **147,** 1522-9.

Sendtner, M., Arakawa, Y., Stockli, K. A., Kreutzberg, G. W., and Thoenen, H. (1991). Effect of ciliary neurotrophic factor (CNTF) on motoneuron survival. *J Cell Sci Suppl* **15,** 103-9.

Sensenbrenner, M., Lucas, M., and Deloulme, J. C. (1997). Expression of two neuronal markers, growth-associated protein 43 and neuron-specific enolase, in rat glial cells. *J Mol Med* **75,** 653-63.

Senut, M. C., Menetrey, D., and Lamour, Y. (1989). Cholinergic and peptidergic projections from the medial septum and the nucleus of the diagonal band of Broca to dorsal hippocampus, cingulate cortex and olfactory bulb: a combined wheatgerm agglutinin- apohorseradish peroxidase-gold immunohistochemical study. *Neuroscience* **30,** 385-403.

Shimohama, S., Rosenberg, M. B., Fagan, A. M., Wolff, J. A., Short, M. P., Breakefield, X. O., Friedmann, T., and Gage, F. H. (1989). Grafting genetically modified cells into the rat brain: characteristics of E. coli beta-galactosidase as a reporter gene. *Brain Res Mol Brain Res* **5,** 271-8.

Silver, J. (1994). Inhibitory molecules in development and regeneration. *J Neurol* **242,** S22-4.

Smith, G. V., and Stevenson, J. A. (1988). Peripheral nerve grafts lacking viable Schwann cells fail to support central nervous system axonal regeneration. *Exp Brain Res* **69,** 299-306.

Staal, F. J., Bakker, A. Q., Verkuijlen, M., van Oort, E., and Spits, H. (1996). Use of bicistronic retroviral vectors encoding the LacZ gene together with a gene of interest: a method to select producer cells and follow transduced target cells. *Cancer Gene Ther* **3,** 345-51.

Stewart, H. J., Bradke, F., Tabernero, A., Morrell, D., Jessen, K. R., and Mirsky, R. (1996). Regulation of rat Schwann cell Po expression and DNA synthesis by insulin-like growth factors in vitro. *Eur J Neurosci* **8,** 553-64.

Stichel, C. C., Lips, K., Wunderlich, G., and Muller, H. W. (1996). Reconstruction of transected postcommissural fornix in adult rat by Schwann cell suspension grafts. *Exp Neurol* **140,** 21-36.

Suzuki, M., and Raisman, G. (1994). Multifocal pattern of postnatal development of the macroglial framework of the rat fimbria. *Glia* **12,** 294-308.

Takeda, Y., Asou, H., Murakami, Y., Miura, M., Kobayashi, M., and Uyemura, K. (1996). A nonneuronal isoform of cell adhesion molecule L1: tissue- specific expression and functional analysis. *J Neurochem* **66,** 2338-2349.

Taniuchi, M., Clark, H. B., and Johnson, E. M., Jr. (1986). Induction of nerve growth factor receptor in Schwann cells after axotomy. *Proc Natl Acad Sci U S A* **83,** 4094-8.

Tennekoon, G. I., Yoshino, J., Peden, K. W. C., Bigbee, J., Rutkowski, L., Kishimoto, Y., DeVries, G. H., and McKhann, G. M. (1987). Transfection of Neonatal Schwann Cells with SV-40 Large T Antigen Gene under Control of the Metallothionein Promoter. *J Cell Biol* **105,** 2315-2325.

Tessier Lavigne, M., and Goodman, C. S. (1996). The molecular biology of axon guidance. *Science* **274,** 1123-1133.

Thi, A. D., Evrard, C., and Rouget, P. (1998). Proliferation and differentiation properties of permanent Schwann cell lines immortalized with a temperature-sensitive oncogene. *J Exp Biol* **201,** 851-60.

Towbin, H., Staehelin, T., and Gordon, J. (1979). Electrophoretic transfer of proteins from polyacrylamide gels to nitrocellulose sheets: procedure and some applications. *Proc Natl Acad Sci USA* **76,** 4350-4.

Tubulekas, I., Berglund, P., Fleeton, M., and Liljestrom, P. (1997). Alphavirus expression vectors and their use as recombinant vaccines: a minireview. *Gene* **190,** 191-5.

Tuszynski, M. H., Weidner, N., McCormack, M., Miller, I., Powell, H., and Conner, J. (1998). Grafts of genetically modified Schwann cells to the spinal cord: survival, axon growth, and myelination. *Cell Transplant* **7,** 187-96.

Vaudano, E., Campbell, G., Anderson, P. N., Davies, A. P., Woolhead, C., Schreyer, D. J., and Lieberman, A. R. (1995). The effects of a lesion or a peripheral nerve graft on GAP-43 upregulation in the adult rat brain: an in situ hybridization and immunocytochemical study. *J Neurosci* **15,** 3594-611.

Ward, W. W., and Bokman, S. H. (1982). Reversible denaturation of Aequorea green-fluorescent protein: physical separation and characterization of the renatured protein. *Biochemistry* **21,** 4535-40.

Watabe, K., Fukuda, T., Tanaka, J., Honda, H., Toyohara, K., and Sakai, O. (1995). Spontaneously immortalized adult mouse Schwann cells secrete autocrine and paracrine growth-promoting activities. *J Neurosci Res* **41,** 279-290.

Watabe, K., Fukuda, T., Tanaka, J., Toyohara, K., and Sakai, O. (1994). Mitogenic effects of platelet-derived growth factor, fibroblast growth factor, transforming growth factor-beta, and heparin- binding serum factor for adult mouse Schwann cells. *J Neurosci Res* **39,** 525-534.

Watabe, K., Yamada, M., Kawamura, T., and Kim, S. U. (1990). Transfection and Stable Transformation of Adult Mouse Schwann Cells with SV-40 Large T Antigen Gene. *J Neuropathol Exp Neurol* **49,** 455-467.

Wendt, J. S., Fagg, G. E., and Cotman, C. W. (1983). Regeneration of rat hippocampal fimbria fibers after fimbria transection and peripheral nerve or fetal hippocampal implantation. *Exp Neurol* **79,** 452-61.

Xu, X. M., Chen, A., Guenard, V., Kleitman, N., and Bunge, M. B. (1997). Bridging Schwann cell transplants promote axonal regeneration from both the rostral and caudal stumps of transected adult rat spinal cord. *J Neurocytol* **26,** 1-16.

Xu, X. M., Guenard, V., Kleitman, N., and Bunge, M. B. (1995). Axonal regeneration into Schwann cell-seeded guidance channels grafted into transected adult rat spinal cord. *J Comp Neurol* **351,** 145-60.

Yazaki, T., Martuza, R. L., and Rabkin, S. D. (1996). Expression of L1 in primary astrocytes via a defective herpes simplex virus vector promotes neurite outgrowth and neural cell migration. *Brain Res Mol Brain Res* **43,** 311-20.

Yen, S. H., and Fields, K. L. (1981). Antibodies to neurofilament, glial filament, and fibroblast intermediate filament proteins bind to different cell types of the nervous system. *J Cell Biol* **88,** 115-26.

Yoshimoto, Y., Lin, Q., Collier, T. J., Frim, D. M., Breakefield, X. O., and Bohn, M. C. (1995). Astrocytes retrovirally transduced with BDNF elicit behavioral improvement in a rat model of Parkinson's disease. *Brain Res* **691,** 25-36.

You, S., Petrov, T., Chung, P. H., and Gordon, T. (1997). The expression of the low affinity nerve growth factor receptor in long-term denervated Schwann cells. *Glia* **20,** 87-100.

Zaheer, A., Zhong, W., and Lim, R. (1995). Expression of mRNAs of multiple growth factors and receptors by neuronal cell lines: detection with RT-PCR. *Neurochem Res* **20,** 1457-1463.

Zhang, G., Gurtu, V., and Kain, S. R. (1996). An enhanced green fluorescent protein allows sensitive detection of gene transfer in mammalian cells. *Biochem Biophys Res Commun* **227,** 707-11.

Zhang, Y., Campbell, G., Anderson, P. N., Martini, R., Schachner, M., and Lieberman, A. R. (1995a). Molecular basis of interactions between regenerating adult rat thalamic axons and Schwann cells in peripheral nerve grafts I. Neural cell adhesion molecules. *J Comp Neurol* **361,** 193-209.

Zhang, Y., Campbell, G., Anderson, P. N., Martini, R., Schachner, M., and Lieberman, A. R. (1995b). Molecular basis of interactions between regenerating adult rat thalamic axons and Schwann cells in peripheral nerve grafts. II. Tenascin-C. *J Comp Neurol* **361,** 210-224.

Zorick, T. S., and Lemke, G. (1996). Schwann cell differentiation. *Curr Opin Cell Biol* **8,** 870-6.

Appendix

Figure A1 Limited restriction map of pRc/CMV

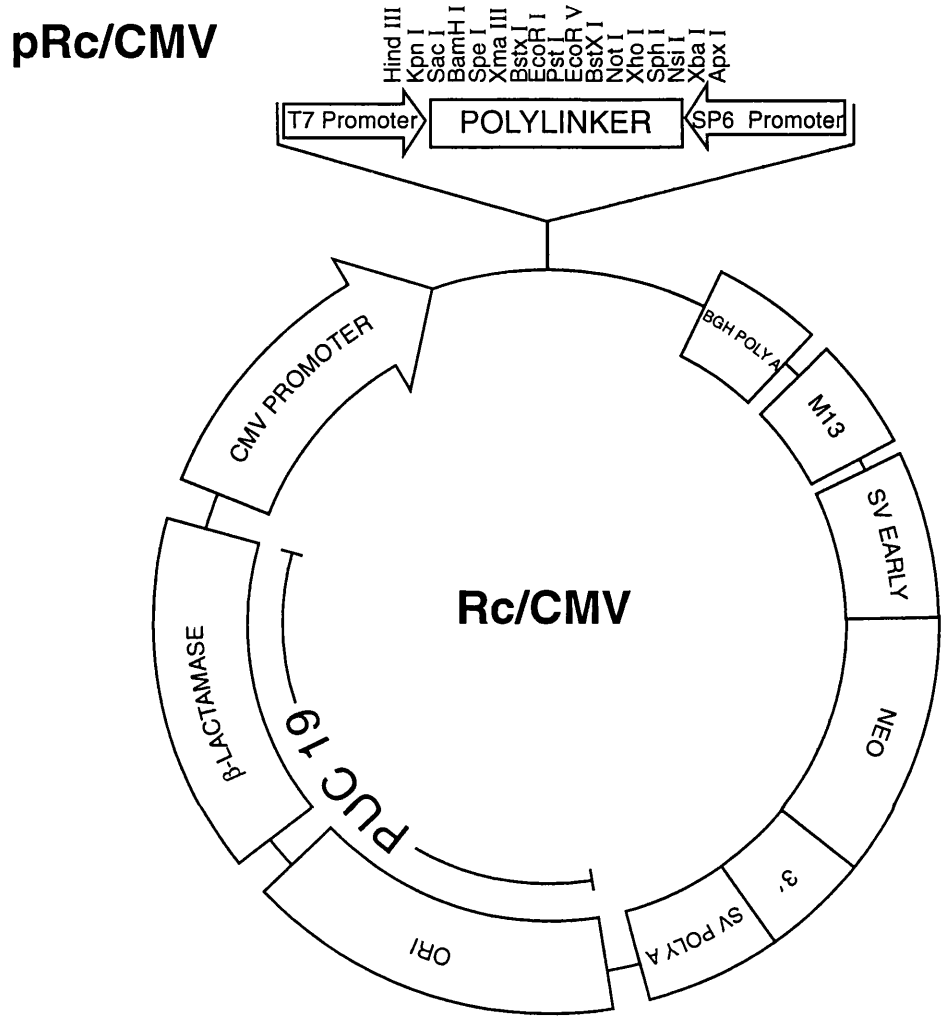

DNA Length: 5,446 bp

CMV promoter begins at base 209
The T7 promoter begins at base 865
The polylinker begins at base 891
The Sp6 promoter begins at 1,019
The M13 origin begins at base 1285
The neomycin gene begins at base 2,120
The pUC 19 backbone, origin and beta-lactamase gene begins at base 3,236

Restriction Enzyme Sites for HindIII and NotI:

HindIII + 891
NotI + 966

Figure A2 G418 killing curve data

Dish No.	[G418] / μg/ml	Number of surviving cells in each of 10 randomly chosen fields*										
		1	2	3	4	5	6	7	8	9	10	Average score per well
(Experiment 1)												
1	50	18	11	32	10	8	7	12	14	9	15	14
2	150	2	0	1	3	2	2	0	2	7	4	2
3	300	5	3	6	2	0	12	7	2	4	4	5
4	450	0	1	2	5	5	12	1	5	31	9	7
5	600	0	0	0	1	0	0	0	0	1	0	0
6	750	1	1	5	2	3	1	3	0	2	0	2
(Experiment 2)												
1	350	0	0	0	1	0	1	0	0	0	1	0
2	450	0	1	24	3	29	3	1	0	0	0	6
3	550	0	0	0	0	0	0	0	0	0	0	0
4	650	0	0	0	0	0	0	0	0	0	0	0
5	350	0	0	0	0	0	0	1	0	0	0	0
6	450	0	0	0	0	0	0	0	0	0	4	0
7	550	0	3	0	0	1	0	0	2	0	1	1
8	650	0	0	0	0	0	0	0	0	0	0	0
9	0											>1000

*cells were counted in fields of view at a magnification of x200

Figure A3 Lipofection of Schwann cells with pCMV-g

[LipoFECTIN] / μg	Transfection efficiency / %	
	Series 1	Series 2
22.5	14	-
30	19	-
35	18	27
40	22	24
45	17	25
50	26	30

Figure A4 Cell proliferation assays of 2 STAG cell lines compared with neonatal SCs (NSCs)

Cell line	Number of fluorescence-stained cells/Total number of cells*									
	1	2	3	4	5	6	7	8	9	10
NSC	4/56	4/45	10/69	3/55	6/71	3/63	4/80	0/71	0/94	5/55
1A1a	10/34	13/63	14/57	20/74	16/46	24/50	20/65	16/51	23/59	21/89
3C3	9/50	25/52	10/42	26/82	12/50	10/37	26/53	21/45	28/59	16/41

*values represent counts from 10 randomly chosen fields of view at a magnification of x200

Figure B1 Effectene Transfection-4: Transfection efficiency with [DNA]

[DNA] / μg	Total no. of fluorescent cells*	Average no. of fluorescent cells
0.2	0	0
0.3	49	5
0.4	102	11
0.5	54	6
0.6	54	6
0.7	47	5

*cells counted under fluorescence microscopy at a magnification of x200

Figure B2a Puromycin killing curve data, PKC-1

	Puromycin			
	0.5µg/ml	1µg/ml	2µg/ml	3µg/ml
Day 1	4 4 0 3 2 2 4 4 4 4 4 4	3 1 2 1 4 4 3 2 4 3 4 2	1 2 4 4 2 4 4 4 2 2 4 4	4 4 4 4 3 3 3 3 4 2 1 4
	1 3 4 4 3 4 1 2 4 4 4 4	1 2 1 2 3 3 4 2 1 3 4 0	4 3 4 4 1 4 4 4 2 3 2 4	3 4 4 4 4 4 4 4 4 1 2 4
	4 4 3 0 1 2 0 0 4 4 4 4	4 4 4 3 1 4 2 3 4 4 4 4	3 2 2 2 4 2 3 3 3 3 3 4	3 3 4 4 1 0 3 1 3 3 2 0
	4 0 3 0 4 4 3 4 4 4 4 4	4 4 4 4 4 4 2 2 4 4 2 3	3 4 4 0 4 3 4 4 2 2 2 1	4 4 3 4 3 2 0 1 3 2 0 1
Day 2	2 4 4 2 3 2 2 4 4 4 4 4	2 1 1 0 4 4 4 4 4 4 4 3	4 4 0 0 2 1 2 0 1 2 3 0	1 3 2 0 1 1 3 2 1 0 2 1
	4 4 3 3 4 2 4 4 4 4 4 4	1 3 2 2 4 4 3 4 1 1 1 3	1 1 2 4 1 1 4 1 1 1 2 2	2 3 2 1 4 2 0 1 2 0 1 0
	4 4 2 3 4 2 4 4 4 4 4 4	3 2 3 4 2 3 2 4 4 3 3 3	4 2 2 0 2 1 1 0 2 1 2 3	2 3 1 1 3 3 2 1 1 0 1 0
	2 4 4 4 2 3 4 4 4 4 4 4	4 4 3 4 4 3 1 1 4 2 2 2	3 2 2 0 1 1 1 0 1 2 1 0	2 1 1 3 1 3 1 2 1 1 1 1
Day 5	4 4 4 4 4 4 4 4 4 4 4 4	4 1 0 0 4 4 4 4 3 3 4 3	2 3 3 3 2 2 1 0 0 0 0 0	0 0 0 0 1 1 1 2 2 3 1 2
	2 2 3 4 4 4 4 4 4 4 4 4	2 1 1 1 3 4 3 4 3 2 3 4	3 2 2 3 2 3 2 1 0 0 0 0	1 1 1 0 2 2 1 0 1 1 3 3
	3 4 4 3 4 4 4 4 4 4 4 4	1 1 1 0 4 3 3 4 4 4 4 4	3 4 3 3 0 0 0 0 2 0 0 0	2 0 0 0 1 3 2 2 1 2 1 2
	4 4 4 4 4 4 4 4 4 4 4 4	2 1 4 3 4 4 4 4 3 1 1 4	3 3 1 2 2 1 0 0 1 0 0 0	2 0 0 0 1 3 2 1 1 2 0 1
Day 6	4 4 4 4 4 4 4 4 4 4 3 4	1 0 0 1 3 4 4 2 3 2 3 3	2 0 0 0 2 0 2 1 2 3 1 2	1 1 1 1 1 0 1 1 2 1 1 0
	4 4 4 4 4 4 4 4 4 4 4 4	2 1 1 1 1 3 1 4 4 3 0 0	1 3 1 0 1 2 2 3 1 4 2 3	1 4 1 0 4 3 3 2 2 0 3 1
	4 4 4 4 4 4 4 4 4 4 4 4	4 3 1 2 4 4 4 4 4 4 3 3	4 4 2 3 1 1 0 0 4 2 1 3	1 1 0 0 3 0 4 0 2 0 1 0
	4 4 4 4 4 4 4 4 4 4 4 4	2 4 3 0 3 2 4 4 4 4 4 3	2 0 1 2 3 1 1 1 3 4 3 1	2 1 0 0 3 2 0 2 3 1 2 1
Day 7	2 4 4 4 4 4 4 4 3 3 4 4	2 0 0 0 2 3 1 1 3 4 4 4	0 0 0 0 2 3 0 0 0 0 0 0	1 0 0 0 1 1 0 1 1 1 2 2
	4 4 4 4 4 4 4 4 4 4 4 4	1 0 0 0 1 2 4 2 3 2 3 3	1 1 0 0 2 0 0 0 0 0 0 0	1 2 1 1 2 0 2 0 1 1 0 0
	4 4 4 4 4 4 4 4 4 4 4 4	3 1 2 3 4 4 3 2 3 1 0 0	1 0 0 0 1 1 1 0 1 1 0 0	1 2 0 0 2 0 0 1 2 2 1 1
	4 4 4 4 4 4 4 4 4 4 4 4	1 2 2 1 1 4 0 3 3 1 1 3	2 0 1 0 0 0 0 0 1 1 0 1	1 1 0 0 2 0 0 0 2 1 0 0
Day 8	4 4 4 4 4 4 4 4 4 4 4 4	3 3 2 0 4 2 3 4 2 0 2 2	1 0 0 0 2 0 2 1 1 0 1 0	2 0 1 1 1 0 0 0 2 0 0 1
	4 4 4 4 4 4 4 4 4 4 4 4	4 4 4 4 3 3 4 4 4 4 2 2	1 0 0 0 2 0 0 0 0 0 0 0	1 1 0 0 2 1 1 2 1 0 1 1
	4 4 4 4 4 4 4 4 4 4 4 4	4 3 2 4 4 4 3 3 2 2 2 0	0 0 0 0 3 2 0 1 1 1 0 1	1 0 0 0 2 1 2 1 1 0 0 0

	0.5μg/ml												1μg/ml												2μg/ml												3μg/ml											
	4	4	4	4	4	4	4	4	4	4	4	4	3	4	4	2	3	3	4	2	3	3	0	1	1	1	0	0	1	1	1	1	1	0	1	0	2	0	1	0	2	0	0	2	1	1	0	0
Day 9	4	4	4	4	4	4	4	4	4	4	4	4	0	0	0	0	4	4	4	4	2	0	1	2	1	0	0	0	1	3	3	1	1	1	0	0	1	0	0	0	1	1	0	2	1	2	2	1
	4	4	4	4	4	4	4	4	4	4	4	4	1	0	0	0	4	4	4	4	2	2	0	1	0	0	0	0	4	4	3	3	0	0	0	0	1	1	0	0	2	1	2	1	3	1	0	0
	4	4	4	4	4	4	4	4	4	4	4	4	1	1	0	0	4	4	4	4	2	1	2	2	0	0	0	0	4	3	1	2	0	0	0	0	1	0	0	0	1	2	1	2	1	0	0	0
	4	4	4	4	4	4	4	4	4	4	4	4	1	0	0	0	4	4	4	4	2	0	2	2	1	1	0	0	3	0	2	1	1	1	0	0	0	0	0	0	2	3	2	1	1	0	0	0
Day 12	4	4	4	4	4	4	4	4	4	4	4	4	3	4	0	3	1	2	3	1	3	0	2	1	1	0	0	0	4	4	4	3	1	0	0	0	1	1	1	0	4	4	2	4	1	0	0	0
	4	4	4	4	4	4	4	4	4	4	4	4	0	0	0	0	4	3	2	1	2	2	0	2	1	1	0	0	4	4	3	4	0	0	0	0	0	0	0	0	4	1	2	2	3	1	0	0
	4	4	4	4	4	4	4	4	4	4	4	4	1	1	1	0	3	3	2	1	2	2	0	0	3	0	0	0	4	3	4	2	1	0	0	0	1	2	0	0	3	1	4	3	2	1	1	0
	4	4	4	4	4	4	4	4	4	4	4	4	1	2	0	0	3	0	2	2	1	1	2	3	0	0	0	0	4	4	3	2	0	0	0	0	1	0	0	0	3	3	2	3	1	1	1	0
Day 13	4	4	4	4	4	4	4	4	4	4	4	4	1	1	1	1	4	4	4	4	1	3	1	1	1	1	1	1	2	1	2	1	1	0	0	0	1	0	0	0	1	0	0	0	2	1	0	0
	4	4	4	4	4	4	4	4	4	4	4	4	2	1	0	0	4	4	4	4	2	1	2	0	1	0	0	0	2	0	1	1	1	0	0	0	1	2	0	0	1	2	1	1	1	0	0	0
	4	4	4	4	4	4	4	4	4	4	4	4	0	0	0	0	4	4	4	4	0	0	0	0	1	2	1	0	1	1	1	1	2	0	0	0	1	1	0	0	1	0	0	0	1	0	0	0
	4	4	4	4	4	4	4	4	4	4	4	4	3	0	0	0	4	4	4	4	3	1	3	0	1	1	0	0	3	2	1	1	1	0	0	0	3	0	0	0	1	0	0	0	1	0	0	0
Day 14	4	4	4	4	4	4	4	4	4	4	4	4	1	1	0	0	3	3	3	4	3	2	0	2	1	0	1	0	3	3	3	3	1	1	0	0	1	0	0	0	1	0	0	0	2	1	0	0
	4	4	4	4	4	4	4	4	4	4	4	4	1	0	0	0	3	4	4	3	2	1	2	1	1	1	0	0	1	3	2	0	1	1	0	0	1	2	0	0	1	2	1	1	1	0	0	0
	4	4	4	4	4	4	4	4	4	4	4	4	1	0	0	0	3	2	3	4	1	3	0	0	2	2	0	0	1	2	2	2	1	0	0	0	0	0	0	0	1	1	0	0	1	0	0	0
	4	4	4	4	4	4	4	4	4	4	4	4	0	0	0	0	4	4	1	1	2	2	2	2	0	0	0	0	2	2	0	3	0	0	0	0	2	1	0	0	3	0	0	0	1	0	0	0
Day 15	4	4	4	4	4	4	4	4	4	4	4	4	1	1	0	0	3	3	3	4	3	2	0	2	1	0	1	0	3	3	3	3	1	1	0	0	0	0	0	0	2	1	1	0	1	2	0	0
	4	4	4	4	4	4	4	4	4	4	4	4	1	0	0	0	3	4	4	3	2	1	2	1	1	1	0	0	1	3	2	0	1	1	0	0	1	0	0	0	1	0	2	0	1	1	2	0
	4	4	4	4	4	4	4	4	4	4	4	4	1	0	0	0	3	2	3	4	1	3	0	0	2	2	0	0	1	2	2	2	1	0	0	0	1	1	1	0	2	2	1	1	1	0	0	0
	4	4	4	4	4	4	4	4	4	4	4	4	0	0	0	0	4	4	1	1	2	2	2	2	0	0	0	0	2	2	0	3	0	0	0	0	0	0	0	0	1	1	2	0	1	0	0	0

The data above represents the PKC scores obtained from fNX cells in 0.5, 1, 2 and 3 μg/μl puromycin, as described in 5.3.3 and Fig. 5.5

Figure B2b Puromycin killing curve data, PKC-2

Puromycin 2μg/ml*																								
Day 1	4	4	4	4	4	4	4	4	4	4	4	4	Day 7	3	1	2	4	1	0	1	0	3	3	3	3
	4	4	4	4	4	4	4	4	4	4	4	4		1	3	3	4	2	1	1	1	4	3	3	4
	4	4	4	4	4	4	4	4	4	4	4	4		3	3	3	1	2	1	2	1	3	2	4	3
	4	4	4	4	4	4	4	4	4	4	4	4		3	4	4	3	2	2	0	0	3	3	4	4
	4	4	4	4	4	4	4	4	4	4	4	4		3	1	2	2	4	4	4	4	3	4	4	4
	4	4	4	4	4	4	4	4	4	4	4	4		3	2	4	4	4	4	4	4	4	4	4	4
	4	4	4	4	4	4	4	4	4	4	4	4		4	4	4	4	4	4	4	4	3	3	4	4
	4	4	4	4	4	4	4	4	4	4	4	4		4	4	4	2	4	4	4	4	4	4	4	3
	4	4	3	4	4	4	4	4	4	4	4	4		2	4	0	0	4	4	4	4	1	1	2	2
	4	4	4	4	4	4	4	4	4	4	4	4		4	3	3	3	4	4	4	4	2	4	2	0
	4	4	4	4	4	4	4	4	4	4	4	4		2	1	1	3	4	4	4	4	2	4	4	4
	4	4	4	4	4	4	4	4	4	3	4	4		3	3	4	2	4	4	4	4	2	3	4	2
Day 2	4	4	4	4	4	4	4	4	4	4	4	4	Day 8	2	0	0	2	3	3	4	4	1	0	0	0
	4	4	4	4	4	4	4	4	4	4	3	4		2	3	1	1	1	0	1	2	1	1	2	0
	4	4	4	4	4	4	4	4	4	4	4	4		1	0	0	0	3	3	1	2	1	2	3	0
	4	4	4	4	4	4	4	4	4	4	4	4		1	0	0	0	2	2	1	4	1	2	1	0
	4	4	3	4	4	4	4	4	4	4	4	4		0	0	0	0	1	0	0	0	1	1	1	0
	4	4	4	4	4	4	4	4	4	4	4	4		0	0	0	0	2	0	0	0	1	0	0	1
	3	4	4	4	4	4	4	4	4	4	4	4		0	0	0	0	0	0	0	0	1	1	0	0
	4	4	4	4	4	4	4	4	4	4	4	4		0	0	0	0	0	0	0	0	1	1	0	0
Day 3	2	0	1	3	4	4	4	4	4	4	4	4	Day 10	0	0	0	0	1	0	0	0	1	0	0	0
	1	1	1	0	4	4	4	4	4	4	4	4		0	0	0	0	2	0	0	0	1	1	1	0
	1	0	0	0	4	4	4	4	4	4	4	4		1	0	0	0	3	0	0	0	1	1	1	0
	1	2	3	0	4	4	4	4	4	4	4	4		1	0	0	0	1	1	1	0	2	0	0	1
	4	4	4	4	4	4	4	4	4	4	4	4													
	4	4	3	4	4	4	4	4	2	4	4	4													
	4	4	4	4	4	4	4	4	4	4	4	4													
	4	4	4	4	4	4	4	4	4	4	4	4													
Day 4	2	1	0	0	4	4	4	4	4	4	4	4													
	2	1	2	3	4	4	4	4	4	4	4	3													
	1	3	2	1	4	4	4	4	4	4	3	4													
	1	2	3	3	4	4	4	4	4	4	4	4													

PKC2 was carried out in duplicate; the data above represent PKC scores counted at 3 points within each of 2 wells for each day of the experiment (see 5.3.3 and Fig. 5.5)

*Cells in the control well containing 0μg/ml puromycin were confluent from day 1 to day 10, and all scores during this period were '4'

Figure B3 Viral transduction of 3T3 cells

Expt.	Virus source	Harvest time / d	Target cell	Viral dilution	Transduction efficiency / %	Notes
VT-1-1	CP5A	2	3T3(I)	1.00	78.7	
VT-1-2	CP5A	2	3T3(I)	0.33	31.4	
VT-1-3	CP5A	2	3T3(I)	0.10	11.2	
VT-1-4	CP5A	2	3T3(I)	0.33	5.2	
VT-1-5	CP5B	2	3T3(I)	1.00	86.9	
VT-1-6	CP5B	2	3T3(I)	0.33	43.6	
VT-1-7	CP5B	2	3T3(I)	0.10	20.6	
VT-1-8	CP5B	2	3T3(I)	0.03	5.2	
VT-1-9	CP5C	2	3T3(I)	1.00	72.3	
VT-1-10	CP5C	2	3T3(I)	0.30	56.6	
VT-1-11	CP5C	2	3T3(I)	0.10	24.4	
VT-1-12	CP5C	2	3T3(I)	0.03	7.5	
VT1-13	CP5C	2	3T3(I)	0.00	1.0	control no virus
VT-2-1	CP5A	2	3T3(II)	1.00	73.5	
VT-2-2	CP5B	2	3T3(II)	1.00	77.0	
VT-2-3	CP5C	2	3T3(II)	1.00	35.7	
VT-2-4	CP5A	2	3T3(II)	1.00	51.9	re-frozen and re-thawed
VT-2-5	CP5B	2	3T3(II)	1.00	67.3	re-frozen as above
VT-2-6	CP5C	2	3T3(II)	1.00	23.2	re-frozen as above
VT-2-7	CP3	2	3T3(II)	1.00	60.5	
VT-2-8	CP3	3	3T3(II)	1.00	70.5	
VT-2-9	CP3	8	3T3(II)	1.00	15.7	
VT-2-10	CP3	12	3T3(II)	1.00	17.7	
VT-2-11	CP3	12	3T3(II)	1.00	28.0	fresh virus used
VT-2-12	no virus	n/a	3T3(II)	na	4.8	control no virus
VT-2-13	CP3	8	3T3(II)	1.00	74.7	Nos. 13-18 are identical
VT-2-14	CP3	8	3T3(II)	1.00	69.0	
VT-2-15	CP3	8	3T3(II)	1.00	67.8	
VT-2-16	CP3	8	3T3(II)	1.00	77.1	
VT-2-17	CP3	8	3T3(II)	1.00	75.8	
VT-2-18	CP3	8	3T3(II)	1.00	77.1	
VT-2-19	CP3	8	3T3(II)	1.00	91.0	non-specific fluorescence from cell death
VT-2-20	CP3	8	3T3(II)	1.00	94.3	as above
VT-2-21	CP3	8	3T3(II)	1.00	93.6	as above
VT-2-22	CP3	8	3T3(II)	1.00	93.5	as above
VT-2-23	CP3	8	3T3(II)	1.00	87.2	as above
VT-2-24	CP3	12	3T3(II)	1.00	62.0	fresh virus used
VT-stag1-1	CP3	12	stag3Faii	1.00	11.6	dp for 10mins on ice
VT-stag1-2	CP3	12	stag3Faii	1.00	16.8	fresh virus used
VT-stag1-3	CP3	12	stag3Faii	1.00	9.8	dp for 10mins at rT
VT-5-1	CP9A	3	3T3(II)	1.00	49.8	
VT-5-2	CP9A	3	3T3(II)	0.75	27.9	0.75ml virus, 0.75ml media
VT-5-3	CP9A	3	3T3(II)	0.50	22.2	0.5ml virus, 0.5ml media
VT-5-4	CP9A	3	3T3(II)	0.33	18.7	
VT-5-5	CP9A	3	3T3(II)	0.20	12.4	
VT-5-6	CP9A	3	3T3(II)	0.11	15.9	

Expt.	Virus source	Harvest time / d	Target cell	Viral dilution	Transduction efficiency / %	Notes
VT-5-7	CP9B	3	3T3(II)	1.00	32.9	
VT-5-8	CP9B	3	3T3(II)	0.75	24.0	
VT-5-9	CP9B	3	3T3(II)	0.50	21.0	
VT-5-10	CP9B	3	3T3(II)	0.33	18.0	
VT-5-11	CP9B	3	3T3(II)	0.20	15.7	
VT-5-12	CP9B	3	3T3(II)	0.11	15.2	
VT-5-13	CP9A	2	3T3(II)	1.00	15.5	
VT-5-14	CP9A	2	3T3(II)	0.75	11.6	
VT-5-15	CP9A	2	3T3(II)	0.50	10.6	
VT-5-16	CP9A	2	3T3(II)	0.33	9.3	
VT-5-17	CP9A	2	3T3(II)	0.20	7.0	
VT-5-18	CP9A	2	3T3(II)	0.11	8.1	
VT-5-19	CP3	2	3T3(II)	1.00	15.5	
VT-5-20	CP3	3	3T3(II)	1.00	31.5	
VT-5-21	CP3	8	3T3(II)	1.00	18.8	
VT-5-22	CP3	10	3T3(II)	1.00	13.6	
VT-5-23	CP3	10	3T3(II)	1.00	15.9	
VT-5-24	no virus	n/a	3T3(II)	0.00	5.7	control no virus
VT-7-1	CP11-2	2	3T3(II)	1.00	23.4	FACS at 24h (all VT7)
VT-7-2	CP11-2	2	3T3(II)	1.00	22.1	as above
VT-7-5	CP11-4	2	3T3(II)	1.00	28.5	as above
VT-7-6	CP11-4	2	3T3(II)	1.00	25.9	as above
VT-7-9	no virus	n/a	3T3(II)	1.00	0.5	control with dp
VT-7-10	no virus	n/a	3T3(II)	1.00	0.3	control with pb
VT-7-11	no virus	n/a	3T3(II)	1.00	0	control no virus
VT-7-13	CP10-2	6	3T3(II)	1.00	21.1	FACS at 24h
VT-7-14	CP10-2	6	3T3(II)	1.00	19.2	as above
VT-7-15	CP10-2	6	3T3(II)	1.00	15.7	as above
VT-8-1	CP12-1	2	3T3(II)	1.00	6.3	
VT-8-2	CP12-1	2	3T3(II)	1.00	1.1	
VT-8-3	CP12-1	3	3T3(II)	1.00	11	
VT-8-4	CP12-1	3	3T3(II)	1.00	8.8	
VT-8-5	CP12-2	2	3T3(II)	1.00	3.5	
VT-8-6	CP12-2	2	3T3(II)	1.00	4.1	
VT-8-7	CP12-2	3	3T3(II)	1.00	4.3	
VT-8-8	CP12-2	3	3T3(II)	1.00	4.4	
VT-8-9	CP12-3	2	3T3(II)	1.00	6.4	
VT-8-10	CP12-3	2	3T3(II)	1.00	6.1	
VT-8-11	CP12-3	3	3T3(II)	1.00	3.3	
VT-8-12	CP12-3	3	3T3(II)	1.00	4.9	
VT-8-13	CP12-4	2	3T3(II)	1.00	4.4	
VT-8-14	CP12-4	2	3T3(II)	1.00	5	
VT-8-15	CP12-4	3	3T3(II)	1.00	4.6	
VT-8-16	CP12-4	3	3T3(II)	1.00	6.2	
VT-8-17	CP10-2	8	3T3(II)	1.00	8.3	nos.17-19 in dp for 4h
VT-8-18	CP10-2	8	3T3(II)	1.00	4.5	as above
VT-8-19	CP10-2	8	3T3(II)	1.00	5	as above

Expt.	Virus source	Harvest time / d	Target cell	Viral dilution	Transduction efficiency / %	Notes
VT-8-20	CP10-2	8	3T3(II)	1.00	2.5	nos.20-22 in dp overnight
VT-8-21	CP10-2	8	3T3(II)	1.00	3	as above
VT-8-22	CP10-2	8	3T3(II)	1.00	2.5	as above
VT-8-23	no virus	n/a	3T3(II)	1.00	2.1	control no virus
VT-9-1	CP14-1	2	3T3(I)	1.00	82.6	dp/virus on ice 10 mins.
VT-9-2	CP14-1	2	3T3(I)	1.00	64.2	no dp/virus incubation
VT-9-3	CP14-2	2	3T3(I)	1.00	81.4	dp/virus on ice 10 mins.
VT-9-4	CP14-2	2	3T3(I)	1.00	81.4	no dp/virus incubation
VT-9-5	CP10-2	2	3T3(I)	1.00	48.6	dp/virus on ice 10 mins.
VT-9-6	CP10-2	2	3T3(I)	1.00	43.8	no dp/virus incubation
VT-9-7	no virus	n/a	3T3(I)	1.00	4.2	dp/media on ice 10 mins.

*days after fNX cell transfection

dp = dotap

pb = polybrene

VT6 was discontinued prematurely because of contamination

missing nos. in VT7 represent failed pb-mediated transductions

3T3(I) and 3T3(II) are the first and second 3T3 lines, respectively, used for transduction (see 5.4.3 for details)